Louisiana Highway Research

FRICTION PILE CAPACITY PREDICTION IN SOFT LOUISIANA SOILS USING ELECTRIC QUASI-STATIC PENETRATION TESTS

INTERIM RESEARCH REPORT NO. 1

Louisiana Department of Transportation and Development
Research and Development Section

FRICTION PILE CAPACITY PREDICTION IN SOFT LOUISIANA SOILS USING ELECTRIC QUASI-STATIC PENETRATION TESTS

INTERIM RESEARCH REPORT NO. 1

By

Mehmet T. Tumay
Professor
Department of Civil Engineering
Louisiana State University

Manouchehr Fakhroo
Staff Engineer
Woodward-Clyde Consultants
New Orleans, Louisiana

State Project No. 736-04-55

Research Project No. 79-1S

September 1981

LOUISIANA STATE UNIVERSITY
Baton Rouge, Louisiana 70803
1981

TECHNICAL REPORT STANDARD TITLE PAGE

1. Report No.	2. Government Accession No.	3. Recipient's Catalog No.
FHWA/LA/LSU - 82		

4. Title and Subtitle	5. Report Date
FRICTION PILE CAPACITY PREDICTION IN SOFT LOUISIANA SOILS USING ELECTRIC QUASI-STATIC PENETRATION TESTS	SEPTEMBER 1981
	6. Performing Organization Code

7. Author(s)	8. Performing Organization Report No.
MEHMET T. TUMAY AND MANOUCHEHR FAKHROD	LA. RESEARCH STUDY 79-1S

9. Performing Organization Name and Address	10. Work Unit No.
CIVIL ENGINEERING DEPARTMENT LOUISIANA STATE UNIVERSITY BATON ROUGE, LOUISIANA 70803	11. Contract or Grant No. 736-04-55
	13. Type of Report and Period Covered INTERIM #1 JANUARY 1979 TO SEPTEMBER 1981
12. Sponsoring Agency Name and Address LOUISIANA DEPARTMENT OF TRANSPORTATION & DEVELOPMENT P.O. BOX 44245, CAPITOL STATION BATON ROUGE, LOUISIANA 70804	14. Sponsoring Agency Code

15. Supplementary Notes

CONDUCTED IN COOPERATION WITH THE LOUISIANA DEPARTMENT OF TRANSPORTATION & DEVELOPMENT AND THE U.S. DEPARTMENT OF TRANSPORTATION, FEDERAL HIGHWAY ADMINISTRATION

16. Abstract

THE MAIN OBJECTIVE OF THIS STUDY WAS TO INVESTIGATE THE POSSIBILITY OF USING THE ELECTRONIC CONE PENETROMETER DATA TO PREDICT THE LOAD CARRYING CAPACITY OF PILES DRIVEN IN SOFT COHESIVE SOILS. SELECTION OF THE LOCATIONS INVOLVED IN THIS STUDY WAS BASED ON THEIR SUBSOIL CONDITION, ACCESSIBILITY, AND WHETHER THEY CONTAINED TEST PILE (S) OF KNOWN CAPACITIES. A TOTAL OF 10 SITES AND 37 FULL SCALE TEST PILES COVERING VARIOUS SHAPES LENGTHS, AND MATERIALS WERE CHOSEN. THE CONE PENETRATION TESTS WERE PERFORMED AS CLOSELY AS POSSIBLE TO THE LOCATION OF THE TEST PILES USING TIPS OF DIFFERENT SIZE AND ANGLE. HOWEVER, THE RESULTS OF THE STUDY PRESENTED ARE BASED ON THE DATA COLLECTED USING AN ELECTRONIC CONE PENETROMETER OF 60° TIP ANGLE AND 10 CM^2 BASE AREA PUSHED AT THE RATE OF 2 CM/S.

THE INTENT WAS TO UTILIZE THE PENETRATION RESULTS DIRECTLY IN COMPUTATION OF PILE CAPACITIES. THE TIP BEARING CAPACITY WAS PREDICTED BY THE TIP RESISTENCE (Q_C) READINGS, IMPLEMENTING A PROCEDURE SIMILAR TO THAT PROPOSED FOR SANDY SOILS. TWO PROCEDURES ARE RECOMMENDED TO ESTIMATE THE PILE SIDE FRICTIONAL CAPACITY IN COHESIVE SOILS WHICH ARE THE CONE-M METHOD AND THE LAMBDA-CONE METHOD. THE PROPOSED PROCEDURES RESULTED IN CLOSE PREDICTIONS OF THE TEST PILES' ULTIMATE CAPACITIES. THE ULTIMATE CAPACITIES OF THE TEST PILES WERE ALSO COMPUTED BY THREE STATIC ANALYSIS TECHNIQUES WHICH WERE THE ALPHA METHOD, THE LAMBDA METHOD, AND THE BETA METHOD. THE RESULTS OF THESE PROCEDURES WERE COMPARED WITH THE ONES OBTAINED BY APPLYING THE TWO PROPOSED CONE METHODS. IT IS CONCLUDED THAT THE ELECTRONIC CONE PENETROMETER DATA CAN INDEED BE UTILIZED TO DESIGN PILE FOUNDATIONS IN COHESIVE SOILS.

17. Key Words	18. Distribution Statement
PILE CAPICITY, ELECTRIC CONE PENETROMETER SOFT COHESIVE SOILS, UNIT PILE FRICTION, FRICTION SLEEVE RESISTANCE UNDRAINED SHEAR STRENGTH	NO RESTRICTIONS, THIS DOCUMENT IS AVAILABLE TO THE PUBLIC THROUGH THE NATIONAL TECHNICAL INFORMATION SERVICE SPRINGFIELD, VIRGINIA 22161

19. Security Classif. (of this report)	20. Security Classif. (of this page)	21. No. of Pages	22. Price
UNCLASSIFIED	UNCLASSIFIED	275	

Form DOT F 1700.7 (8-69)

TABLE OF CONTENTS

LIST OF TABLES

LIST OF FIGURES

LIST OF SYMBOLS

A = adhesion factor

A_p = pile tip bearing area

A_s = total surface area of pile in contact with soil

A_t = tip bearing area

B = pile width or diameter

$\bar{C}$ = average undrained cohesion at pile tip

C_a = developed adhesion between the soil and pile

C_m = mean undrained cohesion for depth of pile

C_u = undrained cohesion

$\bar{C}_u$ = mean undrained cohesion

D = pile diameter

D_c = critical depth

d = diameter of pile

d_p = pile diameter

F_t = total friction

f = unit pile side friction

f_s = cone local friction

$\bar{f}_s$ = average cone local friction

K = coefficient of lateral earth pressure

K_s = Nottingham's local friction correction factor in sand

L = depth to which local friction values considered

m = cone adhesion factor

N_c = bearing capacity factor

N_k = ratio of cone tip resistance to undrained cohesion

N_q = bearing capacity factor

N_γ = bearing capacity factor

n = ratio of undrained cohesion to cone local friction

P = circumference of the pile

P_{c1} = average cone resistance 8d above the pile tip

P_{c2} = average cone resistance 4d below the pile tip

P_d = specific pile point resistance

Q_p = pile tip capacity

Q_s = total pile frictional capacity

Q_t = tip bearing capacity

q_a = average of the minimum $\bar{q}_c$ values, 8D above the tip

q_{b1} = average of the $\bar{q}_c$ values, 4D below the pile tip

q_{b2} = average of the minimum $\bar{q}_c$ values, 4D below the pile tip

q_c = cone tip resistance

$\bar{q}_c$ = average cone tip resistance

q_o = unit tip bearing capacity of pile

r = a proportionality constant

S_u = undrained shear strength

Z = pile settlement

α = Tomlinson's adhesion factor

α' = Nottingham's adhesion factor applied to cone friction data

β = Burland's pile friction factor

γ = total unit weight of soil

δ = pile-soil friction angle

λ = Vijayvergia and Focht's pile friction factor

λ_c = pile friction factor used in Lambda-Cone Method

$\bar{\sigma}_h$ = average horizontal pressure for the length of the pile

$\bar{\sigma}_m$ = mean effective overburden pressure

$\bar{\sigma}_v$ = effective vertical overburden pressure

$\bar{\sigma}_{vm}$ = mean effective vertical pressure for the pile length

$\bar{\sigma}_o$ = effective overburden pressure

ϕ = angle of internal friction

ϕ_d = drained angle of internal friction

χ = pile friction factor used in Beta-Chi Method

ABSTRACT

The main objective of this study was to investigate the possibility of using the electronic cone penetrometer data to predict the load carrying capacity of piles driven in soft cohesive soils. Selection of the locations involved in this study was based on their subsoil condition, accessibility, and whether they contained test pile(s) of known capacities. A total of 10 sites and 37 full scale test piles covering various shapes, lengths, and materials was chosen. The cone penetration tests were performed as closely as possible to the location of the test piles using tips of different size and angle. However, the results of the study presented are based on the data collected using an electronic cone penetrometer of 60° tip angle and 10 cm^2 base area pushed at the rate of 2 cm/s.

The intent was to utilize the penetration results directly in computation of pile capacities. The tip bearing capacity was predicted by the tip resistance (q_c) readings, implementing a procedure similar to that proposed for sandy soils. Two procedures are recommended to estimate the pile side frictional capacity in cohesive soils which are the Cone-m Method and the Lambda-Cone Method. The proposed procedures resulted in close predictions of the test piles' ultimate capacities. The ultimate capacities of the test piles were also computed by three static analysis techniques which were the Alpha Method, the Lambda Method, and the Beta Method. The results of these procedures were compared with the ones obtained by applying the two proposed cone methods.

It is concluded that the electronic cone penetrometer data can indeed be utilized to design pile foundations in cohesive soils.

Chapter 1

INTRODUCTION

1.1 Research Justification

Pile foundations are generally used where upper soil strata are weak or compressible. The ultimate capacity of a pile is either due to failure of the pile or the soil, but in most circumstances it is governed by soil failure. A pile foundation is an indeterminate structure to a very high degree. The ultimate capacity (Q_u) of a pile is generally considered to be due to the soil resistance developed by friction or adhesion between the soil and the pile shaft (Q_s), and to the end bearing capacity (Q_t) at the tip of the pile. There are three methods commonly applied to estimate the total pile capacity: (1) the static analysis techniques based on an evaluation of properties of the soil into which the pile will be driven, (2) the dynamic formulas, and (3) the load test program.

The ultimate (Q_u) of a pile by the static analysis techniques is determined as follows:

$$Q_u = Q_s + Q_t = f \times A_s + q_o \times A_t \qquad (1.1)$$

where

Q_s = pile side friction capacity

Q_t = pile tip bearing capacity

f = unit pile friction

A_s = pile shaft surface area

q_o = unit tip bearing capacity

A_t = pile tip area

The main problem associated with this type of analysis is the proper evaluation of f and q_o. The procedure involved for the cohesionless (sandy) soils differs from that for cohesive (clayey) soils. In general, f and q_o are computed as follows:

$$f = A \times C_u \qquad \text{(saturated clays, } \phi = 0) \qquad (1.2)$$

$$f = K \bar{\sigma}_o \tan \delta \qquad \text{(sandy soils, } C_u = 0) \qquad (1.3)$$

$$q_o = 9 \bar{C} \qquad \text{(clayey soils)} \qquad (1.4)$$

$$q_o = \bar{\sigma}_o N_q \qquad \text{(sandy soils)} \qquad (1.5)$$

where

A = the adhesion factor

C_u = undrained cohesion along the pile shaft

K = coefficient of lateral earth pressure

$\bar{\sigma}_o$ = average effective overburden pressure

δ = pile-soil friction angle

$\bar{C}$ = average undrained cohesion at the pile tip

N_q = bearing capacity factor (function of ϕ)

The difficulties lie in the proper determination of the mentioned parameters. The task is more troublesome in sandy soils than in the clayey soils due to the following reasons.

1. It is nearly impossible to obtain an undisturbed sample of cohesionless soils. Presently, shear strength parameters such as the angle of internal friction (ϕ) are evaluated from the standard penetration test results. However, the nature of the relationship is not well understood and the test itself has numerous shortcomings.

2. The side friction parameters such as K and δ are very difficult to define and determine. The values of the former vary between 0.3 to 3.0 and those of the latter have a range between 10° to 24° (the limit is ϕ).

3. The bearing capacity factor (N_q) is a function of the internal friction angle (ϕ) which should be measured in-situ. Provided that ϕ is evaluated properly, the N_q term value differs greatly depending on the failure pattern or mechanism assumed. For ϕ = 35°, the factor is about 55 by Terzaghi (1943), but on the other hand, it is as high as 400 by DeBeer (1945) criterion. The question is which one should be used in bearing capacity calculations?

The difficulties associated with this technique are less in cohesive soils. There is not much dispute over the exact form of the relationship for computing the unit tip capacity (q_o). However, the major portion of the load carrying capacity of piles driven in clays is contributed by the shaft frictional capacity (Q_s). Thus, the procedure is heavily dependent on the proper determination of the adhesion factor (A). There are several relationships relating the adhesion to the undrained cohesion such as the one suggested by Tomlinson (1957). All of the investigators agree that the adhesion factor decreases as the shear strength increases. Nevertheless, the values can vary by a factor of 2 at certain levels of C_u, depending upon the relationship adopted. Although the procedure produces fairly good results (mostly conservative), many investigarors believe that the friction should be related to the drained rather than the undrained strength.

The dynamic analysis of determining pile capacity is based on work-energy principles. The axial capacity of piles is related to the resistance against penetration developed during driving. This procedure suffers from the following drawbacks.

1. The difficulties involved in determination of energy losses are numerous.
2. The pile driving action generates high excess pore pressures particularly in fine saturated soils. An estimated capacity based on a soil in such condition is different from the capacity that develops after the dissipation of pore pressures. Thus, for cohesive soils the analysis is even less reliable. Most of the dynamic formulas (i.e. the engineering news) are developed for point bearing piles (driven into sand) and their utilizations cannot be justified for friction piles.
3. The factor of safety adopted when utilizing such analysis may be as high as 6 due to the uncertainties involved.

Full scale pile tests are conducted to determine the actual ultimate capacity due to the shortcomings of the previously mentioned procedures. The test pile programs are also run to determine the pile penetration depth, the load-settlement characteristics, and the most efficient type of pile to be used. Even though the test pile programs are required and cannot be eliminated, it is preferable to keep the number involved to a minimum for the following reasons.

1. The program is very expensive to perform. The cost ranges from $1,500 to $150,000 (average $50,000) per test pile. A project might require several test piles.

2. The program is time consuming. It may take 2 to 3 weeks to complete a test pile program.
3. The program is sometimes run while the project is in progress which is too late to make any changes.
4. There is a dispute over the amount of settlement which would constitute a failure. Chellis (1951) summarized 16 different methods to obtain the failure from the load-settlement information provided by a pile testing program.

Surprisingly, a factor of safety of 2.5 is usually assumed for determining the allowable load. It appears that performing a costly, time-consuming test pile program should reduce the uncertainties and lead to adoption of a smaller factor of safety.

The quasi-static cone penetration test (QCPT) which can be regarded as a model test pile, has been used in the Netherlands for the design of piles foundations for many years. This test provides information to estimate the in-situ continuous profile of both unit tip bearing capacity (q_o) and unit friction (f). Because of the geological condition of the countries where QCPT has developed, most of the efforts have been directed toward prediction of the tip bearing capacity of piles driven in sand. Little work is available with respect to utilizing QCPT data to predict pile capacity in cohesive soils.

Most of the test piles involved in this study are driven in cohesive soils (friction piles). The tip bearing capacities of the test piles were predicted by a method similar to that proposed by Dutch engineers. This was done because the procedure for estimating the tip bearing capacity using the cone resistance (q_c) data were well established. The frictional capacity of a pile was related either by

the total friction along the sounding tubes or by q_c data, prior to the development of the friction sleeve penetrometer by Begemann in 1953. This "new" version of the penetrometer capable of providing local friction (f_s) readings opened the door to a more direct and rational estimate of the unit pile side friction (f).

1.2 Purpose and Scope

One of the major goals of this research was to develop procedure(s) requiring direct utilization of f_s data in computations of the frictional capacity (Q_s) which contributes the major portion of the total ultimate capacity of piles driven in cohesive soils. Two different procedures are proposed for computing the unit friction f in conjunction with direct utilization of the cone local friction: (1) the Cone-m Method and (2) the Lambda-Cone Method. The Cone-m Method relates the unit friction f to the average f_s values by an adhesion factor called m. The Lambda-Cone Method is similar to the method proposed by Vijayvergia and Focht (1972) except for the fact that the mean undrained cohesion term is evaluated from the average f_s readings. The two mentioned procedures resulted in close predictions of the test piles' ultimate capacities.

The ultimate capacities were also computed by three static analysis techniques: The Alpha Method (Tomlinson, 1957), the Lambda Method (Vijayvergia and Focht, 1972), and the Beta Method (Burland, 1973). The results of these procedures were compared with the ones obtained by applying the two suggested cone methods. The Alpha Method resulted in conservative results, the Lambda Method provided close predictions, and the Beta Method produced estimations which had to be corrected by a friction factor depending on pile length.

It was concluded that the cone penetrometer data could be utilized to design pile foundations in cohesive soils. Also, in light of the close predictions made by the proposed procedures, it is hoped that adoption of such methods in conjunction with further research in this area would allow smaller factor of safety and minimize the number of costly and time consuming test pile programs required for a project.

Chapter 2

THE CONE PENETRATION TEST

2.1 General

The western and northern European soils engineers have made the major contributions toward development of the cone penetrometers. Several types of penetrometers have been developed and utilized by engineers throughout the world since the early days. These range from hand-pushed penetrometers of small diameter to large penetrometer probes almost one foot in diameter.

The quasi-static cone penetration test (QCPT) requires the measurement of the force on a cone-shaped point during its penetration into the soil. The base area and the tip angle of the cone are usually 10 cm^2 and 60°, respectively. The pressure against penetration exhibited by the soil is called the cone resistance (q_c) and is obtained by dividing the measured penetration thrust by the projected base area of the tip.

The original version of QCPT equipment consisted of a conical point connected to a steel push-rod. This equipment was developed at the Delft Soil Mechanics Laboratory during the early 1930's. One of the problems associated with this penetrometer was that soil particles sometimes entered its mechanism resulting in erroneous readings because of the friction developed between the moving parts. The Delft Laboratory eliminated this problem by designing the mantle cone which proved to be very efficient. The Dutch mantle cone has been used in

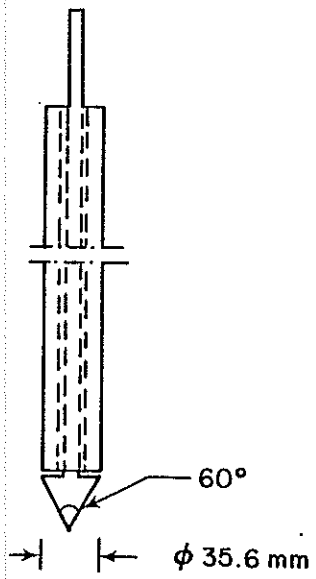

a. Original Dutch Cone Penetrometer

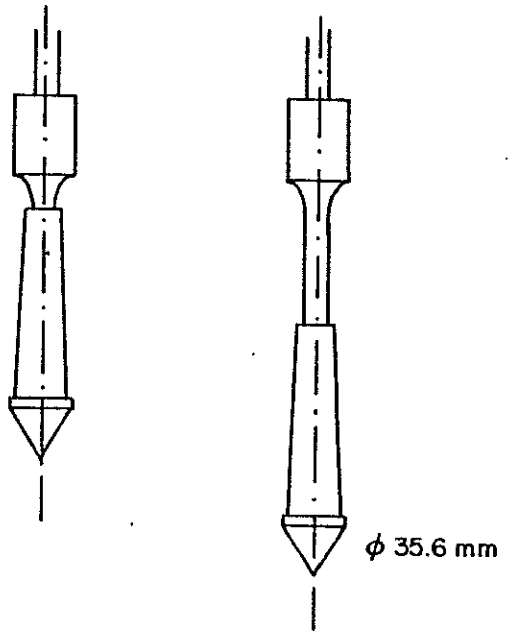

b. Dutch Mantle Penetrometer

c. Begemann Friction Sleeve Penetrometer

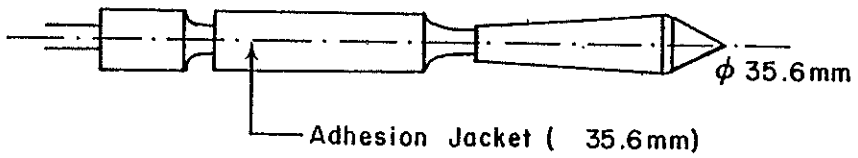

Figure 2.1 Different Types of Mechanical Cone Penetrometers (Heijnen, 1974)

Netherland for design of deep foundations for many years. This was done by measuring the total friction along the rods penetrated.

The Dutch friction-jacket cone was developed after Begeman became discontent with using total rod friction for estimating pile side friction. This penetrometer is similar to the mantle cone, except for the fact that it provides a movable friction sleeve just above the tip for measurement of local friction (f_s). This data could be implemented in the design of pile foundations and has proven to be a useful tool in estimating the shear strength of cohesive soils. The three different types of cone penetrometers discussed here are shown in Figure 2.1.

The Fugro electronic cone penetrometer was used for all of the soundings performed in this study (Figure 2.2). This recent version has the same base area as the mechanical cone, however, it has a cylindrical shape rather than tapered one as in the case of the mechanical cone. There is no relative movement between the parts of the electrical cone, and it is advanced simultaneously and continuously over a length of 1 m which is the length of a single tube. Nottingham (1975) listed the differences between the electrical and mechanical cone penetrometers in his report. There are no systematic differences found between the q_c readings obtained by the two cone penetrometers. However, marked differences have been found in the measurement of local friction (f_s) depending on the type of penetrometer used.

DeRuiter (1971) described general features of electronic penetrometers which may incorporate inclinometers and piezometers.

Many years of experience have revealed that the cone penetration test (QCPT) could be a useful tool in such various geotechnical engineering problems as soil classification, determination of soil shear

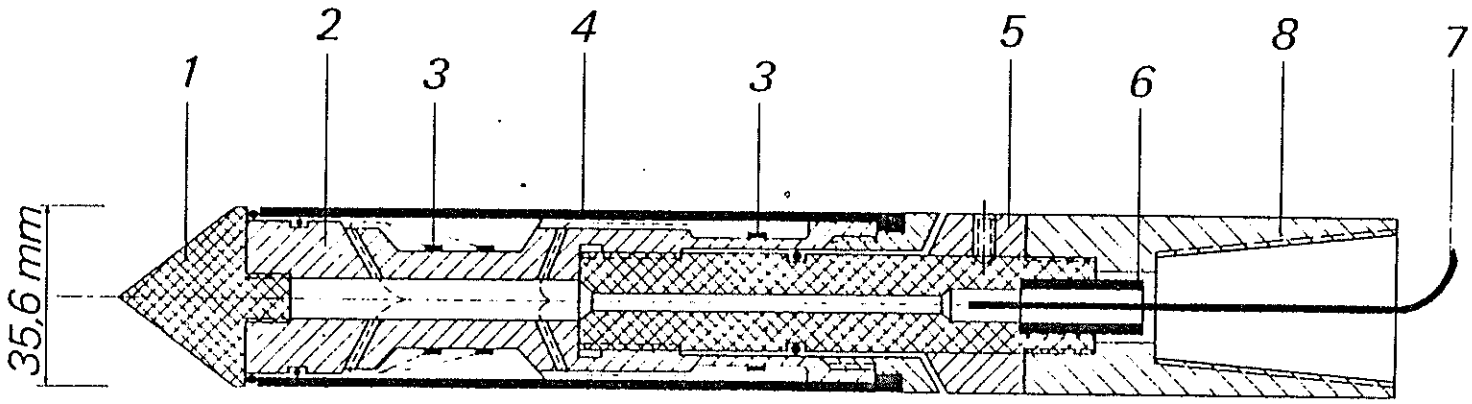

1 Conical point (10 cm^2)
2 Load cell
3 Strain gauges
4 Friction sleeve
5 Adjustment ring
6 Waterproof bushing
7 Cable
8 Connection with rods

Figure 2.2 Fugro Electronic Friction Sleeve Penetrometer (Krause, 1973)

strength properties, settlement computations, and bearing values for design of both shallow and deep foundations.

2.2 Prediction of Pile Capacity Using QCPT Data

2.2.1 General

Based on the published literature, it seems that general soil exploration and pile design have been the main areas of use for QCPT data. The test can be considered as a model test pile, offering an alternative approach to the pile capacity prediction problem.

QCPT has been used in the Netherlands for more than 40 years in the determination of the bearing capacity of piled foundations. Early efforts involved using QCPT data to estimate the maximum depth that a pile could be driven at a given site. Begemann (1969b) reported that the maximum depth that could be achieved by driving a normal concrete pile was taken as the depth where the total resistance (point resistance plus total rod friction) reached 4500 to 5000 kg. This procedure was later abandoned in favor of utilizing QCPT data to arrive directly at the unit tip resistance and friction resistance of a driven pile.

2.2.2 Early Pile Point Capacity Prediction Methods

The cone penetration test which replicates a model displacement pile could provide data to develop an in-situ continuous resistance profile. Since the early days, engineers have been well aware of the relationship between the cone resistance (q_c) and pile point resistance. There are several relationships recommended by engineers; however, there is considerable dispute over the failure mechanism and the relationship between q_c and the unit pile point resistance. Regardless of the form, all of the methods suggest implementing some kind of averaging procedure to arrive at the unit pile point resistance when using QCPT data.

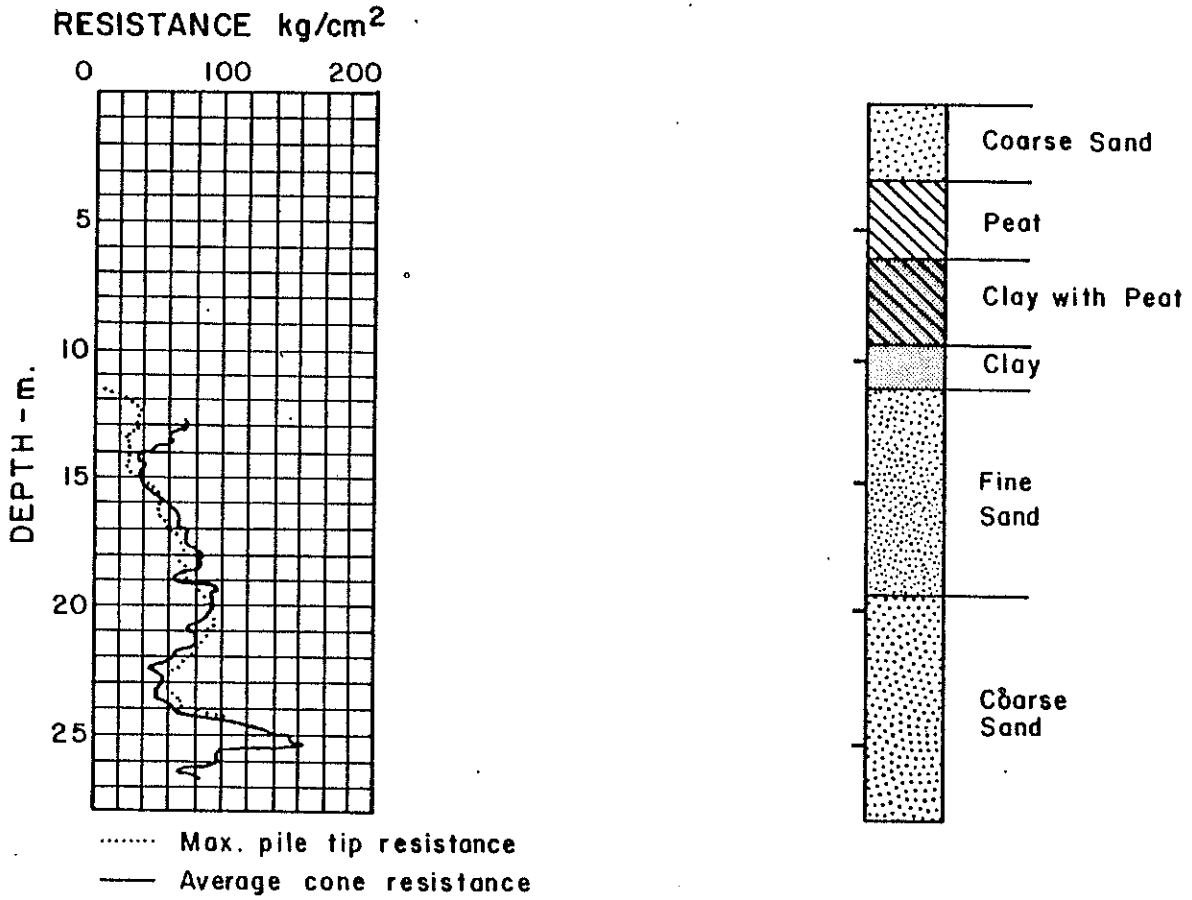

Figure 2.3 Plantema's Experimental Pile Point Resistance Data (Plantema, 1948)

Plantema (1948) performed an interesting experiment to explain the connection between q_c data and pile point resistance. He achieved this by placing a steel sleeve around a 42.6 cm^2 concrete pile in order to eliminate the side friction and measured the pile point resistance while it was being jacked into the soil. He also performed six QCPT soundings and compared their average with the pile point resistance profile as shown in Figure 2.3. The average q_c readings were higher than the pile resistance for the top 3 m of penetration. However, the agreement appeared to be very good. The fact that q_c may be higher than pile resistance in some cases, became a matter of great concern among the engineers. Meyerhof (1951) noted the danger in extrapolating q_c data to obtain pile resistance. He realized that when a pile penetrated a short distance into a dense layer, the q_c readings were higher than pile resistance, because of the difference in diameters. The phenomenon is called the scale effect.

Van der Veen and Boersma (1957) took the scale effect into consideration when relating the q_c readings to pile point resistance. This was done by averaging cone resistance values over a depth interval of aB above the pile base to bB below the pile base where B is the equivalent pile diameter (see Figure 2.4). It was noted that the value of a could vary from 1.5 to 12 and the value b could range from 1 to 2. They recommended the most probable values for a and b which appeared to be 3.75 and 1.0, respectively.

Bogdanovic (1961) suggested that finer pile point resistance predictions are obtained by averaging cone resistance values from an envelope drawn through the minimum q_c values rather than by averaging the actual values. He arrived at this conclusion by taking a 30 x 30 cm

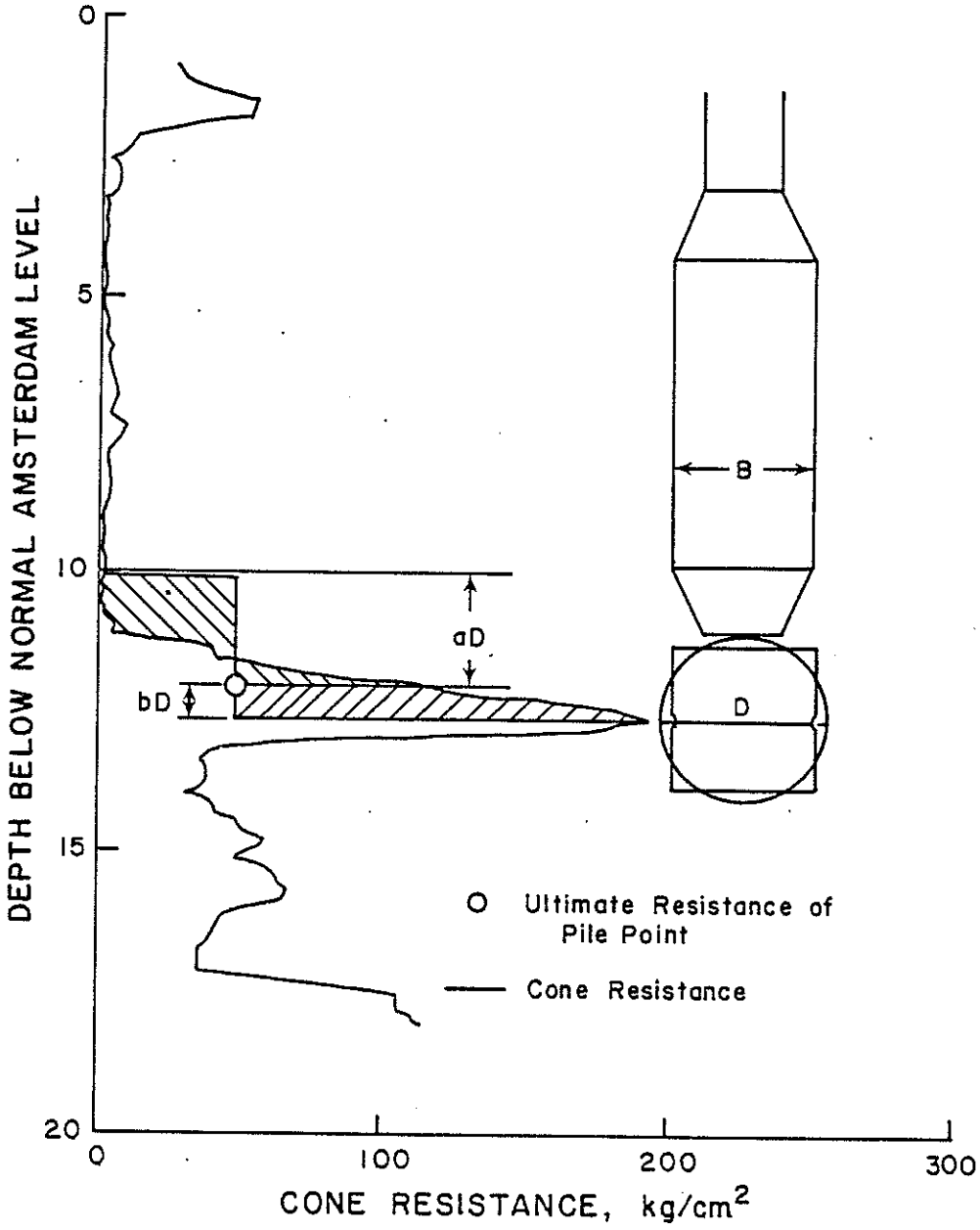

Figure 2.4 Method of Determining Anticipated Pile Bearing Capacity from CPT (after Van der Veen and Boersma, 1957)

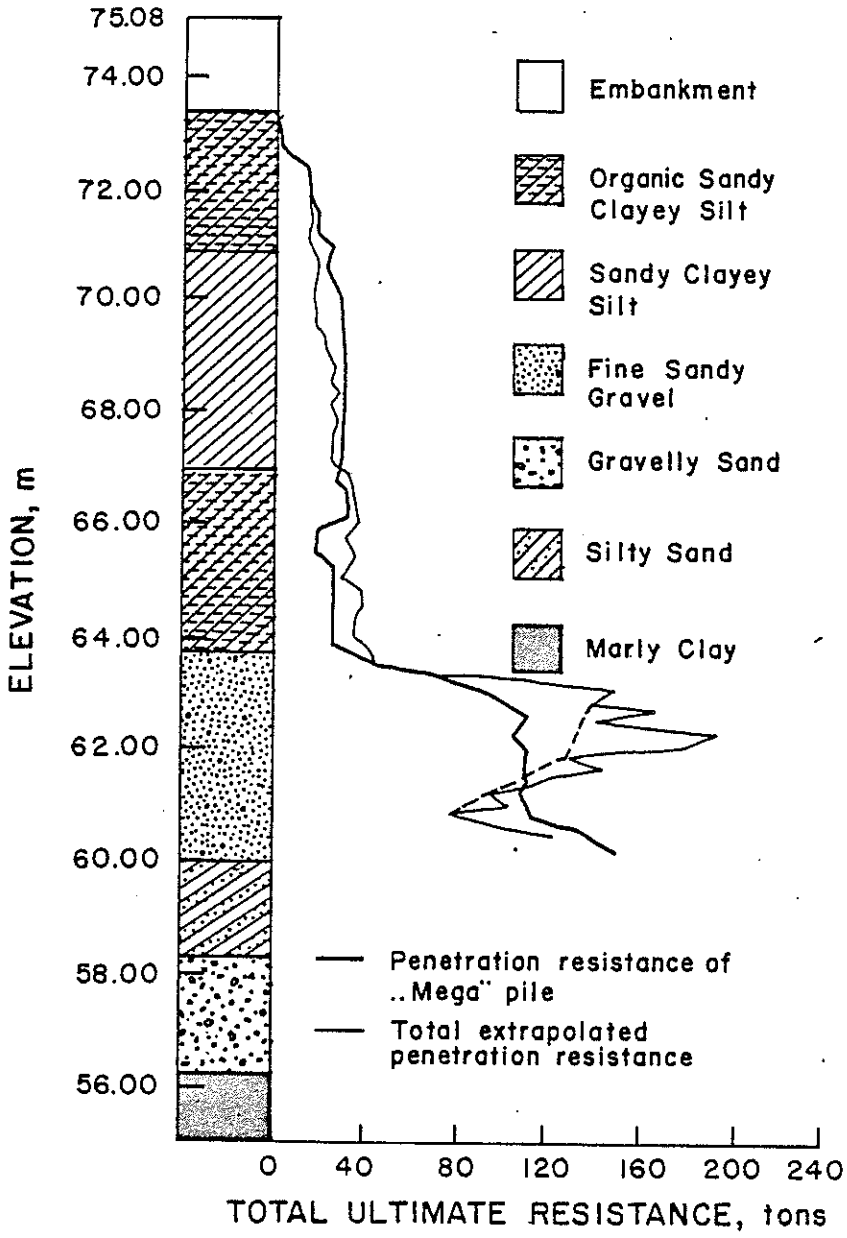

Figure 2.5 Diagram of Penetration Resistance of "Mega" Pile and Total Extrapolated Penetration Resistance (after Bogdanovic, 1961)

"mega" pile to a depth of 13 m and recorded the penetration resistance continuously. The pile point resistance was calculated by averaging the q_c values from 4B above the pile base to 2B below the base, or as the average of the minimum q_c values over the same interval. The pile shaft resistance was calculated from the total penetrometer shaft resistance data. The measured resistance of the jacked-in pile agreed closely with the estimated resistance except when the pile was penetrating the upper portion of the dense layer as shown in Figure 2.5.

The cone resistance q_c may be taken as equal to that of a large diameter pile provided that the soil is homogeneous and penetration is performed at a steady rate. Begemann (1963) investigated the influence of pile diameter for the case of a layered and non-homogeneous soil. He presented a two layered system of a homogeneous clay overlaying a homogeneous sand layer with specific cone resistances of 200 psi and 2200 psi, respectively. This sudden transition can only be sensed as such by a cone of a zero diameter as shown in Figure 2.6. He suggested that each of the ground layers above and below the base of the cone contribute about half to the measured cone resistance. This meant that a cone with a diameter greater than zero, placed with its base exactly on the boundary between the layers, would have a specific resistance equal to the average of the cone resistances in the two layers; in this case,

$$\frac{200 + 2200}{2} = 1200 \text{ psi}$$

The theoretical failure surface was approximated by a logarithmic spiral as presented in Figure 2.7. Therefore the full value of 2200 psi would not be encountered until a penetration depth of 8 to 10 diameter

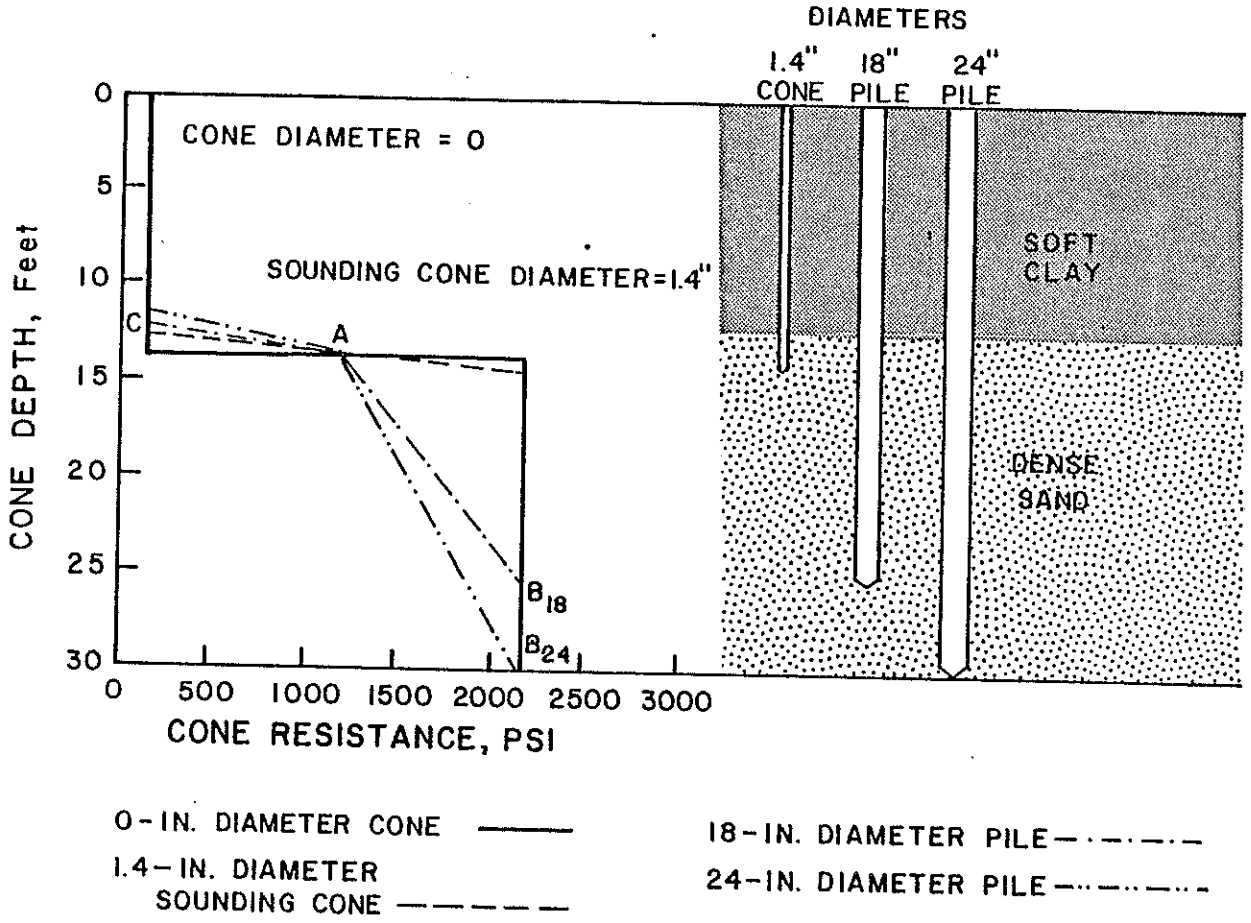

Figure 2.6 Point Resistance in Relation to Depth for a Cone and Piles of Different Diameters (Smith, 1975)

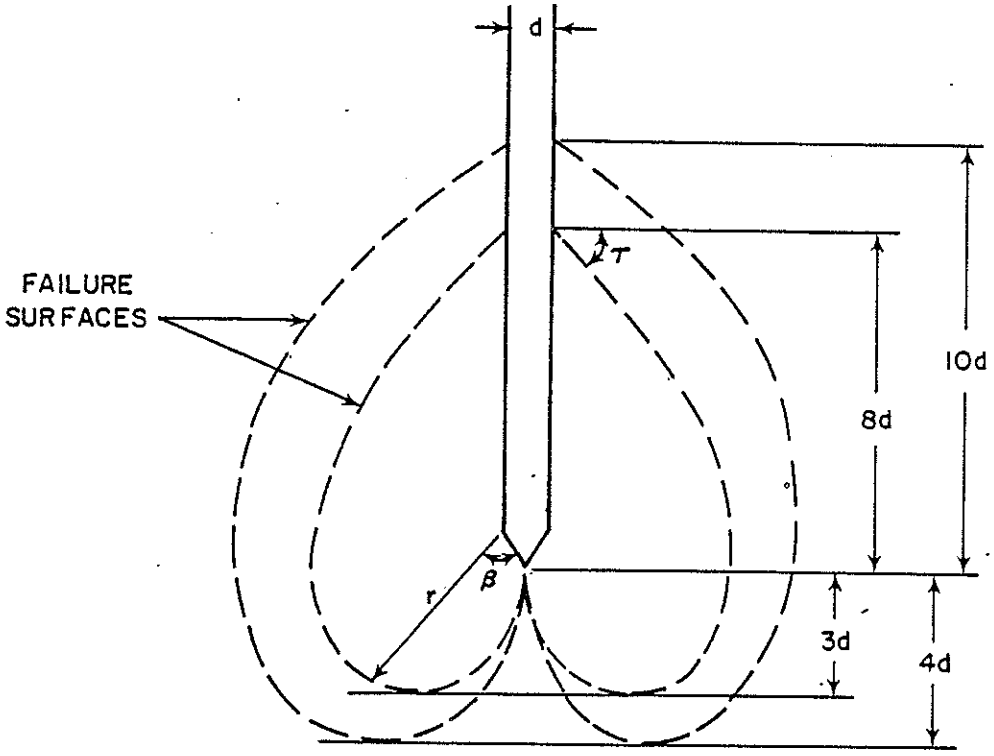

Figure 2.7 Theoretical Failure Surface
(Smith, 1975)

was reached in the sand layer (Fig. 2.6). The specific cone resistance increases from that of the upper soil layer to point A, or the average of the two layers, and is defined by line C-A. This occurs at an elevation of 3 to 4 diameters above the theoretical "zero" line. The maximum pile resistance is not reached until a depth of penetration of 8 to 10 diameters is achieved. Lines A-B define the pile's unit tip resistance at a point between the average (point A) and the maximum (point B) resistance. The equation of this line for any diameter pile can be expressed as follows:

$$P_d = \frac{1}{2} (P_{c1} + P_{c2}) \qquad (2.1)$$

where

P_d = specific point resistance for a pile with diameter d

P_{c1} = the average cone resistances over a distance 8 d above the full section of the pile point

P_{c2} = the average cone resistance below the full section for 3 to 4 d

Begemann further underlined the importance of layer thickness when cone resistances of the soil layers immediately below the pile tip are not constant. Taking into account the above notation as well as the significance of the shape of the failure surface, he recommended a new formula to calculate P_{c2} which follows:

$$P_{c2} = [P_1 + P_2 \cdot \cdot \cdot P_n + n\, P_n]/[2 \cdot n] \qquad (2.2)$$

where

$P_1, P_2, \cdot \cdot \cdot P_n$ = the sounding values at regular intervals to a depth of 3.5 d below the full section of the pile point

The influence of the horizontal portion of the failure surface passing through the P_n layer was taken into consideration by the addition of an equal number of values of the final sounding point ($n \cdot P_n$).

2.2.3 Research Concerning the "Critical Depth"

Sanglaret (1972) was not completely optimistic of taking q_c data directly or of using the proposed averaging procedures because he had encountered cases in which the measured pile point resistance was only a fraction of the q_c value at the same level. Kerisel (1964) also noted that the bearing capacity of large piles was significantly less than that of the penetrometers in dense sand before a certain depth was reached (see Figure 2.8).

DeBeer (1963) investigated the scale effect and revealed that eventually after a certain depth is reached, all penetrometers should attain the same point resistance (see Figure 2.9). This depth is called the critical depth (D_c) at which the bearing capacity failure changes from that of a shallow foundation to that of a deep foundation. Point resistance increases linearly before this depth is reached; however, after the deep foundation condition is encountered, point resistance only increase slightly with depth. A pile point resistance will not reach its maximum value unless it is driven at least a depth equal to D_c into the bearing layer.

Meyerhof (1951) and DeBeer (1963) have shown that D_c is a function of the foundation size. The critical depth ratio D_c/d_p (critical depth/pile tip diameter) also influences the value of point bearing attained by a pile. Experimental and theoretical works in this field have indicated that D_c/d_p for sand is function of density and varies from 5 to 20 for loose sands and dense sands, respectively. Meyerhof (1976) reported

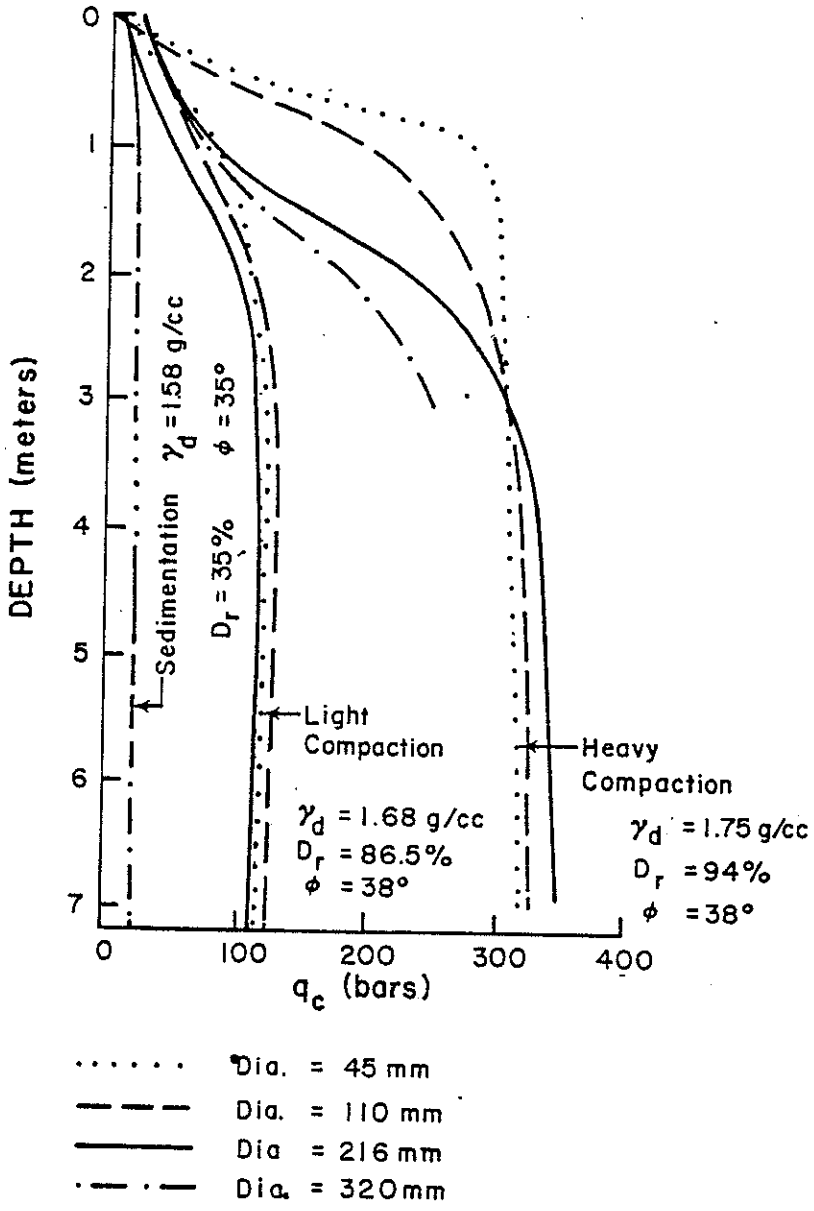

Figure 2.8 Kerisel's Experimental Penetration Resistance Curve (Kerisel, 1964)

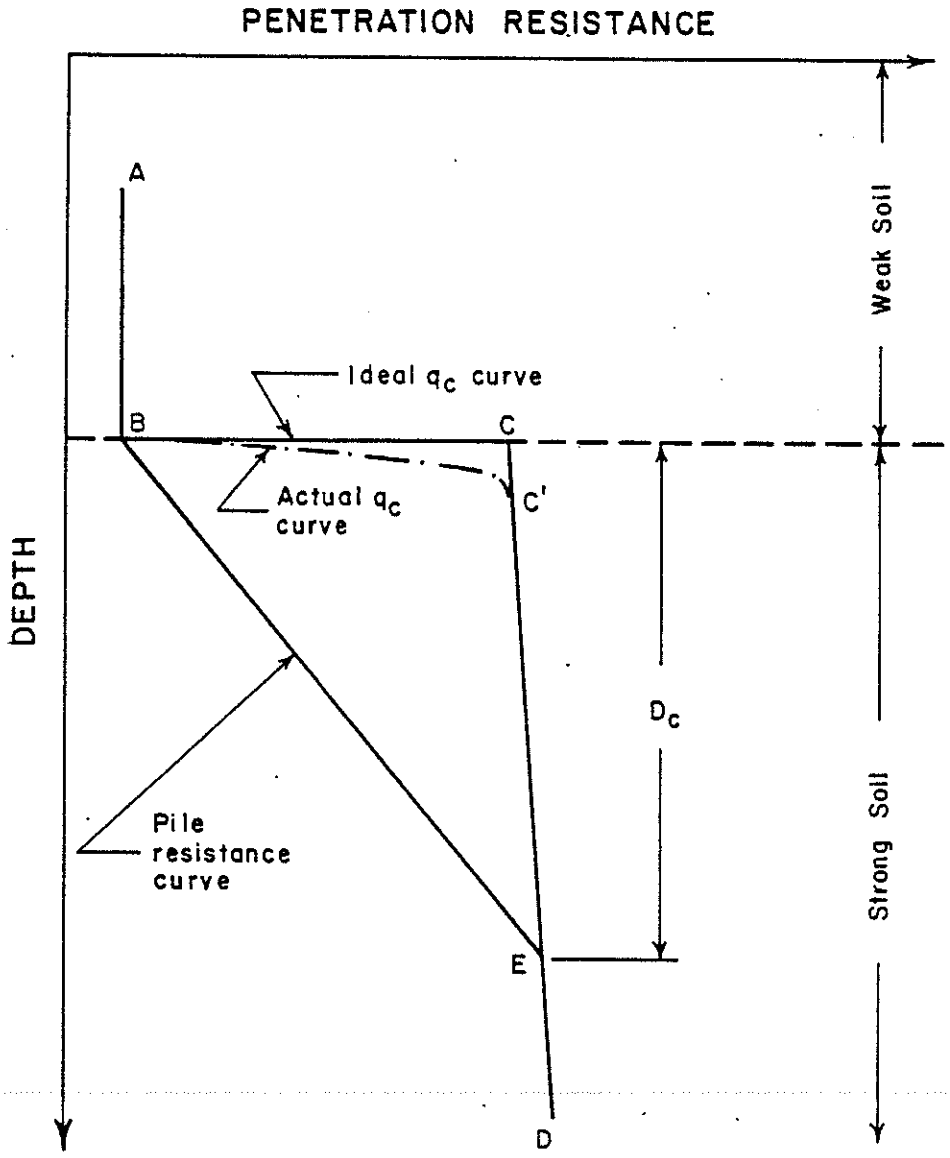

Figure 2.9 DeBeer Scale Effect Diagram
(DeBeer, 1963)

that critical depth ratio (D_c/d_p) was also influenced by friction angle, compressibility and ground water condition, which could range from 1 at $\phi = 0°$ to 25 at $\phi = 45°$.

The scale factor has no significance when the actual embedment is greater than D_c as long as the soil resistance remains constant.

2.2.4 Recent Pile Point Prediction Method Using CPT Data

Recently the procedures mentioned earlier have been further revised to account for the presence of thin layers or zones of weak soil which could affect the shape and position of the rupture surface at the pile base. Heijnen (1974) presented the Dutch method for determining the pile point resistance which follows (see Figure 2.10):

Step 1 - determine average q_c for a distance of 3.75 d below the pile tip from line 1, 2, 3, 4 = q_c (1, 2, 3, 4)

Step 2 - determine the q_c [average from line 4, 3, 5 = q_c (4, 3, 5)]

Step 3 - determine the q_c (average) below pile point

q_c (below) = [q_c (1, 2, 3, 4) + q_c (4, 3, 5)]/2

Step 4 - determine average, q_c, above pile point

q_c (above) = q_c (5, 6, 7, 8)

Step 5 - determine the unit pile point resistance q_u as follows:

$$q_o = \frac{q_c \text{ (above)} + q_c \text{ (below)}}{2} \qquad (2.3)$$

The minimum q_c (below) has to be found for the bearing capacity calculation of the pile. This is achieved by gradually varying the size of the area between 0.7 d to 3.75 d.

Little work has been done with respect to the use of QCPT data for predicting pile point resistance in cohesive soils. This is mainly due

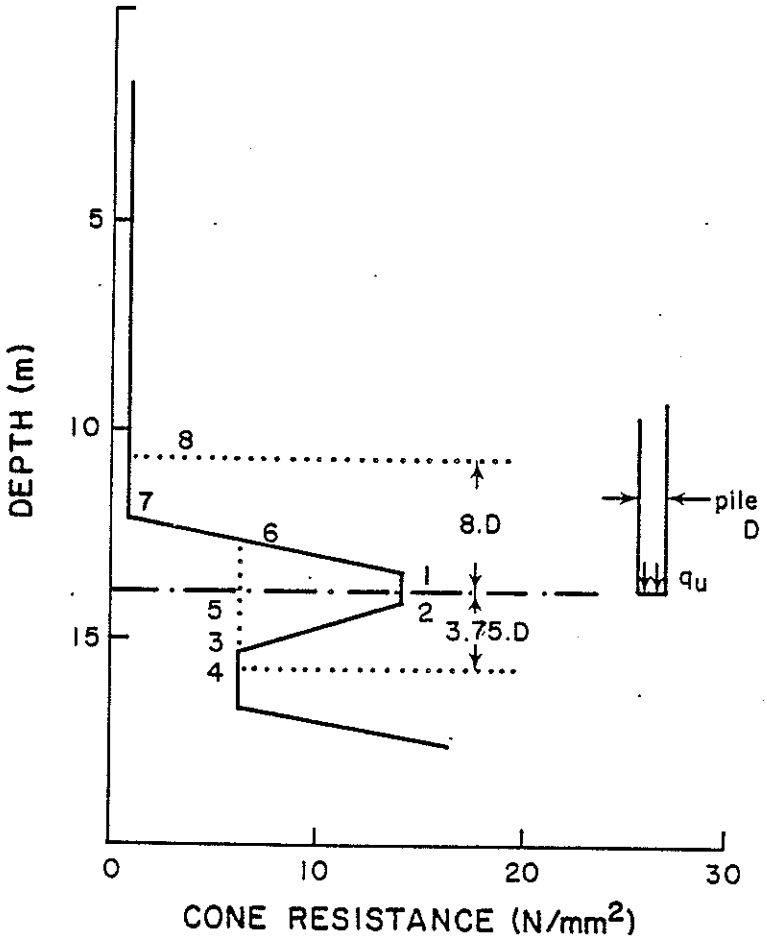

Figure 2.10 Computation of the End Bearing Capacity from CPT Data (Heijnen, 1974)

to the geological conditions of the countries where QCPT was originated. Many engineers suggest applying the same methods which are used for sandy soils to predict pile point resistance in cohesive soils. In this report a procedure similar to the Dutch cone method was implemented to predict pile point resistances and results were satisfactory.

2.3 QCPT Methods for Predicting Side Friction

2.3.1 General

Most of the early attempts were directed toward using cone resistance (q_c) to estimate pile point resistance. Prior to development of the adhesion jacket cone, it was common to relate q_c results to unit pile friction. This was done either by assuming the unit friction as some percentage of q_c or by estimating the shear strength properties of the soil penetrated from the cone resistance (q_c) data. The invention of the adhesion jacket cone opened the door to the more direct measurement of the unit pile friction resistance. Performing the QCPT with the aid of the friction sleeve to measure the local friction (f_s), provides engineers the means to develop the in-situ friction resistance profile of a given site.

2.3.2 Early Methods for Predicting Side Friction

Prior to development of the adhesion jacket cone, it was customary to measure the total friction along the sounding tubes. Begemann (1953) cited that the total friction was used as an indicative of the friction to be expected in the various layers. The total resistance (friction plus cone) was also used to predict the maximum depth of penetration that could be reached for a given pile. However, it was later found that the friction measured along the deep sounding tubes was unreliable

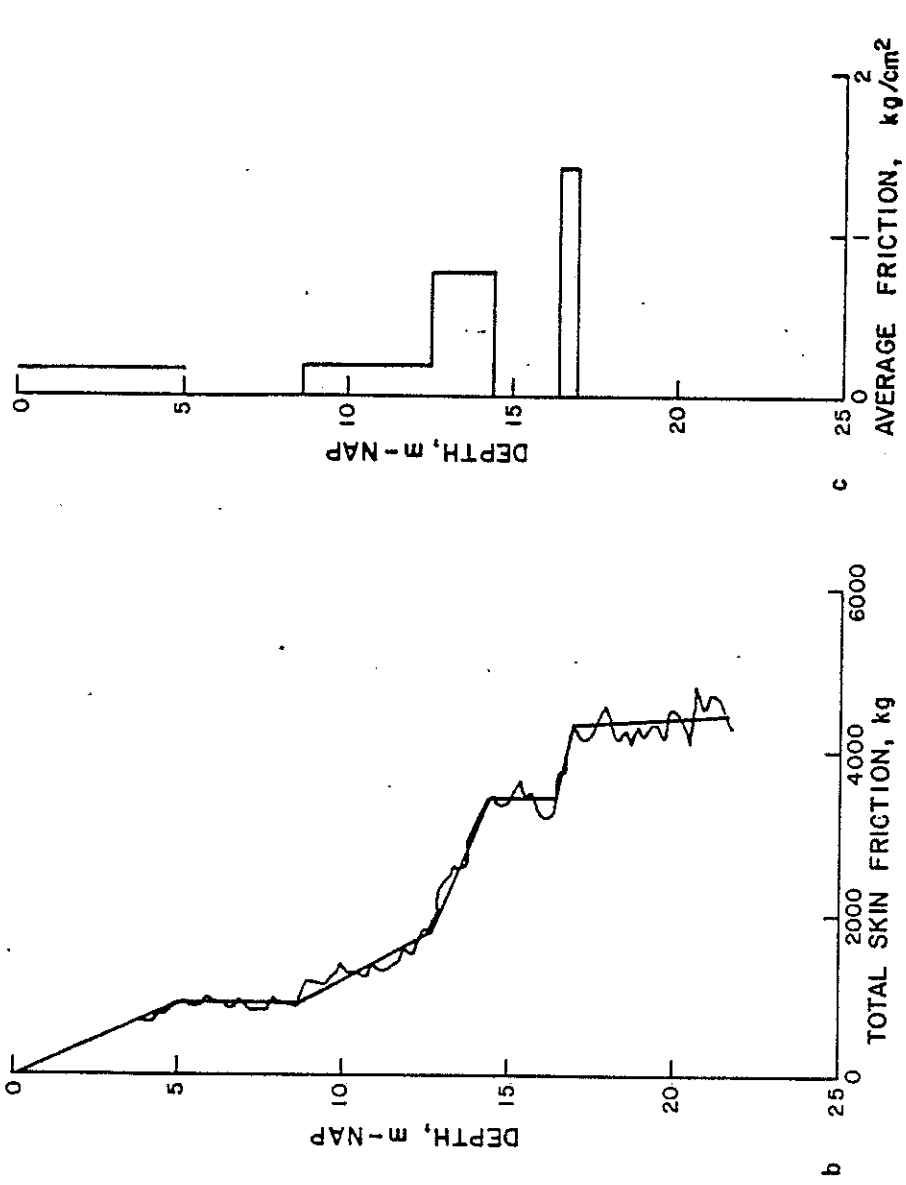

Figure 2.11 Average Local Friction Obtained from Total Friction Along the Rods (Begemann, 1969)

and the idea was abandoned. Begemann (1953 and 1969) presented some typical curves showing variation of total rod friction with penetration and explained the reasons why reasonable pile side estimations from the total friction data could not be expected. He showed several cases where the total rod friction decreased with additional penetration, indicating a soil layer had been encountered which was applying negative friction to the rods, a situation which could not possibly exist. Some cases were also presented where the total friction curve ran practically vertical, indicating that there was no friction in those layers (Figure 2.11). Begemann realized that the lateral movement of the cone rods would tend to enlarge the hole surrounding them and reduce the friction. He also noted the loss of strength due to remolding as more and more rods passed a certain soil layer, which was believed to be the cause of the apparent negative friction.

Bogdanovic (1961) and Huizinga (1951), calculated the pile side friction capacity from the total friction data obtained by the cone penetrometer. This was done by assuming that the unit pile friction was equal to the unit cone friction acting on the cone rods. The pile friction was estimated by multiplying the total rod friction by the ratio of the diameters of the rods and pile. It was realized that the above assumptions would result in conservative results because the unit pile side friction would be much greater than that of the smooth cone rods. Huizinga also noted that predictions assuming equal friction on the pile and rods would be 50% of the actual measured friction of pile.

Begemann (1953) developed the adhesion jacket cone which provided the measurements of the local friction (f_s). By that time he was certain that the total friction data were reasonable as long as the

friction measured in the upper layers kept the same value when more rods passed through the soil. He cited that the ratio of the local friction (f_s) and the cone resistance (q_c) could be an indication of the type of soil penetrated.

Begemann (1965) devised a method to determine frictional resistance of piles in tension. The results of his work are presented in Figure 2.12. The diagram on the left is entered by knowing the local friction (f_s) and cone resistance (q_c). This locates the point A on the $q_c - f_s$ graph. Point B is then found by extending a straight line through the origin and Point A to intersect the right margin of the $q_c - f_s$ diagram. The graph on the right is then entered until the appropriate pile type curve (point C) is intersected. The reduction factor is determined by projecting a vertical line through point C to intersect the reduction coefficient scale. The unit pile friction is estimated by multiplying the average local sleeve friction by the reduction coefficient. A reduction factor of 100% would result in no reduction at all, and a small reduction coefficient amounts to a large reduction.

It should be realized that these design curves were originated on the basis of the uplift tests. The procedure provides an estimate of uplift pile friction rather than friction capacity under compression loading. However, Begemann reported that some test results showed the discrepancies between friction in compression and tension (uplift) are small enough to be ignored.

The unit pile friction (f) may be estimated by either q_c or f_s results. The latter would provide a more direct and meaningful determination of the unit pile friction. The unit friction (f) could be

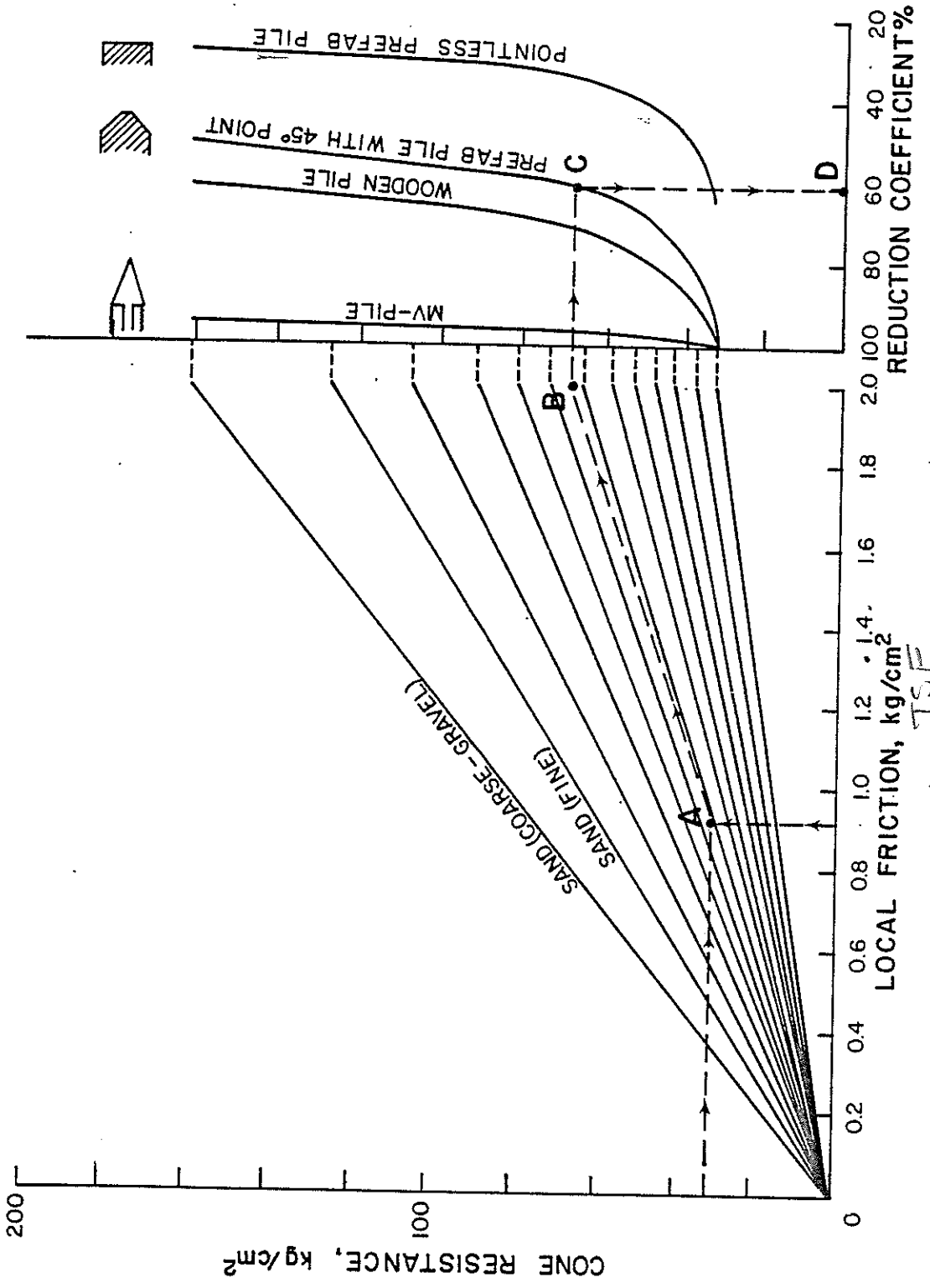

Figure 2.12 Begemann's Graph for Estimating Pile Side Friction (Begemann, 1965 and 1969)

determined by either of the following methods: (a) assuming a proper relationship between f and either of the QCPT data (q_c or f_s), or (b) estimating the shear strength properties of the penetrated soil by either q_c or f_s and then predicting f by using conventional static analysis techniques.

The procedures available differ for cohesive or cohesionless soils which will be treated separately in this section.

2.3.3 Cohesionless Soils

Unit friction along the shaft of a pile driven in sand could be predicted by using either cone resistance (q_c) or local friction (f_s) data.

Meyerhof (1956) proposed the following relationship between q_c and unit frictional resistance of pile:

$$f = \frac{q_c}{200} \tag{2.4}$$

Further study of this matter by Mohan and Kumar (1963) revealed that in soils of average stiffness (q_c between 10 - 100 kg/cm^2) the value of unit skin friction of a pile is roughly 2% of the average cone resistance; therefore

$$f = \frac{q_c}{50} \tag{2.5}$$

The addition of the adhesion jacket to QCPT permits more direct and accurate determination of the unit pile friction (f). Nottingham (1975) developed a procedure using f_s data obtained by QCPT (both electrical and mechanical) to predict pile side friction capacity. The method takes the local friction data (f_s), and corrects them for the type of penetrometer used, the type of soil penetrated, the pile material and taper, and the relative depth of the penetration. His procedure is as follows:

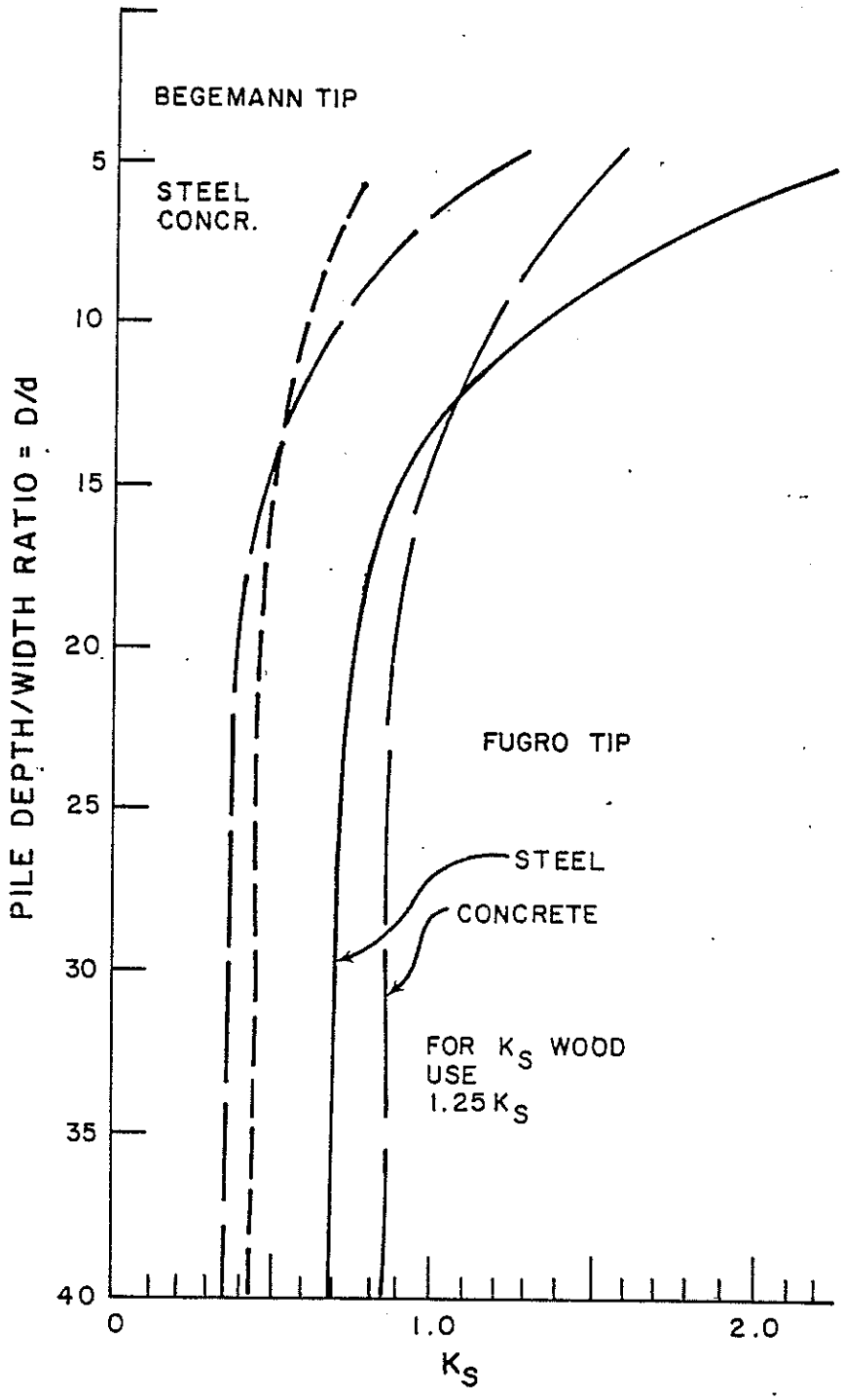

Figure 2.13 Penetrometer Design Curves for Pile Side Friction in Sand (Nottingham, 1975)

$$Q_s = K_s\left[\sum_{L=0}^{8\,d}\left(\frac{L}{8\,d}\right) f_s\, A_s + \sum_{8\,d}^{D} f_s\, A_s\right] \qquad (2.6)$$

where

Q_s = total ultimate side friction resistance

K_s = f_s correction factor in sand (Figure 2.13)

L = depth to which the f_s values considered

d = pile diameter or width

f_s = unit local friction sleeve resistance

A_s = pile-soil contact area per f_s depth interval

D = total embedded length of pile

The first summation term represents a depth-of-embedment correction applied only over 8 d penetration from the ground surface. Nottingham applied the Dutch end bearing and his side friction prediction method to 17 full-scale piles. His prediction error for total ultimate capacity ranged from about -40% to +20% with an algebraic average error of -11.0%.

2.3.4 Cohesive Soils

Unit pile friction estimation in clays could be made using conventional static analysis techniques based on undrained strength as suggested by Tomlinson (1957) in conjunction with cone resistance (q_c) data. The procedure requires determination of the undrained shear strength values using q_c data and a proper q_c/s_u ratio. The ratio could vary from about 5 to 70, but probably the range is between 5 and 25 as suggested by Bjerrum (1973).

Nottingham (1975) presented the following equations applicable to electrical and mechanical penetrometers, to estimate pile side friction using q_c data:

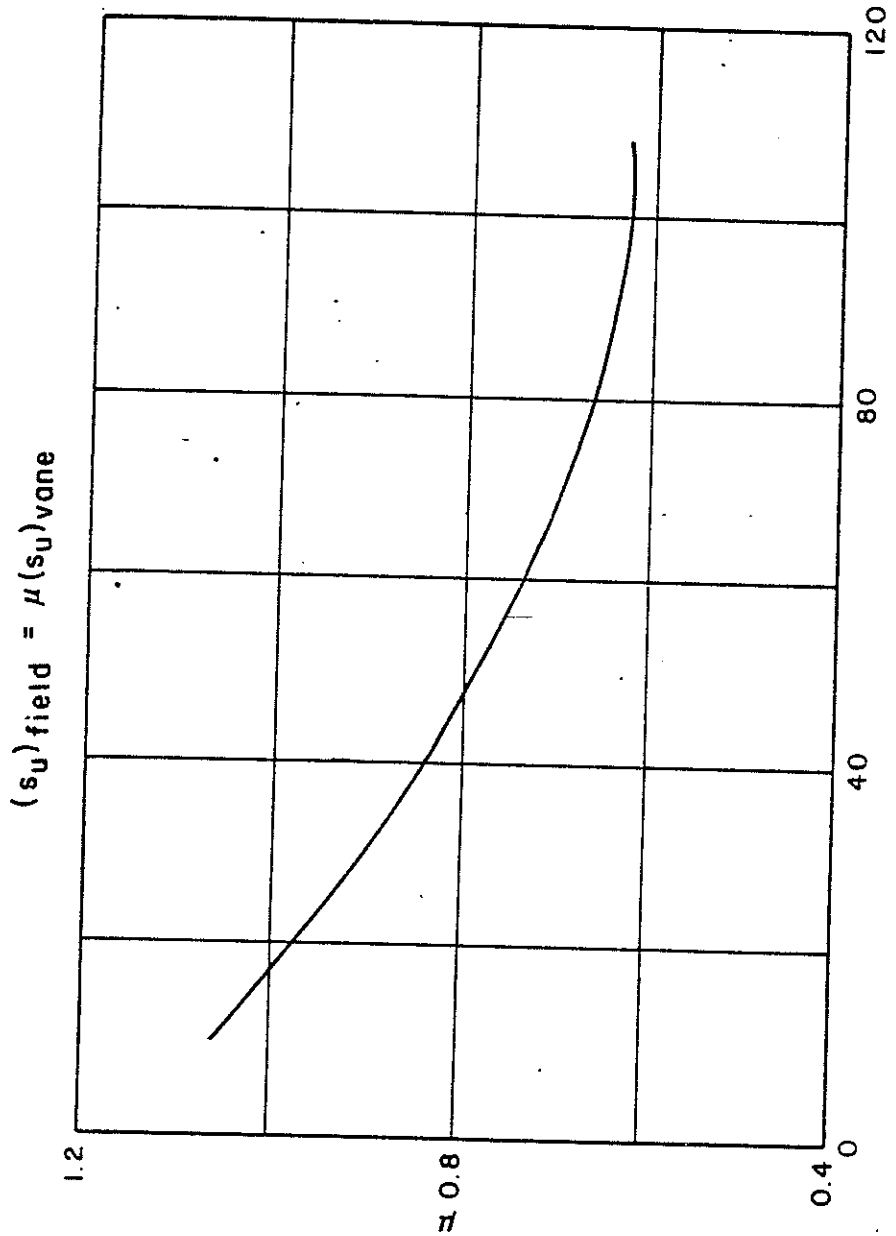

Figure 2.14 Bjerrum's Field Vane Shear Strength Correction Curve (Bjerrum, 1972)

$$Q_s = 0.10\ \mu\ q_c\ A_s \qquad (2.7)$$

or

$$Q_s = 0.067\ \mu\ q_c\ A_s \qquad (2.8)$$

Where the μ term is Bjerrum's (1972) field vane shear strength correlation factor as shown in Figure 2.14.

More reasonable prediction of unit side pile friction could be made if the local friction (f_s) data were available. Begemann (1965) suggested that the value of friction resistance (f_s) could be set equal to the undrained shear strength (s_u). Experimental correlation of the relationship between f_s and s_u was also presented by Wesley (1967) and showed f_s to be slightly higher than s_u. Therefore, it is also possible to make unit pile friction prediction using f_s in conjunction with available static analysis methods.

Nottingham (1975) proposed the following formula to predict the total ultimate side friction of piles driven in cohesive soils:

$$Q_s = \alpha'\ \bar{f}_s\ A_s \qquad (2.9)$$

where

α' = ratio of unit pile to sleeve friction in clay (Figure 2.15)

$\bar{f}_s$ = average sleeve friction

A_s = total pile-soil contact area

His recommendation was primarily based on the model pile studies. The α' curve shown in Figure 2.15 is identical to Tomlinson's α curve, except that α' curve is plotted as function of $\bar{f}_s$ rather than undrained cohesion C_u.

The unit pile friction may be estimated either by directly relating the QCPT data (q_c or f_s) to unit side friction f or by estimating the shear strength of the soil from QCPT results. However, it is believed

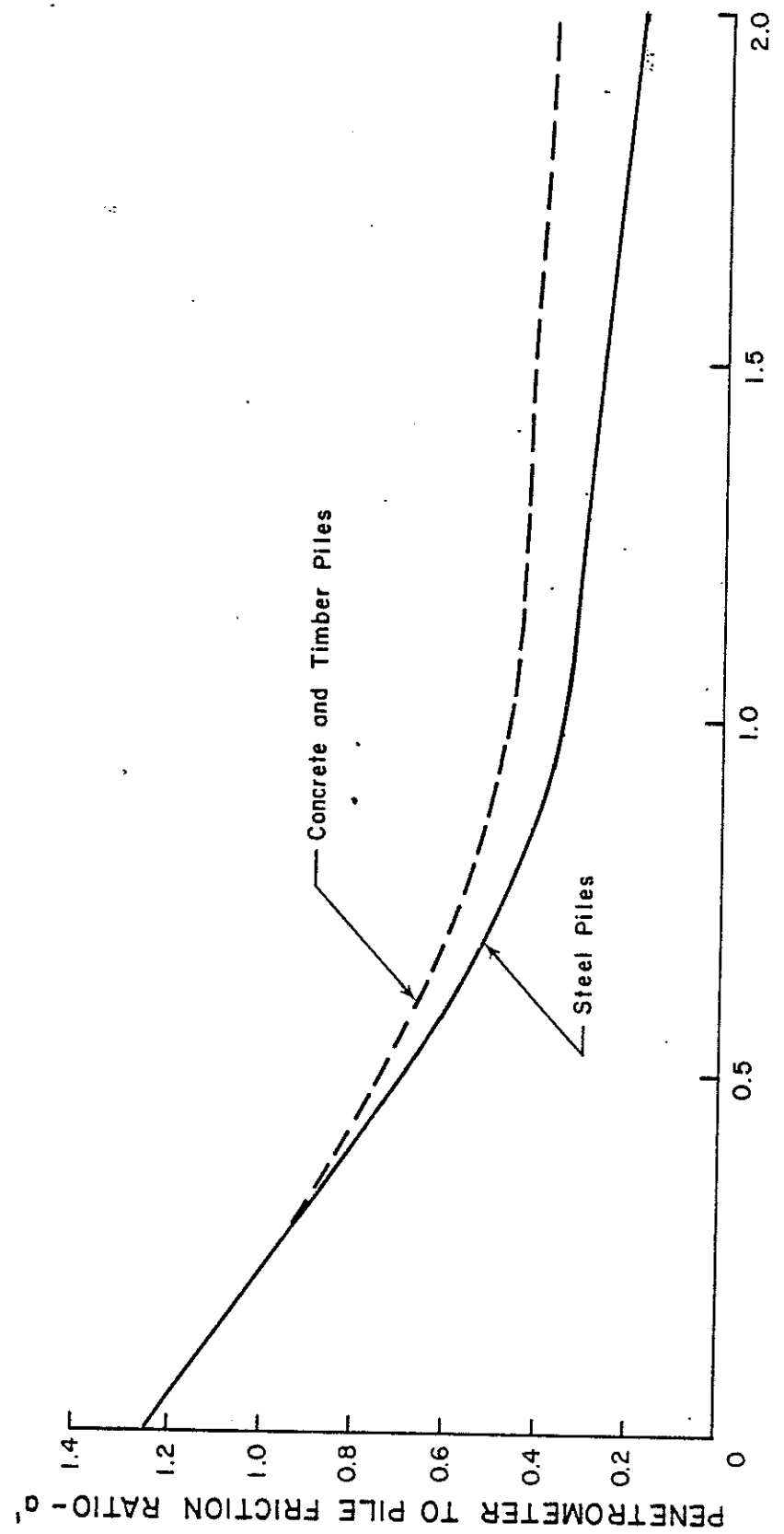

Figure 2.15 Penetrometer Design Curve for Pile Side Friction in Clay (Nottingham, 1975)

that more meaningful prediction of f is possible using f_s results directly. This attitude was followed in this study and attempts were made to arrive at definite relationships between f and f_s.

2.4 Summary

The cone penetration test which could be thought of as a model displacement pile provides means to develop continuous resistance profile in the field. The cone resistance (q_c) results could be utilized to estimate the tip bearing capacity of piles driven into cohesionless soils. This is of great importance because of problems involved in determining in-place shear strength properties of sandy soils and the dispute over the failure pattern. The procedures available for using QCPT data to predict pile tip bearing capacity have proven to be successful even though the rupture surfaces assumed in developing them are not fully understood. Most of the methods suggested are developed for sandy soils and little work has been done for cohesive soils. However, procedures similar to those recommended for sandy soils may be used for clayey soils because of the following reasons:

1. The total point bearing capacity of a pile driven into cohesive soils contributes little to its total capacity. Thus, the exact prediction of tip bearing capacity does little to improve the accuracy of estimating the total capacity.
2. The cone resistance (q_c) values in cohesive soils are very low and uniform as compared with q_c values obtained in sandy soils. Therefore, regardless of the averaging procedure chosen or the rupture surface assumed, the same unit tip bearing would be achieved.

3. The intent was to avoid complication of the matter.

A procedure similar to the Dutch cone method was used in this study and will be explained later in this report.

The development of the adhesion jacket cone by Begemann enhanced the ability of engineers to estimate the frictional resistance of piles. Prior to that time, the total friction along the sounding tubes was used to predict the frictional capacity. This approach was later abandoned because of the lack of accuracy. The local friction (f_s) values obtained from the adhesion jacket cone can be used to directly estimate the unit pile friction. This attitude was adopted by the author. From there relationships between f_s and the unit side friction of piles driven in cohesive soils were developed.

Chapter 3

STATIC ANALYSIS TECHNIQUES FOR COMPUTING TOTAL PILE CAPACITY IN COHESIVE SOILS

3.1 General

There are three methods commonly used to estimate total pile capacity: (1) load tests, (2) dynamic formulas, and (3) static analysis techniques based on evaluation of the soil into which the pile will be driven. The last procedure is the subject of this chapter.

The total downward capacity (Q_t) of a pile depends on soil conditions provided the pile has adequate structural strength to carry the imposed loading. The ultimate capacity of a pile is due to soil resistance developed by friction or adhesion between the soil and pile shaft (Q_s) and the end bearing at the tip of the pile (Q_p). Therefore, the total load carry capacity (Q_t) may be expressed as follows (Figure 3.1):

$$Q_t = Q_p + Q_s \tag{3.1}$$

$$Q_t = q\,A_p + f\,A_s \tag{3.2}$$

where

q = unit tip bearing capacity

A_p = pile tip bearing area

f = average unit skin friction

A_s = Total surface area of pile in contact with soil

Procedures available to calculate Q_p and Q_s depend on type of soil, and the methods differ for cohesive and cohesionless soils. The majority of test piles involved in this study are friction piles driven into cohesive soils. Therefore, only the techniques available to compute Q_p and Q_s in clayey soils will be explained in this chapter.

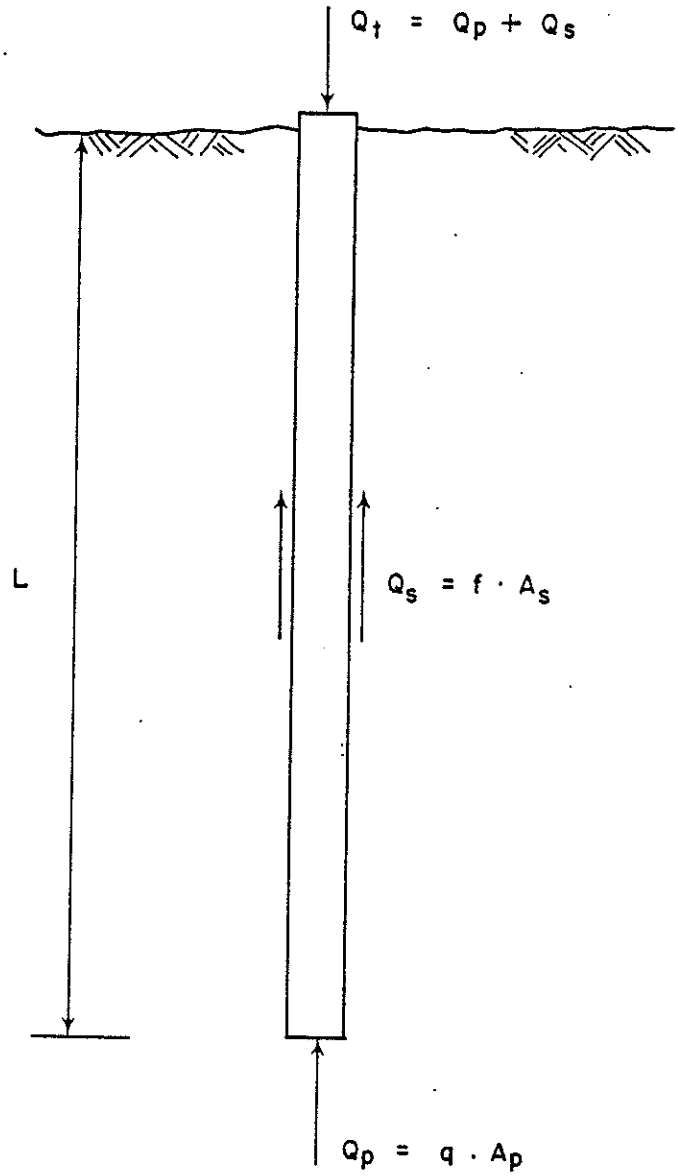

Figure 3.1 Forces Acting on a Pile

3.2 Tip Bearing Capacity in Cohesive Soils

The location of failure surface is less understood for deep foundations than for shallow foundations. However, the principles of bearing capacity recommended for shallow foundations also hold for deep foundations. Dependings on the type of failure pattern assumed, engineers have calculated values of the bearing capacity factors. Terzaghi (1943) suggested the following equation for computing pile end bearing capacity by static analysis method:

$$Q_p = A_p\, q = A_p\, (C\, N_c + 0.5\, \gamma\, B\, N_\gamma + \gamma\, D\, N_q) \qquad (3.3)$$

where

Q_p = ultimate tip bearing capacity

A_p = pile tip area

q = ultimate unit tip bearing capacity

C = soil cohesion

γ = unit weight of soil

B = pile width or diameter

D = pile tip depth

N_c, N_γ, N_q = bearing capacity factors

For piles driven in cohesive soils this equation may be reduced to the following:

$$Q_p = A_p\, (CN_c + \gamma\, D) \qquad (3.4)$$

For $\phi = 0$ degree case, assuming that the weight of the pile is equivalent to the soil displaced, the equation is stated:

$$Q_p = A_p\, C\, N_c \qquad (3.5)$$

Meyerhof (1976) stated that in saturated homogeneous clay under undrained conditon, theory and experience have indicated that the value of N_c below the critical depth varies with the sensitivity and

deformation characteristics of the clay. The value of N_c could range from 5 for very sensitive brittle normally consolidated clay to about 10 for insensitive stiff overconsolidated clay. The most frequent value used for the N_c of piles driven into cohesive soils is 9 which provides sufficient accuracy; therefore,

$$Q_p = 9\ A_p\ C \tag{3.6}$$

where C is the average of the undrained cohesion values up to about 5 pile diameter below the tip.

It is evident that there is not much argument about the exact value of N_c. However, the importance of the pile bearing contribution in relation to total load carrying capacity is very little in cohesive soils. Therefore, precisely estimating tip bearing capacity in cohesive soils provides little to improve the accuracy of the total capacity determined from a static analysis.

3.3 Skin Friction Capacity in Cohesive Soils

3.3.1 General

The total frictional capacity of a driven pile may be expressed as

$$Q_s = A_s \times f \tag{3.7}$$

where A_s and f are referred to the total pile surface in contact with soil and the unit skin friction of pile, respectively. Total side friction capacity could be estimated by the following formula:

$$Q_s = P \times L\ (C_a + \bar{\sigma}_h\ \text{tang}\ \phi_d) \tag{3.8}$$

in which

P = circumference of the pile

L = depth of pile penetration

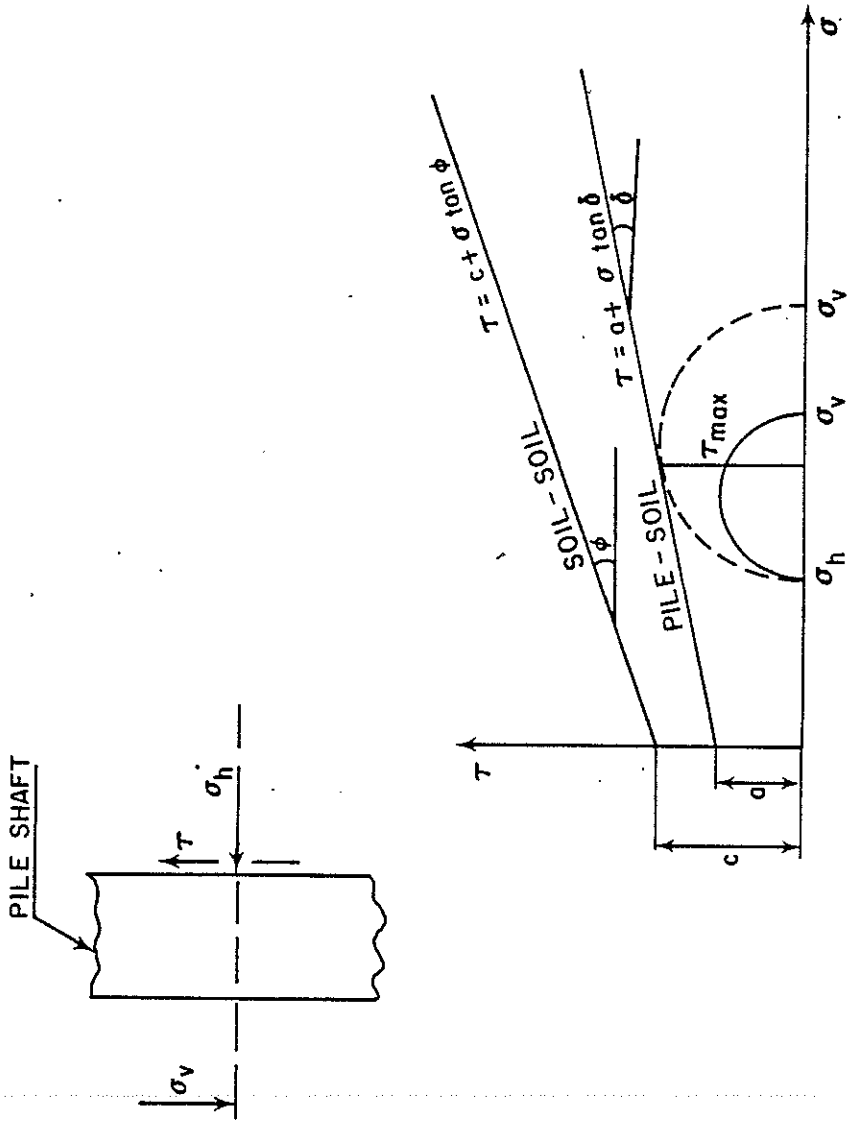

Figure 3.2 Stress Condition on Pile Shaft (Winterkorn & Fang, 1975)

C_a = developed adhesion between the soil and pile

$\bar{\sigma}_h$ = average horizontal pressure for the length of the pile

ϕ_d = developed angle of friction between the soil and pile

The skin friction capacity relationship was derived on the basis of Coulomb's Law by using distribution of normal stresses provided that the vertical displacement of the pile is large enough to mobilize the total shear resistance between soil and pile shaft (see Figure 3.2).

The average ultimate unit skin friction f, in homogeneous saturated clay ($\phi = 0°$) is expressed by

$$f = C_a \tag{3.9}$$

The skin friction, or adhesion, that develops between the soil and pile shaft has been related to the undisturbed undrained cohesive strength (C_u) of the clay. Several relationships between the adhesion (C_a) and the cohesion (C_u) have been proposed, the most famous one being recommended by Tomlinson (1957). The procedures used to predict ultimate frictional capacity of piles driven in clay which assume unit friction being equal to adhesion, are called "adhesion method". This distinction is felt necessary because not all of the methods proposed to calculate unit friction involve the above simplistic assumption. It is believed by many engineers that the frictional capacity of a pile is influenced by drained rather than undrained friction. There are empirical semi-effective procedures available to estimate the unit friction f, such as: (1) lambda (λ) method suggested by Vijayvergia and Focht (1972), and (2) beta method (β) proposed by Burland (1973).

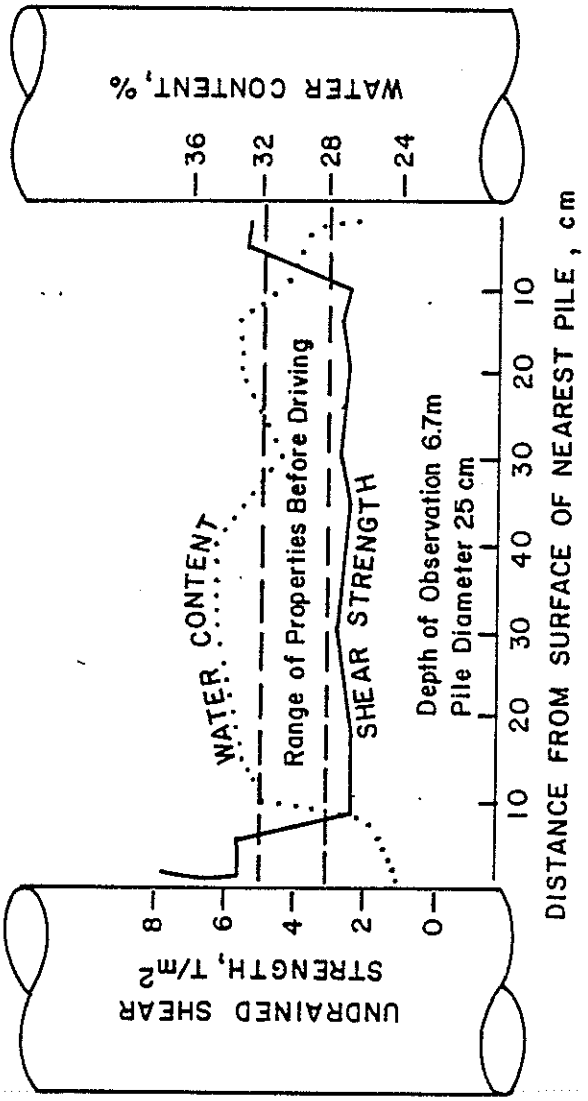

Figure 3.3 Shear Strength and Water Content Variation Between Two Driven Piles (Flatte, 1972)

3.3.2 The Adhesion Approach

The penetration of piles into saturated clays will cause the soils near the pile shaft to be displaced and remolded to a distance of up to one pile diameter. The pore water pressure induced by pile driving sets up a consolidation process in the zone of the highly disturbed soil. After the dissipation of the excess pore pressure, the clay adjacent to driven piles may have a greater shear strength and smaller water content at some distance away from the piles than it had before the pile driving (Figure 3.3). However, in very sensitive or stiff overconsolidated clays, the final shear strength or adhesion may be less than that of the undisturbed soil. The frictional capacity is a function of time and is also influenced by the nature of the soil, the dimensions of the pile and other factors. Because of the phenomenon of strength gain with time (thixotropy), load tests on piles in clays should be performed some weeks after installation to obtain a reliable indication of actual capacity.

The unit skin friction, or adhesion that develops between the soil and pile shaft has been related to undrained cohesion by

$$f = A\, C_u \qquad (3.10)$$

where

f = unit skin friction

C_u = undrained cohesion

A = adhesion factor relating adhesion to undrained cohesion

The adhesion factor, A, has been empirically related to undrained cohesion by various investigators.

Tomlinson (1957) showed that the observed adhesion decreases with increase in undisturbed cohesion. He related adhesion to undisturbed

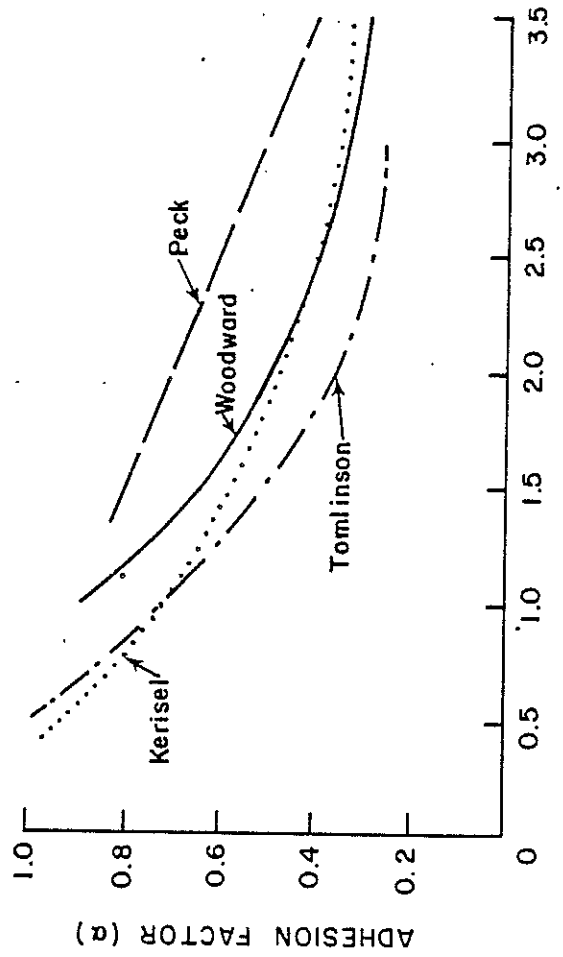

Figure 3.4 Correlation of Adhesion Factor with Undrained Shear Strength (McClelland, 1974)

cohesion by a factor called alpha (α) which could vary from as high as 1.0 in very soft clays to 0.25 in very stiff clays. Tomlinson noted that a partial gap formed by transverse vibrations during pile driving caused the loss in adhesion. He further explained that in soft clays the soil would reconsolidate and close-up the gap, thus achieving 100 percent adhesion. However, in stiff overconsolidated clays only partial reconsolidation would take place resulting in low adhesions.

Woodward, et al. (1961), Peck (1958) and Kerisel (1964) have also recommended relationships between the adhesion factor and the undrained cohesion. The adhesion factor curves determined by the above mentioned investigators are presented in Figure 3.4. All of the relationships presented agree that the adhesion factor is equal or slightly higher than 1.0 for soft clays and may be as little as 0.25 for stiff clays. Although all of the curves exhibit the same trend (i.e., the factor decreases with increase in cohesion), they differ greatly concerning the stiffer clays.

3.3.3 The Lambda Method

Estimating the value of unit skin friction by the adhesion methods has proved to be less reliable for very long piles. The reason may be attributed to experimental errors in determining the adhesion factor. However, some investigators believe that a more probable reason is that unit pile friction is not a simple function of undrained cohesion. Recent findings indicate that the unit skin friction developed in clay may be related to an effective lateral pressure.

Vijayvergia and Focht (1972), suggested that the skin friction is influenced by the passive pressure caused by the displaced soil during pile driving which mobilizes passive pressure in soil surrounding the

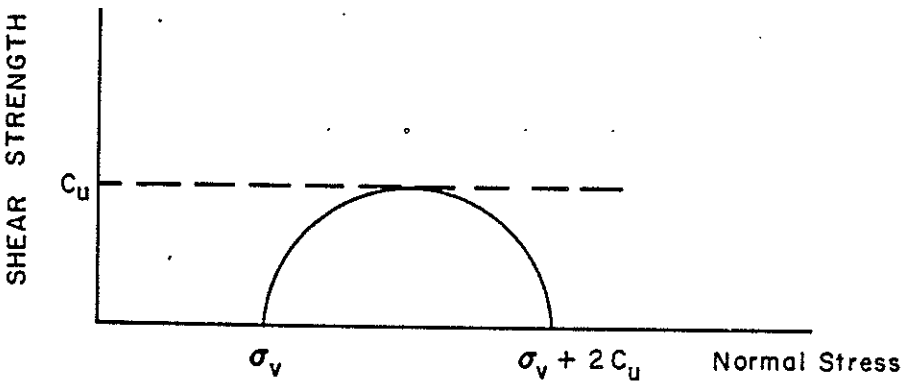

Figure 3.5 Mohr's Circle Presentation Indicating Relation Between Vertical Pressure and Maximum Horizontal Pressure

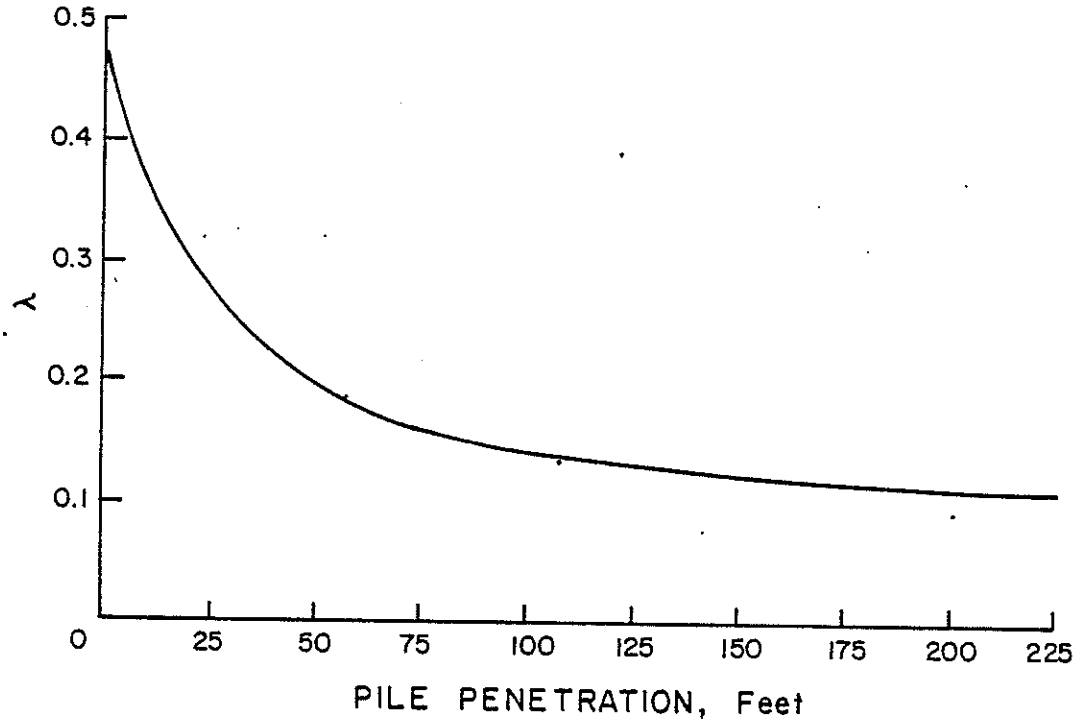

Figure 3.6 Relation Between Friction Capacity Coefficient Lambda and Pile Length (Vijayvergia and Focht, 1972)

pile. If the effective vertical pressure in a soil mass is $\bar{\sigma}_v$, the maximum horizontal passive pressure is $\bar{\sigma}_v + 2\ G_u$ from the Mohr circle analysis for undrained shear strength, (see Figure 3.5). Accordingly, they noted that a relationship might be found between unit pile friction, f, and Rankine passive pressure $\bar{\sigma}_v + 2\ C$. Therefore, it was suggested that the unit friction, f, may be expressed as

$$f = \lambda\ (\bar{\sigma}_v + 2\ C_u) \tag{3.11}$$

where

λ = a friction capacity coefficient

C_u = undrained cohesion of the clay

The total frictional capacity Q_s for a pile would be

$$Q_s = \lambda\ (\bar{\sigma}_{vm} + 2\ C_m)\ A_s \tag{3.12}$$

where

$\bar{\sigma}_{vm}$ = mean effective vertical pressure for the embedded length

C_m = mean undrained cohesion of clay for depth of pile

A_s = surface area of pile shaft in contact with soil

The values of λ have been empirically determined for various pile length which are presented in Figure 3.6. The λ curve was developed using undrained shear strength values obtained by unconfined compression or miniature laboratory vane shear tests.

3.3.4 The Beta Method

Several investigators have indicated that the long term capacity of piles driven in cohesive soils is influenced by drained friction at the pile-soil interface. Shortly after pile driving, the shaft resistance is governed by the undrained shear strength of the remolded clay. However, after the dissipation of pore pressure caused by pile driving, the skin resistance is controlled by the effective drained shear

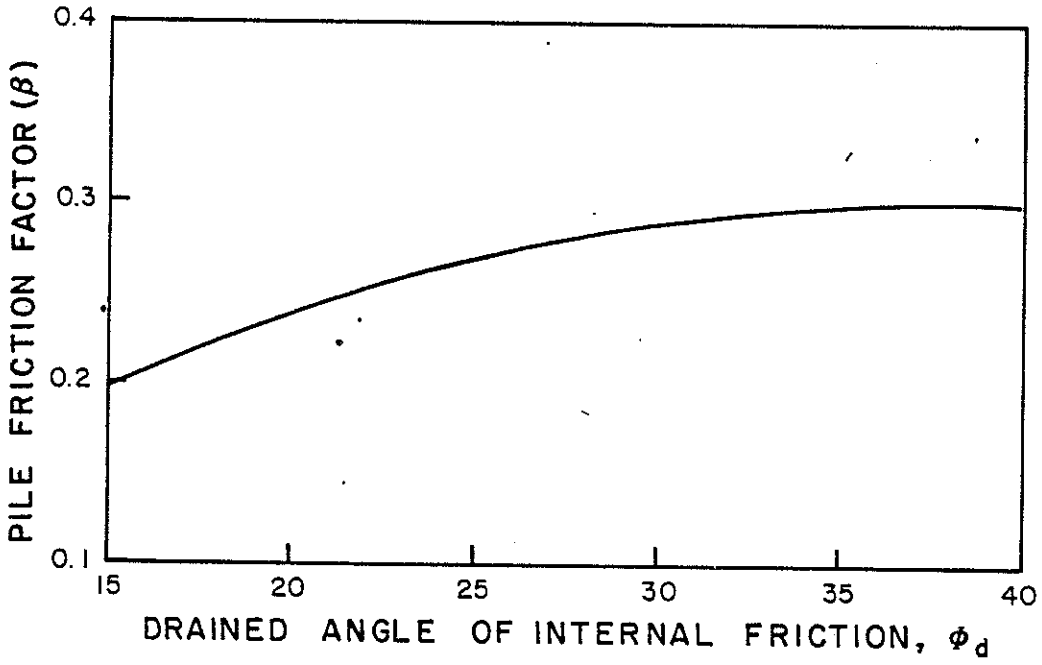

Figure 3.7 Relation Between Friction Factor Beta and Drained Friction Angle (Burland, 1973)

strength parameters C and ϕ, of the remolded clay surrounding the pile shaft. The cohesion of the remolded clay in drained condition may be taken as zero.

Burland (1973), suggested that the ultimate unit shaft resistance, f, developed in clay may be calculated as follows:

$$f = \beta \bar{\sigma}_v \tag{3.13}$$

where

β = the skin friction factor

The term β may be expressed as

$$\beta = K \text{ tang } \phi_d \tag{3.14}$$

where

ϕ_d = angle of internal friction in drained shear

K = lateral earth pressure coefficient

The lateral earth pressure coefficient K for normally consolidated clays is given by the following:

$$K = (1 - \sin \phi_d) \tag{3.15}$$

Therefore, the unit skin friction of piles in clays can finally be expressed as follows:

$$f = (1 - \sin \phi_d) \text{ tang } \phi_d \bar{\sigma}_v \tag{3.16}$$

For clays, the angle of internal friction in drained shear normally ranges between 15 and 30 degrees. The skin friction β for normally consolidated clays should only vary a small range of about 0.24 to 0.29, as shown in Figure 3.7. The lateral earth pressure can not be easily determined for overconsolidated soils. Therefore, the application of this approach should be limited to normally consolidated soils where β factor does not vary over a wide range.

3.4 Summary

According to static analysis, the ultimate capacity of a pile is due to the shaft frictional resistance (Q_s), and the end bearing capacity (Q_p) at the tip of the pile.

There is not much disagreement about the precise relationship between the soil properties and the unit bearing capacities of piles driven into cohesive soils. However, the importance of the tip bearing contribution in relation to total load carrying capacity is very little, thus, eliminating the need to predict it accurately.

The most common procedure to predict the unit skin friction in clays is the adhesion method (i.e., alpha method). This approach requires a relationship between the adhesion or unit skin friction and the undrained cohesion of the soil. This method has been shown unreliable for long piles which has led many investigators to believe that the unit friction is not a simple function of undrained shear strength.

In recent years many engineers have suggested that the frictional capacity is controlled by drained friction at the pile soil interface. Two empirical semi-effective methods were discussed in this chapter: (1) the Lambda Method and (2) the Beta Method.

Although the Lambda Method provides satisfactory results, the nature of the empirically determined λ coefficient is not well known.

Limited research is available on the Beta Method and it is not commonly used because of the difficulties associated with evaluating the drained shear strength properties of the cohesive soils. The application of this approach should also be limited to normally consolidated clays for which the β factor varies over a small range.

The ultimate bearing capacity of the test piles involved in this study were calculated by the adhesion approach (using Tomlinson's adhesion curve), the Lambda Method and the Beta Method. The results were later compared with the predictions of the ultimate load capacities determined by the cone penetrometer methods.

Chapter 4

THE ULTIMATE LOAD CRITERION

4.1 General

Vesic (1974) stated that soil under a deep foundation always fails in the same manner, i.e. in punching shear under the foundation point, accompanied or preceded by direct shear failure of the soil along the foundation shaft.

The definition of the ultimate load is arbitrary, it may be taken as when a predetermined amount of settlement has occurred or when the slope of load-settlement plot is no longer proportional.

4.2 Definition of Failure Load

The ultimate failure load is usually determined by defining a point on the load-settlement curve obtained from the pile load test results. Chellis (1951) summarized sixteen different methods which had been used for selecting this point. More recently, Peck (1977) presented some of the rules for determination of ultimate load which can be found in Table 4.1.

The following definitions are generally accepted for the failure load of a piled foundation:

1. The load at which a predetermined amount of settlement has occurred: This definition may not be applicable for all different size of piles. Recent research on pile behavior has indicated that the full mobilization of skin resistance

Table 4.1

Rules for Determination of Ultimate Load
(Peck, 1977)

1. Limiting total settlement

   (a) Absolute — 1.0 in. (Holland, New York City Code)
   (b) Relative — 10% of pile tip diameter (England)

2. Limiting plastic settlement

   0.25 in. (AASHTO)
   0.33 in. (Magnel)
   0.50 in. (Boston Code)

3. Limiting ratio plastic settlement/elastic settlement

   1.5 (Christiani and Nielsen)

4. Maximum ratio $\frac{\text{elastic settlement increment}}{\text{plastic settlement increment}}$

   (Szechy, 1961)

5. Limiting ratio settlement/load

   (a) Total — 0.01 in./ton (California, Chicago)
   (b) Incremental — 0.03 in./ton (Ohio)
   0.05 in./ton (Raymond Co.)

6. Limiting ratio plastic settlement/load

   (a) Total — 0.01 in./ton (New York City Code)
   (b) Incremental — 0.03 in./ton (Raymond Co.)

7. Maximum ratio $\frac{\text{settlement increment}}{\text{load increment}}$

   (Vesic, 1963)

8. Maximum curvature of log w/log Q line

   (DeBeer, 1967)

9. Van der Veen postulate

   $$w = \beta \ln \left(1 - \frac{Q}{Q_{max}}\right)$$

   (Van der Veen, 1953)

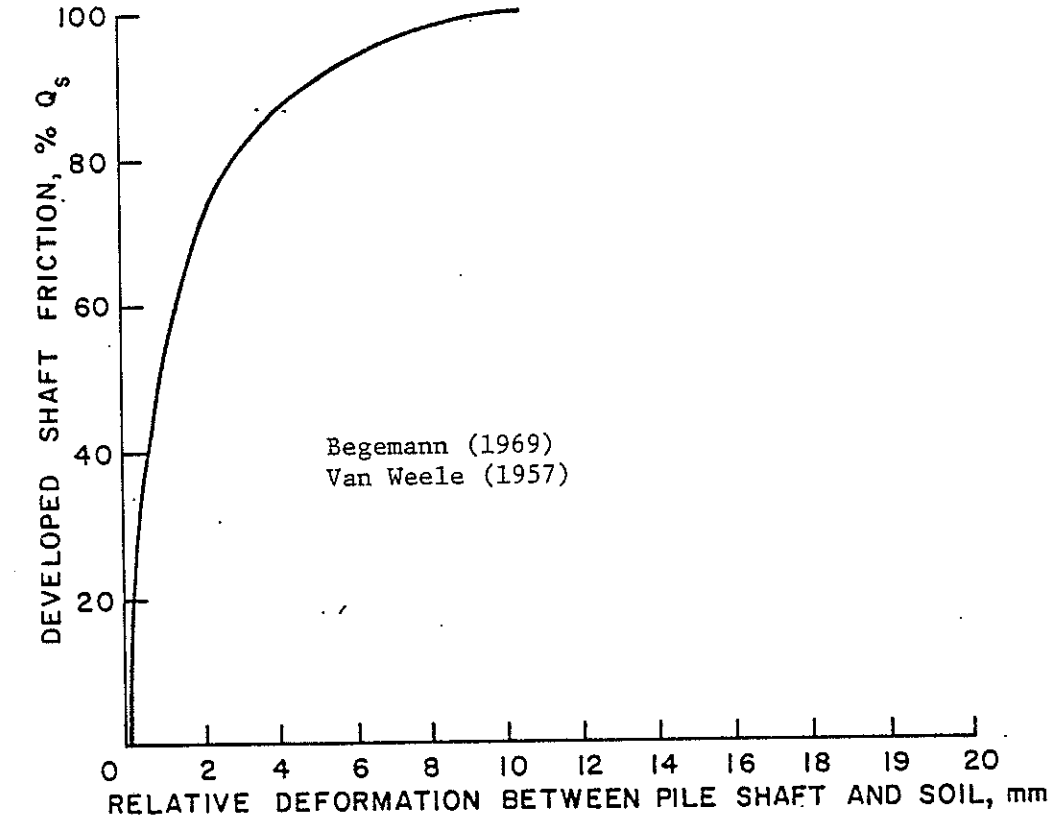

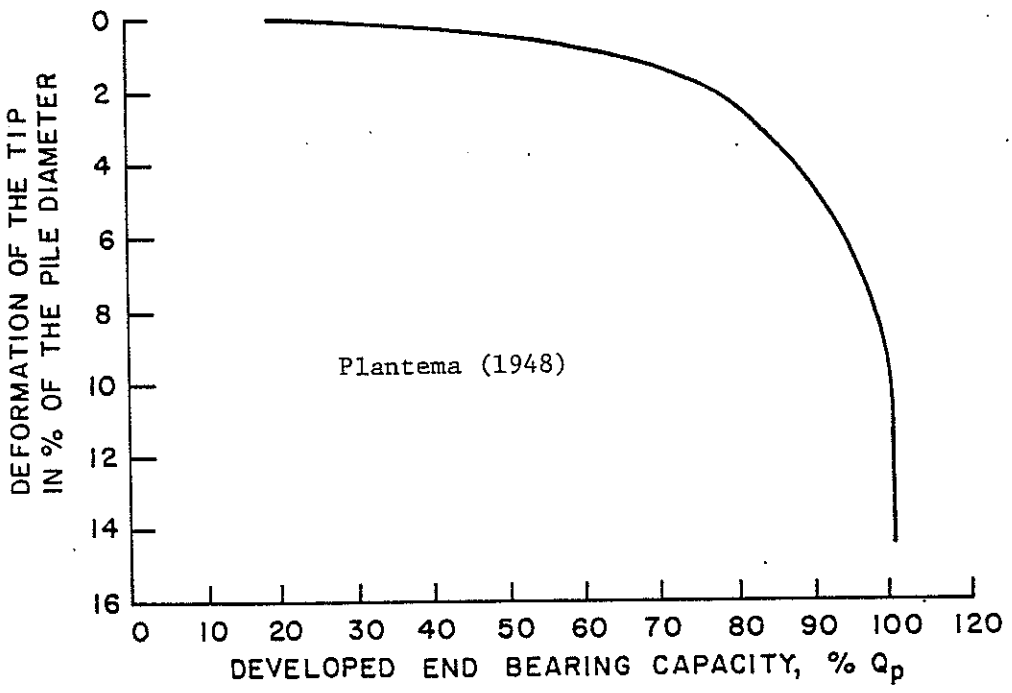

Figure 4.1 Developed Shaft Friction and End Bearing Capacity as a Function of Deformation

requires a relative displacement between the pile shaft and surrounding soil of 6 to 10 mm, regardless of pile size and length. On the other hand, full mobilization of ultimate load point resistance of a pile requires a displacement of approximately 10 percent of pile-tip diameter for driver piles (Figure 4.1). Therefore, it is evident that a predetermined amount of settlement might indeed mobilize the ultimate load of a small diameter pile, but only a fraction of the ultimate load of a much larger pile.

2. The load at which the slope of the load settlement plot is no longer proportional: The ultimate resistance of a pile is usually defined as a load, at which an infinitely small increase causes an infinitely large settlement, or as the point where the load-settlement curve moves downward vertically. This definition is very much influenced by the scales chosen for plotting the load-settlement curve. For example, if the scale on which the settlement data is plotted is changed, the curve will take a different shape. As illustrated in Figure 4.2, the drawing on the upper part suggests that the ultimate resistance has been reached at about 100 tons, whereas, the curve on the lower part suggests that the ultimate resistance is not yet reached.

Plantema (1948) presented the load-settlement curve in a slightly different manner. He plotted the settlement of pile toe versus the load applied to pile as a percentage of the ultimate resistance (Figure 4.3). Van der Veen (1953) noted that the curve resembled a well known function in biology which represented the growth of a living individual as a

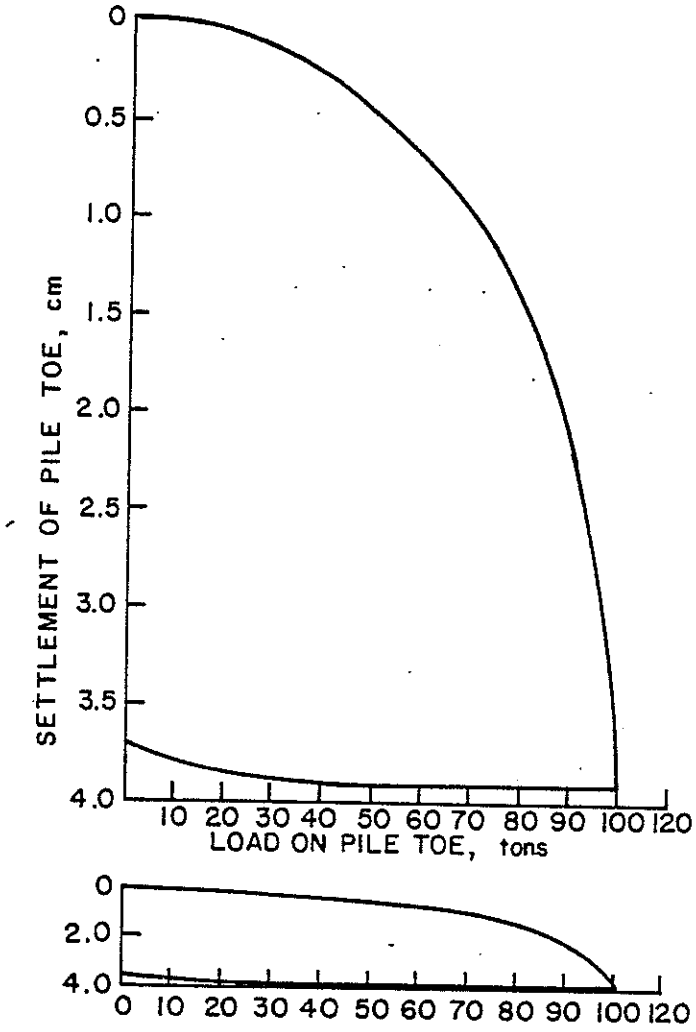

Figure 4.2 Load Settlement Curve of a Concrete Pile in the Harbour Area of Amsterdam (Van der Veen, 1953)

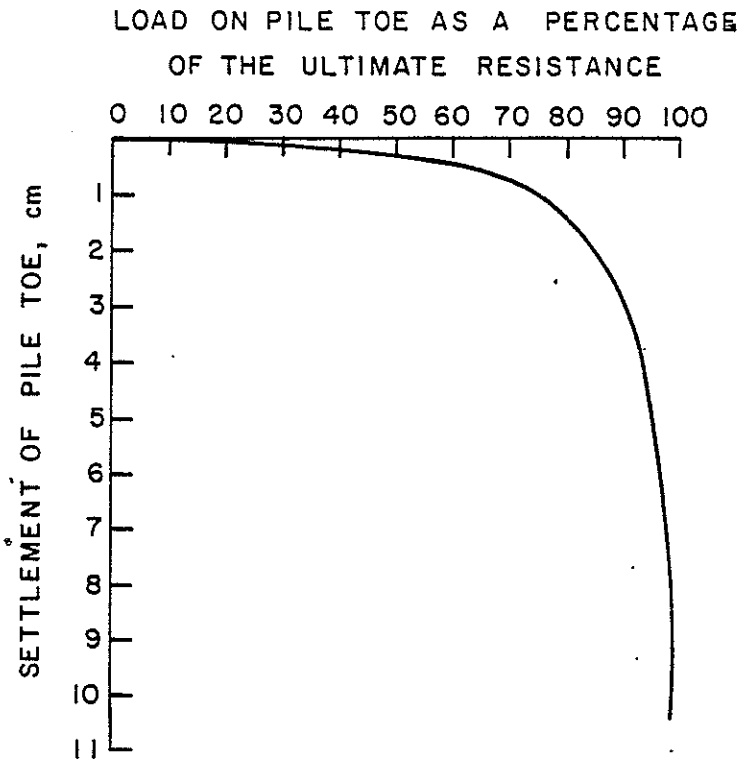

Figure 4.3 Load-Settlement Curve of the Plantema Sounding Pile (Plantema, 1948)

function of time. Therefore, he suggested that the load-settlement curve could be represented by the following expression:

$$Q = Q_u (1 - e^{-rz}) \qquad (4.1)$$

where

Q = applied load causing settlement z

Q_u = ultimate load

r = coefficient of proportionality

Magnitude of r influences the shape of the load-settlement curve. This procedure may be utilized if the loading to failure is not possible due to practical difficulties.

4.3 Application of Van der Veen's Expression in this Study

The ultimate loads of the test piles involved in this study were computed using Equation 4.1. This was done by selecting two points from the load settlement-curve of each test pile. As it is evident in Figure 4.4, this expression should hold for any two points; therefore,

$$Q_1 = Q_u (1 - e^{-rz1})$$

and

$$Q_2 = Q_u (1 - e^{-rz2})$$

This represents a system of two equations and two unknowns which could be solved for Q_u and r. At least five pairs of data points were selected from the load-settlement of each test pile under study. Theoretically, the solution to the equations of each pair must be the same and equal Q_u and r should be obtained regardless of the pair chosen. However, some of the pairs of data points resulted in incorrect prediction of the ultimate load (Q_u). It was noted that the pairs including one point from the middle and the other point from the end of

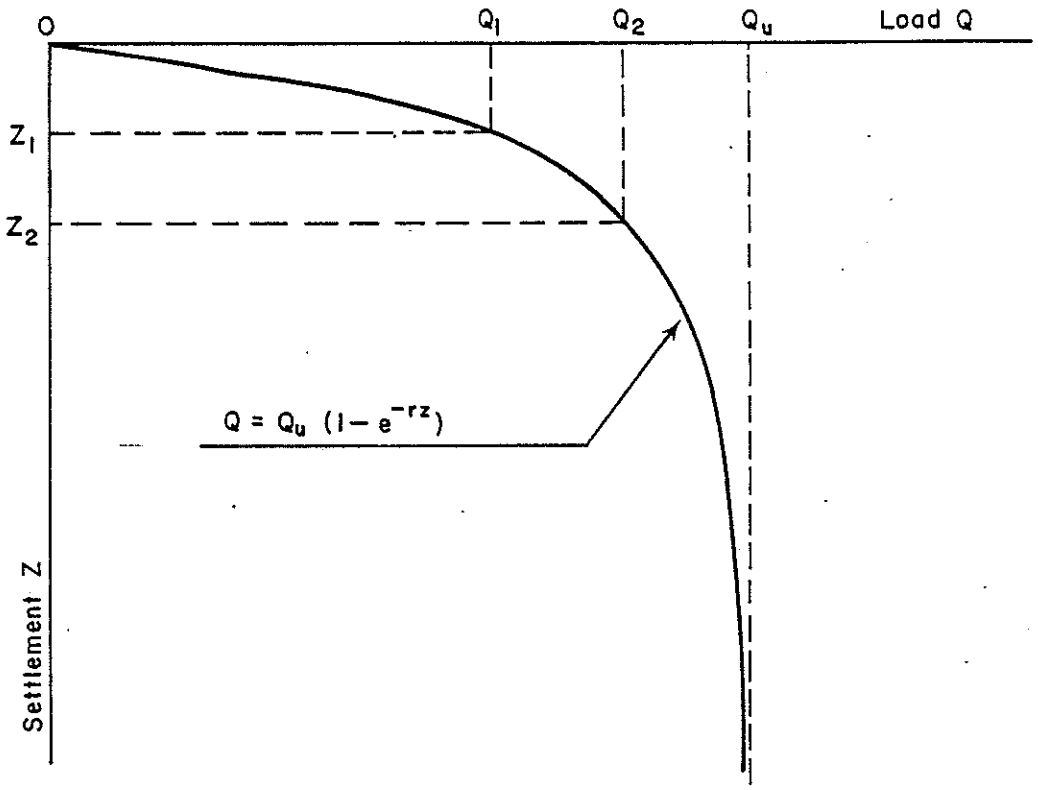

Figure 4.4 Application of Van der Veen's Expression in the Study

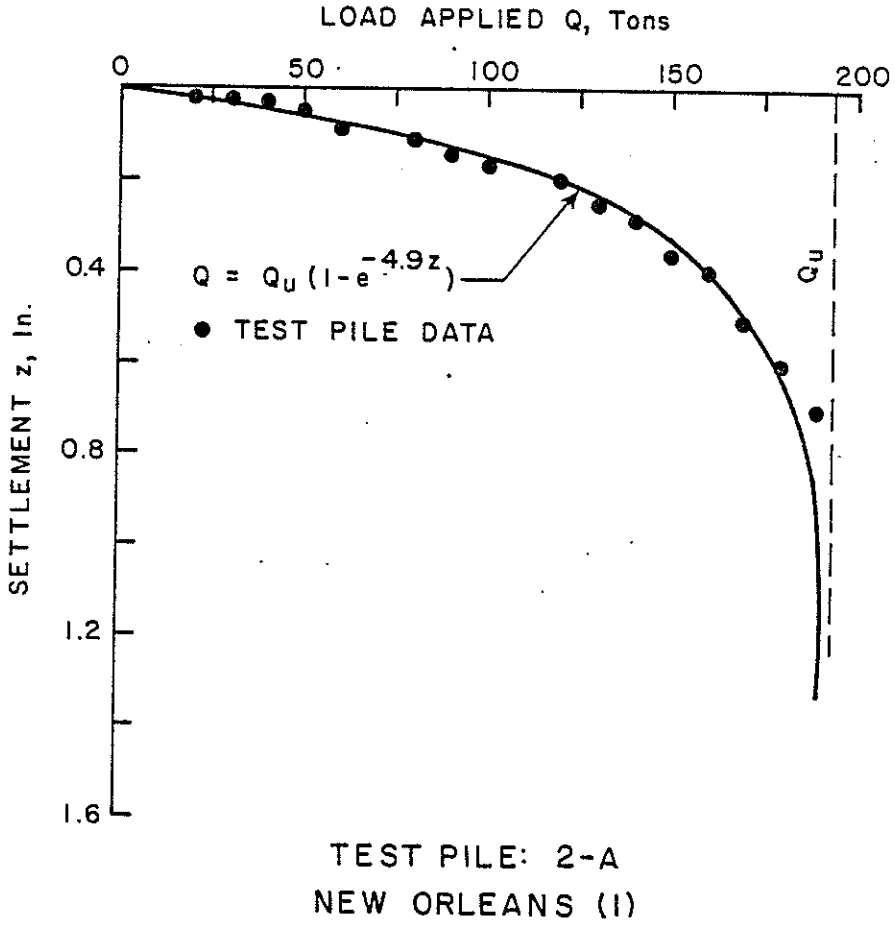

Figure 4.5 Actual Pile Load Test Data and the Load Settlement Curve Obtained by Applying Van der Veen's Expression

the test pile program (i.e., the last load applied) would give reasonable estimate of Q_u. In conclusion, a pair of data points resulting in a Q_u which reasonably fits the load-settlement plot should be selected. The ultimate capacities (Q_u) of all of the test piles in this study were computed by the above mentioned procedure and the results were treated as the measured ultimate capacities. The measured capacities were later compared with the estimation of ultimate capacities based on the static analysis techniques and cone penetrometer prediction methods. The test piles were loaded to either 2.5 times the design load or to loads causing a settlement of about 1/2 inch on the average. The ultimate capacities computed using the Equation 4.1 were about 12 percent higher than the last load applied to each test pile. It is believed that if the test piles were loaded to Q_u, a plunging type of failure would have occurred. The load-settlement data and the theoretical load-settlement curve for all of the test piles were plotted (see Appendix A). An example of such a plot is given in Figure 4.5. It was noted that 99 percent of the ultimate load (0.99 Q_u) occurred at an average settlement of about 0.90 inch for all of the test piles.

The proportionality constant (r) ranged from 3.1 to 10.5 with an average of 5.3 and a standard deviation of 1.8. The results are summarized in Figure 4.6. It is possible to assume a value for r and compute the ultimate capacity (Q_u) knowing only one data point on the load-settlement diagram. This is of great value for cases where it is not possible to load the pile to a definite failure. As it was mentioned earlier, the test piles were either loaded to some multiple of the design load (i.e., 2.5) or where a settlement of about 1/2 inch was reached. Except for a few, none of the test piles experienced a true

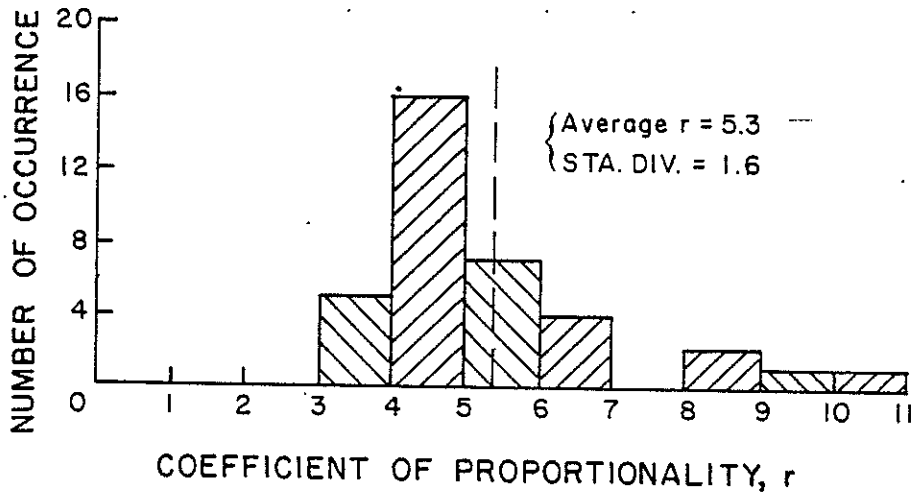

Figure 4.6 Range of the Proportionality Constant (r)

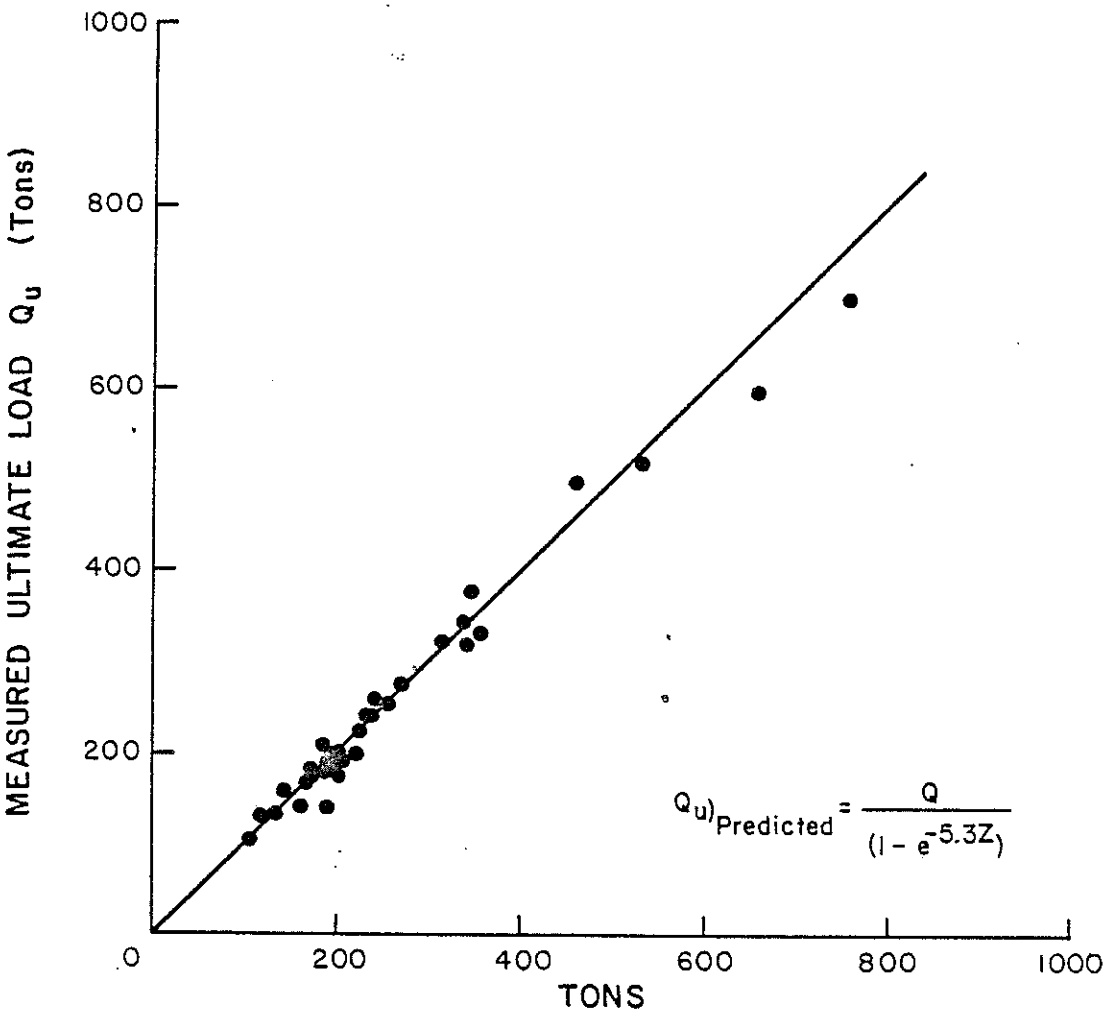

Figure 4.7 Pile Capacity Prediction by Equation 4.1 and a Point (Last Load Applied) on the Load-Settlement Diagram

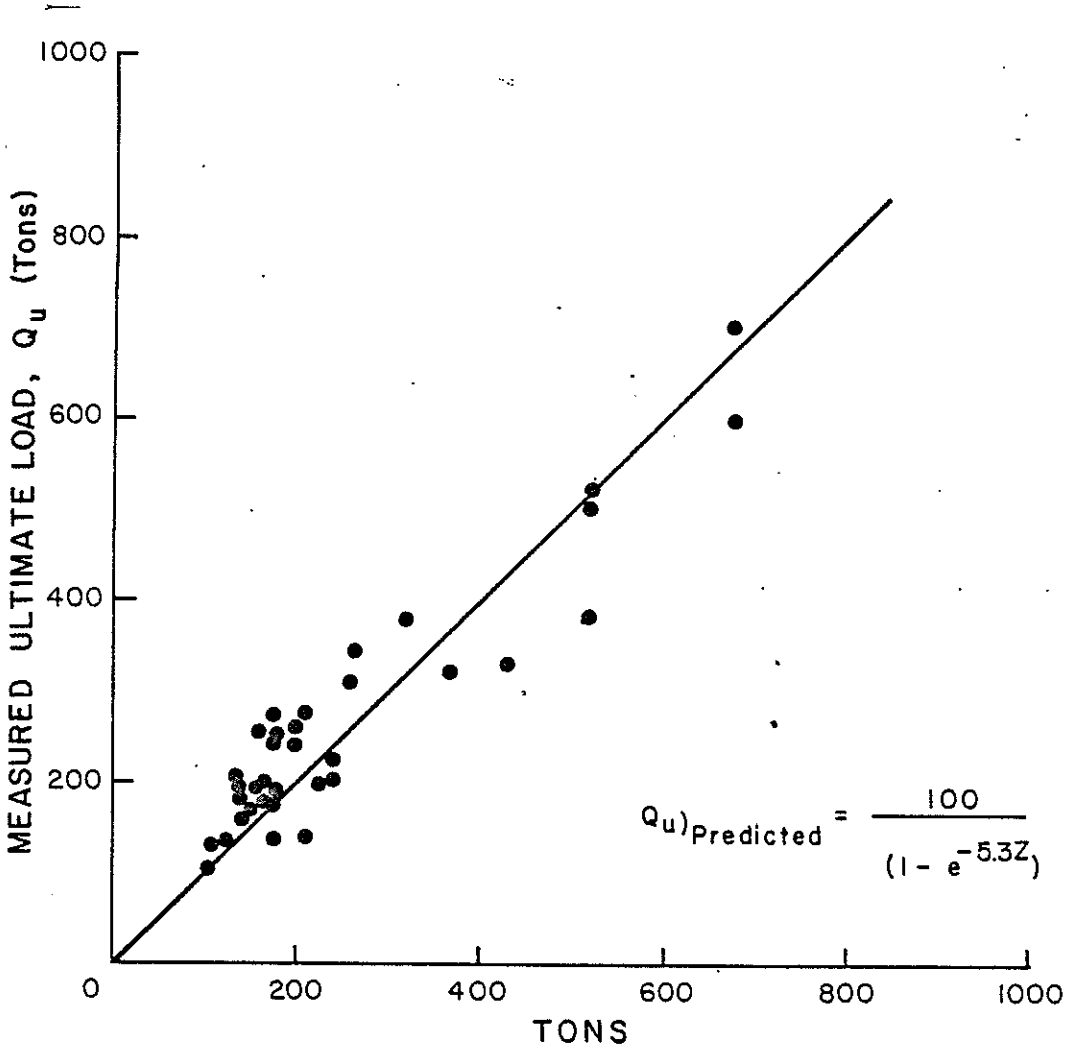

Figure 4.8 Pile Capacity Prediction by Equation 4.1 and a Point (Load (p) = 100) on the Load-Settlement Diagram

(plunging type) failure. An attempt was made to compute the ultimate capacity (Q_u) using the data of the last load applied in conjunction with Equation 4.1. The average r (5.3) was assumed for all the sites and test piles. The predictions were good and the prediction errors were calculated using the following expression:

$$\% \text{ Error} = \frac{\text{Predicted-Measured}}{\text{Measured}}^{1} \times 100 \qquad (4.2)$$

The algebraic mean of the % errors was about 1.1 percent with standard deviation of about 0.09. The results are shown in Figure 4.7.

There are instances when it is not possible to load the test pile to a large magnitude of load because of equipment limitations, cost, time, etc. However, it is essential to have an idea about the failure load. An attempt was made to determine the ultimate load (Q_u) using Equation 4.1 and knowing a point at the start of the loading program. This load was taken as 100 tons for all of the test piles and r was also assumed as the average r (i.e. 5.3) for all of the sites. The algebraic mean of the % errors was found to be 6.0 percent with standard deviation of about 0.20. The results are shown in Figure 4.8.

4.4 Summary

The proposed procedure in conjunction with Van der Veen expression (4.1) appears to result in reasonable and meaningful determination of the ultimate capacity (Q_u) of a pile. The capacities computed with this approach were treated as the actual capacities of the test piles and were termed "the measured ultimate capacity" in this study. The

---

[1] Evaluated from the load-settlement data provided by the pile load tests in conjunction with expression 4.1.

measured ultimate capacities were later used to compare with the predictions based on the available static analysis techniques and the methods using CPT data. The procedure results in a non-biased determination of Q_u which is the load which would have caused a continuous movement of the pile (true failure) if it were applied.

Chapter 5

FIELD TESTING

5.1 General

Selection of the sites involved in this study was based on their subsoil conditions, accessibility, and whether or not they contained test piles of known ultimate capacities. All together there were ten sites under study and all of them were part of projects for the Louisiana Department of Transportation and Development. A total of thirty-seven test piles was selected for this study covering a variety of length, shape, and material. The majority of them were loaded to failure. The QCPT tests were performed as closely as possible to the location of the test piles using different types of cones and tip angles.

5.2 Site Selection

The sites selected for this project were designated as follows: 1) Morgan City, 2) Houma, 3) New Orleans (IIA), 4) New Orleans (I), 5) Ruddock, 6) Baton Rouge (I), 7) Baton Rouge (II), 8) Alexandria, 9) Borgne (I), and 10) Borgne (II) (see Fig. 5.1). All of these sites were parts of projects for the Louisiana Department of Transportation and Development (LDOTD). However, the names given to these sites merely reflect their locations and do not necessarily match their LDOTD designations. The detailed maps of the site locations are presented in Appendix B. These maps also contain information regarding location of

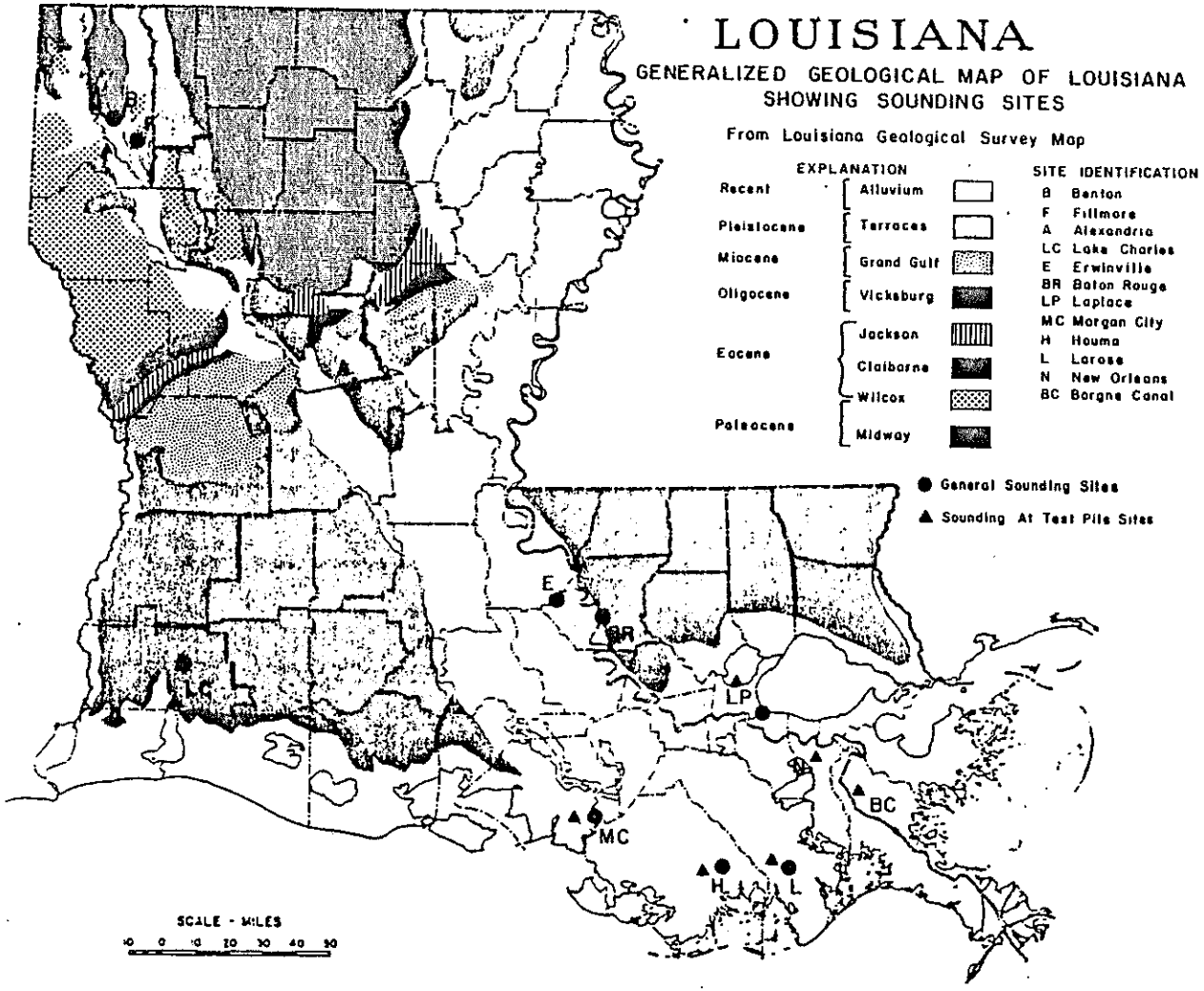

Figure 5.1 General Location of the Sites Under Investigation

the test piles and CPT soundings, LDOTD project name and number, and the location of the borings performed in the vicinity of each site. A search was conducted for choosing the appropriate sites with the following guidelines in mind:

1. The subsurface soil conditions of sites had to be composed of cohesive (clayey) soils.
2. The sites had to contain test pile(s) of known ultimate load(s).
3. The sites had to be accessible by the cone penetrometer truck.

Except for the Ruddock Site, all of the sites chosen met the first criterion. In this site, only the first 45 feet is composed of cohesive soils. All of the sites contain test pile(s) with known ultimate capacities. Nearly all of the test piles were loaded to failure except for a few cases where they were tested to only 2.5 times their design loads. However, the method explained in Chapter 4 was used to determine the ultimate load carrying capacities of those test piles.

The subsurface information of the sites were provided by LDOTD. The borings were performed in the vicinity of each site and information such as the unconfined compression test results, the density and the plasticity index values were used for some of the computations in this study. The subsurface condition of the sites are summarized and presented in Appendix C. The undrained shear strength profiles (undrained cohesion versus depth) of the sites were plotted and presented in Appendix D. It appears that the subsoil condition of the majority of the sites is composed of soft to medium normally consolidated clays. This was true for all the sites except for Baton Rouge and Alexandria where the subsurface investigation indicated that the soils

beneath these locations were stiff overconsolidated clays. The weakest soil was encountered at Borgne (I) Site and the strongest soil was found in Alexandria with mean undrained cohesion of 0.21 TSF and 1.1 TSF, respectively. As a general rule, when one moves from south to north in Louisiana the condition of the soils encountered improves.

5.3 Quasi-Static Cone Penetration Testings

The Fugro electronic cone penetrometer was used in all of the soundings performed for this study. The QCPT soundings were performed as closely as possible to the location of test piles. The depth of penetrations was governed by the embedded lengths of the test piles. The QCPT soundings were conducted to at least 5D (D is diameter of test pile) below the tip of the test piles. A total of 35 soundings for more than 2800 feet was performed using different types of cones and cone tip angles. The following three different tips were used:

1. 60°/10: 60° tip angle/10 cm^2 base area
2. 18°/10: 18° tip angle/10 cm^2 base area
3. 60°/20: 60° tip angle/20 cm^2 base area

The piezometer cone was also utilized in two of the sites. The cone which provided local friction (f_s) and tip resistance (q_c) readings was called the friction cone in this study and was used extensively.

The data furnished by the QCPT soundings (f_s and q_c) were recorded using two different independent systems. One was the strip chart recorder provided by the Fugro cone penetrometer truck and the other was a multipurpose oscilloscope (Nicolet). The strip chart recording is the usual manner of collecting data which uses two different pens for plotting the local friction (f_s) and tip resistance (q_c) readings on a

NEW ORLEANS (I)

PENETRATION RESULTS TEST NO=63 (CONE 60/10)

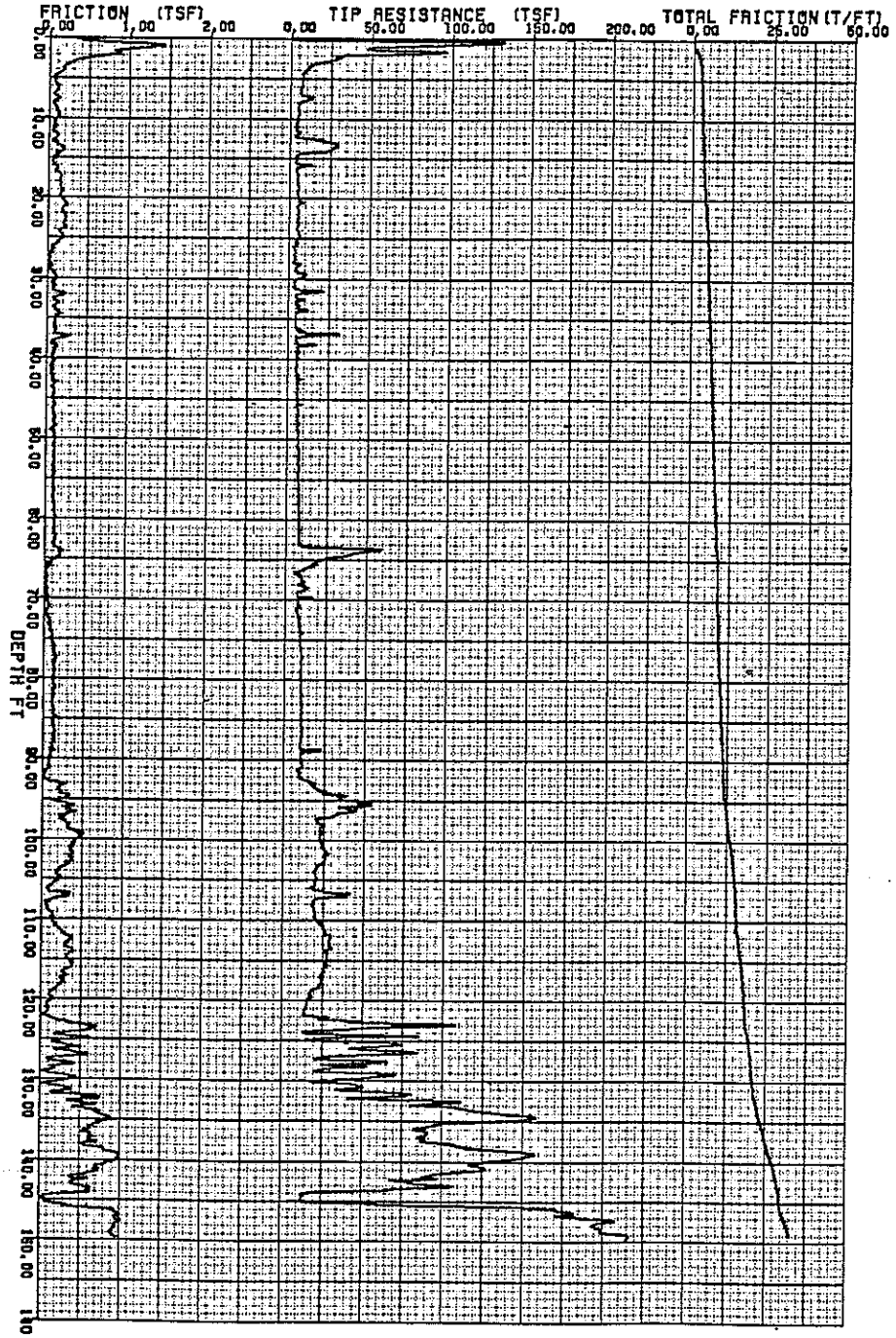

Figure 5.2 Cone Penetration Results Obtained at the New Orleans (I) Site (Using 60/10 Tip)

special type of grid paper. The values of f_s and q_c versus depth could be read from the chart knowing the proper relationships to convert one inch of the pen movements into stress (TSF) or depth (ft). One inch of horizontal movement equals 50.0 TSF of tip resistance (q_c) and 1.0 TSF of local friction (f_s). One inch of vertical pen movement is usually equal to 5 feet depth of penetration.

A multipurpose oscilloscope was also used for the first time to record the cone data (q_c and f_s) readings. The data was displayed on the screen during the penetration of each rod. After complete penetration of each rod (about 1 m) the data was recorded on floppy diskettes. This recording process was automatically performed by the oscilloscope at the end of each 1 m penetration. The data retrieval unit was capable of collecting and recording up to 1024 data points per rod penetrated. Nearly all of the penetrations were done at the rate of 2 cm/s and the unit was able to collect one data point every 50 milliseconds. This means that on the average one data point was collected for every 0.1 cm (0.04 in) of penetration. This procedure was used for all of the penetrations performed in this study. All of the data collected were later transferred from floppy diskettes to computer tapes. This process made possible the use of LSU's computer system for fast and accurate analysis of the data. The collected data could then be retrieved and used for necessary computations. The area under local friction diagram (f_s vs. depth) for each QCPT sounding was computed per foot interval. This information was named "total friction" and became a valuable tool in later computations.

The plottings were done by LSU's Variant plotter. The values of local friction (f_s), tip resistance (q_c) and total friction (F_t) were

Table 5.1

General Information About the Test Piles

No.	Test Pile	Location	Shape	Embedded Length (ft)	Ultimate Load (Q_u) (tons)
1	1	New Orleans (I)	18" Square (C)	120	345
2	2A	New Orleans (I)	Step Taper (S)	123	190
3	3	New Orleans (I)	Monotube (S)	123	275
4	4	New Orleans (I)	Step Taper (S)	123	200
5	5	New Orleans (I)	16" Dia. Pipe (S)	123	320
6	6	New Orleans (IIA)	16" Square (C)	100	225
7	8	New Orleans (IIA)	20" Triangle (C)	100	240
8	9	New Orleans (IIA)	Step Taper (S)	102	135
9	10	New Orleans (IIA)	Step Taper (S)	137	205
10	11	New Orleans (IIA)	Monotube (S)	102	180
11	12	New Orleans (IIA)	Monotube (S)	137	240
12	13	New Orleans (IIA)	Step Taper (S)	102	175
13	14	New Orleans (IIA)	Step Taper (S)	137	200
14	15	New Orleans (IIA)	14" Dia. Pipe (S)	102	200
15	16	New Orleans (IIA)	16" Dia. Pipe (S)	137	260
16	18	New Orleans (IIA)	Step Taper (S)	101	130
17	19	New Orleans (IIA)	Step Taper (S)	138	195
18	1	Houma	18" Square (C)	95	225
19	2	Houma	12" Dia. Pipe (S)	95	140
20	3	Houma	14" Dia. Pipe (S)	95	160
21	4	Houma	Step Taper (S)	95	195
22	5	Houma	Step Taper (S)	152	255
23	10	Houma	Monotube (S)	95	175
24	24-1	Ruddock	24" Square (C)	65	250
25	30-1	Ruddock	30" Square (C)	65	330
26	24-2	Ruddock	24" Square (C)	90	380
27	30-2	Ruddock	30" Square (C)	80	600
28	54-2	Ruddock	54" Round (C)	83	700
29	4A	Morgan City	Step Taper (S)	120	180
30	4B	Morgan City	Step Taper (S)	108	170
31	2A	Baton Rouge (I)	14" Square (C)	45	170
32	4A	Baton Rouge (IIA)	14" Square (C)	43	165
33	1	Alexandria	14" Square (C)	31	105
34	3	Alexandria	14" Square (C)	45	140
35	2	Borgne (I)	36" Round (C)	124	500
36	4	Borgne (II)	36" Round (C)	130	520
37	5	Borgne (II)	24" Square (C)	104	320

C: Concrete; S: Steel

plotted versus depth for all of the QCPT soundings performed. An example of such plot is given in Figure 5.2. The QCPT sounding plots of all of the sites are presented in Appendix E.

5.4 The Test Piles Under Study

There is a total of 37 test piles involved in this study. These test piles cover a variety of shape, length and material. All of the test piles are part of various projects of LDOTD and located at the sites described earlier. The majority of them were loaded to failure or otherwise tested/loaded to 2.5 times their design loads. The test piles located at New Orleans (I), New Orleans (IIA), Houma, and Ruddock sites were parts of "advanced test pile programs" and were meant to be loaded to failure. However, the ultimate load carrying capacities (Q_u) were computed by the procedure described in Chapter 4.

A complete description of the test piles together with their detailed dimensions is presented in Appendix F. The summary of the test piles including their designated names, locations, shape, embedded length, and ultimate capacity (Q_u) are given in Table 5.1.

5.5 Summary

The objective of this study was to determine the feasibility of utilizing the electronic cone penetrometer to design piled foundations in cohesive soils. The sites included a wide range of cohesive soils as far as the shear strength was concerned. All of the penetrations were performed to an adequate depth using different tip angles. The new method of collecting, recording, and retrieving the data made it possible to use LSU's computer for fast and accurate analysis. The test piles were tested (with majority of the time loaded to failure) and

covered all kinds of driven piles. The above facts indicate the existence of sufficient possible means to perform a statistically sound and accurate analysis to reach the mentioned objective.

Chapter 6

RECOMMENDED PILE CAPACITY PROCEDURES FOR COHESIVE SOILS USING CPT DATA

6.1 Introdution

The quasi-static cone penetration test (QCPT) has been used extensively in the Netherlands and other western European countries for design of piled foundations. However, most of the developments have been toward predictions of the tip bearing capacities of piles driven in sand. The frictional capacity of a pile was related to the total friction along the tubes, or q_c data, prior to development of the friction sleeve penetrometer by Begemann in 1953. This "new" version of the penetrometer was capable of providing frictional resistance, f_s readings which opened the door to a more direct and rational estimation of the unit pile side friction, f.

One of the major goals of this research was to develop procedure(s) using f_s data directly in computations. This was done by relating f_s data to the unit pile friction (f) or by estimating undrained shear strength to be used in conjunction with available static analysis techniques. The proposed procedures resulted in close predictions of the test piles' ultimate capacities. However, the tip bearing capacities were estimated by a method similar to the Dutch method. This was done because the procedures for prediction on the tip bearing capacity using q_c data were already well established. Most of the research concentrated on developing procedures for estimating the frictional

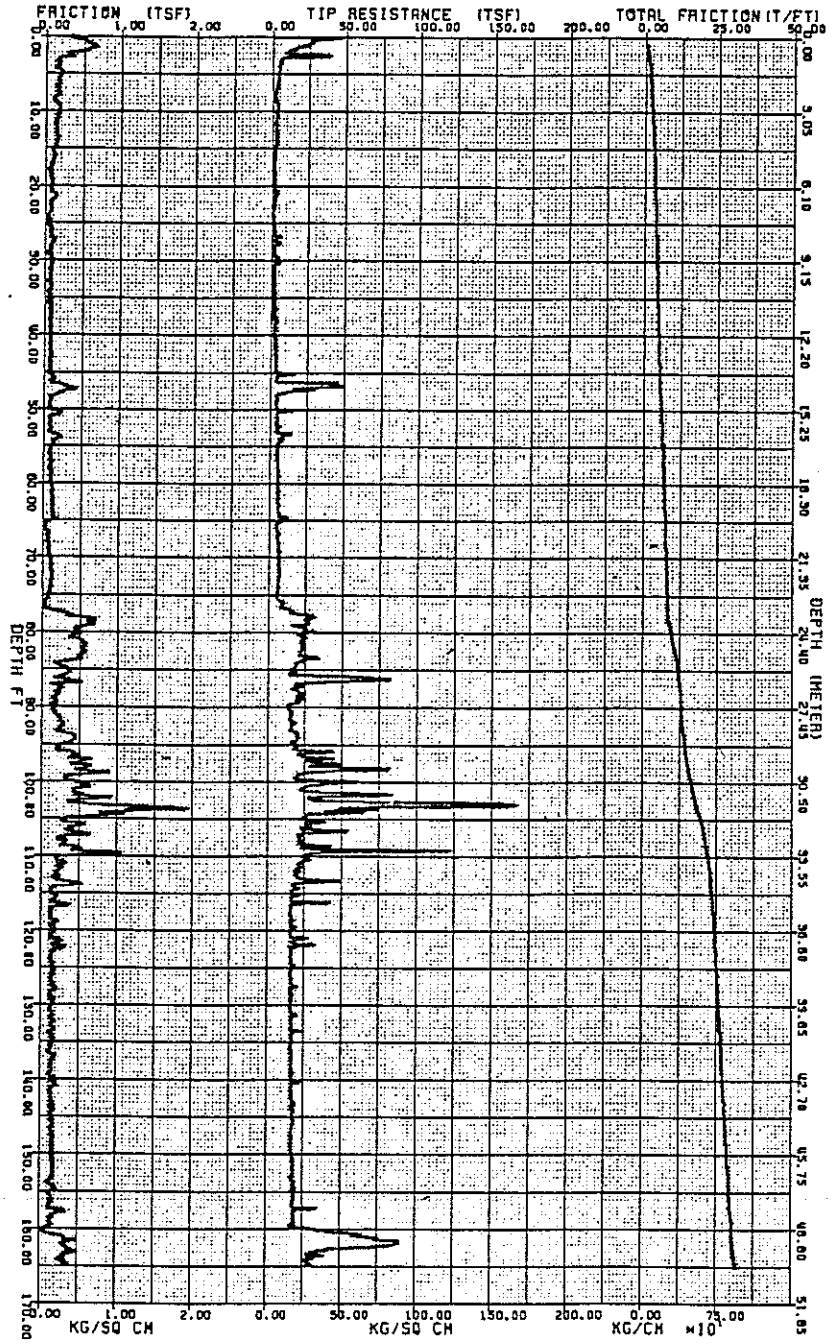

Figure 6.1 The Electronic Cone Penetration Results in New Orleans (IIA) Site

capacity since it contributes the major portion of the loading carrying capacity of piles driven in cohesive soils.

It was concluded that the QCPT data could be utilized to design pile foundations in soft cohesive soils. Also, in light of the close predictions made by the proposed procedures, it is hoped that adoption of such methods in conjunction with further research in this area would minimize the number of costly and time consuming test pile programs required for a project.

6.2 Tip Bearing Capacity Predictions

The quasi-static cone penetration test (QCPT) which represents a model displacement pile provides data to develop a continuous in-situ resistance profile. Because of the geological conditions of the countries where QCPT has developed, most of the efforts are related to the use of the cone resistance (q_c) data in cohesionless soils, and little work is conducted in case of the cohesive soils. Numerous methods and procedures are available with regard to the use of the cone resistance data for estimating the unit pile tip bearing capacity (q_o). However, all of the procedures recommend some kind of averaging procedure applied to q_c data for calculating the tip bearing capacity. The most recent one is the Dutch method originally suggested by Begemann (1963) which was explained and successfully applied by Nottingham (1975). The theory and practice of using QCPT data for predicting the unit tip bearing capacity were covered in Chapter 2.

Nearly all of the test piles under study are of "friction" type piles driven in cohesive soils. The tip bearing capacity does not contribute much to the ultimate total capacity (Q_u) of a pile driven in

NEW ORLEANS II-A

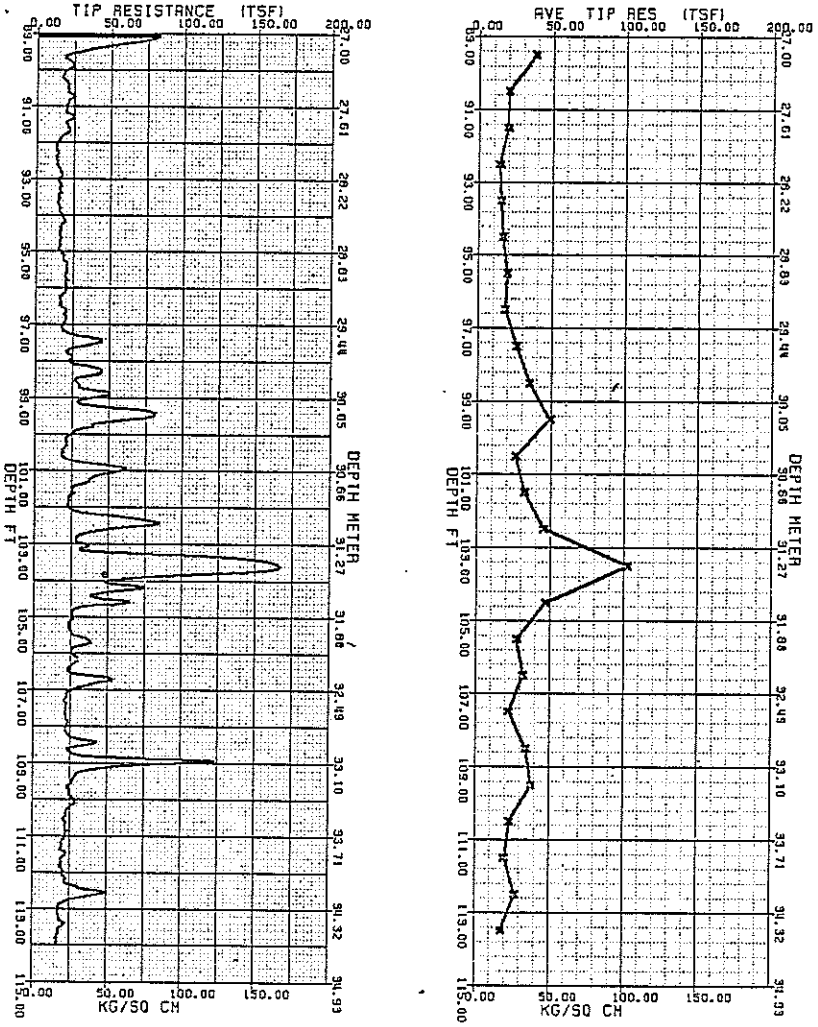

Figure 6.2 The Average Tip Resistance Results in New Orleans (IIA) Site (One Foot Intervals)

clayey soils. Thus, most of the procedures were developed for precisely estimating the frictional capacity. For this reason, a procedure similar to the one suggested for sandy soils was adopted in this study. The method should not cause any major error due to the following reasons.

1. The tip resistance values are low and uniform in cohesive soils; therefore, regardless of the failure surface pattern, or the procedure used, the same unit tip bearing capacity (q_o) would be obtained. For example, there are five test piles driven to a a depth of about 138 ft in New Orleans (IIA) site (Fig. 6.1). The unit tip bearing capacity (q_o) can be taken as 17.0 tsf regardless of the procedure applied.
2. The contribution of the tip bearing capacity (Q_t) is very little (about 10%) to the total ultimate load (Q_u); consequently, the need for measuring it precisely is eliminated.
3. The critical depth ratio (D_c/d_p) is one for cohesive soils ($\phi = 0$). This point which was discussed in Chapter 2, indicates that a pile does not have to be penetrated by a large amount (greater than the critical depth) into a layer, for performing a sound correlation between the cone resistance readings (q_c) and q_o. It was also intended to keep the procedure simple and consistant with the presently available methods.

The average of the q_c data for each foot of penetration was computed. The average values were utilized in the tip bearing capacity calculations. Fig. 6.2 presents the average cone resistance ($\bar{q}_c$) data

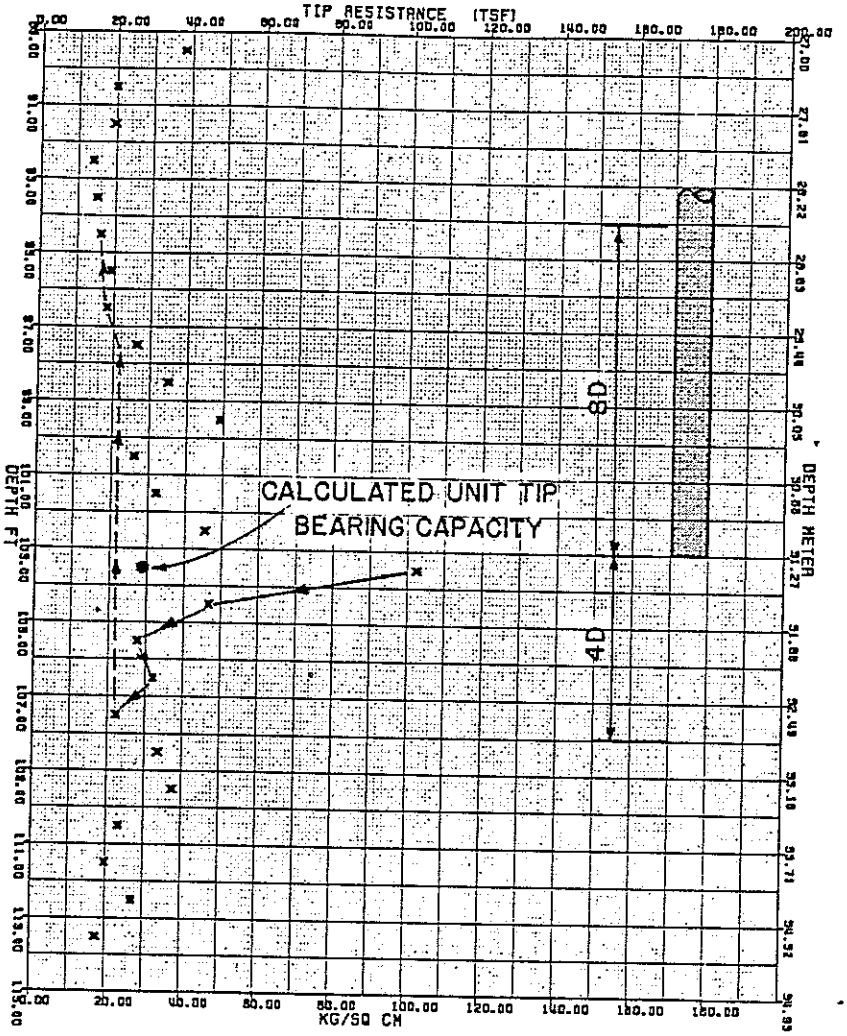

Figure 6.3 Tip Bearing Capacity Calculations by the Proposed Procedure (14.0 in Diameter Pipe Pile, New Orleans (IIA) Site)

collected between depths of 89.0 ft and 115.0 ft, in the New Orleans (IIA) site. The equation implemented for calculating the unit tip bearing (q_o) of piles driven in cohesive soils follows:

$$q_o = \frac{(q_{b1} + q_{b2})/2 + q_a}{2} \qquad (6.1)$$

where

q_{b1} = the average of the $\bar{q}_c$ data, 4D below the pile tip

q_{b2} = the average of the minimum $\bar{q}_c$ data, 4D below the pile tip

q_a = the average of the minimum $\bar{q}_c$ data, 8D above the pile tip

D is the diameter or equivalent of the diameter of the pile. The difference between this procedure and the recent version of the Dutch method is that in the latter, the term $(q_{b1} + q_{b2})/2$ is calculated using q_c values obtained from XD below pile tip, X is varied between 0 to 3.75, and minimum $(q_{b1} + q_{b2})/2$ is chosen in q_o calculations.

The tip bearing capacity of the test piles were determined using the above mentioned procedure. The average cone resistance ($\bar{q}_c$) values collected in the New Orleans (IIA) site is presented in Fig. 6.3.

The test pile No. 15 has a diameter of 14.0 in and is penetrated to a depth of 103.0 ft. The unit tip bearing capacity (q_o) for this pile was calculated as follows:

$$q_{b1} = \frac{1}{5}(102 + 47 + 28 + 32 + 22) = 46 \text{ tsf}$$

$$q_{b2} = \frac{1}{5}(5 \times 22) = 22 \text{ tsf}$$

$$q_a = \frac{1}{9}(6 \times 22 + 2 \times 18 + 16) = 20 \text{ tsf}$$

$$q_o = \frac{(q_{b1} + q_{b2})/2 + q_a}{2} = \frac{(46 + 22)/2 + 20}{2} = 27 \text{ tsf}$$

The above calculations are recommended for tip bearing calculations of piles driven to sandy, or silty clays where q_c readings are high and erratic. In the case of pure cohesive soils, the unit tip bearing

calculations may be done by simply averaging the q_c values around the depth where the pile tip is located. This means that for clayey soils, adherence to the proposed procedure is not necessary.

6.3 Frictional Capacity Prediction Using QCPT Data

Prior to the development of the adhesion jacket cone in 1953 by Begemann, the frictional capacity of a pile was related to the total friction along the tubes penetrated or the unit pile friction (f) was related to q_c data. The first idea was abandoned because Begemann (1953 and 1969) presented cases where the total rod friction decreased with additional penetration. Theoretically this meant that certain layers of soil exhibited negative local friction, which was an impossible situation. The unit friction (f) may be directly related to q_c data as Meyerhof (1956) suggested. The frictional capacity in cohesive soils may be estimated by assuming a proper q_c/S_u (i.e., N_k) ratio. The estimated S_u may then be utilized in conjunction with available static analysis techniques such as the one suggested by Tomlinson (1957) to compute f.

Many investigators believe that the local friction (f_s) data is a better indication of the undrained shear strength (S_u) and the unit friction (f) of piles driven in clays, than the tip resistance (q_c) data. Experimental correlation of f_s and S_u presented by Wesley (1967) indicated f_s to be slightly higher than S_u. The estimated S_u from such a correlation could also be utilized in conjunction with a static analysis technique to compute f.

Begemann (1965) and Vesic (1967) suggested that the unit friction (f) could be directly obtained from the local friction (f_s) data.

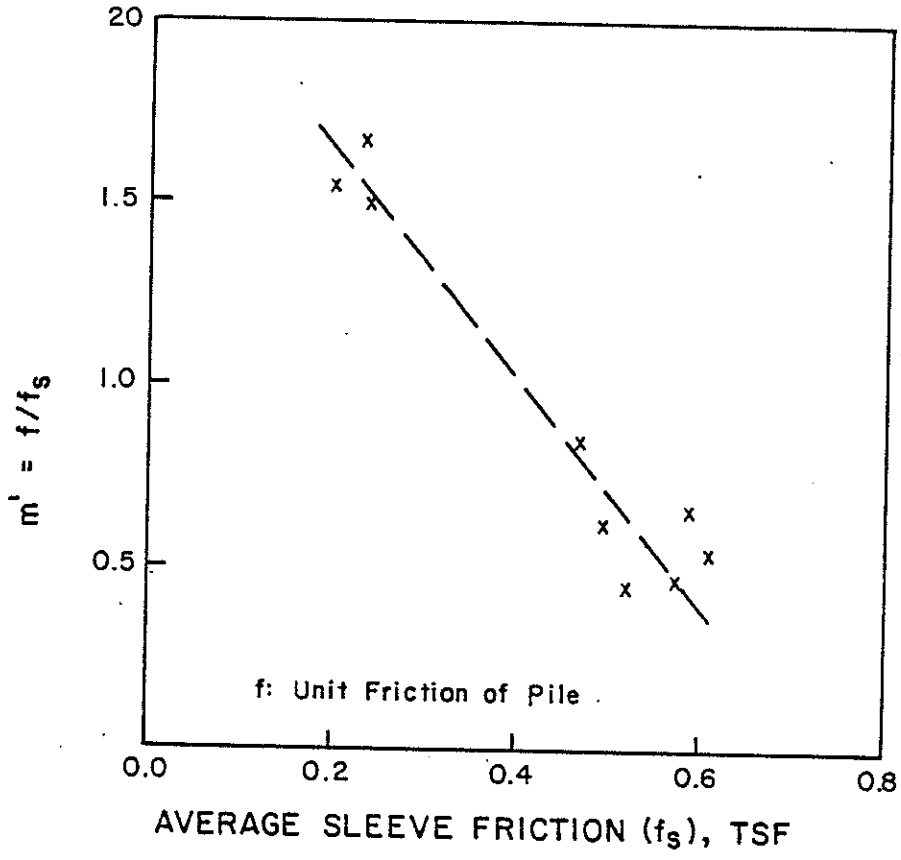

Figure 6.4 Plot of the f/f_s Ratios Versus f_s Values (Model Test Piles, Nottingham 1975)

Begemann recommended that f may safely be taken as equal to f_s; however, Vesic suggested that f should be taken as two times the f_s readings. Although the relationships proposed by Begemann and Vesic do not agree with each other, they are correct for the particular soils studied by the two investigators. This indicates that f cannot be related to f_s by a constant for all soils. Nottingham (1975) assumed f_s to be equal to the undrained cohesion (C_u), and related f to f_s by the adhesion factor (α) suggested by Tomlinson (1957). Nottingham applied this procedure to compute the frictional capacity of model test piles, and the results were fairly successfull. He also realized that f cannot be related to f_s by a constant for clays of different strength; on the contrary, the two may be correlated by an adhesion factor such as α which decreases as the shear strength increases.

The intent was either to relate the unit friction (f) to the local friction (f_s) data or to estimate the undrained cohesion (C_u) from f_s and employ static analysis techniques to compute f. Consequently, two different procedures, the Cone-m Method and the Lambda-Cone Method, are suggested for computing f from f_s. The Cone-m Method relates f to f_s by a recommneded adhesion factor called m. The Lambda-Cone Method is similar to the original Lambda Method (Vijayvergia and Focht, 1972), except for the fact that the mean undrained cohesion term is determined from the local friction (f_s) readings. The procedures are explained and presented in this chapter.

6.3.1 The Cone-m Method

In order to develop a rational relationship between the QCPT data and the frictional capacity (Q_s) of a pile, it is essential to determine

the portion of the ultimate load carrying capacity (Q_u) which is supported by the pile shaft. Ideally the study would use instrumented test piles to measure the frictional capacities directly and accurately. However, one of the advantages of working with piles driven in cohesive soils (i.e., friction pile) is that the contribution of the tip bearing capacity (Q_t) to the ultimate capacity (Q_u) is very little. Thus, the frictional capacity (Q_s) may reasonably be estimated by subtracting Q_t from Q_u.

Nottingham (1975) conducted a study with instrumented model test piles driven in clays and predicted the shaft capacity (Q_s) by assuming f_s to be equal to C_u and applying Tomlinson's adhesion factor (α) to compute f.

The data collected by Nottingham was treated in a different manner in this study. The average unit friction (f) of the test piles were first computed. The ratio of f to the average local friction ($\bar{f}_s$) data collected in the vicinity of the model test piles was calculated. The plot of the $f/\bar{f}_s$ ratios versus $\bar{f}_s$ is presented in Fig. 6.4. As expected, it is evident that the $f/\bar{f}_s$ ratio is not a constant for all soils but decreases as shear strength increases.

The same type of analysis which was applied to Nottingham's model test pile data was also performed on the full scale test piles under study. The unit pile friction (f) of the test piles was calculated based on the total frictional capacity (Q_s). The average local friction readings ($\bar{f}_s$) obtained at the vicinity of the test piles were determined by the following expression:

$$\bar{f}_s = \frac{F_t}{L} \qquad (6.2)$$

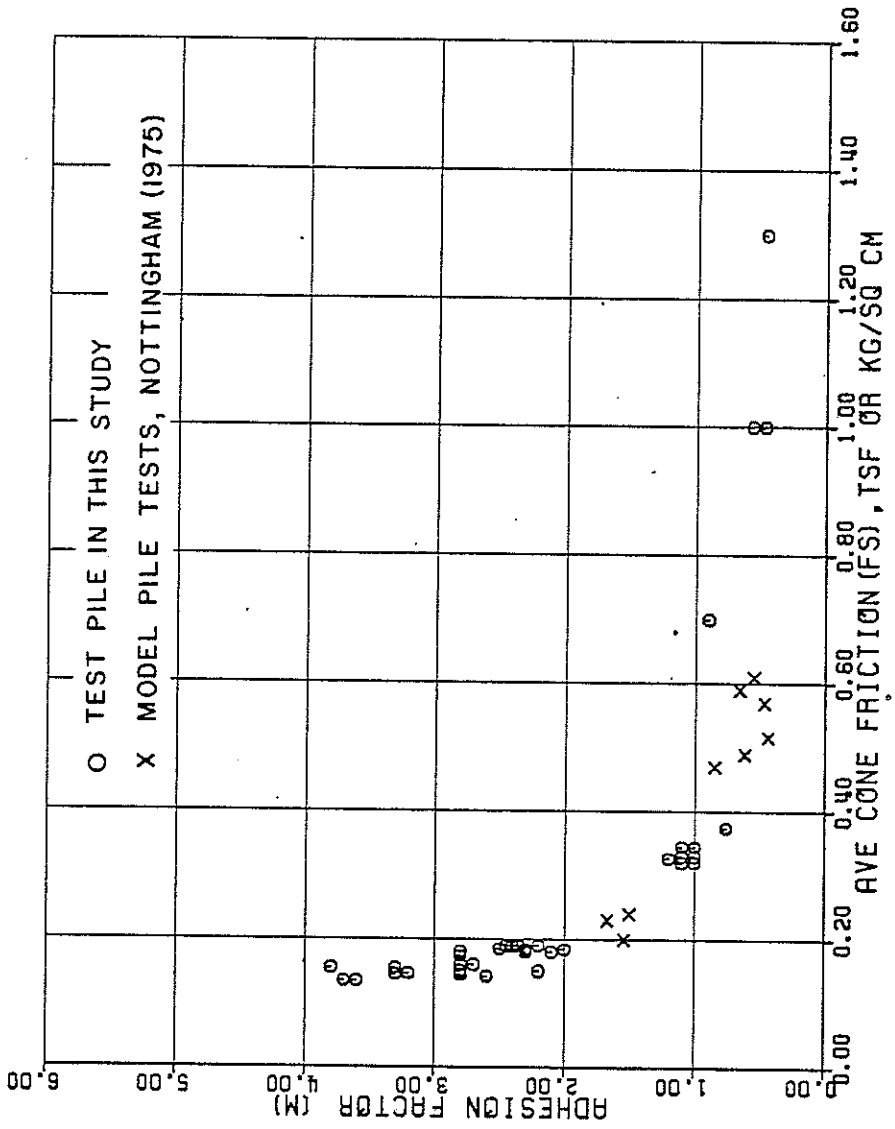

Figure 6.5 The Adhesion Factor (m) Values Obtained From the Test Pile Results

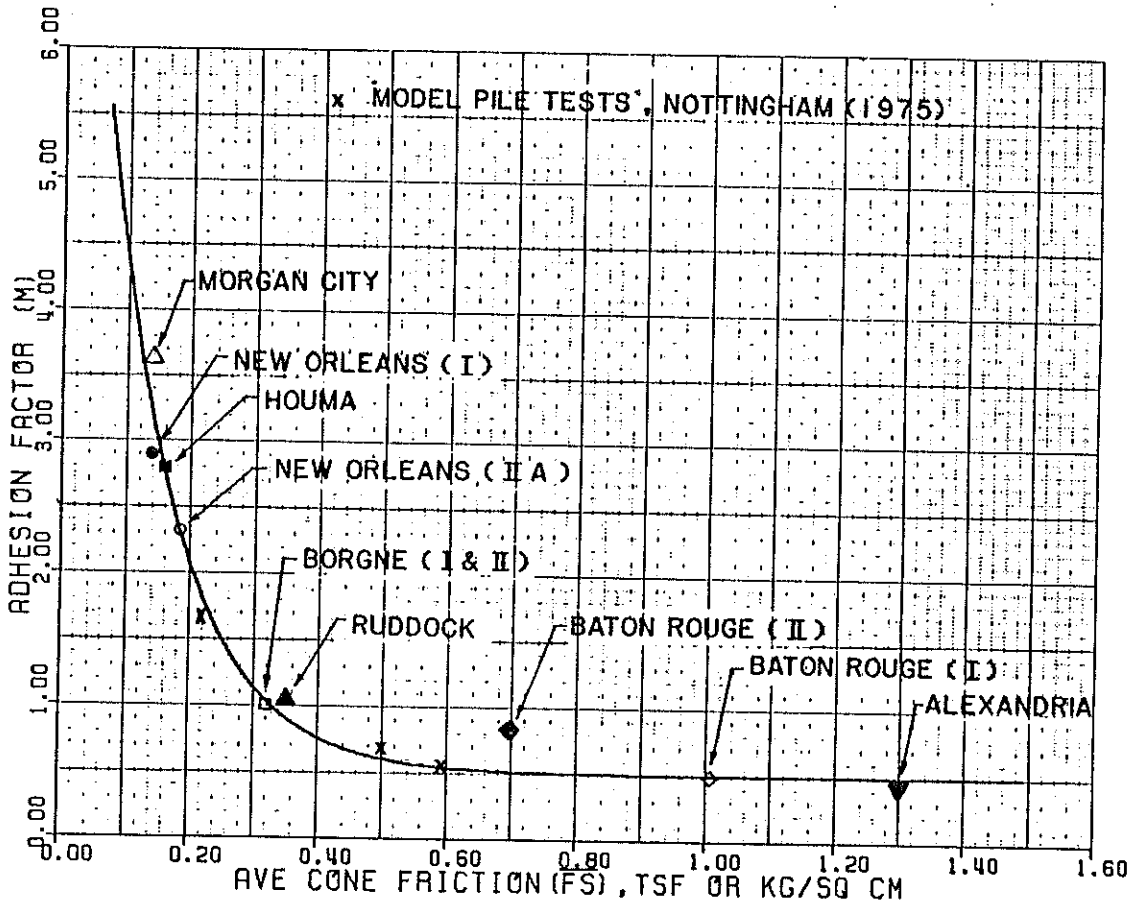

Figure 6.6 The Adhesion Factor (m) Curve (Average Values of the Sites are Shown)

where F_t is the total area in (T/ft) under f_s diagram for the pile penetration (L). The area under f_s was calculated for each foot of interval. The areas were then integrated for a given depth (L) to compute the total friction (F_t) for that depth. The total friction data (F_t) is plotted next to f_s and q_c data versus depth for a given site (see Fig. 6.1).

The ratios of the unit friction (f) and $\bar{f}_s$ were calcualted and plotted versus $\bar{f}_s$ for all of the test piles. The $f/\bar{f}_s$ ratio was called the adhesion factor m. The m versus $\bar{f}_s$ plot shown in Fig. 6.5 was developed by analyzing 37 full scale test piles in ten different sites. The $f/\bar{f}_s$ ratios gathered from Nottingham's model test pile study are also presented in Fig. 6.5. It is evident that there is a clear and definite relationship between m and $\bar{f}_s$. A curve fitting process was conducted on m and $\bar{f}_s$ values which resulted to the following expression for m:

$$m = 10.0 - 9.5\ (1 - e^{-9.0\ \bar{f}_s}) \qquad (6.3)$$

The graph of this expression and the average data obtained for each site is presented in Fig. 6.6. The unit friction (f) may then be expressed as shown in Fig. 6.7, where

$$f = m \times \bar{f}_s < 0.75 \text{ tsf} \qquad (6.4)$$

The reasons for setting an upper limit for f will be explained later in this chapter.

The shape and the trend of the m curve resembles other suggested adhesion factor curves versus the soil's shear strength. The suggested adhesion (m) factor decreases as the soil's strength increases which is reflected by the $\bar{f}_s$ data for a given site. Equation 6.3 suggested that m could vary between 0.50 to 10.5 for all soils. This is in sharp

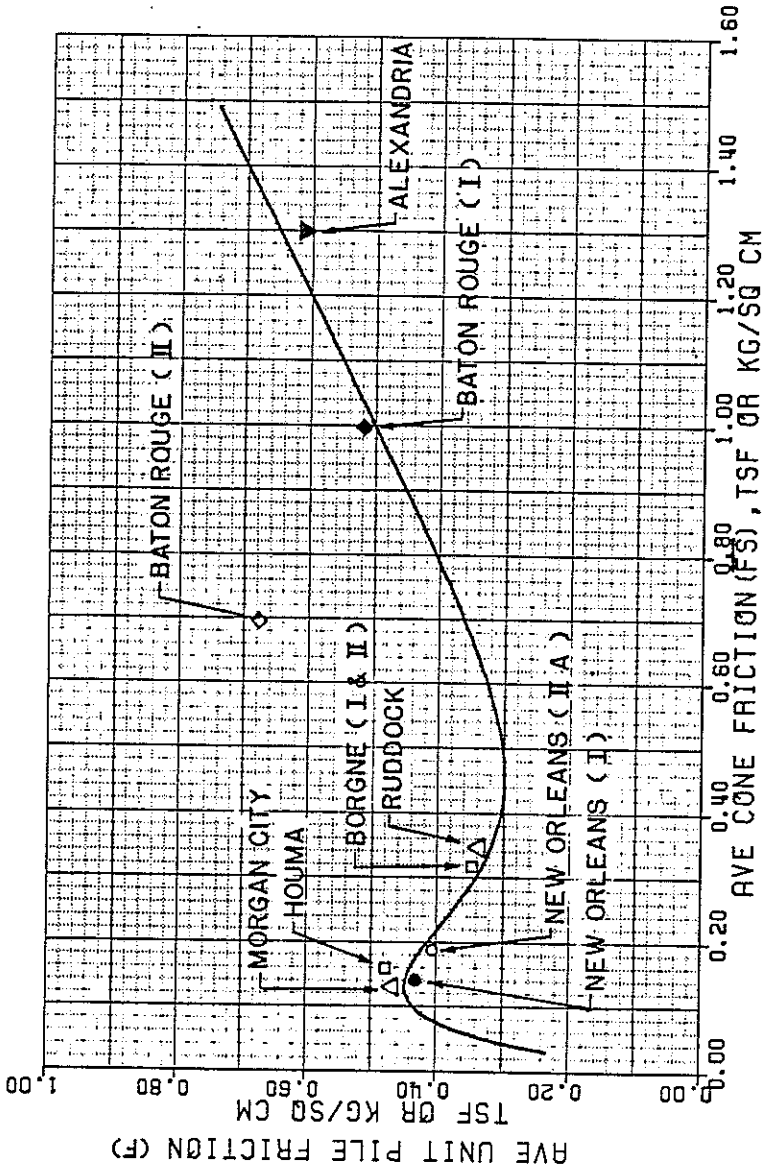

Figure 6.7 Pile Adhesion Versus the Average Local Friction (f_s) Values

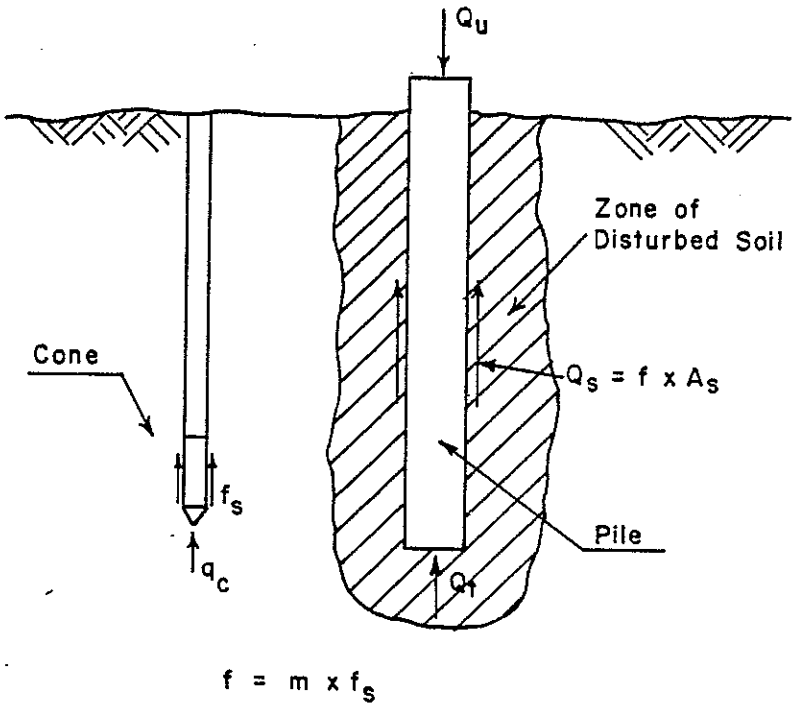

Figure 6.8 The Mechanism Involved in Obtaining f and f_s

contrast with the present belief that f could be related to f_s by a correlation factor of 1 or 2 as suggested by the mentioned investigators. The reason for this may be that f and f_s are obtained from two different mechanisms which involve different types of failure criterion and condition. The local friction (f_s) data is collected by the smooth friction sleeve from soil layers which have experienced a definite failure caused by the penetration. On the other hand, f is obtained from the information provided by a test pile program conducted after the pile driving is completed. This argument is depicted in Fig. 6.8. It may be concluded that f_s represents an undrained type of friction whereas f is a friction related to the drained condition.

The f_s readings are either increased by a factor (m) greater than one for soft clays ($\bar{f}_s < 0.30$ tsf) or decreased by an m less than one for medium to stiff ($\bar{f}_s > 0.30$ tsf) clayey soils. This is explained by the fact that the pile driving causes excess pore pressures in the zone of highly disturbed soils around the pile shaft. The excess pore pressures set up a consolidation process which eventually increases the strength of surrounding soils after adequate time is allowed for the excess pore pressures to be dissipated. Although remolding affects the soil around the pile shaft, the strength gained from the reconsolidation/densification process seems to be more dominant. But for medium to stiff soils ($\bar{f}_s > 0.30$ tsf) the reconsolidation process is less prominant. The vigorous action of pile driving causes the soil to heave at the surface; consequently a gap is created between the pile shaft and the surrounding soils. The gap does not allow a full mobilization of the shear strength which causes the adhesion factor to be smaller than one.

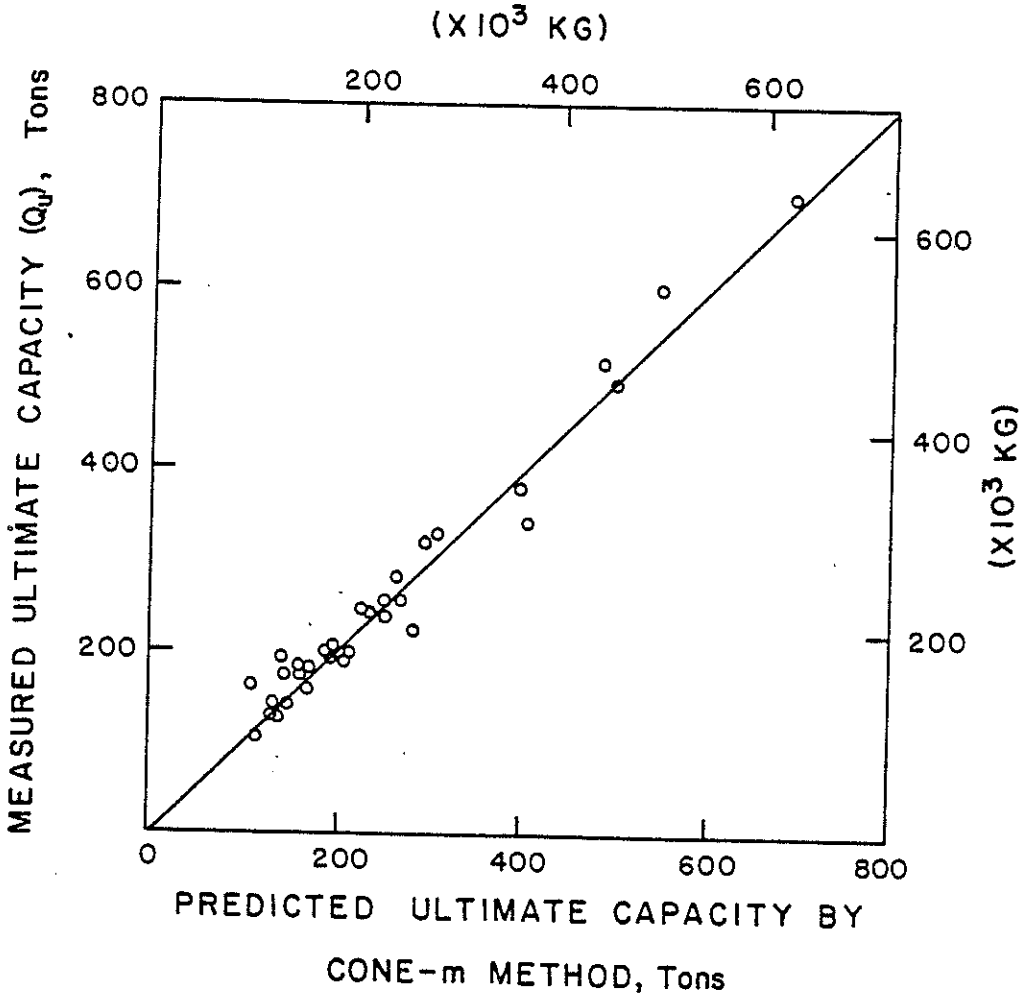

Figure 6.9 Pile Capacity Predictions by the Cone-m Method

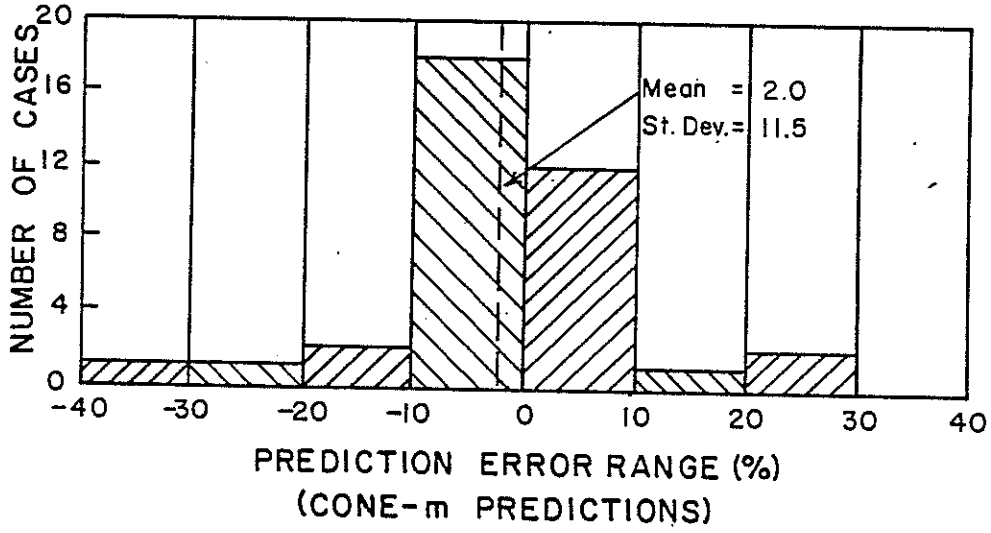

Figure 6.10 The Prediction Error Results
(The Cone-m Method)

The ultimate capacities (Q_u) of the test piles were calculated by applying the Cone-m Method to determine the frictional capacity (Q_s). The tip bearing capacities were calculated by utilizing the Equation 6.1 to compute q_o. The values of the predicted and measured ultimate capacities were plotted in Fig. 6.9. The points are gathered around the one-to-one line which is indicative of close predictions. The prediction errors were computed by the following equation:

$$\% \text{ Prediction Error} = \frac{\text{Predicted-Measured}}{\text{Measured}} \times 100 \qquad (6.5)$$

The algebraic mean of the prediction errors was -2.0% with a standard deviation of 11.5%, as presented in Fig. 6.10. It appears that a very close prediction of a pile ultimate capacity is possible by summing the tip bearing capacity determined by Equation 6.1 and the friction capacity estimated by the recommended Cone-m Method.

6.3.2 The Lambda-Cone Method

This procedure is similar to the one suggested by Vijayvergia and Focht (1972) except the mean undrained cohesion term is replaced by an expression evaluated from the average local friction ($\bar{f}_s$) data. The original Lambda Method indicated that the unit friction (f) is influenced by passive pressures caused by the displaced soil during pile driving. The procedure also suggests that f may be related to the Rankine passive pressure.

The frictional capacity (Q_s) of the test piles was determined by subtracting the tip capacity (Q_t) from the total ultimate capacity (Q_u). The unit friction (f) was calculated knowing Q_s for a given test pile. The pile friction factor Lambda-cone (λ_c) was calculated for all of the test piles applying the following expression:

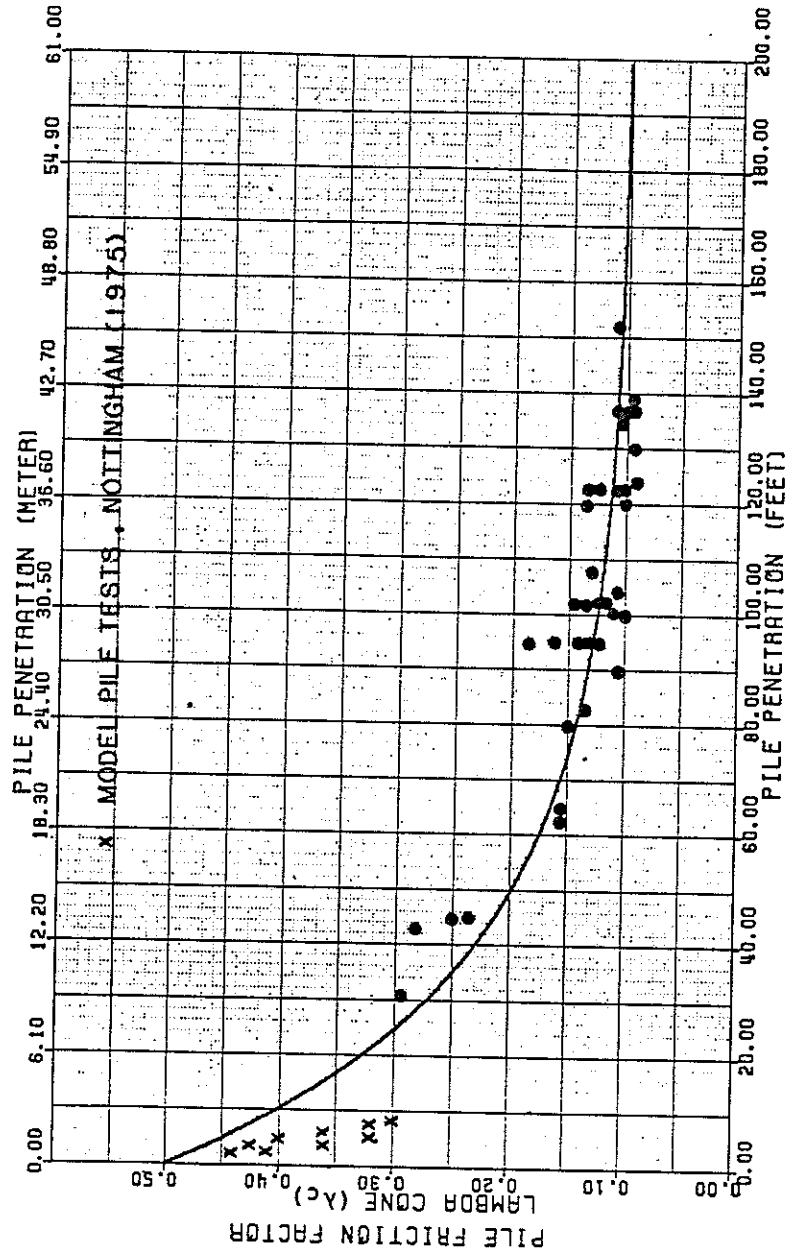

Figure 6.11 The Lambda-Cone (Pile Friction Factor) Curve

$$\lambda_c = \frac{f}{(\bar{\sigma}_m + 2\ m\ \bar{f}_s)} \qquad (6.6)$$

where

λ_c = the Lambda-cone friction factor

$\bar{\sigma}_m$ = mean effective overburden

m = adhesion factor obtained by Equation 6.3

$\bar{f}_s$ = average local friction

The term m x $\bar{f}_s$ is equal to f which was introduced in the Cone-m Method. The λ_c factor was calculated for the test piles and the values were plotted against the corresponding pile penetration (L). The plotted values indicated a definite relationship between λ_c and L. The Lambda-cone values decreased with increasing pile penetration (L). An attempt was made to fit a curve to the plotted data which indicate the following expression for λ_c:

$$\lambda_c = 0.50 - 0.40\ (1 - e^{-0.028\ L}) \qquad (6.7)$$

This points out that λ_c could vary between 0.10 and 0.50. The trend and the shape of λ_c curve is similar to the original Lambda curve presented in Fig. 3.6. Both λ and λ_c are 0.50 for a pile of zero length and remain to a constant for very long piles. It is evident that the reason for λ_c being 0.50 for pile of zero length is that the term $\bar{\sigma}_m$ will be zero, thus, λ_c will be:

$$\lambda_c = \frac{f}{2f} = 0.50$$

However, λ equal to 0.50 (for L = 0) is only possible if cohesion equals unit friction f for all soils. By the same argument, it is possible to calculate λ for zero length as follows:

$$\lambda = \frac{f}{(\bar{\sigma}_m + 2\ C_u)}$$

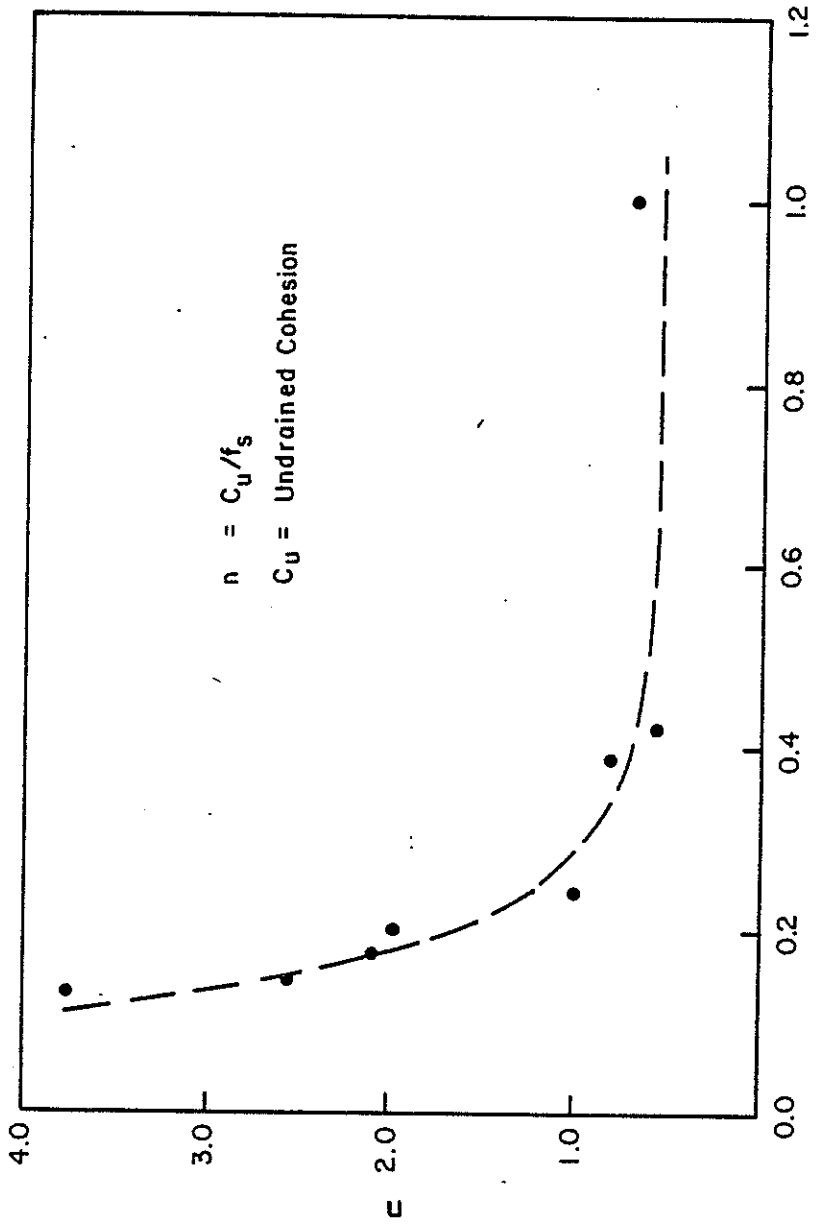

Figure 6.12 Relationship Between Undrained Cohesion (C_u) and Average Local Friction (f_s)

assuming $f = C_u$ and $\bar{\sigma}_m = 0$ for zero pile length, then

$$\lambda = \frac{C_u}{2\ C_u} = 0.50$$

The assumption of $f = C_u$ may be a correct one for soft cohesive soils, but not for all soils. This may be the reason that some engineers believe that the Lambda Method results in overprediction of the frictional capacity of short piles driven in stiff cohesive soils.

The plot of the actual λ_c values and the graph of λ_c values computed by the expression 6.7 is presented in Fig. 6.11. The actual values fit the proposed curve very well. Furthermore, the procedure was applied to Nottingham's model test piles and the λ_c values obtained were superimposed in Fig. 6.11. The results indicate that λ_c may indeed approach 0.50 for very short piles. One of the advantages of the Lambda-Cone Method is that it involves two corrections for determining f. One is λ_c which depends on pile penetration and the other one is m applied to $\bar{f}_s$ which is indicative of the soil's shear strength. The term m x $\bar{f}_s$ is replacing C_m (mean undrained cohesion) in the original Lambda Method. This suggests that m x f which is the same as unit pile friction (f) may be taken as equal to the undrained cohesion. The assumption is correct in the case of soft cohesive soils. The correlation between $\bar{f}_s$ and undrained cohesion indicated that:

$$C_u = n\ \bar{f}_s \qquad (6.8)$$

The plot of n versus $\bar{f}_s$ is given in Fig. 6.12. The graph indicates that n values vary with $\bar{f}_s$ in a manner similar to the adhesion factor (m). This demonstrates that m x f_s may replace the term C_m for computing the unit friction (f) by the Lambda-Cone Method without contributing any major error.

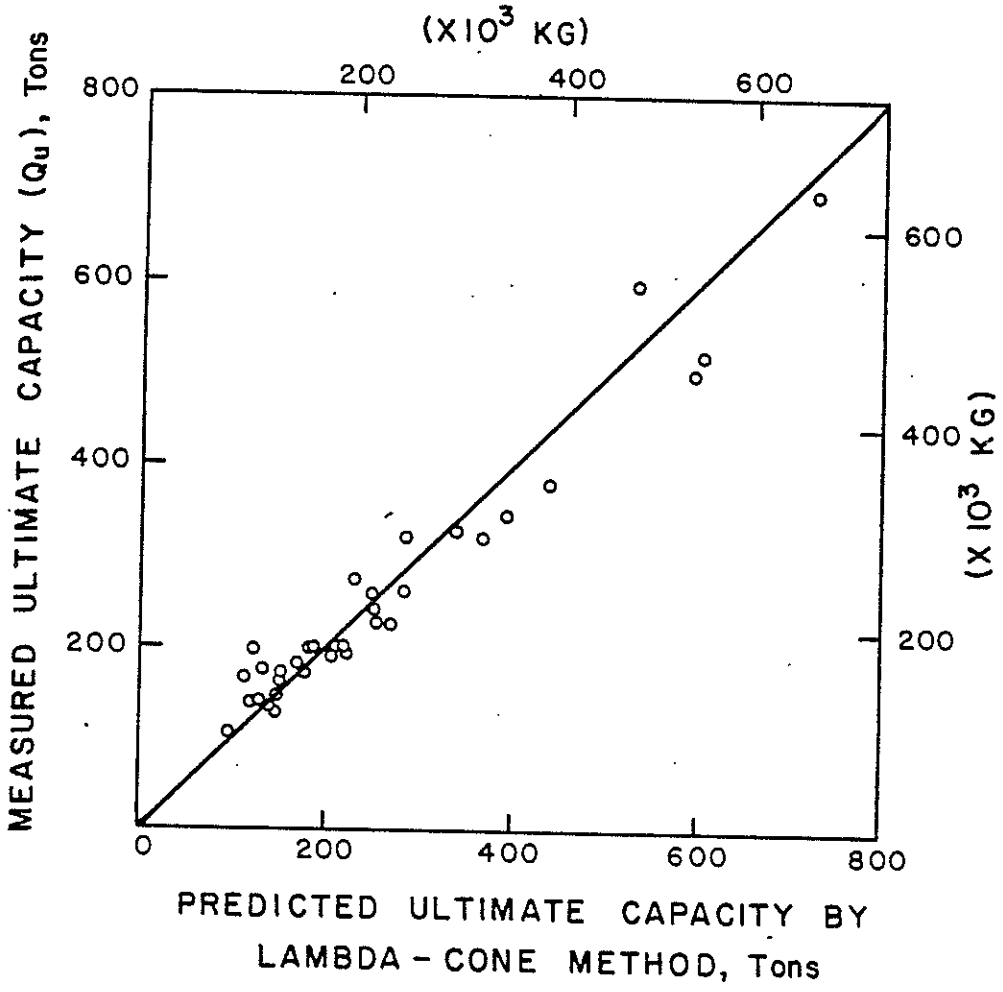

Figure 6.13 Pile Capacity Predictions by the Lambda-Cone Method

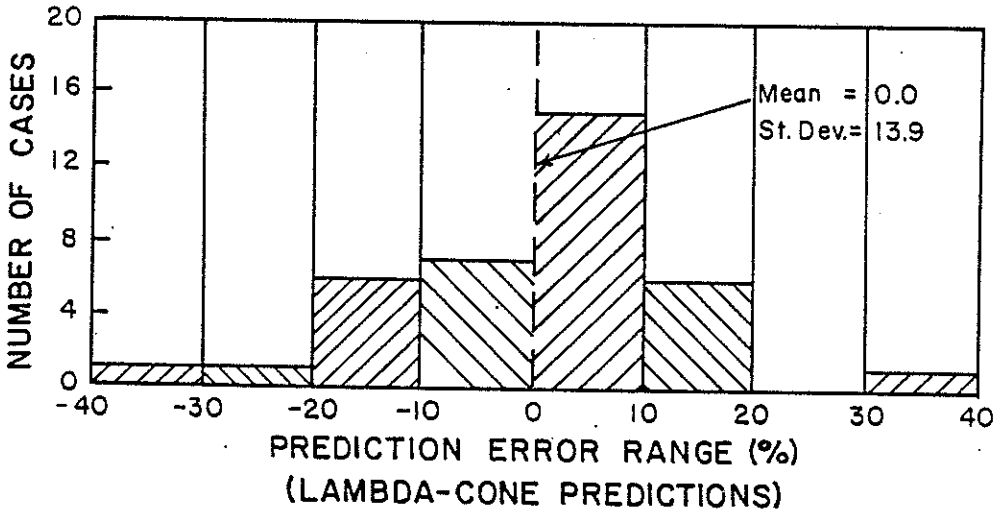

Figure 6.14 The Prediction Error Results
(Lambda-Cone Method)

The ultimate load capacity (Q_u) of the test piles was computed by summing the tip bearing capacity (Q_t) calculated by the expression 6.1 and the frictional capacity was predicted by the Lambda-Cone Method. The pile penetration factor (λ_c) was determined by Equation 6.7. The results are given in Fig. 6.13 which indicate accurate predictions of the ultimate loads by this procedure. The algebraic mean of the prediction errors was 0.0% with a standard deviation of 13.9% (see Fig. 6.14). This proves that the Lambda-Cone can be regarded as a reliable procedure for computing pile capacity in cohesive soils.

Although the predictions made by the Cone-m and Lambda-Cone procedures were in close agreement with the measured values, it was essential to compare the results with the predictions based on the available static analysis techniques. Three procedures, the Alpha Method, Lambda Method and Beta Method were chosen.

6.3.3 Pile Capacity Prediction by the Alpha Method

The ultimate load capacity (Q_u) of the test piles was determined by the static analysis technique called Alpha Method suggested by Tomlinson (1957). The procedure is discussed in Chapter 3 which suggested the following analysis to compute Q_u:

$$Q_u = Q_t + Q_s \tag{6.9}$$

where

$$Q_t = 9 \times A_t \times \bar{C}_u \tag{6.10}$$

$$Q_s = P \times L \times \alpha \times C_u \tag{6.11}$$

The adhesion factor (α) was obtained from Tomlinson's proposed relationship presented in Fig. 3.4. The plot of the predicted versus the measured values is given in Fig. 6.15. It appears that the method results in conservative predictions. This is further illustrated in Fig. 6.16

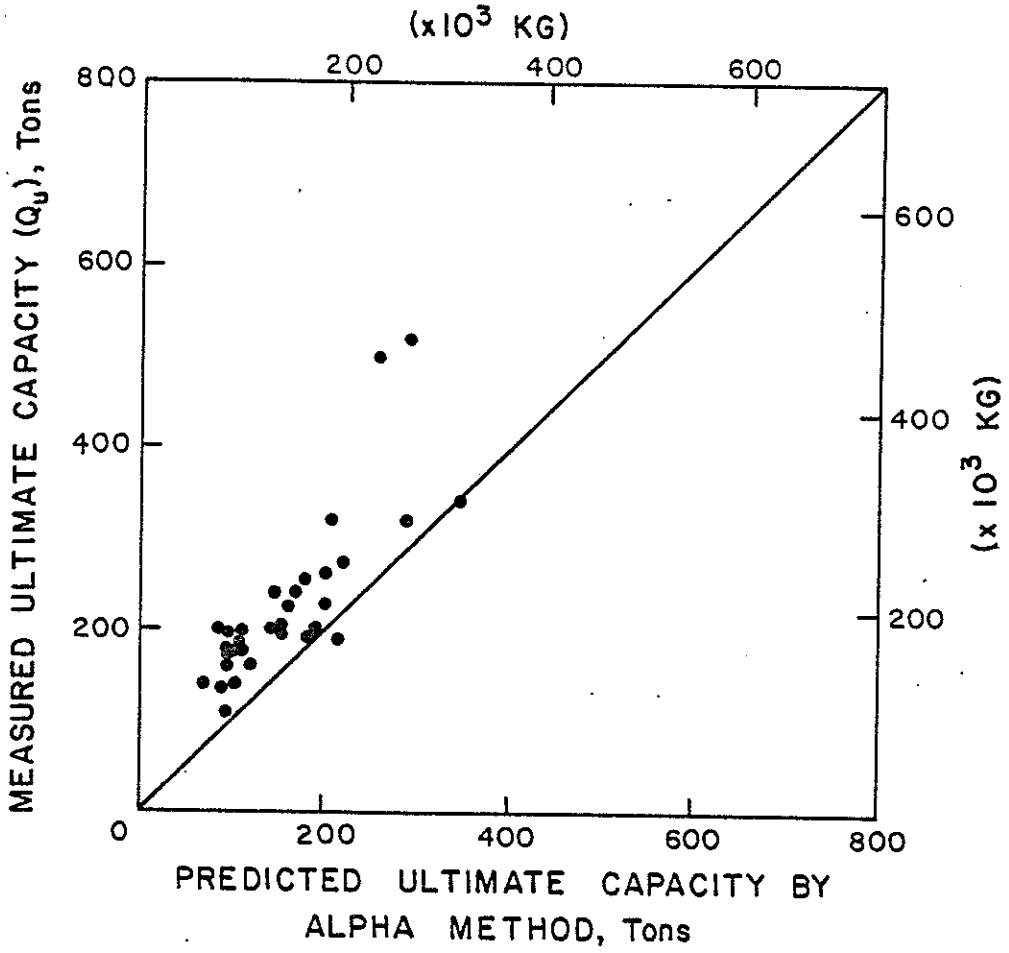

Figure 6.15 The Pile Capacity Predictions by the Alpha Method

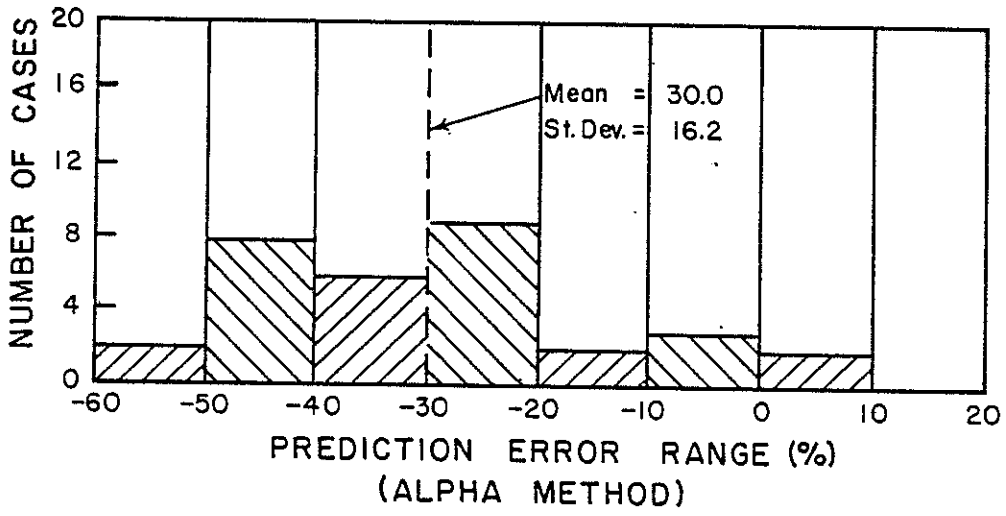

Figure 6.16 The Prediction Error Results
(Alpha Method)

which indicates that the algebraic mean of the prediction errors is -30.0% with a standard deviation of 16.2%. The tip bearing capacity of few test piles had to be predicted from the cone q_c results. This was necessary because those test piles were not driven into pure cohesive soils and the information provided by the conventional subsurface investigation was not sufficient to be used in the classical bearing capacity equations.

6.3.4 Pile Capacity Prediction by the Lambda Method

The ultimate load (Q_u) of the test piles calculated by the Lambda Method recommended by Vijayvergia and Focht (1972). The method is described in Chapter 3 which suggests that

$$Q_u = Q_t + Q_s$$

where

$$Q_t = 9 \times A_t \times \bar{C}_u$$

$$Q_s = \lambda \times P \times L \times (\bar{\sigma}_m + 2\, C_m) \qquad (6.12)$$

The friction factor (λ) values are presented in Fig. 3.6. The predicted versus measured values are shown in Fig. 6.17. It seems that the method provides superior results to the previously mentioned Alpha Method. The prediction errors ranged between -1.0% and +50.0% with an algebraic mean of -0.3% and a standard deviation of 17.8% as shown in Fig. 16.18. The tip bearing capacity of a few test piles had to be estimated by implementing Equation 6.1 for the reasons explained earlier.

6.3.5 Pile Capacity Prediction by Beta Method

The frictional capacity of the test piles was determined by the semi-drained Beta Method suggested by Burland (1973). The procedure is explained in Chapter 3. The method involves the following analysis to compute Q_u:

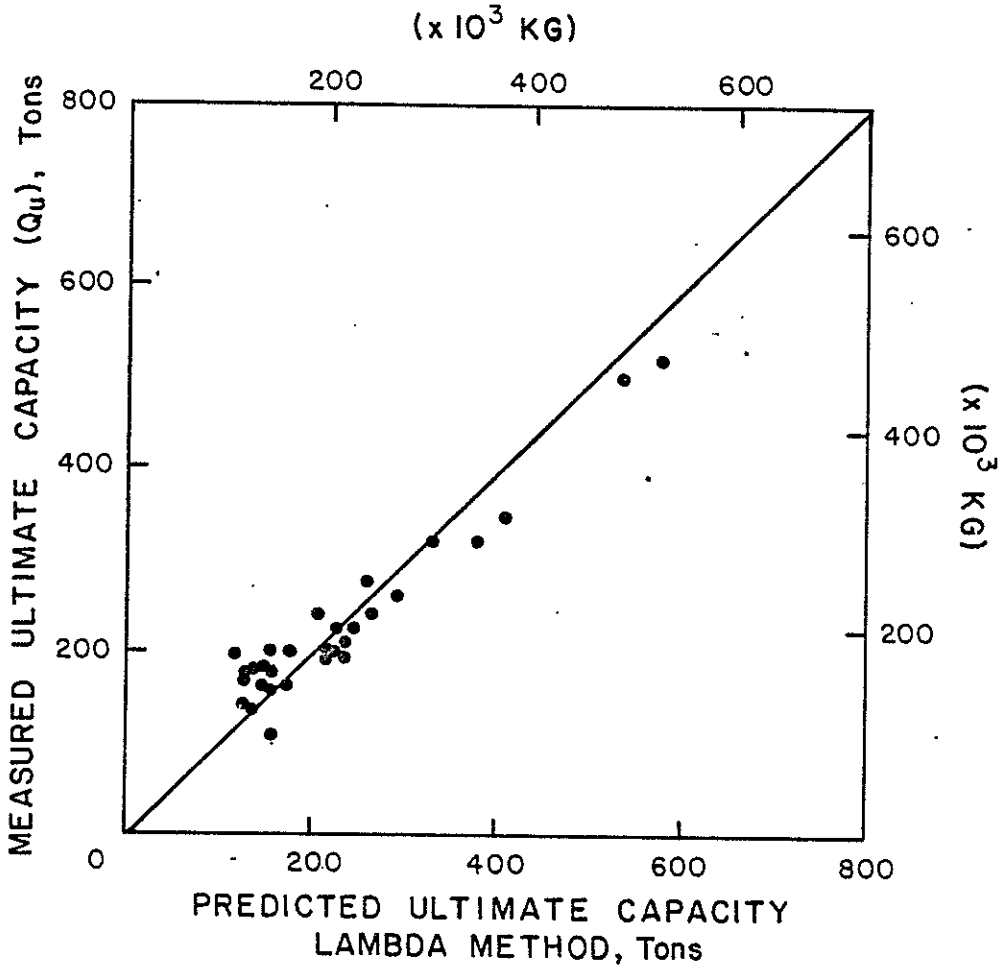

Figure 6.17 Pile Capacity Predictions by the Lambda Method

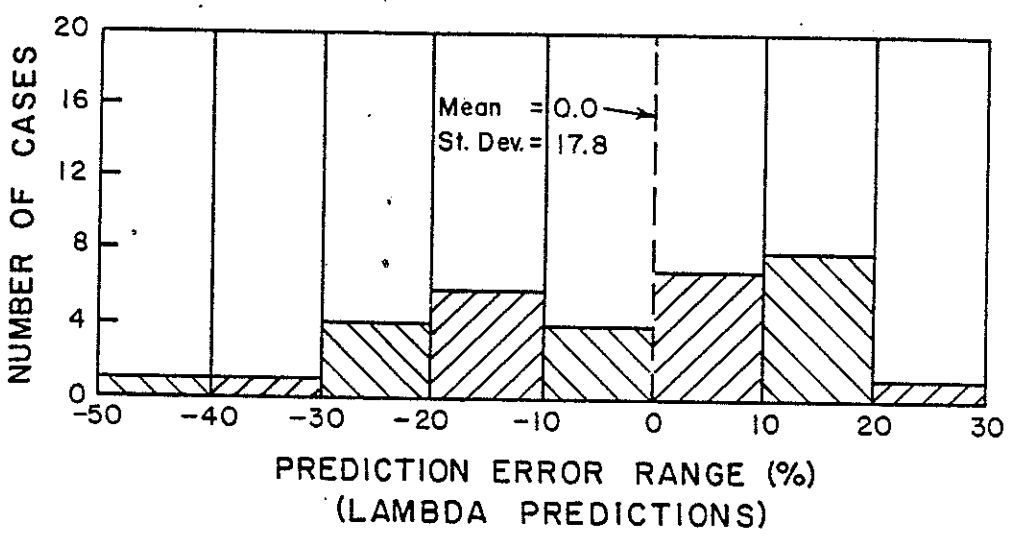

Figure 6.18 The Prediction Error Results
(Lambda Method)

$$Q_u = Q_t + Q_s \tag{6.13}$$

where

$$Q_t = A_t \times q_o \tag{6.14}$$

q_o is calculated from the cone q_c results by utilizing expression 6.1. The frictional capacity (Q_s) is estimated as follows:

$$Q_s = \beta \bar{\sigma}_v$$

where

$$\beta = (1 - \sin \phi_d) \text{ tang } \phi_d$$

in which ϕ_d is the drained angle of friction. The angle of friction (ϕ_d) was determined by using the relationship suggested by Bjerrum and Simons (1960) which is presented in Fig. 6.19. The ultimate load (Q_u) of the test piles were calculated using this procedure. However, it was realized that the analysis resulted in overprediction for long piles and underprediction for short piles. It was noted that the predictions based on this approach had to be corrected by a factor name Chi (χ) which was calculated as follows:

$$\chi = \frac{f \text{ (Measured)}}{f \text{ (predicted by Beta Method)}} \tag{6.15}$$

where f is the average unit pile friction. The plot of the χ values versus pile penetration (L) is given in Fig. 6.20. It is evident that this pile friction factor also depends on the pile penetration length.

The ultimate capacity of the test piles were recalculated by applying both Beta and Chi pile friction factors. This procedure, "Beta-Chi", requires the following analysis to predict total frictional capacity (Q_s) of a pile:

$$Q_s = P \times L \times \chi \times \beta \times \bar{\sigma}_m \tag{6.16}$$

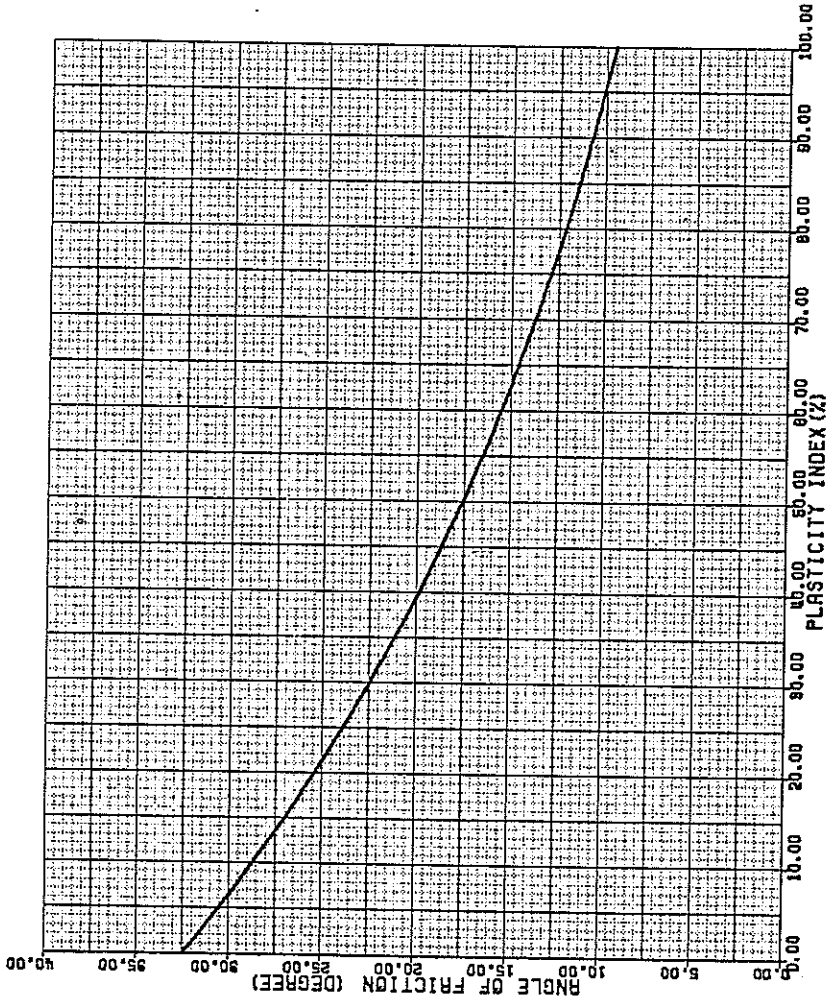

Figure 6.19 Correlation Between Angle of Internal Friction and the Plasticity Index (after Bjerrum and Simons, 1960)

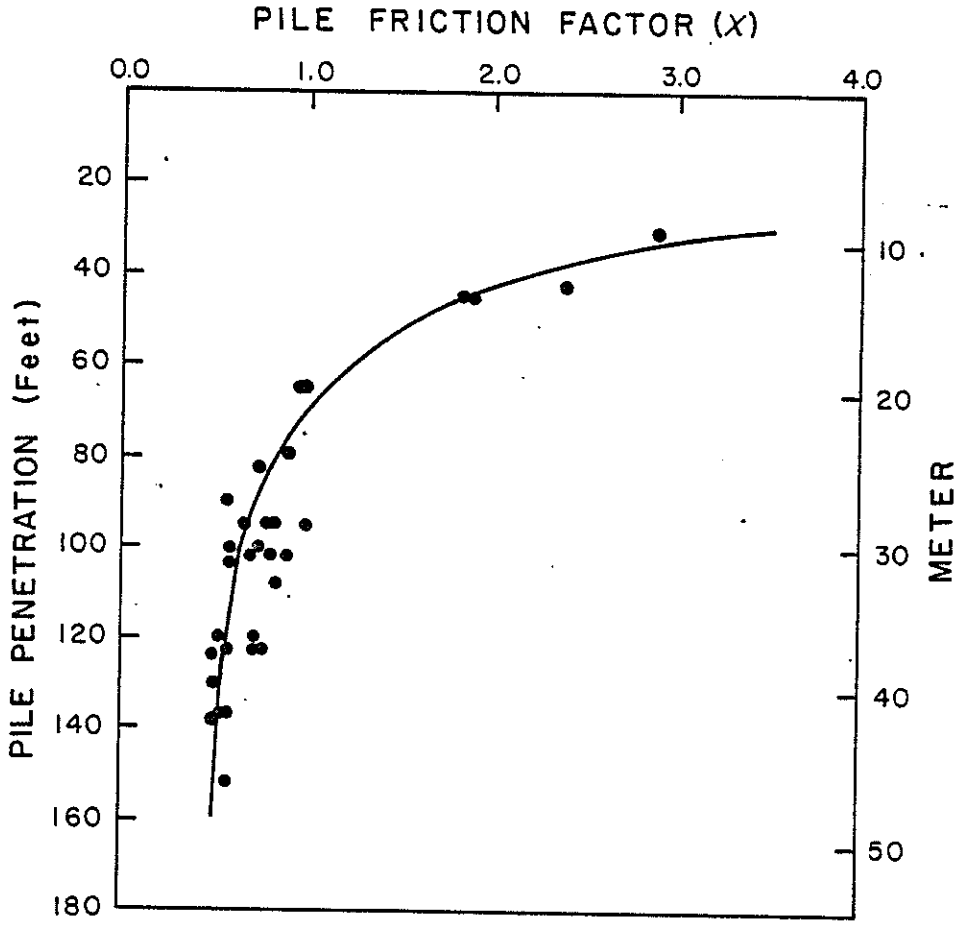

Figure 6.20 The Pile Friction Factor (Chi) Versus the Pile Penetration Length

where

P = pile perimeter

L = pile penetration length

χ = pile friction factor (Fig. 6.20)

$\beta = (1 - \sin \phi_d) \tan \phi_d$

$\bar{\sigma}_m$ = mean effective overburden pressure

The ϕ_d values were estimated by utilizing the relationship given in Fig. 6.19. A weighted average of the plasticity index (PI) values along the pile penetration was computed for determining ϕ_d.

The predicted ultimate loads determined by the Beta-Chi Method versus the measured ultimate loads obtained by test programs are shown in Fig. 6.21. The algebraic mean of the prediction errors is -4.9% with a standard deviation of 13.9% which are presented in Fig. 6.22. The Beta-Chi Method provides reasonable prediction of the ultimate load even though it does not require any knowledge of the shear strength of the soils surrounding a pile. Adoption of such a method would eliminate the need for undisturbed sampling and shear strength testing of soils under consideration. In contrast with other available procedures for calculating the frictional capacity, the method only requires the information about the plasticity index values which are easily obtained from disturbed samples.

6.3.6 Step Taper and Monotube Piles

The step taper and monotube piles were treated in a slightly different manner than the straight edge piles such as pipe piles, etc. For the Cone-m and Alpha Method, a corresponding m or α was applied to $\bar{f}_s$ or $\bar{C}_u$ of a given section for computing the friction capacity (Q_s). However, in the other three methods (Lambda-Cone, Lambda, and Beta-Chi)

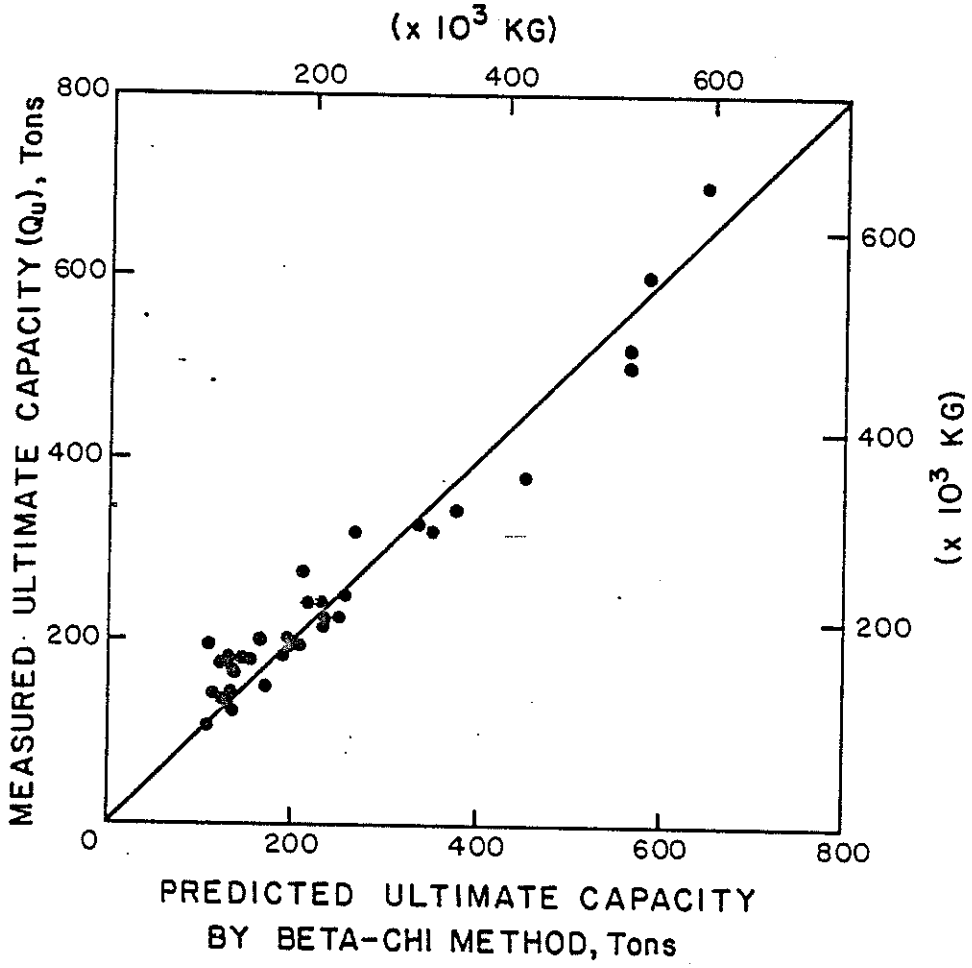

Figure 6.21 Pile Capacity Predictions by the Beta-Chi Method

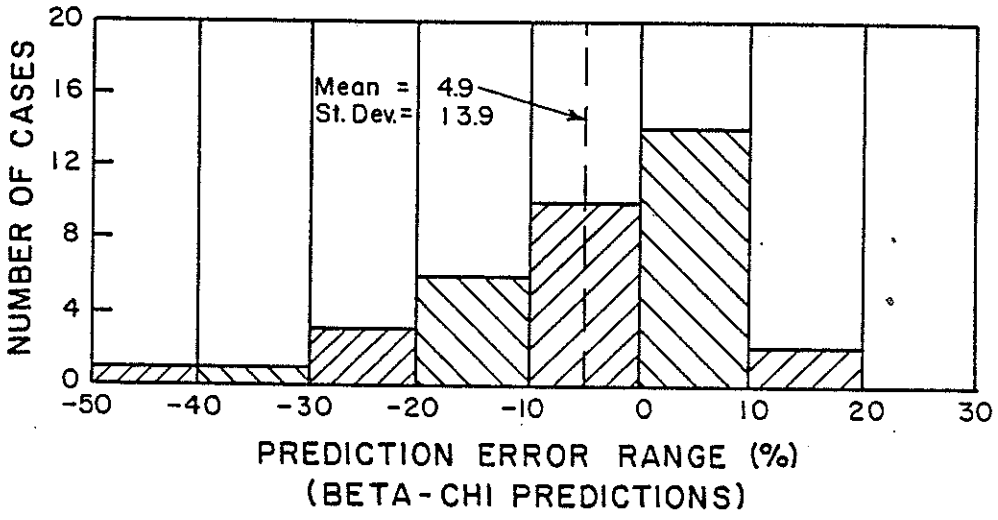

Figure 6.22 The Prediction Error Results
(Beta-Chi Method)

a weighted average of the perimeters was calculated to be used in the unit friction (f) computations. The bearing capacities of the "steps" were ignored and the tip bearing calculations were based on the contribution of the tip only. This approach was adopted for both step taper and monotube test piles. It is believed that the above approach and assumption are correct in cohesive soils. This is due to the fact that the major portion of the load carrying capacity of piles driven in cohesive soils (friction piles) is contributed by the shaft frictional capacity.

6.4 Comparison of the Results

The two proposed procedures for computing the ultimate load of piles driven in cohesive soils, the Cone-m Method and the Lambda-Cone Method, resulted in very close predictions of the measured values. The Alpha Method provided the most conservative predictions. The predictions made by the Lambda Method were also in close agreement with the measured data provided by test pile programs. The Beta-Chi procedure surprisingly resulted in very good estimation of the ultimate loads even though the analysis involved did not require any shear strength data. The prediction quotients were computed for all of the pile capacity determinations made by the mentioned methods. This quotient is expressed as follows:

$$\text{Prediction Quotient} = \frac{\text{Predicted } Q_u}{\text{Measured } Q_u} \qquad (6.17)$$

The ratios were plotted against the pile penetration lengths for predictions made by all of the procedures cited earlier. The results are given in Appendix G. A summary of the results is presented on one page

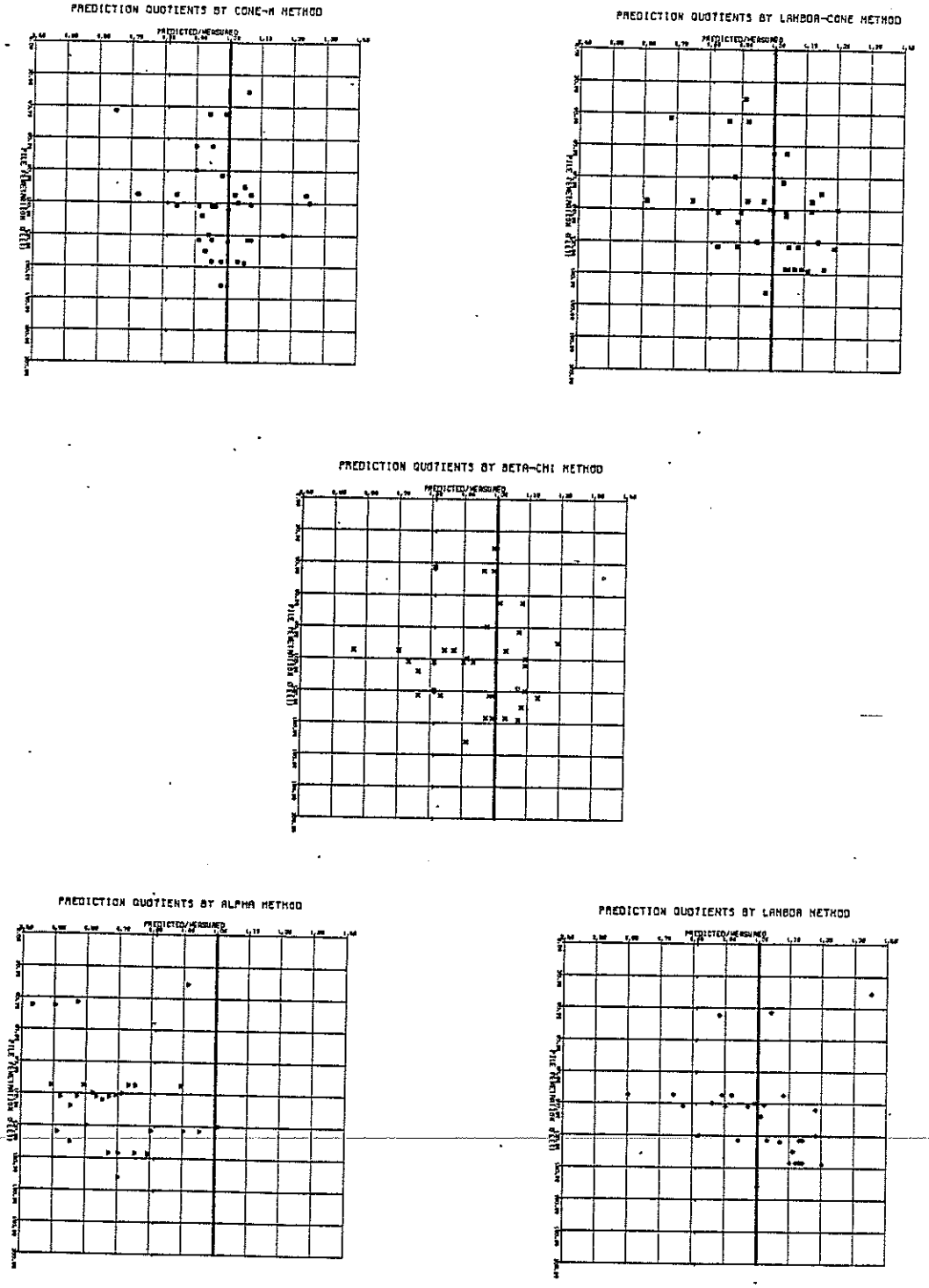

Figure 6.23 Prediction Quotient Results

(Fig. 6.23) for easier comparisons. Further comparisons may be made by referring to Table 6.1. The prediction quotient results also indicate that the Alpha Method provides the most conservative predictions of the test piles' ultimate loads.

Table 6.1

Summary of the Prediction Results

Method Name	Prediction Ratio Results			Mean of Prediction Quotient
	Range (%)	Mean (%)	Standard Deviation (%)	
Cone-m	-35 to 25	- 2.0	11.5	0.997
Lambda-Cone	-38 to 20	0.0	13.9	0.988
Alpha	-57 to 1	-30.0	16.2	0.692
Lambda	-39 to 50	- 0.3	17.8	1.000
Beta-Chi	-44 to 19	- 4.9	13.9	0.943

6.5 The Effects of the Cone Tip Shape and Angle on the QCPT (f_s and q_c) Results

The cone penetration testings were performed using three different tips. However, the findings of this study are based on results obtained by a penetrometer of 60° tip angle and 10 cm^2 base area penetrated at the rate of 2 cm/s. The three types of tips used were (see Fig. 6.24):

1. 60/10: 60° tip angle/10 cm^2 base area
2. 60/18: 18° tip angle/10 cm^2 base area
3. 60/20: 60° tip angle/20 cm^2 base area

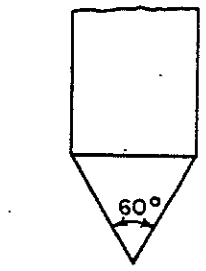

a. 60/10 TIP

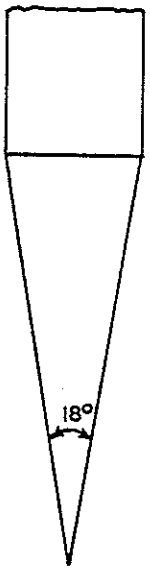

b. 18/10 TIP

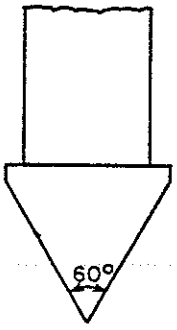

c. 60/20 TIP

Figure 6.24 The Three Types of Tips Used in the Study

The results of the penetrations performed by these tips are given in Appendix E. The influence of the tip angle and shape on q_c and f_s results are discussed separately.

6.5.1 The Effects on the Tip Resistance (q_c)

The q_c values obtained by the three tips generally agree with each other. The "pointed" 18/10 tip's q_c results are not as smooth as those collected by the other two. The "big" 60/20 tip resulted in the smoothest q_c measurements for a given layer. The results of the "regular" 60/10 cone are closer to the "big" tip's q_c values than the 18/10 tip. These differences were not detected in cohesive soils with low q_c values. However, in the case of a sand layer, the 18/10 tip reaches a maximum value faster than the other two and the variations between the q_c values are the greatest. It appears that the 18/10 tip senses and reacts to a layer with high q_c values (i.e., sand) quicker than the other two tips because it is the longest. It should be noted the D_c/d (critical depth/ cone diameter) also influences q_c results. The tip with the smallest D_c/d would reach a maximum q_c value the last. This is in agreement with the fact that the "big" 60/20 with the smallest D_c/d usually reached a maximum q_c the last and gave the smoothest q_c results. The closer D_c/d is to D_c/d_p (critical depth/pile diameter) the better the q_c results correlate with the unit tip bearing capacity (q_o). For this reason, q_c values obtained by the big tip are more indicative of a pile tip bearing capacity than the other two.

6.5.2 The Effects on the Local Friction (f_s)

Contrary to the tip resistance (q_c) results, the tip shape and angle have major effects on the local friction (f_s) data. This is

because f_s readings are influenced by the cavity created by the tip penetration. It should be noted that the f_s values are from soil layers which have been remolded and disturbed by penetration. The cavity created by the tip closes back and the soil grabs the friction sleeve located immediately behind the tip. The level and the intensity of this "grabing" process is influenced by the tip shape which has major effects on the local friction (f_s) readings.

The 18/10 tip opens a cavity which will close back sooner than in the case of the other two tips. This may be due to the fact that this tip has a very sharp pointed front and a smooth transition with the sleeve friction. The f_s values obtained by this tip are usually higher than the f_s readings obtained by the 60/10 tip. The ratio of the f_s values collected by the 18/10 tip, ranged between 1.0 for soft clays to as high as 1.6 for stiff cohesive (clayey) soils (see Appendix H). It appears that in the case of soft soils, the grabing process is independent of the tip shape and angle. However, in the case of the stiff cohesive soils, the cavity created by the penetration will not close back over the full length of the friction sleeve for the 60/10 tip as much as it does for the 18/10 tip.

The f_s readings obtained by the "big" 60/20 tip are not reliable for pile friction estimation. The f_s values obtained by this tip are as low as 10% of the ones obtained by the other two tips regardless of the soil's consistency. Negative total frictions were detected with this tip indicating a layer with negative local friction (f_s) values, which is not possible. This may be attributed to the fact that the friction sleeve of this cone has a diameter much smaller than that of the tip base. The hole created by this tip is large and does not close back over the full length of the friction sleeve.

It is concluded that the q_c values collected by the 60/20 are better indication of the pile capacity. However, the f_s values obtained by this tip need to be studied in further detail. The f_s values gathered by the 18/10 tip are the highest and probably the most representative for a given layer; on the other hand, the q_c values measured by this cone are not as representative as the ones collected by the other two tips. The 60/10 tip which was extensively used in the analysis may be regarded as the "average" tip, compared with the other two. The tip resistance (q_c) values gathered by this tip are as reasonable as the 60/20 tip and the f_s values are as representative as the values obtained by the 18/10 tip. However, the 60/10 tip was the only one that could provide both f_s and q_c values reasonably. A tip of 60° angle and 20 cm^2 base area, coupled with a friction sleeve having a diameter slightly larger than the tip base is recommended for pile capacity prediction. This tip would provide q_c values as representative as the ones obtained by the 60/20 tip for the tip bearing calculations, and f_s readings as reliable as the values obtained by the 60/10 tip for frictional capacity computations. A 60/15 tip has been developed by Fugro which was used recently. The tip provided satisfactory results (Tumay et al., 1981).

6.6 The Unit Pile Friction (f)

It appears that there is an upper and a lower limit for the unit pile friction (f). This argument is further supported by the plot of the actual test piles' unit frictions versus their penetration as shown in Fig. 6.25. The range is between 0.30 tsf to 0.65 tsf. This may be the reason attributing to the shape and trend of the adhesion curve, m.

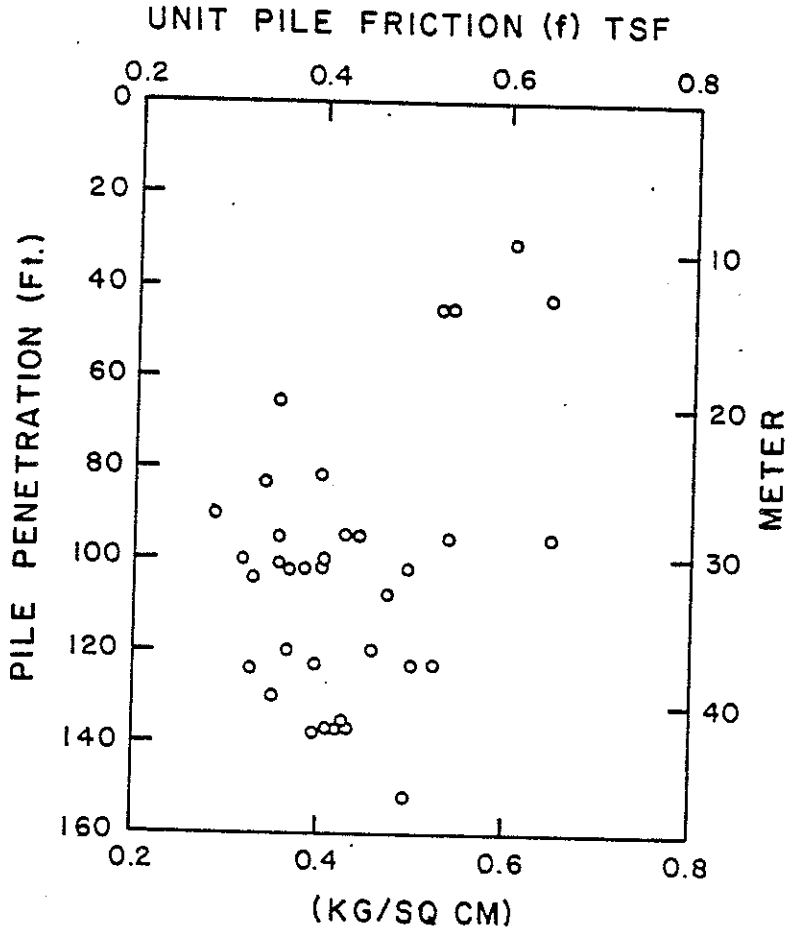

Figure 6.25 Range of the Average Unit Friction (f) of the Test Piles

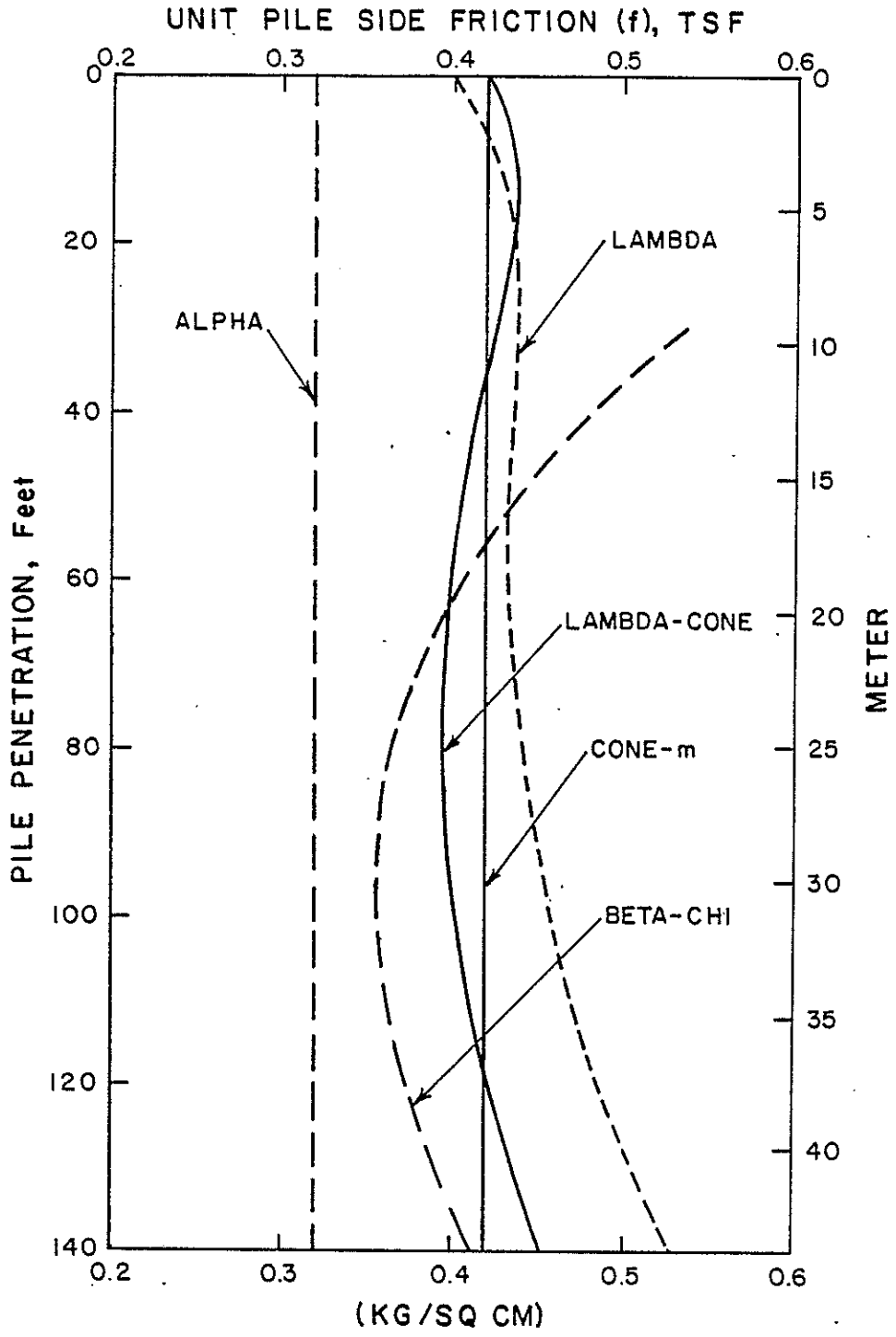

Figure 6.26 The Average Unit Pile Friction (f) Versus Pile Penetration Length (New Orleans IIA Site)

The shape and the trend which resembles other adhesion curves, such as the one proposed by Tomlinson (1957). The m and α values are such that f cannot take a magnitude out of a certain range. This range is usually taken between 0.25 tsf to 0.75 tsf as recommended by many engineers. The adhesion (f) values calculated by Tomlinson's α factor ($f = \alpha C_u$) implies an upper limit of 0.50 tsf for all piles. The upper limit adopted for f values obtained by the Cone-m Method is 0.75 tsf as given by expression 6.4. The f values obtained by the Cone-m method are independent of the pile penetration length. The average unit friction (f) computed by the Alpha Method is also independent of the pile length and values depend only on the undrained cohesion (C_u) of the soil. The Cone-m Method is very similar to the Alpha Method except for the fact that in the former, the cone (f_s) values are utilized instead of the undrained cohesion (C_u) data, and the adhesion factor α is replaced by m.

The Lambda-Cone and the Lambda Methods are similar to each other and the average unit friction (f) calculated by these two procedures do depend on pile penetration length (L). The unit friction (f) computed by these two methods increases with larger pile penetration. This is due to increase in the $\bar{\sigma}_m$ term with increase in depth. On the other hand, the pile friction factors λ_c and λ, decrease with depth, preventing f from taking a value outside its range. This is also true for the Beta-Chi Method in which the term χ also decreases with increasing pile penetration, keeping f in its acceptable range. The summary of the unit pile friction (f) versus pile penetration calculated by the five different procedures used in this study is shown in Fig. 6.26. The mean undrained cohesion and the average local friction (f_s) for this site

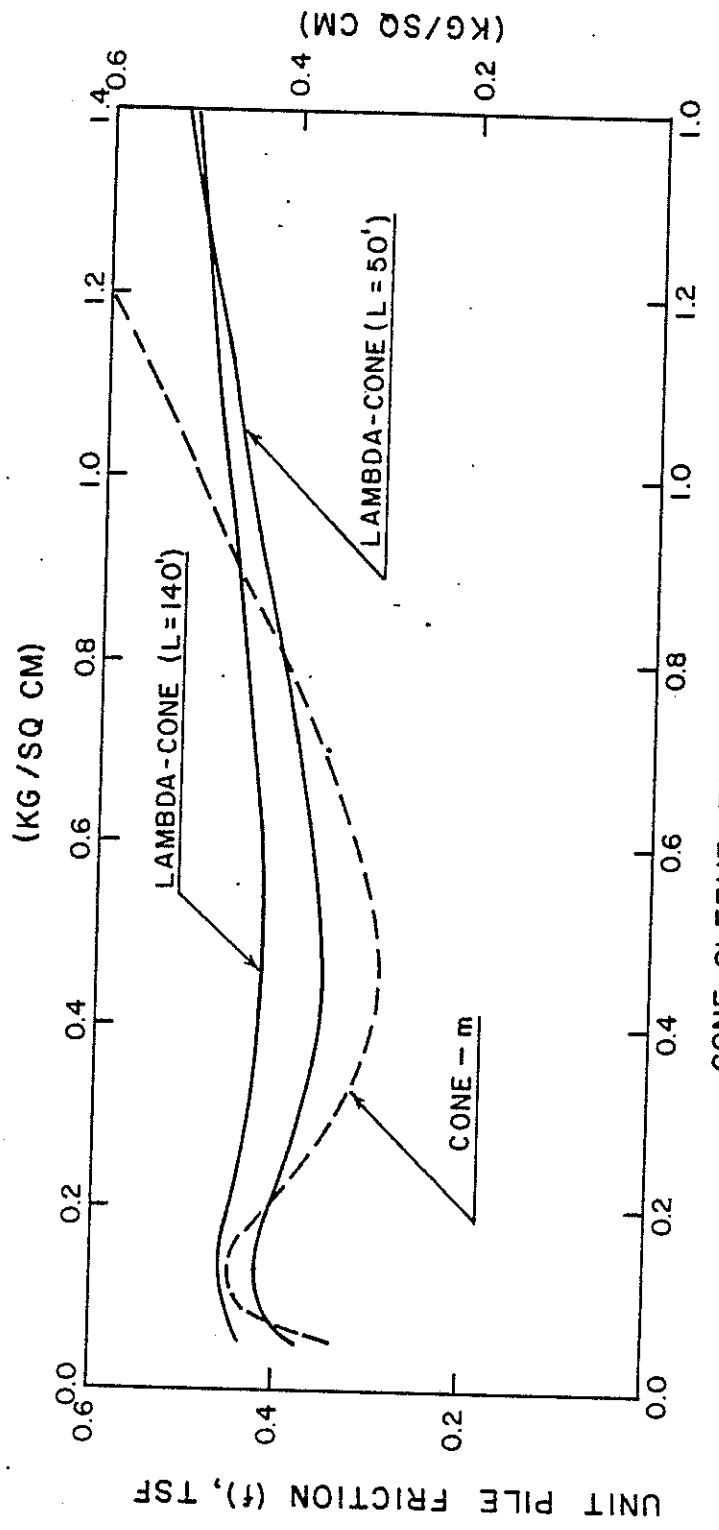

Figure 6.27 The Unit Pile Friction Versus Cone Sleeve Friction (Cone-m and Lambda-Cone Methods)

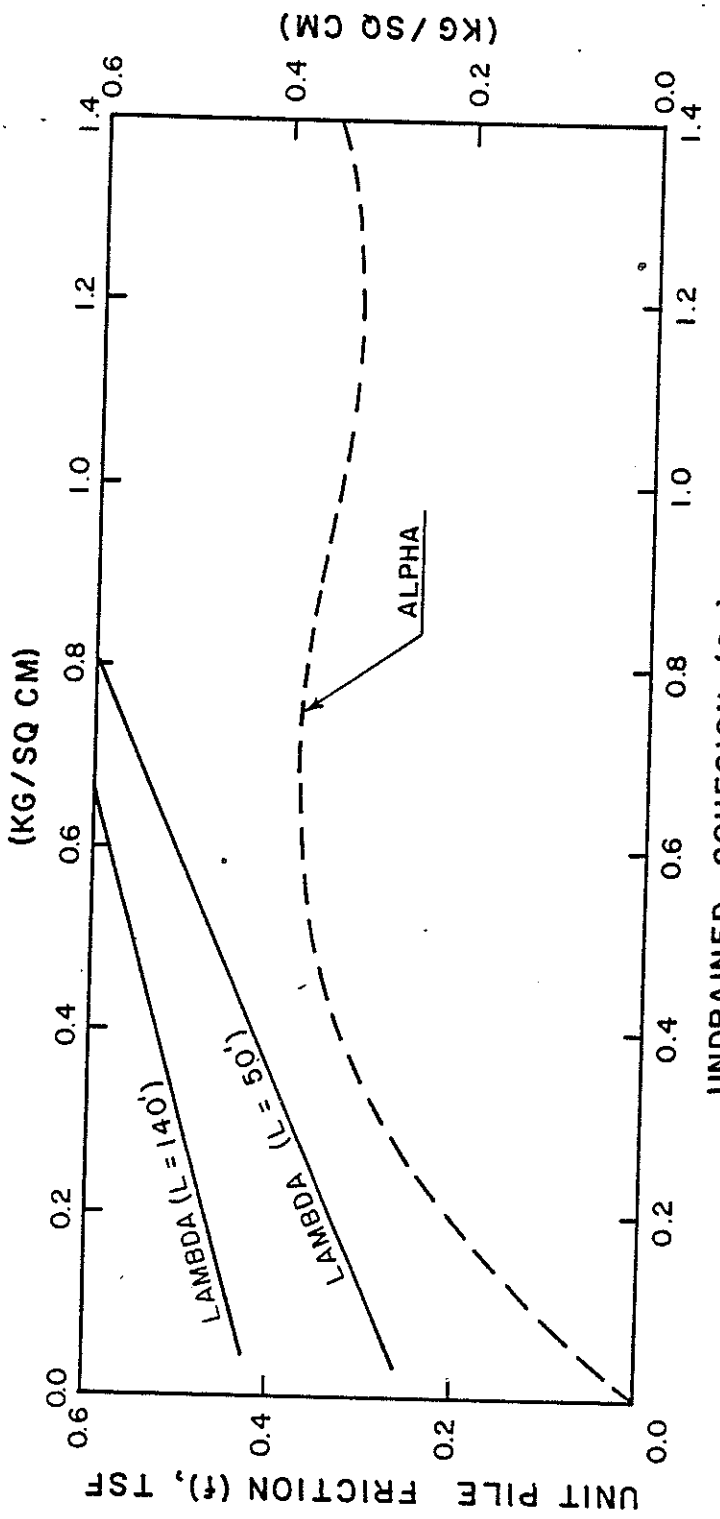

Figure 6.28 The Unit Pile Friction Versus Undrained Cohesion (Alpha and Lambda Methods)

(New Orleans IIA) are 0.40 tsf and 0.20 tsf, respectively. The pile unit friction (f) is 0.32 tsf as determined by the Alpha Method or 0.42 tsf as computed by applying the adhesion factor (m) of the Cone-m Method. These unit friction values are independent of the pile length. However, the f values computed by the Lambda-Cone, Lambda and the Beta-Chi Methods vary with depth. Interestingly, it can be noted that although the procedures are based on different approaches and theories, the unit frictions computed by the methods for different pile lengths are generally in agreement as depicted in Fig. 6.26.

The unit frictions (f) computed by the Cone-m and Lambda-Cone Methods were compared with respect to variations in shear strength. The f values computed by the Cone-m Method ($f = m \times \bar{f}_s$) were compared with f values obtained by the Lambda-Cone Method for two different pile penetrations of 50 and 140 feet. It appears that the unit frictions obtained by the two procedures are in agreement with each other regardless of the soil's shear strength as shown in Fig. 6.27.

The f values determined by the Alpha and Lambda Methods were also compared with respect to variations in soils' shear strength. The agreements are generally good for soils of low shear strength. However, in the case of stiff soils, the values of f computed by the Lambda Method are much higher, as shown in Fig. 6.28. Evidently, the Lambda Method results in overprediction of the frictional capacity of piles driven in stiff cohesive soils.

As mentioned earlier, the Alpha Method results in underprediction of the pile frictional capacity. The algebraic mean of prediction errors and the mean of prediction quotients were -30.0% and 0.692, respectively. The conservative predictions made by this method may be

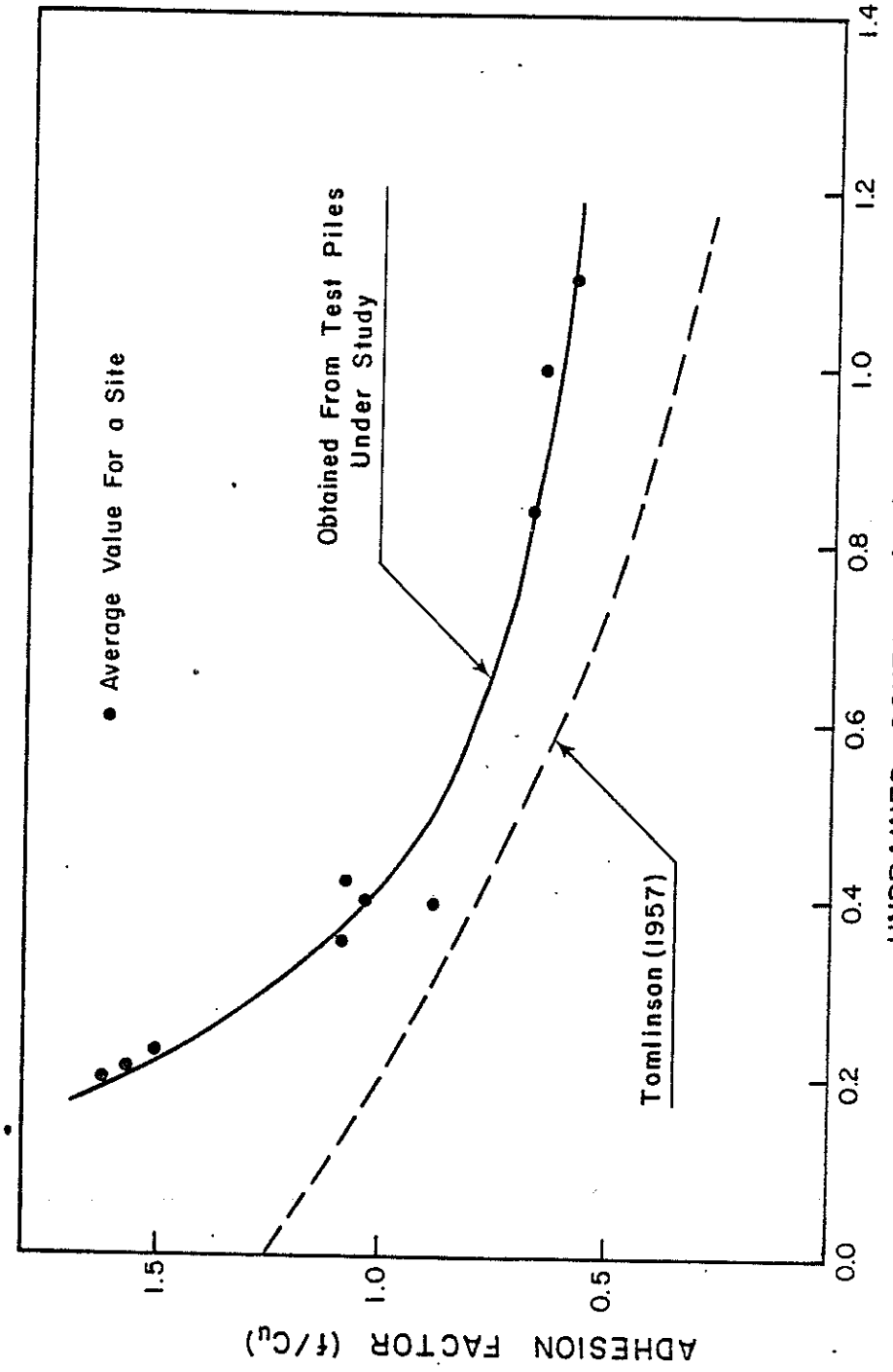

Figure 6.29 Adhesion Factor Values Obtained from the Test Pile Programs

attributed to the fact that the adhesion factor α should take higher values in the case of soft soils. The matter is further clarified by plotting the adhesion factors obtained from the test piles, versus the mean undrained cohesion of the sites investigated in this study. The adhesion factor (α) curve is also presented in Fig. 6.29. It is evident that the measured adhesion factors are much higher than the α factors in the case soft cohesive soils. The measured adhesion factors take values of greater than one which is contrary to the belief of many engineers. The adhesion factor is not allowed to be greater than "one" because the limiting value of the unit friction f is set equal to the undrained cohesion C_u. The argument is valid, however; it should be noted that the adhesion factors are evaluated based on the undisturbed undrained cohesion. In reality, the capacity of a pile is controlled by the remolded soils of the disturbed zone created by pile driving. The pile driving action generates excess pore pressures which, after dissipation, increases the strength of the soils surrounding the pile shaft. The process is only prominant in the case of soft cohesive soils with undrained cohesion of less than 0.40 tsf. This fact is further illustrated in Fig. 6.30 in which

C_1 = undrained cohesion before pile driving (undisturbed)

f_1 = adhesion of a soil with cohesion of C_1

C_2 = undrained cohesion after pile driving

f_2 = adhesion of a soil with cohesion of C_2

Before the pile is driven the limiting value for f_1 is C_1. Consequently, it is true that the adhesion factor (α) cannot take a value greater than "one." However, after the excess pore pressures have dissipated, the soil becomes stronger as the result of the

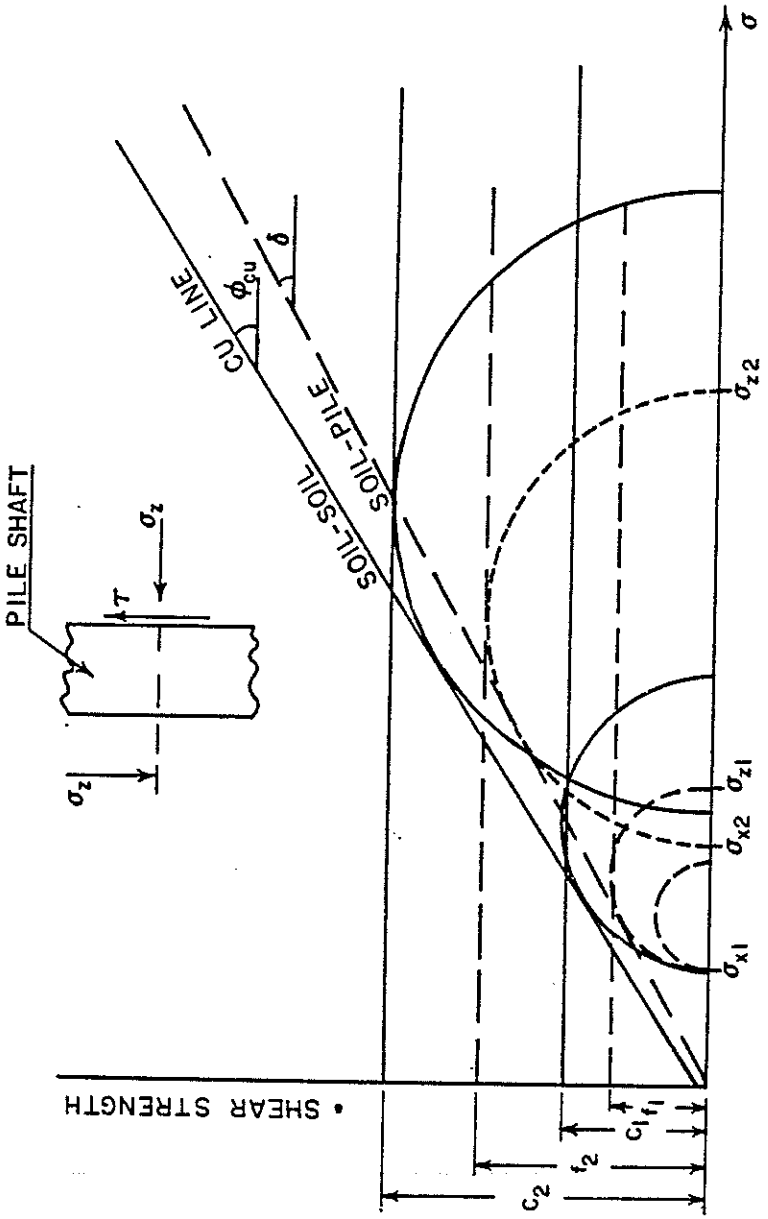

Figure 6.30 Gain in Strength of Soft Cohesive Soils Due to the Pile Driving

reconsolidation/densification process. The process is similar to the consolidated undrained (CU) condition. The pile driving increases the vertical and horizontal stresses in the soils around the pile shaft. The increase in stresses generate excess pore pressures which set up a consolidation process. After the excess pore pressures have dissipated, the surrounding soils gain in strength (C_1 increases to C_2) because of the reconsolidation/densification action. A pile testing program is performed a few weeks after a pile is driven. The frictional capacity is probably controlled by the new shear strength, C_2, and the corresponding adhesion f_2 is limited by C_2 (after pile driving) rather than C_1 (undisturbed). The adhesion factor curves are based on the undisturbed shear strength (C_1) rather than C_2 which contributes to the load carrying capacity of a pile. The reason for the measured adhesion factors taking values greater than "one" (contrary to theory) is that f_2 may be greater than C_1 due to the cited consolidation (gain in strength) process. The limiting factor for the "real" adhesion is post pile driving cohesion (C_2) rather than the pre pile driving cohesion (C_1). It should be stated here that this consideration is significant only in soft cohesive soils.

6.7 Practical Application of the Proposed QCPT Methods in Pile Capacity Prediction

A test pile program is required for accurate measurement of pile capacity due to the uncertainties associated with the present static analysis techniques. The difficulties involved with using the bearing capacity equations for pile tip bearing capacity occur more in the case of sandy soils than in clayey soils. The test pile programs are not only used to determine the load-settlement characteristics, but also to

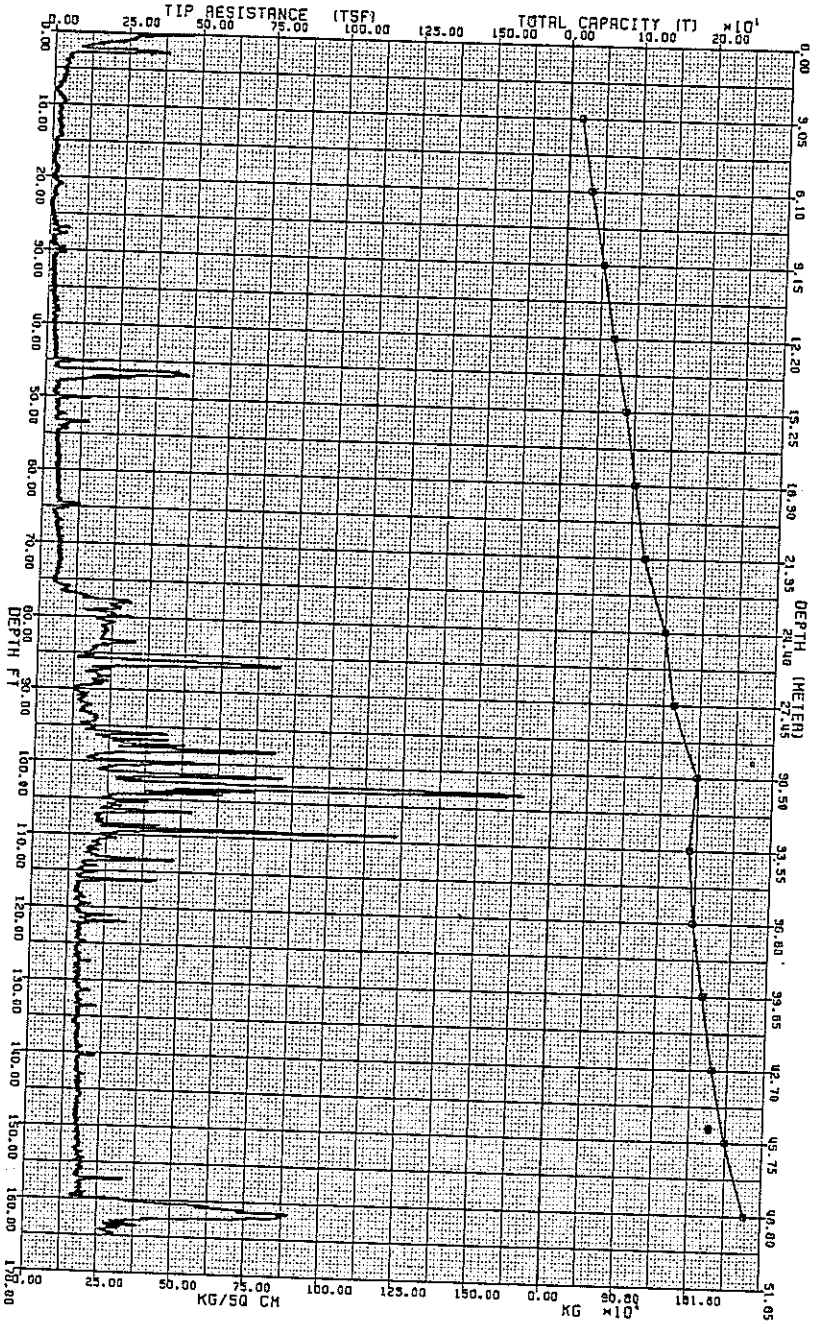

Figure 6.31 Ultimate Pile Capacity Versus Pile Penetration (by the Cone-m Method)

choose the most efficient type and size of pile. The process is costly, time consuming, and performed after or while the project is in progress.

An attempt was made to simulate the function of a test pile program by applying QCPT data in conjunction with the proposed Cone-m Method. The ultimate capacity of a 14.0 inch diameter pipe pile was calculated versus depth at the New Orleans (IIA) Site. The tip bearing capacity was calculated using the expression 6.1 and the frictional capacity was determined by utilizing the adhesion factor, m (Fig. 6.6). The pile penetration length was increased in 10 foot intervals, and the corresponding ultimate loads (Q_u) were computed. In reality, there is a 14.0 inch diameter pile driven to a depth of 103 feet in the New Orleans (IIA) Site. This test pile actually failed under a 200 T of load which is equal to the ultimate load predicted by the Cone-m Method as shown in Fig. 6.31. The same type of analysis may be conducted by utilizing the Lambda-Cone Method.

Presently, the ultimate load capacity versus penetration depth determinations are based on the driving resistance records (blow counts/foot) used in conjunction with a dynamic pile capacity analysis such as the Engineering News Formula. Due to the uncertainties associated with this and other similar procedures, a high factor of safety is usually adopted. The factor of safety applied to a static analysis technique is usually taken as 2.5. This is in addition to the "built-in" factor of safety as part of the analysis, due to the conservative determination of the adhesion factors used to calculate the frictional capacity. As mentioned earlier, the Alpha Method resulted in underprediction of the ultimate loads. The mean of the prediction quotients was 0.692 (for the alpha method) which indicates a "built-in" factor of safety of more than

1.4 (1/0.692). Thus, the real factor of safety adopted is 3.50 (2.5 x 1.4). The higher the factor of safety, the more money and piles required to finish a project. A higher factor of safety also means more confidence in the safe performance of a structure. It should be stated that when predictions are good and uncertainties are minimum, a smaller factor of safety may be considered. A test pile program leaves little doubt with regard to the magnitude of pile failure load. In light of the close predictions made by the Cone-m and the Lambda-Cone Methods, a factor of safety of 2.0 is recommended for computing the allowable load. This suggeston is further supported by the fact that under the allowable loads computed by a factor of safety of 2.0, the average settlement of the test piles is 0.15 inch. This settlement is only 15% of the settlement of 1.0 inch accepted widely to be the failure condition. It is also concluded that with regard to settlement tolerance, the factor of safety is more than 6 (1.0/0.15) under the recommended allowable load ($Q_u/2.0$).

The depth of the cone penetration tests were controlled by length of the longest test pile presented at a site in this study. In practice, this information is not available because the problem is to determine the pile length. The function of the cone penetraton testing is to determine the length of a pile(s) capable of carrying the imposed loading. The length of a pile is computed by utilizing the QCPT data in conjunction with one of the suggested Cone-m or Lambda-Cone Methods. Sufficient amounts of data must be collected to conduct such analysis. The required cone penetration testing depth (CPTD) may be determined in feet by the following equation:

$$CPTD = \frac{Q_a \times F.S.}{p \times 0.30} \qquad (6.18)$$

where

Q_a = allowable pile load (T)

F.S. = factor of safety

p = assumed pile perimeter (ft)

The unit friction (f) is taken as low as possible (f = 0.30 tsf) to ensure adequate amount of penetration. The tip bearing capacity is ignored for further assurance against lack of CPT data to perform a sound pile capacity calculation.

6.8 Summary

The ultimate bearing capacity of a pile can be predicted by utilizing the QCPT data. The tip bearing capacity may be estimated by a procedure similar to the ones suggested for sandy soils. Two procedures were suggested for computing the frictional capacity. The two procedures are the Cone-m Method and the Lambda-Cone Method. Both procedures provide very close predictions of the ultimate loads. Two existing static analysis techniques were also investigated: the Alpha Method and the Lambda Method. The former resulted in conservative, and the latter in close predictions of the test pile's ultimate loads. A modified version of the Beta Method was introduced which provided reliable pile capacity estimations. This method was named Beta-Chi. It was concluded that the undrained cohesion can be estimated from the cone local friction (f_s) data with reasonable accuracy. A cone tip of 60° angle and 20 cm^2 base area in conjunction with a friction sleeve having a diameter slightly larger than the tip base is recommended to be used in pile capacity analysis.

A factor of safety of 2.0 may be adopted when any of the two cone procedures is applied. The QCPT data can be utilized to determine the length and the most efficient type of pile to be used in a project. This is presently done by performing test pile programs. It is believed that analysis involving the utilization of QCPT data in conjunction with the proposed procedures could help minimize the number of test piles required for a project. Further research in this area is strongly recommended. More research may be performed in stiff clays with piles of shorter length which have not been covered extensively in this study.

Chapter 7

CONCLUSIONS

This research has produced several contributions with regard to the use of the electronic cone penetrometer for pile capacity prediction in cohesive soils. Based on the study performed, the following conclusions were drawn:

1. The cone penetration (QCPT) test is capable of providing an in-situ continuous profile of the unit tip bearing capacity (q_o) and the unit pile side friction (f).
2. The tip bearing capacity of piles driven in clays can be predicted by utilizing the cone tip resistance (q_c) data in conjunction with a proposed method similar to that used for sandy soils. The modified version suggested in this study should not cause any major errors for the following reasons:
   a. The cone resistance (q_c) values are low and uniform in cohesive soils. Therefore, regardless of the procedure used, the same unit tip bearing capacity is obtained.
   b. The contribution of the tip bearing capacity to the ultimate load is very little, thus, eliminating the need for precisely determining it.
   c. The pile does not have to be penetrated to a great depth into a cohesive soil layer to make sound correlations between q_c and q_o.

It was also intended to keep the procedure simple and consistant with the available methods.

3. On the average the tip bearing capacity (Q_t) of the test piles comprised only 10% of the total ultimate capacity.

4. The pile frictional capacity may be estimated by a proposed procedure called the Cone-m. The method relates the average unit pile friction to the average f_s readings by an adhesion factor (m). The procedure produced very good results. (The algebraic mean of the prediction errors = -2.0%.)

5. The pile frictional capacity can also be predicted by a recommended procedure called the Lambda-Cone. The method is similar to the one suggested by Vijayvergia and Focht (1972) except that the mean undrained cohesion term is evaluated from the local friction (f_s) data. The procedure employs a pile friction factor (Lambda-Cone) depending on pile length. The predictions made by this method were extremely good. (The algebraic mean of prediction errors = 0.0%.)

6. The undrained cohesion can be related to the average local friction ($\bar{f}_s$) by a factor called n. The shape and the trend of the curve n is very similar to that of the curve m employed in the Cone-m Method.

7. The Alpha Method produced conservative results, especially in soft cohesive soils. (The algebraic mean of the prediction errors = -30.0%.)

8. The adhesion factor should take higher values for soft soils. The factor is not allowed to be greater than "one;" because, the limit of the adhesion is set equal to the undisturbed

undrained cohesion. It is believed that the adhesion is governed by the undrained cohesion of the disturbed soil (after pile driving) rather than that of the undisturbed soil (before pile driving). The pile driving action generates excess pore pressures which set up a consolidation process. The disturbed soils around the pile shaft gain in strength through the reconsolidation process. The magnitude of the adhesion (unit friction) is controlled by the undrained cohesion of the stronger soil, and its value may be greater than the undisturbed cohesion of the soil before pile driving. For this reason, the adhesion factor may take values greater than "one," contrary to common practice. The argument is only valid for soft cohesive soils.

9. The Lambda Method gave close predictions of the ultimate loads. The algebraic mean of the prediction errors was -0.3%. The method produces unconservative results for short piles driven in stiff cohesive soils.

10. The Beta Method produced conservative results for short piles and unconservative results for long piles.

11. The predictions made by the Beta Method had to be corrected by a friction factor depending on the pile length. This factor was called Chi; consequently, the procedure was named Beta-Chi. The method does not require any shear strength data which eliminates the need for the undisturbed samples. However, the plasticity index (PI) values for the soils along the pile shaft is needed. The procedure produced suprisingly good results. (The algebraic mean of the prediction errors = -4.9%.)

12. The Van der Veen's expression can be used to make rational analysis of the load-settlement data provided by load test programs. The ultimate loads obtained by this procedure would cause a plunging type failure of the pile. A pair of points from a load settlement curve may be obtained, and two applications of the expression generate a system of two equations and two unknowns. Solving the system of equations would give the ultimate load (Q_u) and the coefficient of proportionality (r).

13. The ultimate load (Q_u) may be predicted by knowing only one point on the load settlement curve and assuming an average coefficient of proportionality (r). The average r for the test piles under the study was 5.3.

14. The settlement of the test piles under 99% of their ultimate loads was about 1.0 inch (on the average) which is the widely accepted failure criterion.

15. There is an upper and a lower limit for the unit pile friction (f). f ranged between 0.30 tsf to 0.60 tsf, for the test piles under investigation.

16. The unit frictions obtained by the Cone-m Method and the Lambda-Cone Method agreed with each other both with respect to variations in the soil's shear strength and the pile's length.

17. The size and the geometry of the cone tip did not have any significant influence on the cone resistance (q_c) readings. However, q_c values obtained by the "big" 60/20 tip may be considered to be the most reliable for the pile capacity calculations.

18. The cone tip's size and geometry greatly affected the local friction (f_s) measurements. The 60/20 tip provided less reliable local friction data. The 18/10 tip and the 60/10 tip gave reliable f_s readings.

19. A tip of 60° apex angle and 20 cm^2 base area in conjunction with a friction sleeve having a diameter slightly larger than that of the base would give reliable results for pile capacity prediction.

20. The 60/10 tip gives as reliable q_c data as that of the 60/20, and as representative f_s readings as those obtained by the 18/10 tip. The findings of this study were based on a penetrometer of 60° tip angle and 10 cm^2 base area (the 60/10 tip) pushed at the standard rate of 2 cm/s.

21. The ultimate load profile for a given site and pile may be developed by applying either of the two proposed cone procedures. The most efficient type of pile for a particular project can be determined by performing CPT, before the project is undertaken. Presently, this is done by conducting test pile programs which are costly and time consuming. Although the test pile programs cannot be eliminated, reducing the number of test piles required for a project would save a great deal of time and money.

22. A factor of safety of 2.0 may be adopted when either of the proposed cone methods is employed. The test piles settled only 0.15 inch (on the average) under the allowable loads ($Q_u/2.0$) computed by this factor of safety. This amount is only 15% of the 1.0 inch settlement which is the failure

condition widely accepted by the engineers. The commonly assumed factor of safety is 2.5. The 20% reduction in factor of safety (2.5 to 2.0) will lead to savings in money and time without jeoparizing safety.

23. Further study in this area is strongly recommended. More study may be performed in stiff clays and with piles of short lengths which were not covered extensively in this research. The piezo-cone penetration test (PCPT) may be tried in conjunction with such studies to simulate the effects of pore pressures caused by pile driving for a possible drained approach to this problem.

BIBLIOGRAPHY

Al-Awkati, A., "On Problems of Soil Bearing Capacity at Depth," Ph. D. Dissertation, Duke University, Durham, N. C., 1975, 204p.

Alpan, I., "The Empirical Evaluation of the Coefficients K_o and K_{or}," Soils and Foundations, Vol. 7, No. 1, 1967, pp 31-40.

Amar, S. Baquelin, F., Jezequel, J. F. and Le Mehaute, A. "In Situ Shear Resistance of Clays," Proceedings ASCE Specialty Conference on In Situ Measurement of Soil Properties, Raleigh, Vol. I, 1975, pp. 22-45.

Amir, J. M., and Sokolov, M., "Finite Element Analysis of Piles in Expansive Media," Journal of the Geotechnical Engineering Division, ASCE, Vol. 102, No. GT7, July, 1976, pp. 701-719.

Arman, A. and McManis, K.L., "The Effects of Conventional Soil Sampling Methods on the Engineering Properties of Cohesive Soils in Louisiana," Engineering Research Bulletin No. 117, LSU, 1977.

Arman, A., Poplin, J. K. and Ahmad, N., "Evaluation of the Vane Shear Test in Louisiana," Engineering Research Bulletin No. 118, Dec. 1978.

ASTM, Special Procedures for Testing Soil and Rock for Engineering Purposes, ASTM STP 479, 1970, 630 p.

ASTM, "Symposium on Sampling of Soil and Rock," ASTM STP 483, 1970, 193 p.

Bachelier, M., and Parez, L., "Contribution a l etude de la compressibilite a le aide du Penetrometre a cone," Proc. of the 6th Int. Con. Soil Mechanics and found. Eng., Montreal, Vol. 2, 1965, pp. 3-10.

Baladi, G. Y., and Rohani, B., "Elastic-Plastic Model for Saturated Sand," Journal of the Geotechnical Engineering Division, ASCE, Vol. 105, No. GT4, April, 1979, pp. 465-480.

Baligh, M. M., Vivatrat, V., and Ladd, C. C., "Cone Penetration in Soil Profiling," Journal of the Geotechnical Engineering Division, ASCE, Vol. 106, No. GT4, April, 1980, pp. 447-461.

Baligh, M. M., Ladd, C. C., and Vivatrat, V., "Exploration and Evaluation of Engineering Properties of Marine Soils for Foundation Design of Offshore Structures," Sea Grant Project RT-3, MIT and Fugro Inc., Interim Report No. 1, May, 1977, 88p.

Baligh, M. M., "Cavity Expansion in Sands With Curved Envelopes," Journal of the Geotechnical Engineering Division, ASCE, Vol. 102, No. GT11, Nov. 1976, pp 1131-1146.

Baligh, M. M. and Scott, R. F., "Quasi-Static Deep Penetration in Clays", Journal of the Geotechnical Engineering Division, ASCE, Vol. 101, No. GT11, Nov. 1975, pp. 1119-1133.

Baligh, M. M., "Applications of Plasticity Theory to Selected Problems in Soil Mechanics," Soil Mechanics Laboratory Report, California Institute of Technology, Pasadena, California, 1972.

Baligh, M. M. and Scott, R. F., "Analysis of Wedge Penetration in Clay," Geotechnique, Vol. 26, No. 1, 1976, pp. 185-208.

Baligh, M. M., "Theory of Deep Site Static Cone Penetration Resistance," Res. Report R 75-56, No. 517, Dept. of Civil Engineering, Massachusetts Institute of Technology, 1975, 133 p.

Baquelin, F., Jezequel, J. F., Le Mehaute, A., "Expansion of Cylindrical Probes in Cohesive Soils," Journal of the Soil Mechanics and Foundation Division, ASCE, Vol. 98, No SM11, Nov. 1972 pp. 1129-1142.

Begemann, H.K.S., "The Friction Jacket Cone as an Aid in Determining the Soil Profile", Proceedings of the 6th International Conference on Soil Mechanics and Foundation Engineering, Montreal, Vol.I, 1965, pp. 17-20.

Begemann, H.K.S., "Improved Method of Determining Resistance to Adhesion by Sounding Through a Loose Sleeve Placed Behind the Cone," Proceedings of the 3rd International Conference on Soil Mechanics and Foundation Engineering, Zurich, Vol. 1, 1953, p. 213.

Begemann, H.K.S., "The Use of the Static Penetrometer in Holland," New Zealand Engineering, Vol. 18, No. 2, 1963, p. 41.

Begemann, H.K.S., "The Maximum Pulling Force on a Single Tension Pile Calculated on the Basis of Results of the Adhesion Jacket Cone," Proceedings of the 6th International Conference on Soil Mechanics and Foundation Engineering, Montreal, Vol. 2, 1965, p. 229.

Begemann, H. K. S. Ph. (1969a), "The Dutch Static Penetration Test With The Adhesion Jacket Cone," Lab. Voor Grondmechanica, Delft, Medad. XII, No. 4, p. 69.

Begemann, H. K. S. Ph. (1969b), "The Dutch Static Penetration Test With The Adhesion Jacket Cone," Lab. Voor Grondmechanica, Delft, Medad., XIII, No. 1, p. 1.

Berezantsen, V. G. and Yaroshenko, V. A., "Osobennosti Deporмirovania Peschanych Osnovanii pod Fundamentani Glubokogo Zalozhenia," Osnovaniya i Fundamenty, Vol. 4, No. 1, 1962, pp. 3-7.

Berre, T. and Bjerrum, L., "Shear Strength of Normally Consolidated Clays," Proceedings of the 8th International Conference on Soil Mechanical and Foundation Engineering, Moscow, Vol. 1.1, 1973, pp 39-49.

Bishop, A. W., "Shear Strength Parameters for Undisturbed and Remoulded Soil Specimens," Proceedings Roscoe Memorial Symposium on Stress Strain Behavior of Soils, Cambridge, 1971, pp. 3-58.

Bishop, A. W. and Bjerrum, L., "The Relevance of the Triaxial Test to the Solution of Stability Problems," ASCE, Research Conference on the Shear Strength of Cohesive Soils, Boulder, Colorado, 1960, pp. 503-532.

Bishop, R. F., Hill, R. and Mott, N. F., "Theory of Indentation and Hardness Tests," Proceedings of the Physical Society, Vol. 57, Part III, 1945, p. 147.

Bjerrum, L., and N. E. Simons (1960), "Comparison of Shear Strength Characteristics of Normally Consolidated Clays," Proceedings, First ASCE Specialty Conference, pp. 711-726.

Bjerrum, L., "Problems of Soil Mechanics and Construction on Soft Clays, State-of-the-Art Rep. Proceedings of the 8th International Conference on Soil Mechanics and Foundation Engineering, Moscow, Vol. 3, 1973, pp. 111-159.

Bjerrum, L. and Landva, A., "Direct Simple Shear Test on Norwegian Quick Clay," Geotechnique, Vol. 16, No. 1, 1966, pp. 1-20.

Bjerrum, L., and Simono, N., "Comparison of Shear Strength Characteristics of Normally Consolidated Clays," Proc. of ASCE Research Conference on Shear Strength of Cohesive Soils, Boulder, 1960, pp. 711.

Bjerrum, L., "Engineering Geology of Norwegian Normally Consolidated Marine Clays as Related to Settlements of Buildings," 7th Rankine Lecture, Geotechnique, Vol. 17, No. 2, 1967, pp. 81-118.

Bjerrum, L. (1972), "Membankment on Soft Ground," Proceedings of the Specialty Conference on Performance of Earth and Earth - Supported Structures, ASCE, Purdue University, Vol. 2, p. 1.

Bjerrum, L., "Problems of Soil Mechanics and Construction of Soft Clays," State-of-the-Art Report, Session 4, Proceedings of the 8th International Conference on Soil Mechanics and Foundation Engineering, Moscow, Vol.3, 1973, pp. 109-159.

Bogdanovic, L., "The Use of Penetration Test for Determining the Bearing Capacity of Piles," Proceeding of the 5th International Conference on Soil Mechanics and Foundation Engineering, Paris, Vol. 2, 1961, p. 17.

Brand, E. W., Moh, Z-C., and Wirojanagud, P., "Interpretation of Such Cone Test in Soft Bankok Clay", ESOPT, Vol. 2:2, 1974, pp. 51-58.

Brooker, E. W., and Ireland, H. O., "Earth Pressures at Rest Related to Stress History," Canadian Geotechnical Journal, Vol. 2, No. 1, Feb. 1965, pp. 1-15.

Burland, J. (1973), "Shaft Friction of Piles in Clay--A Simple Fundamental Approach," Ground Engineering, Vol. 6, No. 3, p. 30.

Butterfield, R., and Andrawes, K. Z., "An Investigation of a Plane Strain Continuous Penetration Problem," Geotechnique, Vol. 12, No. 4, Dec., 1972, pp 597-617.

Casagrande, A. and Rutledge, P.C., "Cooperative Triaxial Shear Research," Waterways Experiment Station, Vicksburg, Miss., 1947.

Casagrande, A. and Wilson, S., "Effect of Rate of Loading on Strength of Clays and Shales at Constant Water Content," Geotechnique, Vol. 2, No. 3, pp 251-263.

Casagrande, A., "The Determination of the Pre-Consolidation Load and Its Practical Significance," Proceedings of the 1st International Conference on Soil Mechanics and Foundation Engineering, Cambridge, Mass, Vol. 3, 1936, pp. 60-64.

Chadwick, P., "The Quasi-Static Expansion of Spherical Cavity in Metals and Ideal Soils," Quarterly Journal of Mechanics and Applied Mathematics, Vol. 12, Pt.1, 1959, pp. 52-71.

Chellis, R. D. (1951), Pile Foundations, 1st Edition, McGraw-Hill Book Company Inc., New York, N.Y.

Christian, J. T., "Undrained Stress Distribution by Numerical Methods," Journal of the Soil Mechanics and Foundations Division, ASCE, Vol. 94, No. SM6, Nov., 1968, pp 1333-1345.

Crawford, C. B., "The Influence of Rate of Strain on Effective Stresses in Sensitive Clay," ASTM., STP No. 254, 1959, pp. 36-48.

Crooks, J.H.A. and Graham, J., "Geotechnical Properties of the Belfast Estuarine Deposits," Geotechnique 26, 1976, pp 293-315.

Davis, E. H. and Christian, J. T., "Bearing Capacity of Anisotropic Cohesive Soil," Journal of the Soil Mechanics and Foundation Engineering Division, ASCE, Vol. 97, No. SM5, May 1971, pp. 753-769.

Davis, E. H. and Poulos, H. G., "Laboratory Investigations of the Effects of Sampling," Civil Engineering Transactions, Institute of Engineers, Australia, Vol CE9, No. 1, 1967, pp. 68-94.

Davis, E., "Theories of Plasiticity and the Failure of Soil Masses," Soil Mechanics, Selected Topics. Edited by I.K. Lee, American Elsevier Publishing Co., Inc., New York, 1968, pp. 341-380.

De Beer, E. E., "Bearing Capacity and Settlement of Shallow Foundations on Sand," Symposium on Bearing Capacity and Settlement of Foundations, Duke University, 1965, pp. 15.

De Beer, E. E., Etude des Fondations sur Pilotis et des Foundations Directes, Annales des Travaux Publics de Belgique 46, 1945, pp. 1-78.

De Beer, E. E., "The Scale Effect in the Transposition of the Results of Deep Sounding Tests on the Ultimate Bearing Capacity of Piles and Caisson Foundations," Geotechnique, Vol. 8, No. 1, 1963, p. 39.

DeRuiter, J., "Electric Penetrometer For Site Investigations," Journal of the Soil Mechanics and Foundations Division, ASCE, Vol. 97, No. SM2, Feb. 1971, pp. 457-472.

Desai, C. S., editor, "Applications of the Finite Element Method in Geotechnical Engineering," U. S. Army Engineer Waterways Experiment Station, Vicksburg, Mississippi, May, 1972.

Drnevich, V. P., Gorman, C. T., and Hopkins, T. C., "Shear Strength of Cohesive Soils and Friction Sleeve Resistance", ESOPT, Vol. 2:2, 1974, pp. 129-132.

Drucker, D. C., "Some Implications of Work Hardening and Ideal Plasticity," Applied Mathematics, Vol. 7, No. 4., 1950, pp. 411-418.

Duncan, J. M., and Chang, C. Y. "Nonlinear Analysis of Stress and Stain in Soils," Journal of the Soil Mechanics and Foundations Division, ASCE, Vol. 96, No. SM5, Sept., 1970, pp. 1629-1653.

Duncan, J. M. and Seed, H. B., "Strength Variation Along Failure Surfaces in Clay," Journal of the Soil Mechanics and Foundations Division, ASCE, Vol. 92, SM6, Nov. 1966, pp. 81-104.

Durgunoglu, H. T., "Static Penetration Resistance of Soils", Ph.D. Thesis, University of California, Berkeley, 1972.

ESOPT, Proceedings of the European Symposium on Penetration Testing, Swedish Geotechnical Society, Stockholm, Vol. 2, 1974.

Flatte, K. (1972), "Effects of Pile Driving in Clays," Canadian Geotechnic Journal, Vol. 9, No. 1, p. 81.

Fox, G. W., "Dutch Cone Soundings," Foundation Facts, Vol. 9, No. 1, 1973.

Gibson, R. E. and Anderson, W. F., In Situ Measurements of Soil Properties With the Pressuremeter," Civil Engineering and Public Works Review, Vol. 56, 1961, pp. 615-618.

Gibson, R. E., Discussion, Journal of the Institution of Civil Engineers, Vol. 34, 1950, p. 382.

Girijavallabhan, C. V., and Reese, L. C., "Finite Element Method for Problems in Soil Mechanics," Journal of the Soil Mechanics and Foundation Division ASCE, Vol. 94, No. SM2, March, 1968, pp. 473-496.

Golder, H. Q. and Skampton, A. W., "The Angle of Shearing Resistance in Cohesive Soils for Tests at Constant Water Content", Proceedings of the 2nd International Conference on Soil Mechanics, 1948.

Hartman, J. P., "Finite Element Parametric Study of Vertical Strain Influence Factors and the Pressuremeter Test to Estimate the Settlement of Footing in Sand," Dissertation Presented to the Graduate Council of the University of Florida in partial fulfillment of the requirements for the Degree of Doctor of Philosophy, 1974.

Huizinga, T. K. (1951), "Application of Results of Deep Penetration Tests To Foundation Piles," Building Research Congress, London, Div. 1, Part 3, p. 173.

Henkel, D. J., "Effect of Overconsolidation on Behavior of Clays During Shear," Geotechnique, Vol. 6, No. 4, 1956, pp.

Henkel, D. J., "The Relationships Between the Strength, Pore-Water Pressure and Volume Change Characteristics of Saturated Clays," Geotechnique Vol. 9, No. 3, 1959, pp. 119-135.

Hoeg, K., "Finite Element Analysis of Strain-Softening Clay," Journal of the Soil Mechanics and Foundations Division , ASCE, Vol. 98, No. SM1, January 1972, pp. 43-58.

Hill, R., The Mathematical Theory of Plasticity, The Oxford Engineering Science Series, Clarendon Press, 1950.

Hvorslev, M. H., "Surface Exploration and Sampling of Soils for Civil Engineering Purposes," Waterways Experiment Station, Vicksburg, Mississippi, 1949, 521 p.

Hvorslev, M. J., "Condition of Failure for Remolded Cohesive Soils", Proceedings of the 1st International Conference on Soil Mechanics and Foundation Engineering, Vol. 3, 1936, pp. 51.

Hvorslev, M. J., "Physical Components of the Shear Strength of Saturated Clays," Proc. of ASCE Research Conference on Shear Strength of Cohesive Soils, Boulder, 1960, pp. 169.

Hansen, J. B., and Gibson, R. E., "Undrained Shear Strengths of Anisotropically Consolidated Clays," Geotechnique, Vol. 1, No. 3, 1948, pp. 189-204.

Henkel, D. J., "The Shear Strength of Saturated Remolded Clays," ASCE, Research Conference on the Shear Strength of Cohesive Soils, Boulder, Colorado, 1960, pp. 533-554.

Janbu, N., "The Resistance Concept Applied to Deformation of Soils," Proceedings of the 7th International Conference on Soil Mechanics and Foundation Engineering, Mexico, Vol. 1, 1969, pp. 191-196.

Janbu, N. and Senneset, K., "Effective Stress Interpretation of In Situ Static Penetration Tests," Proceedings of the European Symposium on Penetration Testing, ESOPT, Stockholm, Vol. 2.2, 1974, pp. 181-193.

Janbu, N., and Senneset, K., "Interpretation Procedures For Obtaining Soil Deformation Parameters," British Geotechnical Society, London, Vol. 1, 1979.

Jacky, J., "Pressure in Silos," Proceedings of the 2nd International Conference on Soil Mechanics and Foundation Engineering, Rotterdam, Vol. 1, 1948, pp. 103-107.

Jezuquel, J. F., Mieussens, C., "In-situ Measurement of Coefficient of Permeability and Consolidation in Fine Soils," ASCE Specialty Conference on In-situ Measurement of Soil Properties, North Carolina State University, Raleigh, Vol. 1, 1975, pp. 208-224.

Karafiath, L. L., Discussion, Journal of the Geotechnical Engineering Division, ASCE, Vol. 105, No. GT6, June, 1979, pp. 796-799.

Kerisel, J. (1964), "Deep Foundations Basic Experimental Facts," Proceedings of Conference in Deep Foundations, Mexico City, Vol. 1, p. 7.

Kerisel, J., "Foundation Profondes en milieux sebleux," Proc. of the 5th International Conference on Soil Mechanics and Foundation Engineering, Paris, Vol. 2, 1969, pp. 73.

Kjekstad, O., Lunne, T., and Clausen, C. J. F. "Comparison Between In Situ Cone Resistance and Laboratory Strength for Overconsolidated North Sea Clays," Norwegian Geotechnical Institute, Internal Report No. 124, 1978, pp. 1-4.

Kondner, R. L., "Hyperbolic Stress-Strain Response: Cohesive Soils," Journal of the Soil Mechanics and Foundation Division, ASCE, Vol. 89, No. SM1, Feb. 1963, pp. 115-143.

Krause, E. R. (1973), "The Design of Foundation Piles for Offshore Structure," Technical Publication, Fugro-Cesco, Leidschendam, The Netherlands, Offshore Engineering Department.

Ladanyi, B., "Deep Punching of Sensitive Clays," Proceedings of the Third Pan American Conference on Soil Mechanics and Foundation Engineering, Caracas, Vol. 1, 1967, pp. 533-546.

Ladanyi, B., "Expansion of a Cavity in a Saturated Clay Medium," Journal of the Soil Mechanics and Foundation Division, ASCE, Vol. 89, No. SM4, July 1963, pp. 127-161.

Ladanyi, B., and Eden. W. J., "Use of the Deep Penetration Test in Sensitive Clays," Proceedings of the 7th International Conference on Soil Mechanics and Foundation Engineering, Mexico, Vol. I, 1969, pp. 225-231.

Ladd, C. C. "Discussion to L. Bjerrum: State-of-the-Art Rep. Proceedings of the 8th Int. Conf. on Soil Mechanics and Foundation Engineering, Moscow, Vol. 4.2, 1973, pp. 435-464.

Ladd, C. C. and Foott, R., "New Design Procedure for Stability of Soft Clays," Journal of the Geotechnical Engineering Division, ASCE, Vol. 100, No. GT7, July 1975, pp. 763-786.

Ladd, C. C., and Lambe, T. W., "The Strength of Undisturbed Clay Determined From Undrained Tests," Special Technical Publication No. 361, National Research Council of Canada-American Society of Testing and Materials Symposium on Laboratory Shear Testing of Soils, 1963, pp. 342-371.

Ladd, C. C., "Settlement Analyses For Cohesive Soils," M.I.T. Department of Civil Engineering Research Report R 71-2, 1971, 107 p.

Ladd, C. C., Foott, R. Ishihara, K, Poulos, H. G. and Schlosser, F., "Stress Deformation and Strength Characteristics," State-of-the-Art Report for Session I, Proceedings of the 9th International Conference on Soil Mechanics and Foundation Engineering, Tokyo, July, 1977.

Ladd, C. C., "Foundation Design of Embankments Constructed on Connecticutt Valley Varved Clays," Res. Report R75-7, No. 343, Dept. of Civil Engr., Mass., Inst. of Technology, Cambridge, 1975, 439p.

Ladd, C. C., "Stress-Strain Modulus of Clay in Undrained Shear", Journal of the Soil Mechanics and Foundation Division, ASCE, Vol. 90, No. SMS, Sept., 1964, pp. 103-132.

Lamé, M. G., Lecons sur la theorie mathematique de 1 élasticité des Corps Solides, Paris, 1852.

La Rochelle, P., Roy, M., and Tavenas, F., "Field Measurements of Cohesion in Champlain Clays," Proceedings of the 8th International Conference on Soil Mechanics and Foundation Engineering, Moscow, Vol. 1.1, 1973, pp. 229-236.

La Rochelle, P., Lefebvre, G., "Sampling Disturbance in Champlain Clays," Sampling of Soil and Rock, ASTM, STP 483, 1971, pp. 143-164.

Lo, K. Y., and Lee, C. F., "Stress Analysis and Slope Stability in Strain-Softening Materials," Geotechnique 23, Vol. 1, 1973, pp. 1-11.

Lo, K. Y. and Milligen. V., "Shear Strength Properties of Two Stratified Clays," Journal of the Soil Mechanics and Foundations Division, ASCE, Vol. 93, SM1, Jan., 1967, pp. 1-15.

Lunne, T., Eide, O. and De Ruiter, J., "Correlations Between Cone Resistance and Vane Shear Strength in Some Scandinavian Soft to Medium Stiff Clays," Canadian Geotechnical Journal, Vol. 13, No. 4, Nov., 1976, pp.430-441.

McClelland, B. (1974), "Design of Deep Penetration Piles for Ocean Structures," Journal of the Geotechnical Engineering Division, ASCE, Vol. 100, No. 677, p. 709.

Ménard, L., "Mesures in-situ des propriétés physiques des Sols," Annales des Ponts et Chaussees, Paris, Vol. 127, 1957, pp. 357-377.

Meyerhof, G. G., "An Investigation of the Bearing Capacity of Shallow Footings on Dry Sand," Proceedings of the 2nd International Conference on Soil Mechanics, 1948, 1:237.

Meyerhof, G. G., "The Bearing Capacity of Foundations Under Eccentric and Inclined Loads," Proceedings of the 3rd International Conference on Soil Mechanics and Foundation Engineering, Zurich, Vol. 1, 1953, pp. 440.

Meyerhof, G. G., "Influence of Roughness of Base and Ground-Water Conditions on the Ultimate Bearing Capacity of Foundations, Geotechnique, Vol. 5, 1955, pp. 227.

Meyerhof, G. G., "The Ultimate Bearing Capacity of Foundations," Geotechnique, Vol. 2, No. 4, 1951, pp. 301-332.

Meyerhof, G. G., "The Ultimate Bearing Capacity of Wedge - Shaped Foundations," Proceedings of the 5th International Conference on Soil Mechanics and Foundation Engineering, Vol. 2, Paris, 1961, pp. 105-109.

Meyerhof, G. G., "Penetration Tests and Bearing Capacity of Cohesionless Soils," Journal of the Soil Mechanics and Foundations Division, ASCE, Vol. 82, No. SM1, Jan. 1956, p. 1-12.

Meyerhof, G. G., "Bearing Capacity and Settlement of Pile Foundations," Journal of the Geotechnical Engineering Division, ASCE, Vol. 102, No. GT3, Proceedings Paper 11962, March, 1976, pp. 195-228.

Michaud, D., "Contribution á la mesure en place de la résistance non drainee des argiles sensibles a' l'aide de penetrometres statiques," These de maitrise qui sera presentee a' l'universite' Laval pour l'obtention du grade M.Sc.A., 1974.

Mikasa, M., and Takada, N., "Significance of Centrifugal Model Test in Soil Mechanics," Proceedings of the 8th International Conference on Soil Mechanics and Foundation Engineering, Vol. 1, Part 1, Moscow, 1973, pp. 273-278.

Milovic, D. M., "Penetration Test Results of Some Cohesive Soils," ESOPT, Vol. 2:2, 1974, pp. 269-275.

Mitchell, J. K., Durgunoglu, H. T., "In-Situ Strength by Static Cone Penetration Test," Proceedings of the 8th International Conference on Soil Mechanics and Foundation Engineering, Vol. 1, Part 1; Moscow, 1973, pp. 279-286.

Mitchell, J. K. and Lunne, T. A., "Cone Resistance as Measure of Sand Strength," Journal of the Geotechnical Engineering Division, ASCE, Vol. 104, No. GT7, July, 1978, pp. 995-1012.

Mitchell, R. J., "On the Yielding and Mechanical Strength of Leda Clays," Canadian Geotechnical Journal, Vol. 7, No. 3, 1970, pp. 297-312.

Mitchell, R. J. and Wong, K. K., "The Generalized Failure of an Ottawa Valley Champlain Sea Clay," Canadian Geotechnical Journal, Vol. 10, No. 4, 1973, pp. 607-616.

Mohan, D., Jain, G. S., and Kumar, V. (1963), "Load Bearing Capacity of Piles," Geotechnic, Vol. 13, No. 1, p. 76.

Noorany, I. and Seed, H. B., "In-Situ Strength Characteristics of Soft Clays," Journal of the Soil Mechanics and Foundations Division, ASCE, Vol. 91, No. SM2, March 1965, pp. 49-80.

Nottingham, L. C., "Use of Quasi-Static Friction Cone Penetrometer Data to Predict Load Capacity of Displacement Pile," Ph.D. Dissertation, Civil Engineering, University of Florida, Gainesville, Fl., 1975.

Nottingham, L. C., Schmertmann, J. H., "An Investigation of Pile Capacity Design Procedures," Research Report D629, Engineering and Industrial Experiment Station, Gainesville, Florida, September 1975, 159 p.

Oden, J. T., "Finite Elements of Nonlinear Continua," McGraw Hill Book Co., New York, 1972.

Okumura, T., "The Variation of Mechanical Properties of Clay Samples Depending on its Degree of Disturbance," Proceedings of the Specialty Session on Quality in Soil Sampling, Proceedings of the 4th Asian Conference, International Society for Soil Mechanics and Foundation Engineering, Bangkok, 1971, pp. 73-81.

Ottaviani, M, "Three Dimensional Finite Element Analysis of Vertically Loaded Pile Groups," Geotechnique, Vol. 15, No. 2, 1975, pp. 159-174.

Palmer, A. C., "Undrained Plane Strain Expansion of a Cylindrical Cavity in Clay: A Simple Interpretation of the Pressuremeter Test," Geotechnique, Vol. 22, No. 3, 1972, pp. 451-457.

Parry, R. H. G., "Triaxial Compression and Extension Tests on Remolded Saturated Clay," Geotechnique, Vol. 10, No. 4, 1960, pp. 166-180.

Peck, R. B. (1958), "A Study of the Comparative Behavior of Friction Piles," Special Report No. 36, Highway Research Board, Washington, D.C.

Peck, R. B. (1977), "Design of Pile Foundations," Special Report No. 42, Highway Research Board, Washington, D.C.

Perloff, W. H., and Osterberg, T. O., "Stress History Effects on Strength of Cohesive Soils," Highway Research Record No. 48, 1964, pp. 49.

Perloff, W. H., Baron, W., Soil Mechanics Principles and Applications, Ronald Press Company, New York, 1976.

Plantema, G. (1948), "Results of a Special Loading Test on A Reinforced Concrete Pile, A So-Called Pile Sounding," Proceedings of the 2nd International Conference on Soil Mechanics and Foundation Engineering, Rotterdam, Vol. 2, p. 112.

Prager, W., Theory of Plasticity, Brown University, 1942.

Prager, W., An Introduction to Plasticity, Addison-Wesley Publishing Company, London, 1959.

Prager, W. and Hodge, P. G., Theory of Perfectly Plastic Solids, John Wiley & Sons, Inc., New York, 1951.

Raymond, G. P., Townsend, D. L. and Lojkacek, M. J., "The Effect of Sampling on the Undrained Soil Properties of the Leda Soil", Canadian Geotechnical Journal, Vol. 8, No. 4, 1971, pp. 546-557.

Richardson, A. M. and Whitman, R. V., "Effect of Strain-Rate Upon Undrained Shear Resistance of a Saturated Remolded Fat Clay," Geotechnique, Vol. 13, No. 4, 1963, pp. 310-324.

Robinsky, E. I., Morrison, C. F., "Sand Displacement and Compaction Around Model Friction Piles," Canadian Geotechnical Journal, Vol. 1, No. 2, 1964, pp. 81-93.

Roscoe, K. H. and Burland, J. B., "On the generalized stres-strain Behaviour of Wet Clay," Engineering Plasticity edited by J. Heyman and F. A. Leckie, Cambridge University Press, 1968.

Roy, M, Michaud, D., Tavenas, F. A., Leroueil, S., La Rochelle, P., "The Interpretation of Static Cone Penetration Tests in Sensitive Clays," Proceedings of the European Symposium on Penetration Testing, ESOPT, Vol. 2.2, 1974, pp. 323-330.

Rutledge, P. C., "Relation of Undisturbed Sampling to Laboratory Testing," Transactions, ASCE, Vol. 109, 1944, pp. 1155-1216.

Sanchez, J. M., Sagaseta, C. and Ballester, F., "Influence of Stress History on Undrained Behaviour of Soft Clays," British Geotechnical Society, London, Vol. 1, 1979.

Sanglerat, G., The Penetrometer and Soil Exploration, American Elsevier Publishing Company Inc., New York, N.Y., 1972.

Sangrey, D. A., "Normalized Design Procedures in Sensitive Clays," Journal of the Geotechnical Engineering Division, ASCE, Vol. 101, No. GT11, Nov. 1975, pp. 1181-1187.

Sangrey, D. A., "Naturally Cemented Sensitive Soils," Geotechnique, Vol. 22, No. 1, pp. 139-152, 1972.

Schmertmann, J. H., "The Undisturbed Consolidation of Clay," Transactions ASCE, Vol. 120, 1955, pp. 1201-1233.

Schmertmann, J. H., Discussion of paper by M. L. Calhoon, Transactions ASCE, Vol. 121, 1956, pp. 940-950.

Schmertmann, J. H., "Static Cone Penetrometers for Soil Exploration," Civil Engineering, Vol. 37. No. 6, 1967, p. 71.

Schmertmann, J. H., "Static Cone to Compute Static Settlement Over Sand," Journal of the Soil Mechanics and Foundations Division, ASCE, Vol. 96, No. SM3, May 1970, pp. 1011-1043.

Schmertmann, J. H., "Measurement of in situ shear strength," State-of-the-Art, ASCE, Conference on in situ Measurements of Soil Properties. Raleigh, N. C., Proceedings, Vol. 2, 1975, pp. 57-138.

Schmertmann, J. H., "Guidelines for Cone Performance and Design," U.S. Department of Transportation, Washington, D.C., 1977.

Schmertmann, J. H., "Use of the SPT to Measure Dynamic Soil Properties-Yes, But..!," ASTM, STP No. 654, 1978, pp. 341-355.

Schmertmann, J. H., "Statics of SPT," Journal of the Geotechnical Engineering Division, ASCE, Vol. 105, GT 5, May 1979, pp. 655-670.

Schmertmann, J. H. and Palecios, A., "Energy Dynamics of SPT," Journal of the Geotechnical Engineering Division, ASCE, Vol. 105, GT 8, Aug. 1979, pp. 909-926.

Schlutz, E. and Knausenberger, H., "Experiences with Penetrometers", Proceedings of the 4th International Conference on Soil Mechanics and Foundation Engineering, London, Vol. 1, 1957, pp. 249-255.

Seed, H. B, Noorany, I. and Smith, I. M., "Effects of Sampling and Disturbance on the Strength of Soft Clay," University of California, Berkeley, Report TE-64-1, 1964.

Shibata, T. and Karube, D., "Creep Rate and Creep Strength of Clays," Proceedings of the 7th International Conference on Soil Mechanics and Foundation Engineering, Mexico City, Vol. 1, 1969, pp. 361-367.

Skempton, A. W., "The Bearing Capacity of Clays," Build. Res. Congr., London. Pap., Div. 1, Part 3, 1951, pp. 180-189.

Skempton, A. W., and Bishop, A. W., "Soils," Chapter 10 of Building Materials, Their Elasticity and Plasticity, ed. M. Reiner, North-Holland Publishers, Amsterdam, 1954.

Skempton, A. W., "The $\emptyset = 0$ Analysis of Stability and Theoretical Basis," Proceedings of the 2nd International Conference on Soil Mechanics and Foundation Engineering, Rotterdam, Vol. 1, 1948, pp. 72-78.

Skempton, A. W., "Long-Term Stability of Clay Slopes," Geotechnique, Vol. 14, No. 2, 1964, pp. 75-102.

Skempton, A. W., and Bishop, A. W., "The Measurement of the Shear Strength of Soils, Geotechnique, Vol. 2, 1950, pp. 90-108.

Skempton, A. W. and Sowa, V. A., "The Behavior of Saturated Clays During Sampling and Testing," Geotechnique, Vol. 13, No. 4, 1963, pp. 269-290.

Skempton, A. W., "The Pore Pressure Coefficients A and B," Geotechnique, Vol. 4, No. 4, 1954, pp. 143-147.

Smith, I. M., "Incremental Numerical Solution of a Simple Deformation Problem in Soil Mechanics," Geotechnique, Vol. 20, No. 4, 1970, pp. 357-372.

Smith, P. D. (1975), "The Cone Penetrometer For Foundation Investigations," Research Report No. 33, New York State Department of Transportation, Albay, N.Y.

Szechy, C. (1961), "A More Exact Evaluation of Pile Test Loadings," Acta Technica Academia Scientiarum Hungaricae, Vol. XXXIV, No. 3-4, pp. 445-451.

Tavenas, F. and Leroveil, S., "Effects of Stresses and Time on Yielding of Clays," Proceedings of the 9th International Conference on Soil Mechanics and Foundation Engineering, Tokyo, 1977.

Tavenas, F. and Leroveil, S., "Clay Behavior and the Selection of Design Parameters," British Geotechnical Society, London, 1979, Vol. 1, pp. 281-190.

Tavenas, F. A., Roy, M., La Rochelle, P., "An Artificial Material for Simulating Champlain Clays," Canadian Geotechnical Journal, Vol. 10, No. 3, 1973, pp. 489-503.

Terzaghi, K., Theoretical Soil Mechanics, John Wiley and Sons, Inc., New York, 1943.

Thomas, "Deepsounding Test Results and The Settlement of Spread Footings on Normally Consolidated Sands," Geotechnique, Dec. 1968.

Tomlinson, M. J., "The Adhesion of Piles Driven in Clay Soils," Proceedings of the 4th International Conference on Soil Mechanics and Foundation Engineering, London, Vol. 2, 1957, p. 65.

Torstensson, B. A., "Pore Pressure Sounding Instruement," ASCE Specialty Conference on In-Situ Measurement of Soil Properties, North Carolina State University, Raleigh, Vol. II, 1975, pp. 48-54.

Townsend, D. L., Sangrey, D. A., and Walker, L. K., "The Brittle Behavour of Naturally Cemented Soils," Proceedings of the 7th International Conference on Soil Mechanics and Foundation Engineering, Mexico City, Vol. I, 1969, pp. 411-417.

Tumay, M. T., Boggess, F. L. Acar, Y. (1981), Subsurface Investigation With Piezo-Cone Penetrometer, "Contribution to the Symposium on Cone Penetration Testing and Experience,"

Van Der Veen, C., "The Bearing Capacity of a Pile," Proceedings of the 3rd International Conference on Soil Mechanics and Foundation Engineering, Zurich, Vol. 2, 1953, pp. 84-90.

Van Der Veen, C. and Boersma, L., "The Bearing Capacity of a Pile Predetermined by a cone Penetration Test," Proceedings of the 4th International Conference of Soil Mechanics and Foundation Engineering, London, Vol. 2, 1957, p. 72.

Van Weele, A. F., "A Method of Separating The Bearing Capacity of a Test Pile into Skin-Friction and Point-Resistance," Proceedings of the 4th International Conference on Soil Mechanics and Foundation Engineering, London, 1957, Vol. 2, pp. 76-80.

Vesic, A. S., Discussion, Proceedings of the 7th International Conference on Soil Mechanics Foundation Engineering, Mexico City, 1969, pp. 270-272.

Vesic, A. S., "Analysis of Ultimate Loads of Shallow Foundations," Journal of the Soil Mechanics and Foundations Divisibn, ASCE, Vol. 99, No. SM1, January 1973, pp. 45-73.

Vesic, A. S., Lecture Series on Deep Foundations, Geotechnical Group, BSCES/ASCE in cooperation with MIT, March-April 1975, "Principles of Pile Foundation Design" Lecture 1, 1975.

Vesic, A. S., "Expansion of Cavities in Infinite Soil Mass," Journal of the Soil Mechanics and Foundations Division, ASCE, Vol. 98, No. SM3 Proceedings Paper 8790, March 1972, pp. 265-290.

Vesic, A. S., "On Penetration Resistance and Bearing Capacity of Piles in Sand," Discussion, Session 3, Proceedings of the 8th International Conference on Soil Mechanics and Foundation Engineering, Moscow, Vol. 3, 1973.

Vesic, A. S., "Ultimate Loads and Settlements of Deep Foundations in Sand," Proceedings of a Symposium held at Duke University, 1965, pp. 53-68.

Vesic, A. S. "Bearing Capacity of Deep Foundation in Sand," Highway Research Record 39, Highway Research Board, National Research Council, Washington, D. C., 1963, pp. 112-153.

Vitayvergia, V. N. and Focht, J. A. (1972), "A New Way to Predict Capacity of Piles in Clays," Proceedings of the 4th Annual Offshore Technology Conference, Houston, Texas, p. 865.

Walker, L. K., "Undrained Creep in a Sensitive Clay," Geotechnique, Vol. 19, No. 4, 1969, pp. 515-529.

Wesley, L. D. (1967)," The Dutch Penetrometer and Its Use In Indonesia," Proceedings, Southease Asian Conference of Soil Engineering, Bangkok, pp. 223-230.

Winterkorn, H. F., Fand, H. (1975), Foundation Engineering Handbook, Van Nostrand Reinhold Company, New York, N.Y.

Wissa, A.E.Z., Martin, R. T., and Garlenger, J. E., "The Piezometer Probe," Proceedings, ASCE Specialty Conference on In-Situ Measurement of Soil Properties, North Carolina State University, Raleigh, Vol. 1, 1975, pp. 536-545.

Woodward, R. J., Lundgren, R., and Boitano, J. D. (1961), "Pile Loading Tests in Stiff Clay," Proceedings of the 5th International Conference on Soil Mechanics and Foundation Engineering, Paris, Vol. 2, p. 177.

Yilmaz, R. (1981), "In-Situ Determination of Undrained Shear Strength of Louisiana Soils By Quasi-Static Electric Cone Penetration Test," M.Sc. Thesis, Civil Engineering Department, Louisiana State University, Baton Rogue, La.

APPENDIX A

LOAD-SETTLEMENT CURVES

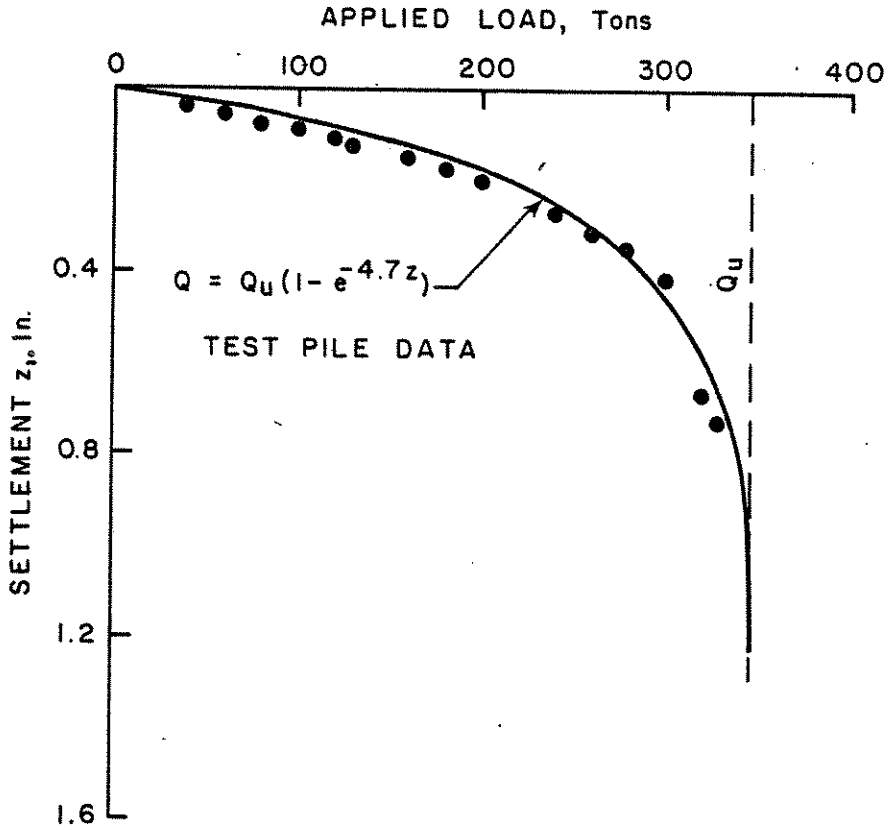

TEST PILE: I

NEW ORLEANS (I)

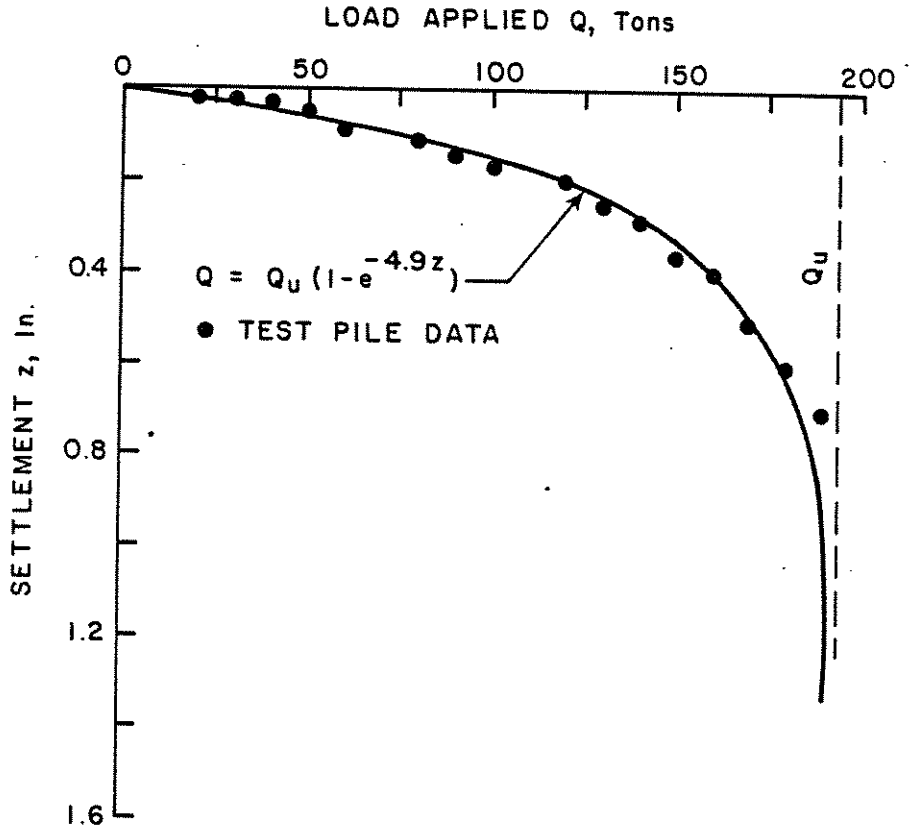

TEST PILE: 2-A
NEW ORLEANS (I)

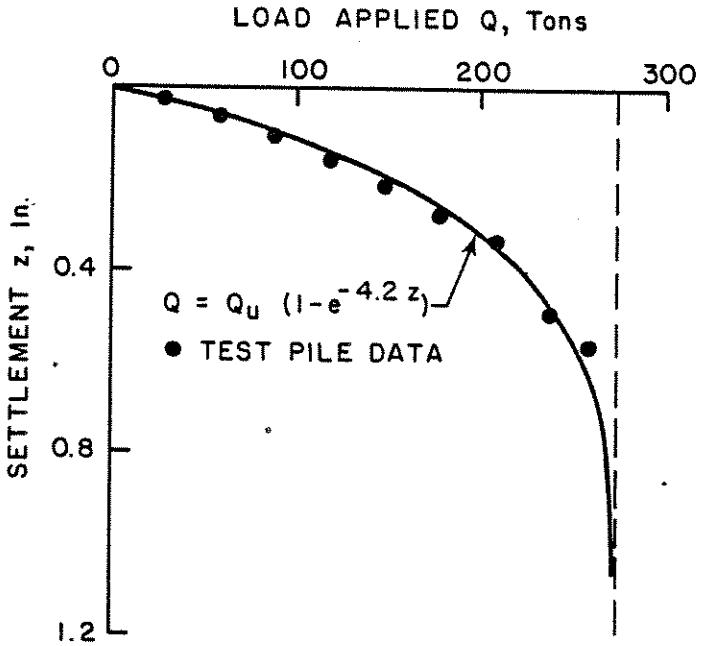

TEST PILE: 3
NEW ORLEANS (I)

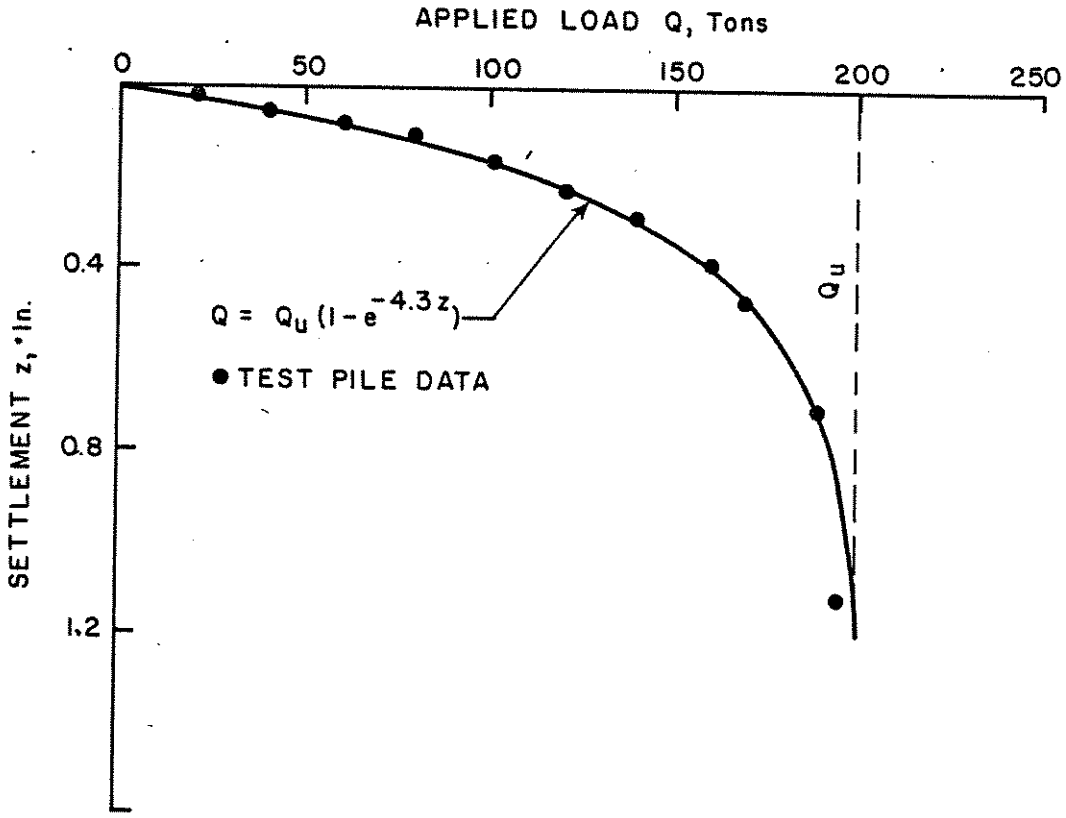

TEST PILE: 4-A

NEW ORLEANS (1)

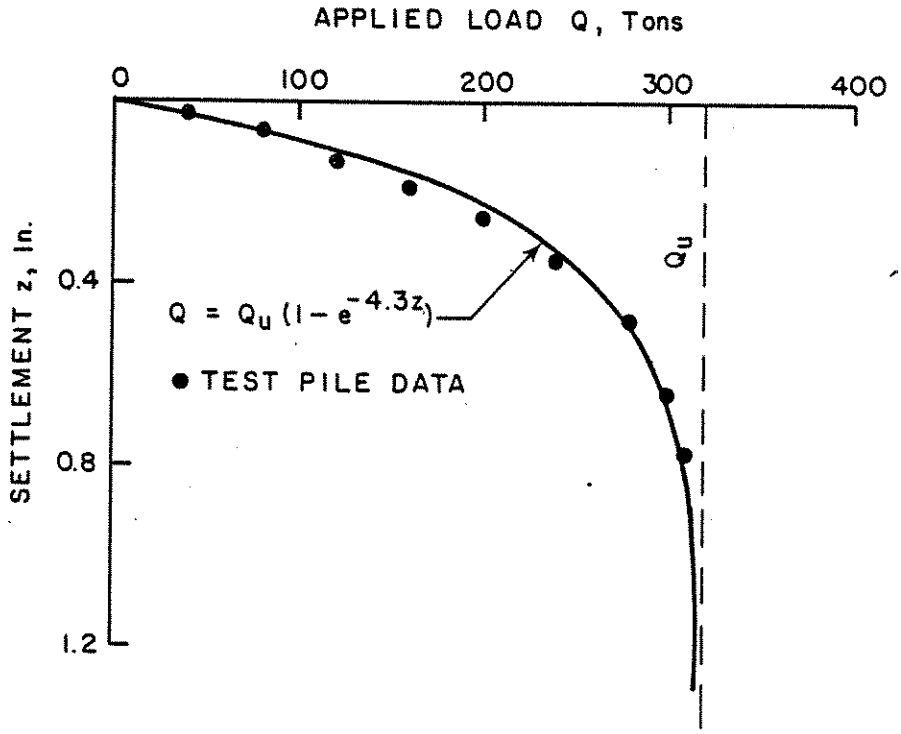

TEST PILE: 5
NEW ORLEANS (I)

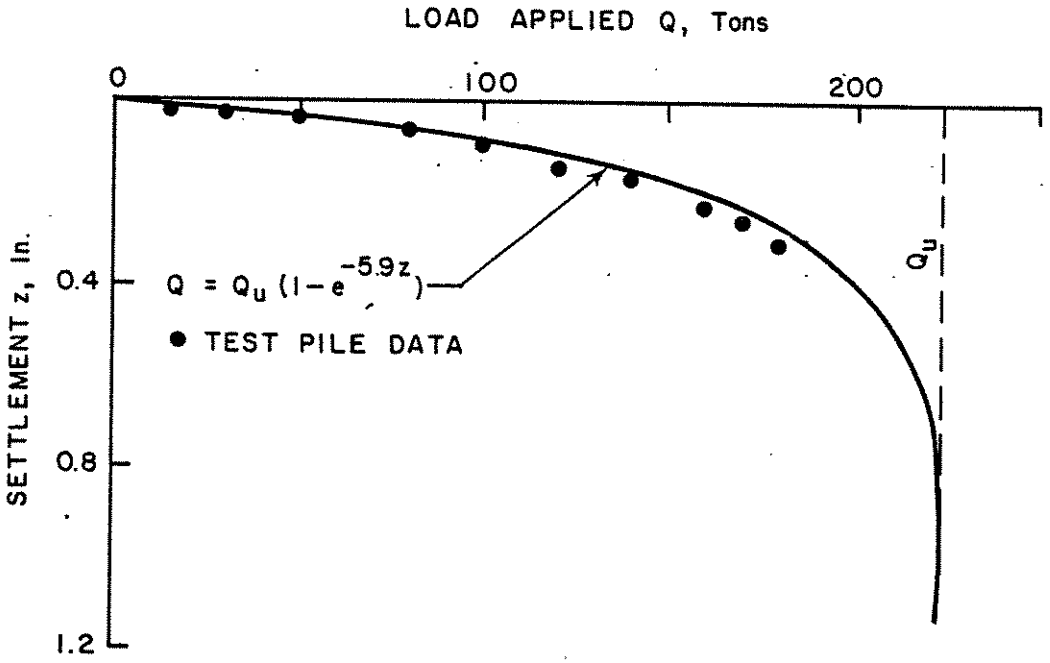

TEST PILE: 6
NEW ORLEANS (II A)

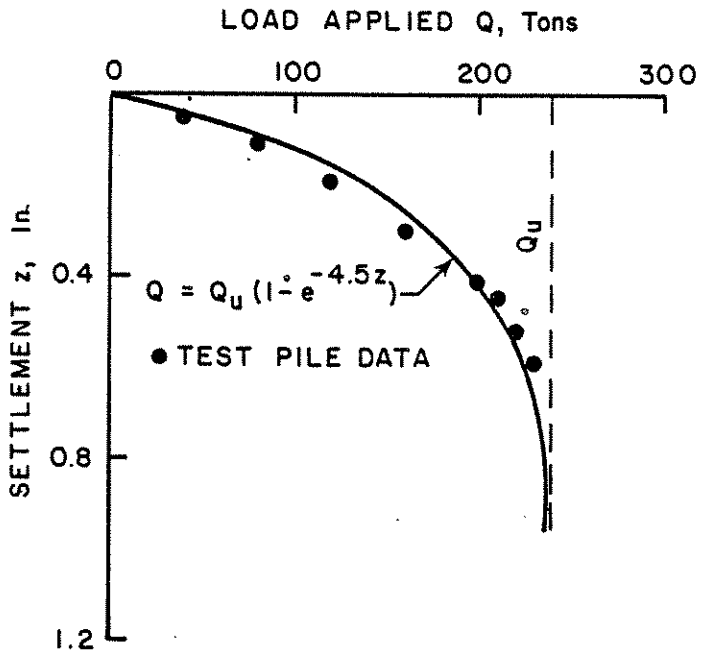

TEST PILE: 8
NEW ORLEANS (IIA)

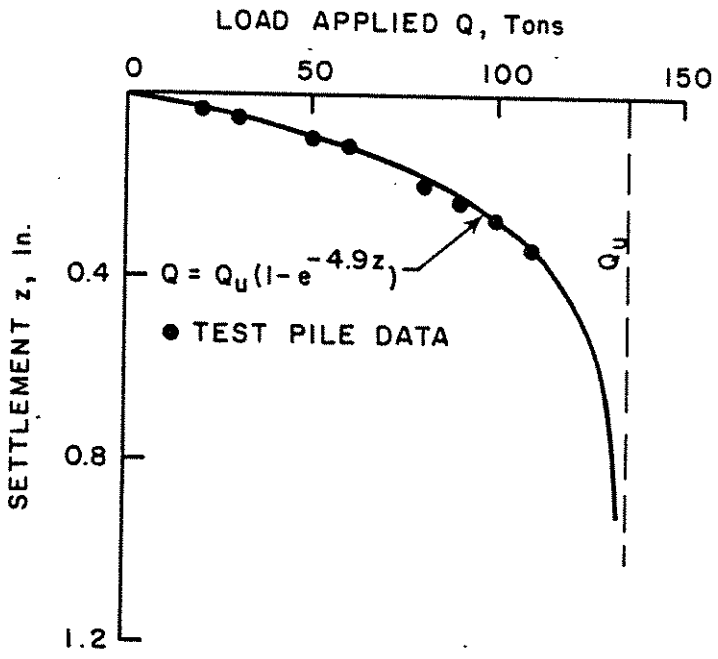

TEST PILE: 9
NEW ORLEANS (II A)

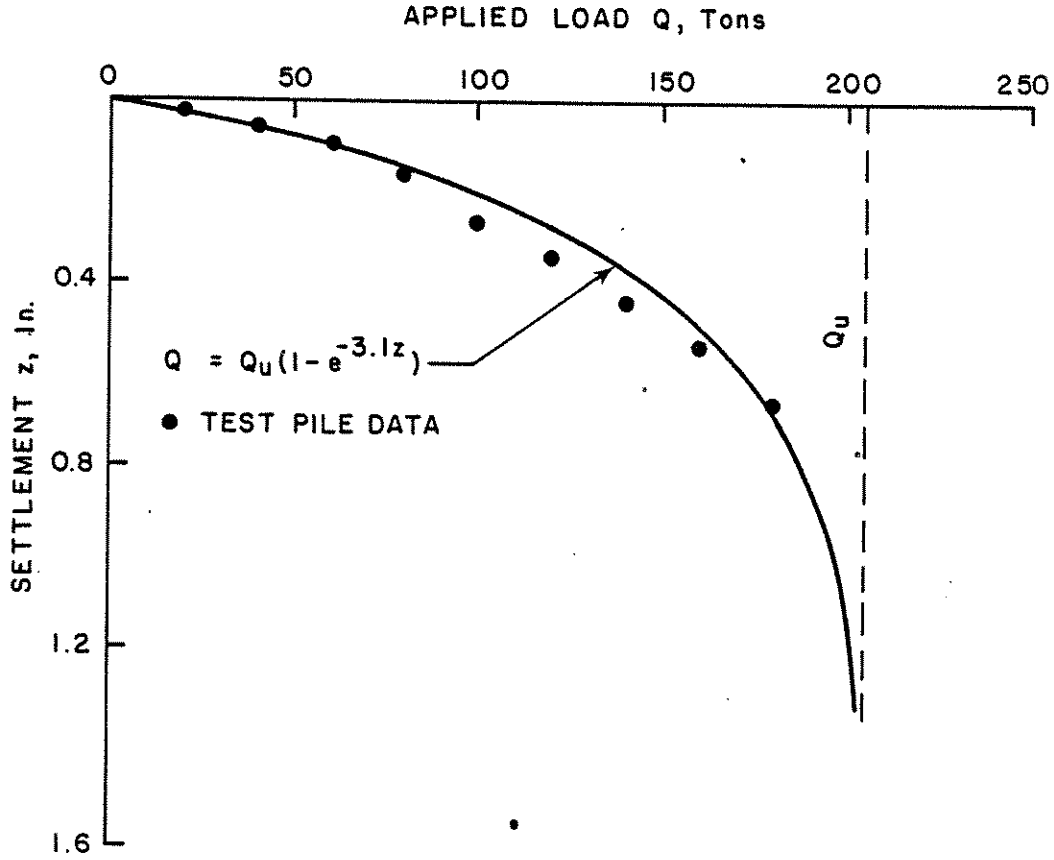

TEST PILE: 10

NEW ORLEANS (11A)

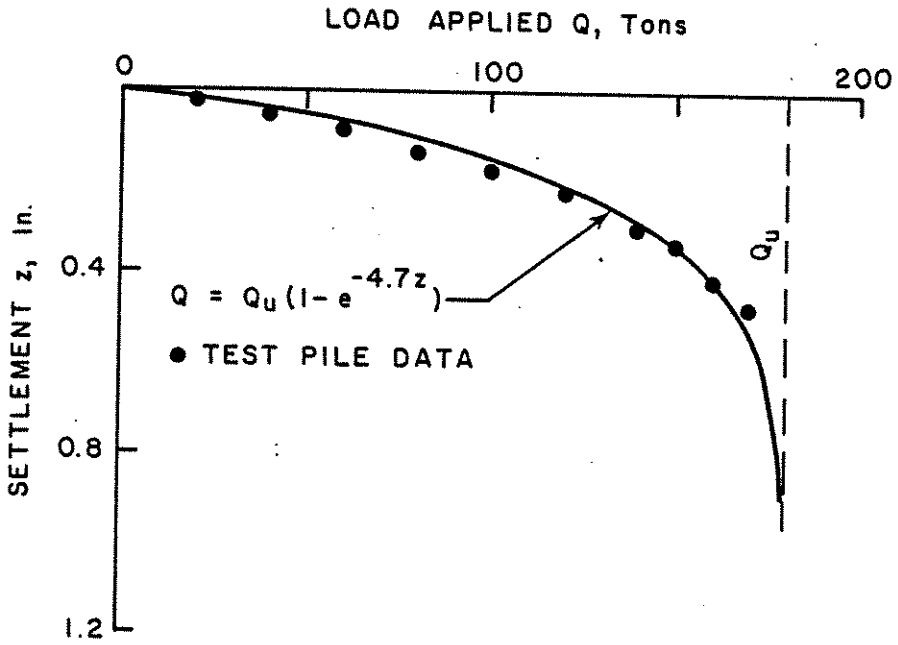

TEST PILE: 11
NEW ORLEANS (11A)

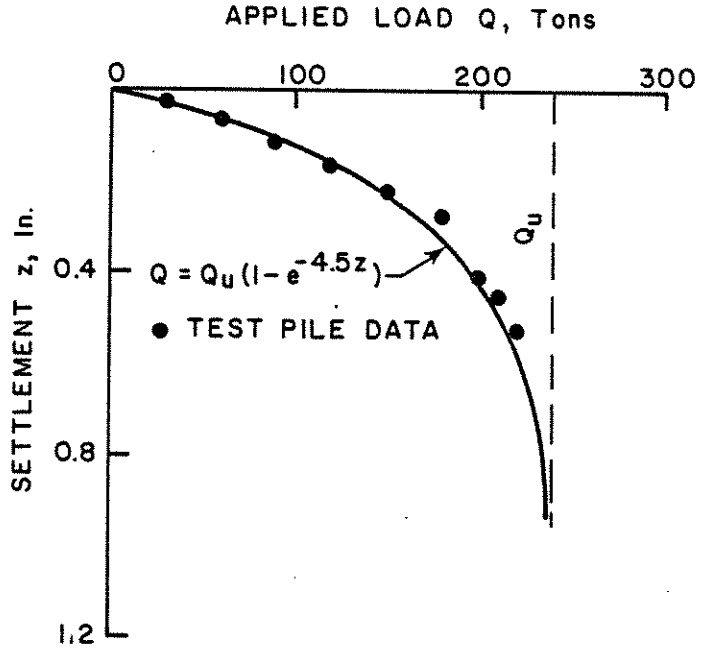

TEST PILE: 12

NEW ORLEANS (11 A)

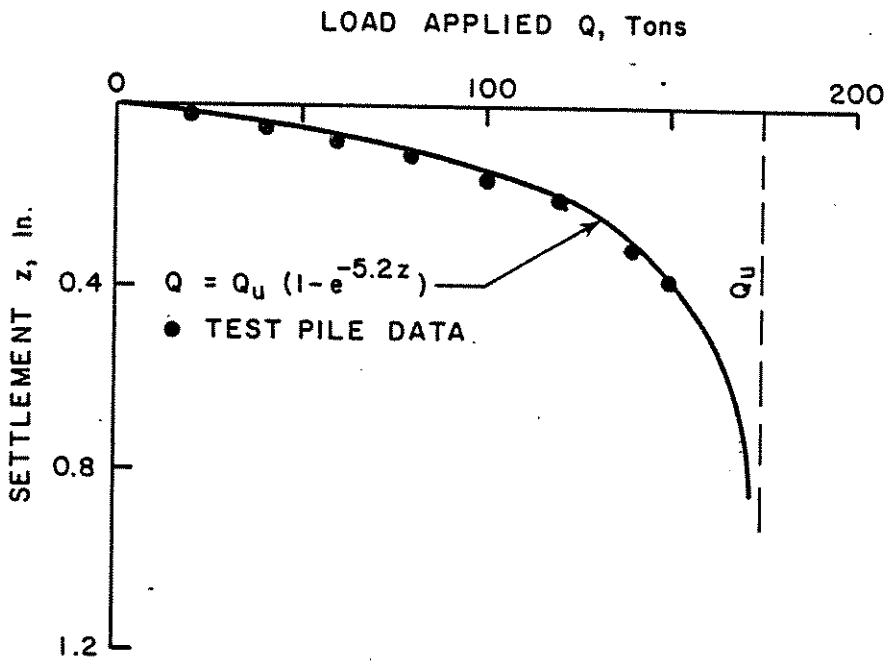

TEST PILE: 13

NEW ORLEANS (II A)

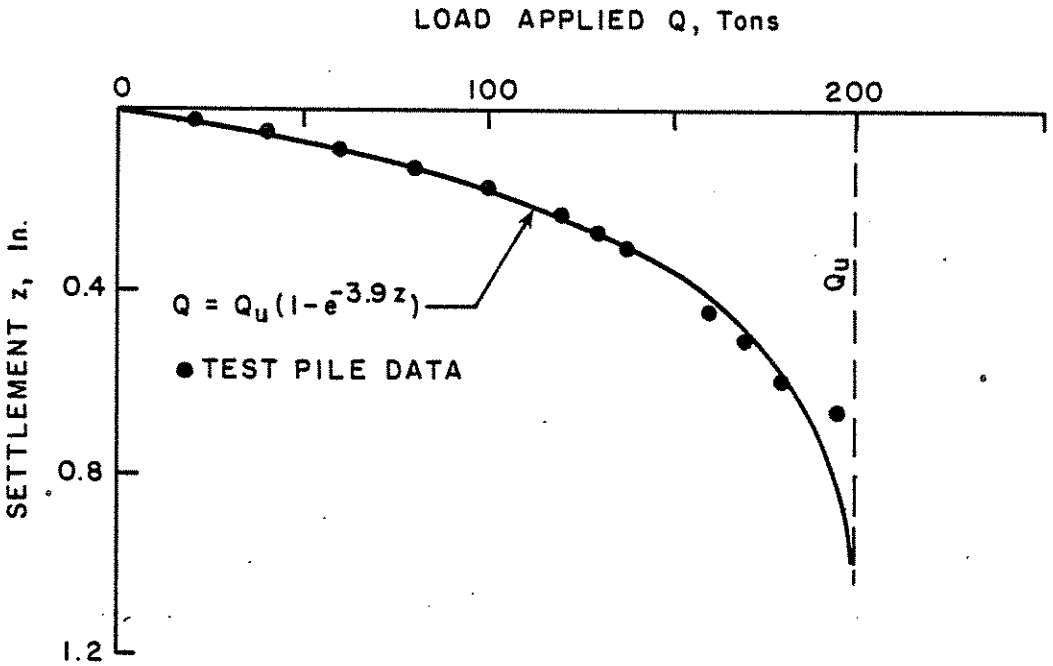

TEST PILE: 14

NEW ORLEANS (11A)

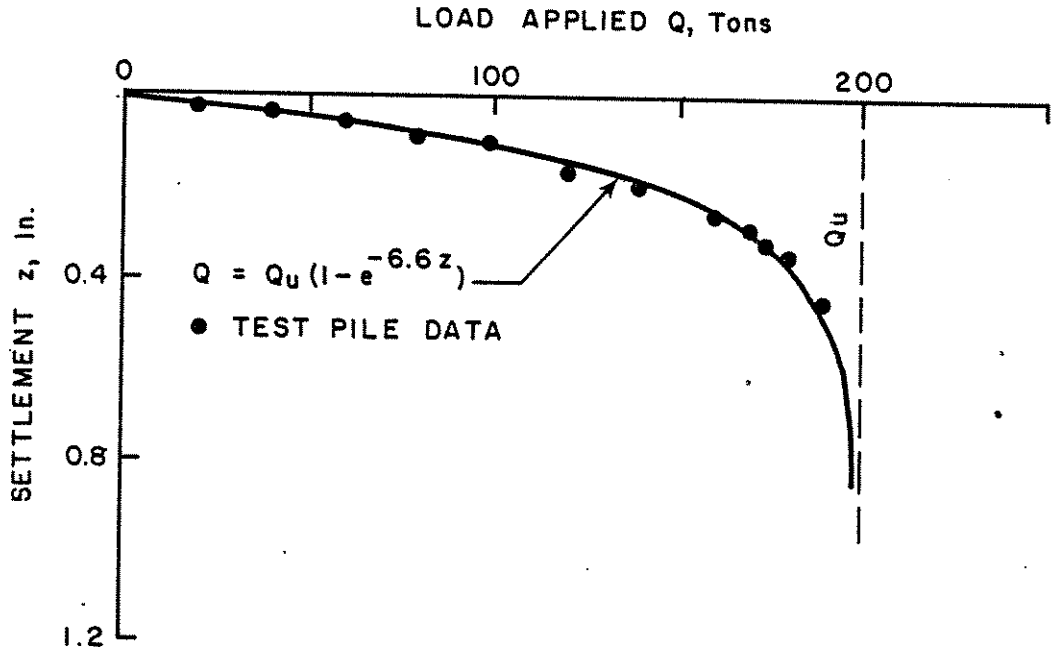

TEST PILE: 15

NEW ORLEANS (11 A)

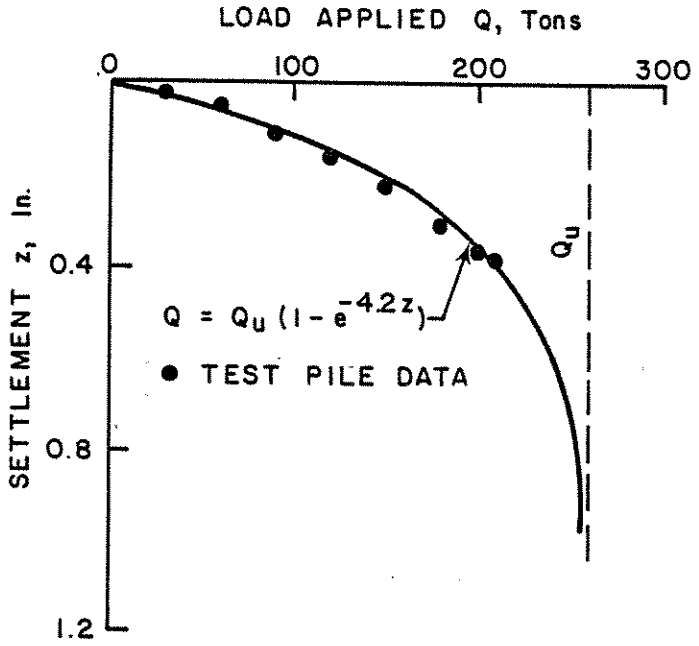

TEST PILE: 16

NEW ORLEANS (11 A)

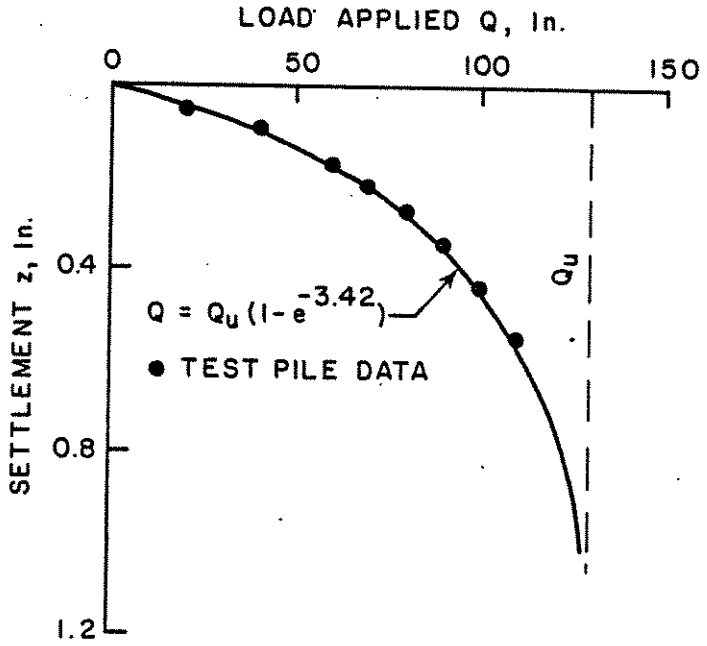

TEST PILE: 18
NEW ORLEANS (11A)

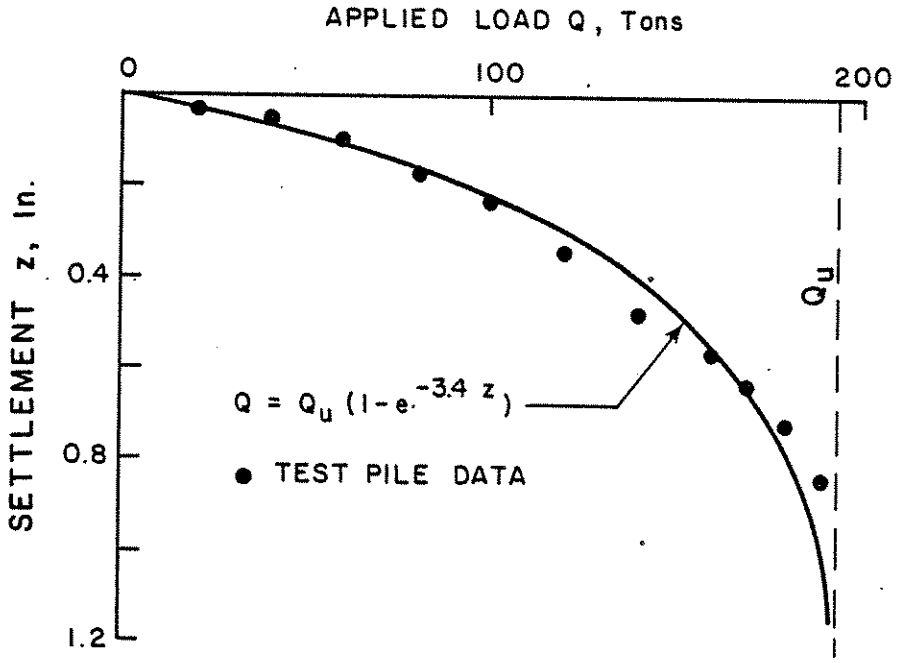

TEST PILE: 19
NEW ORLEANS (11A)

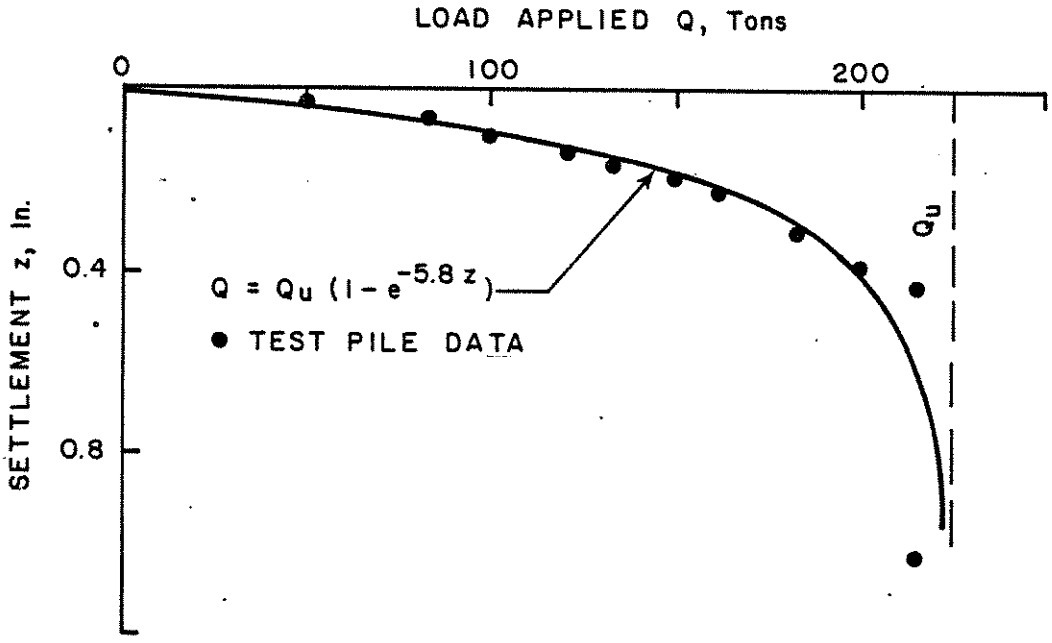

TEST PILE: I
HOUMA

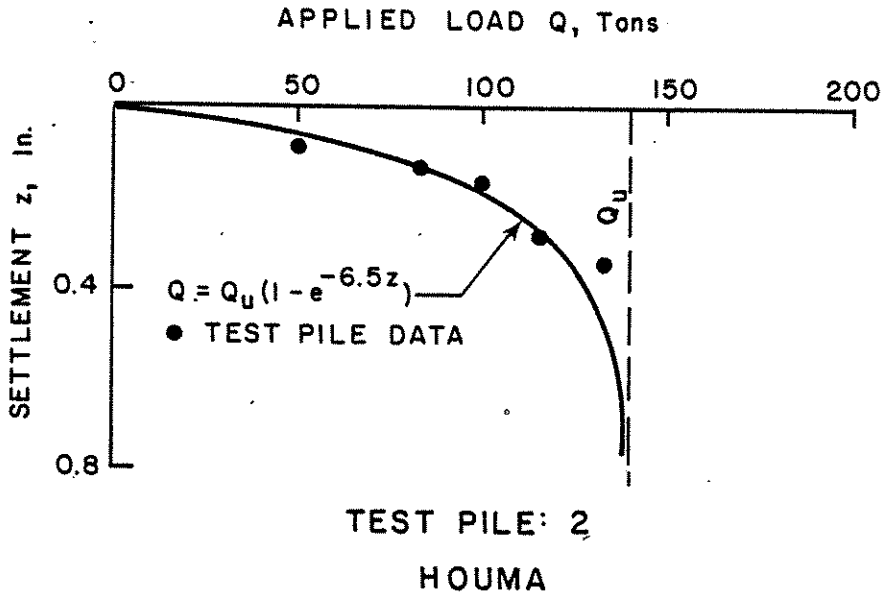

TEST PILE: 2

HOUMA

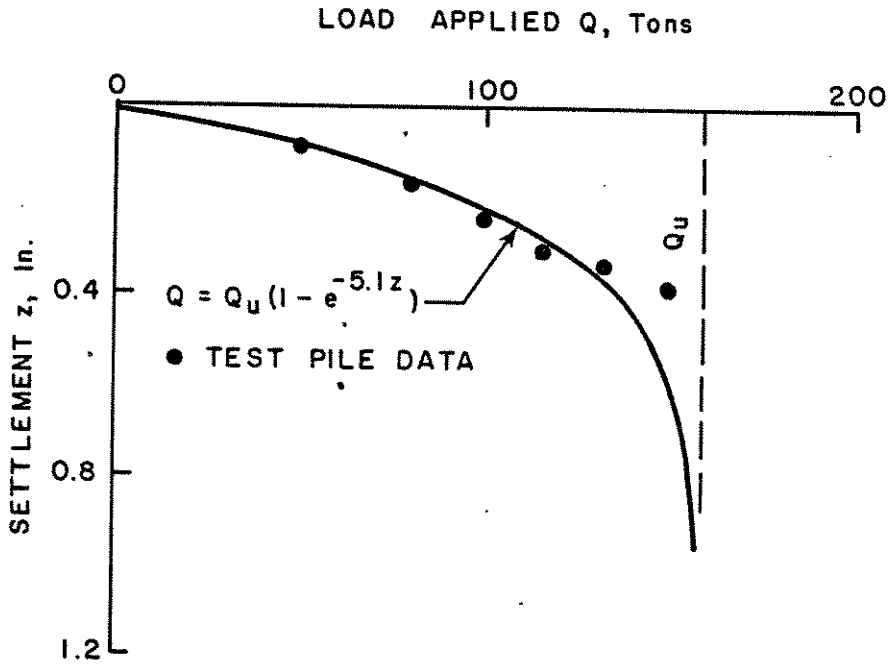

TEST PILE: 3
HOUMA

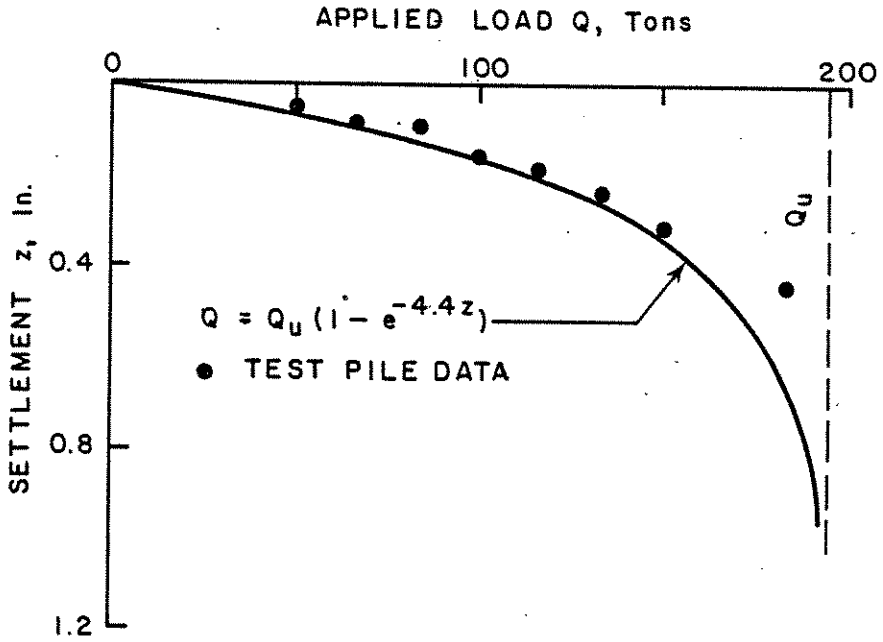

TEST PILE: 4

HOUMA

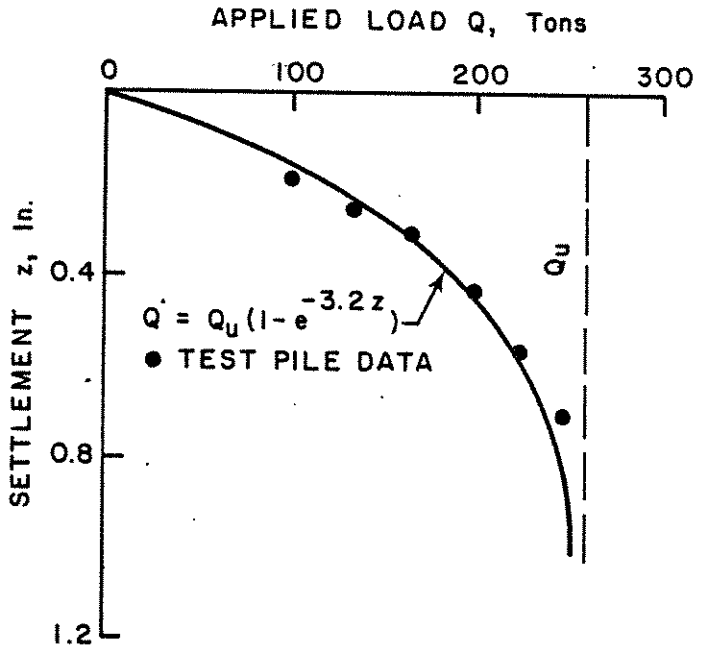

TEST PILE: 5

HOUMA

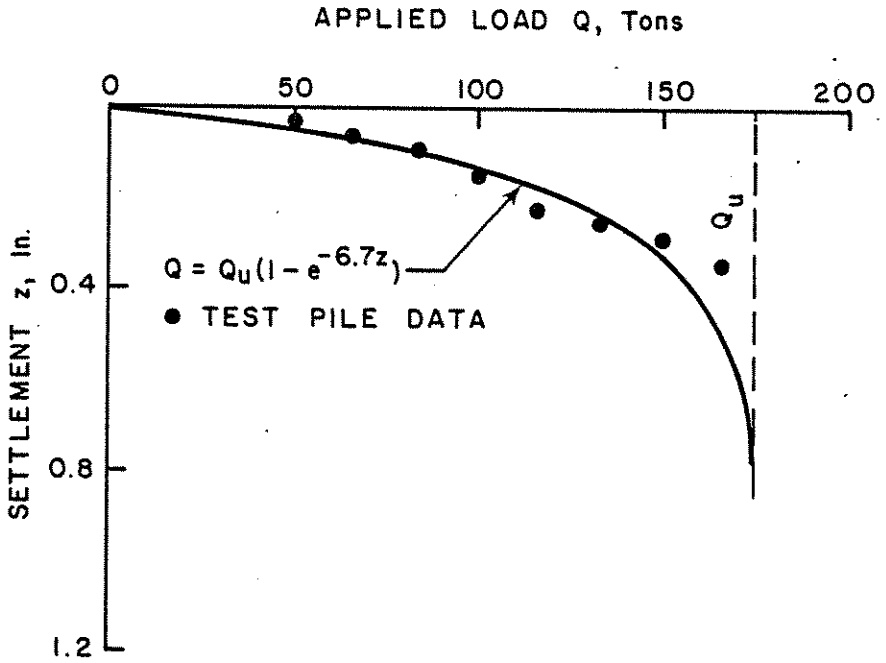

TEST PILE: 10

HOUMA

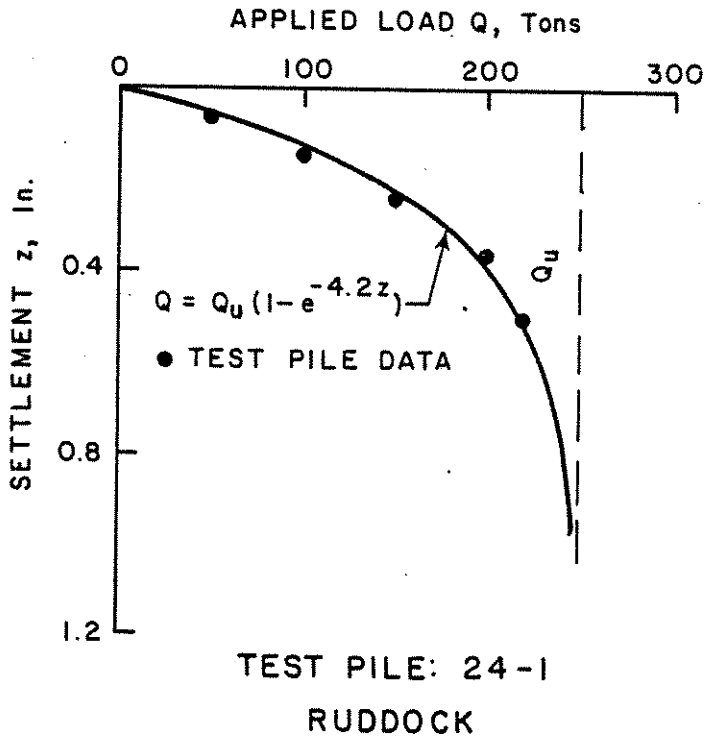

TEST PILE: 24-1
RUDDOCK

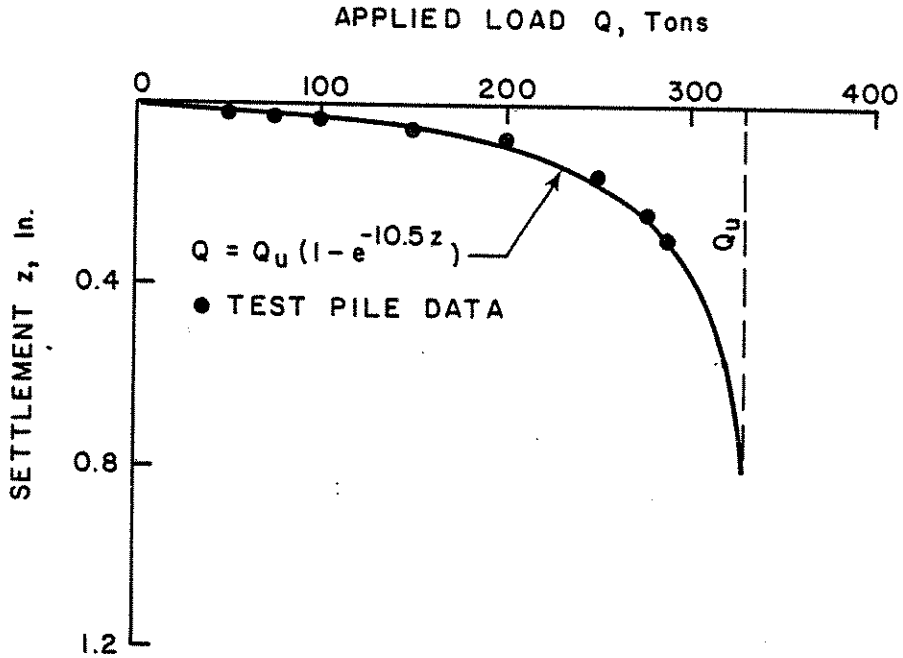

TEST PILE: 30-1

RUDDOCK

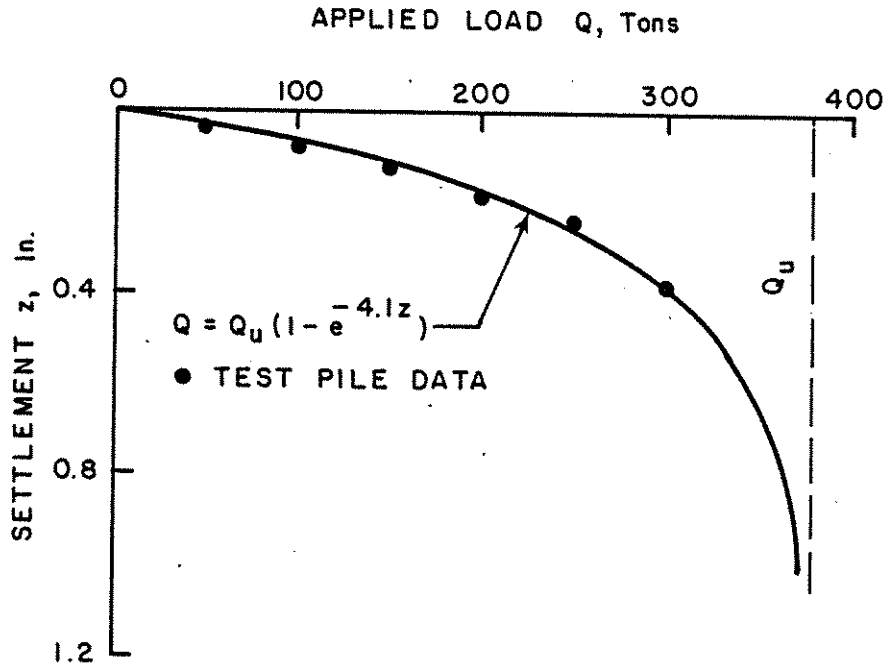

TEST PILE: 24-2

RUDDOCK

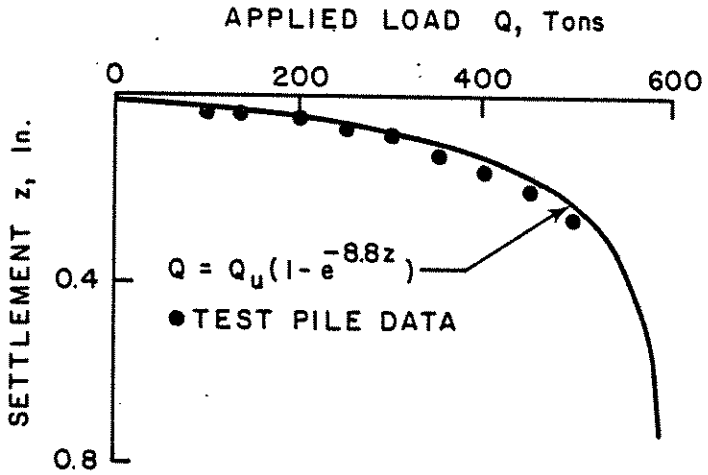

TEST PILE: 30-2

RUDDOCK

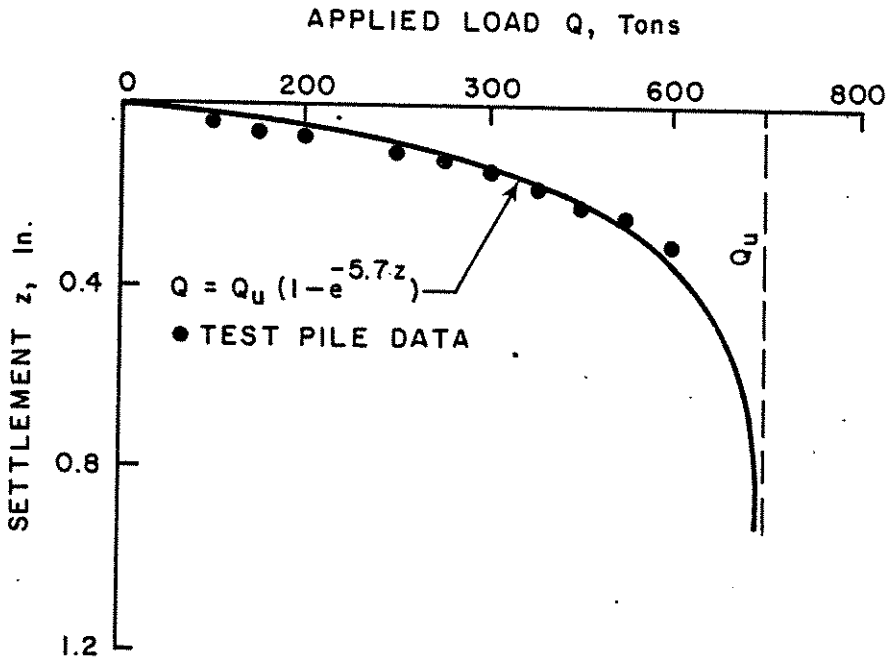

TEST PILE: 54-2
RUDDOCK

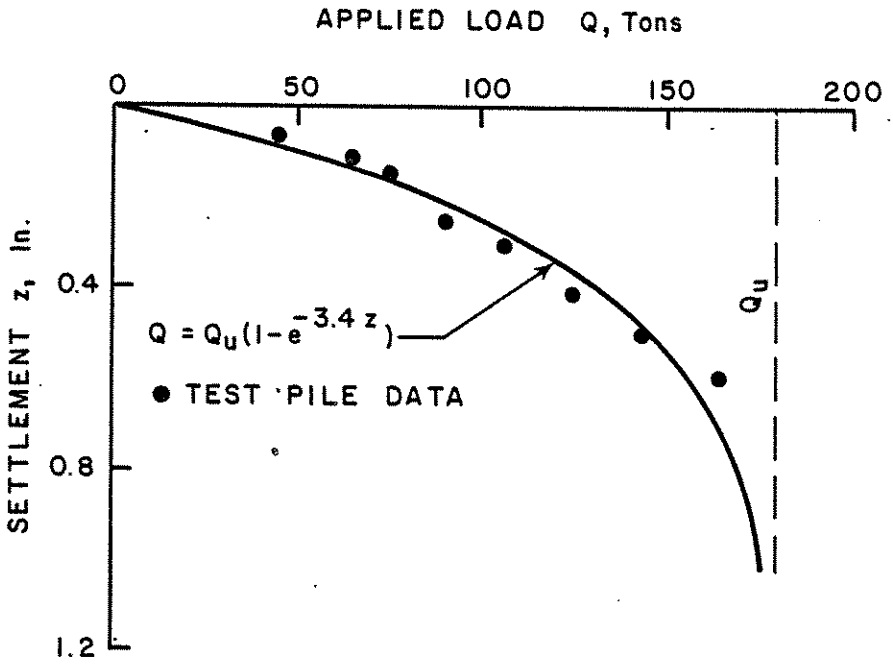

TEST PILE: 4A

MORGAN CITY

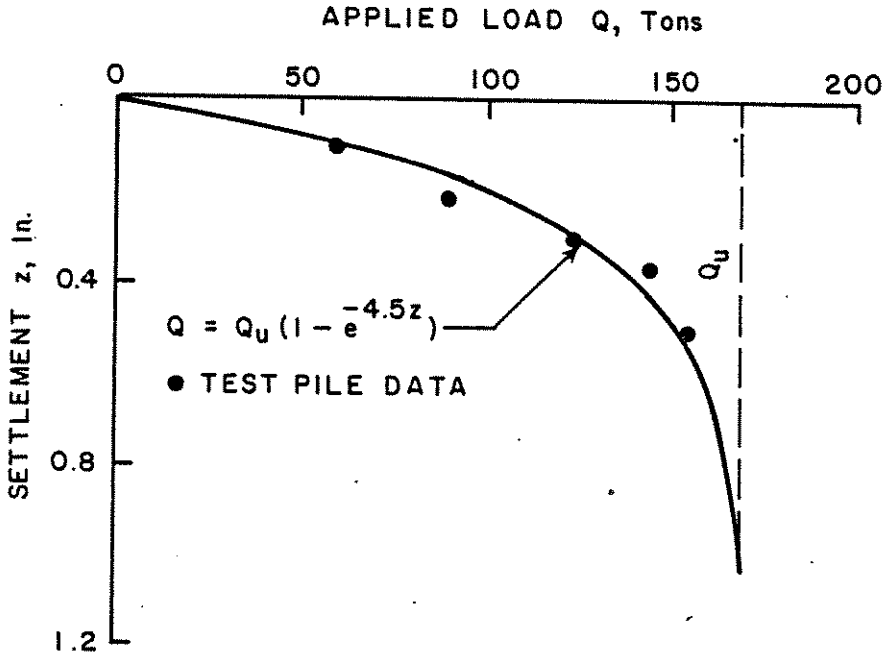

TEST PILE: 4B

MORGAN CITY

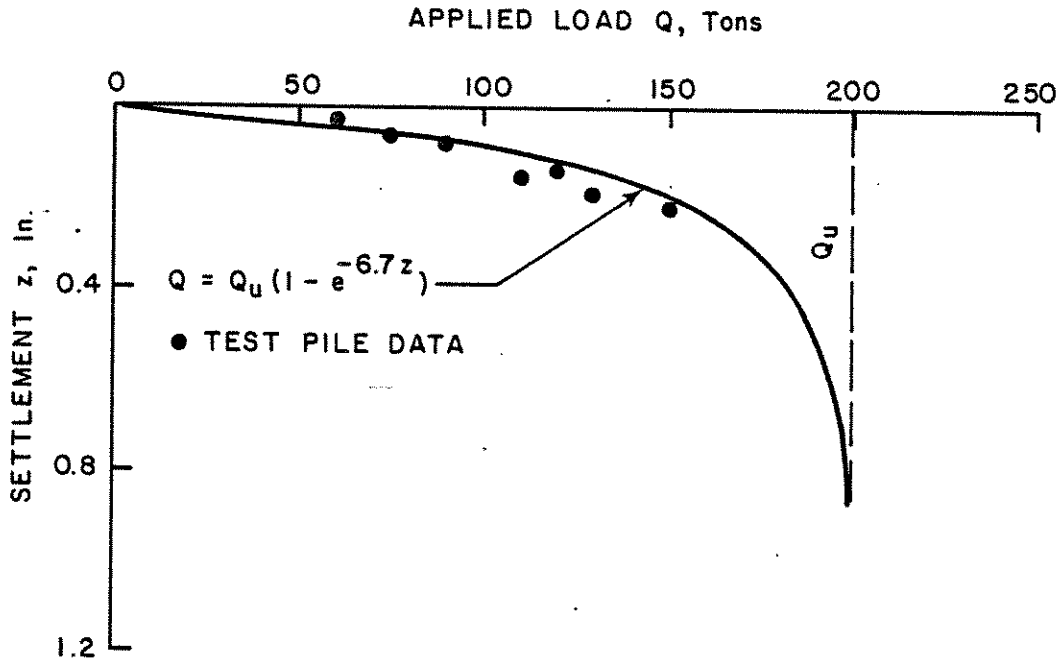

TEST PILE: 2A
BATON ROUGE

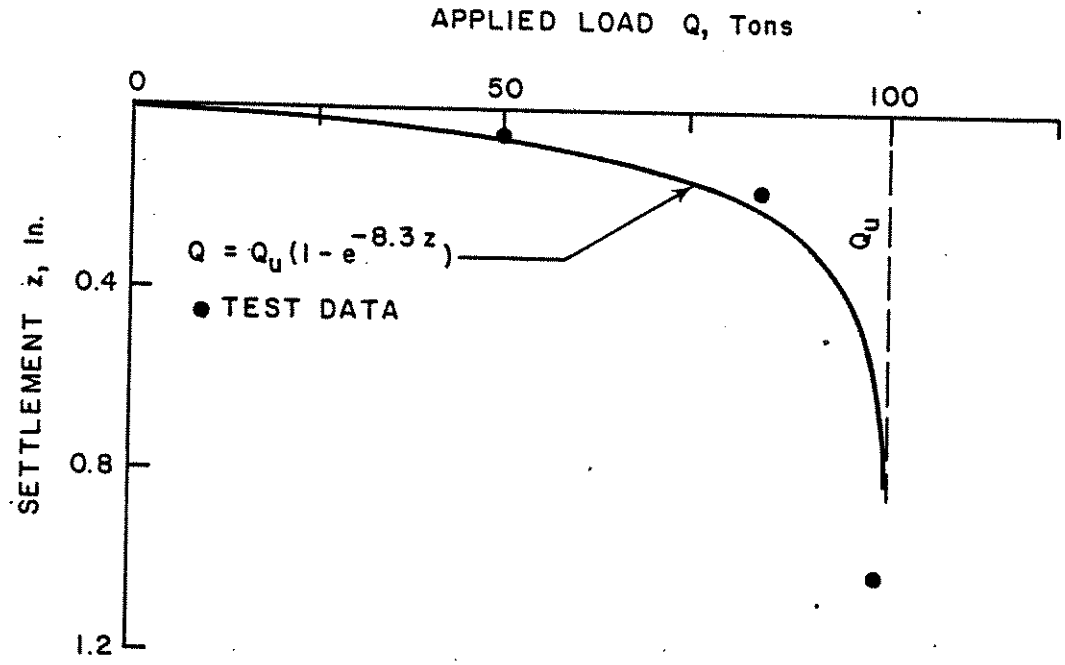

TEST PILE: I

ALEXANDRIA

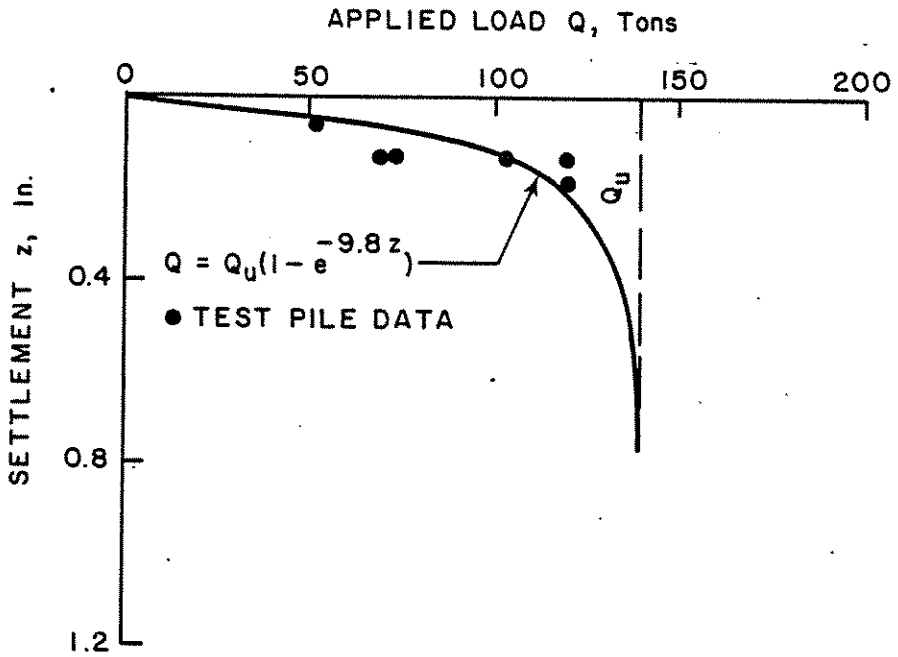

TEST PILE: 3
ALEXANDRIA

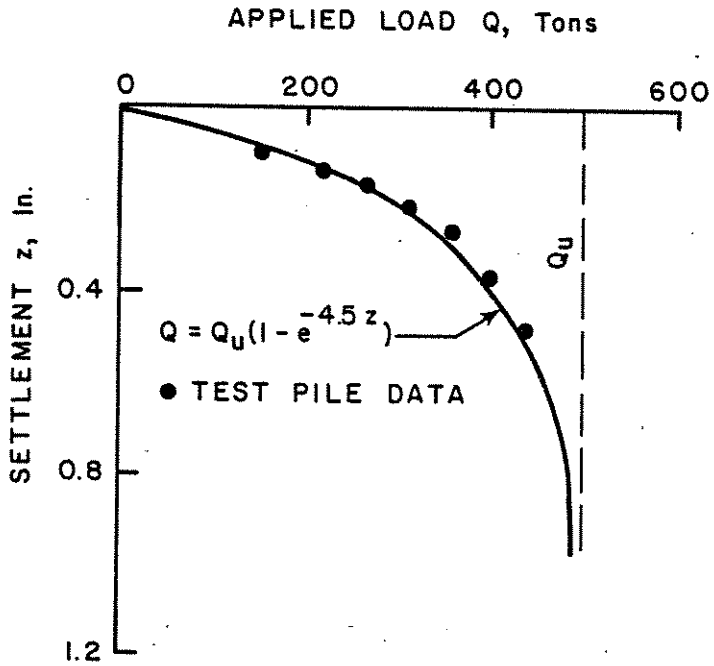

TEST PILE: 2

BORGNE (I)

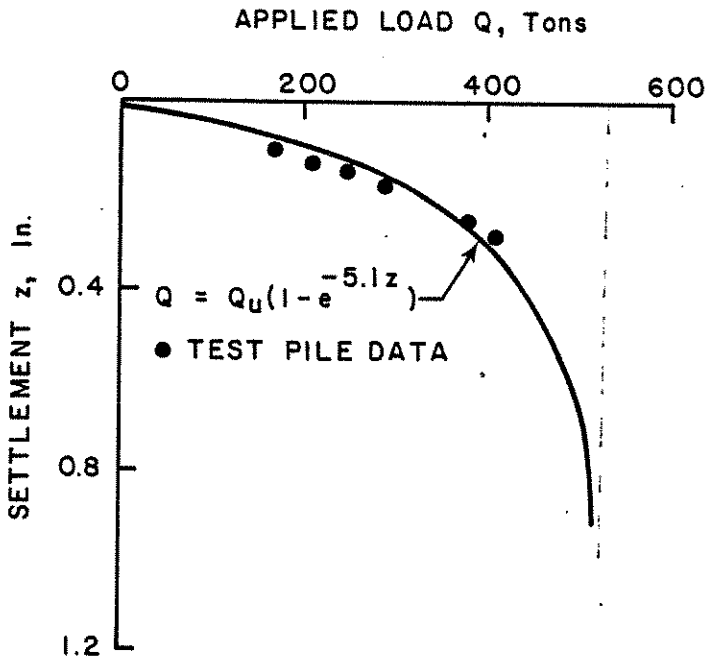

TEST PILE: 4
BORGNE (11)

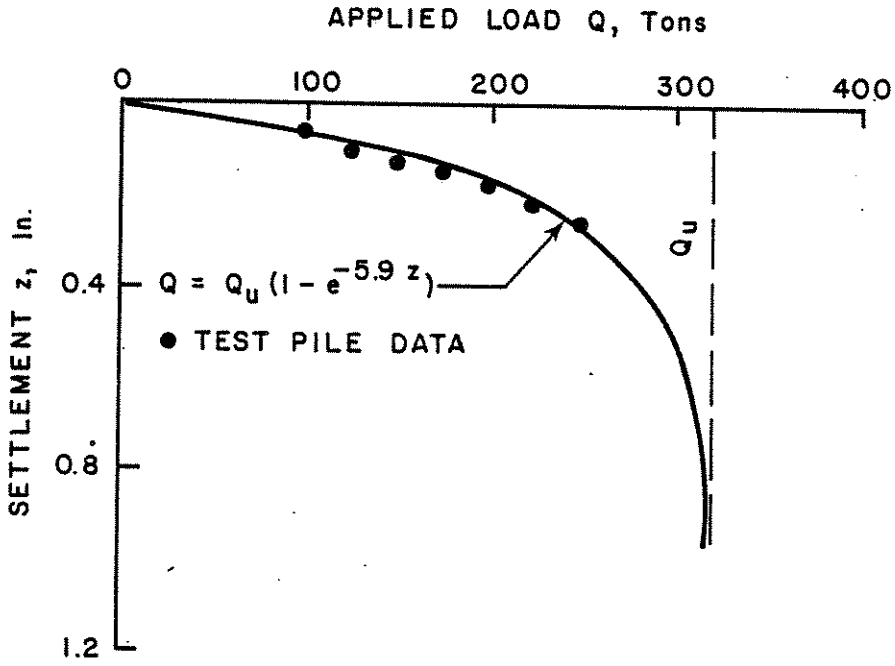

TEST PILE: 5
BORGNE (11)

APPENDIX B

LOCATION OF THE SITES

ATCHAFALAYA RIVER BRIDGE

BERWICK APPROACH

STATE PROJECT 424-05-32

PARISH: SAINT MARY

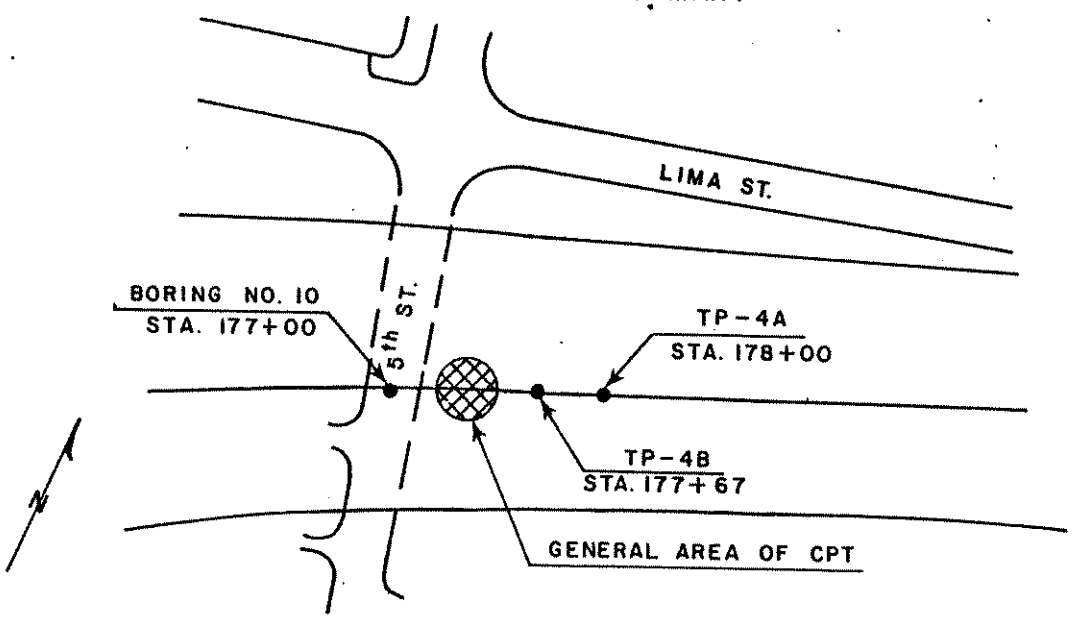

MORGAN CITY SITE

INTERCOASTAL WATERWAY BRIDGE

(PROSPECT AVENUE EXTENTION)

STATE PROJECT: 855-14-03

PARISH: TERREBONNE

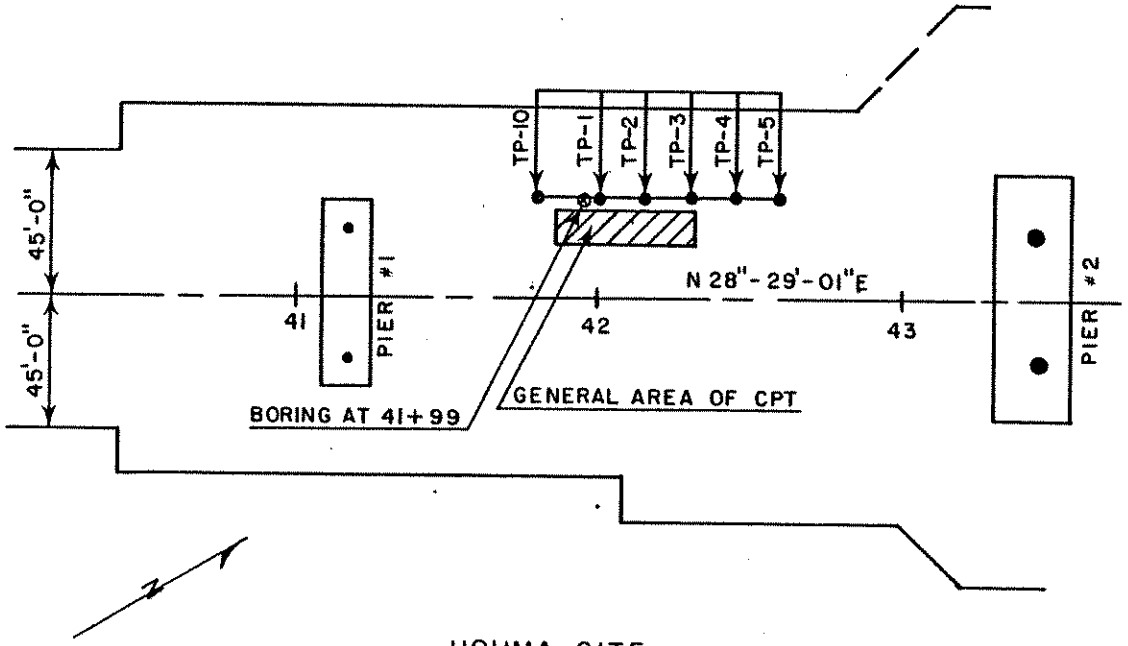

HOUMA SITE

WEST BANK EXPRESSWAY

STATE PROJECT: 283-09-52

PARISH: JEFFERSON

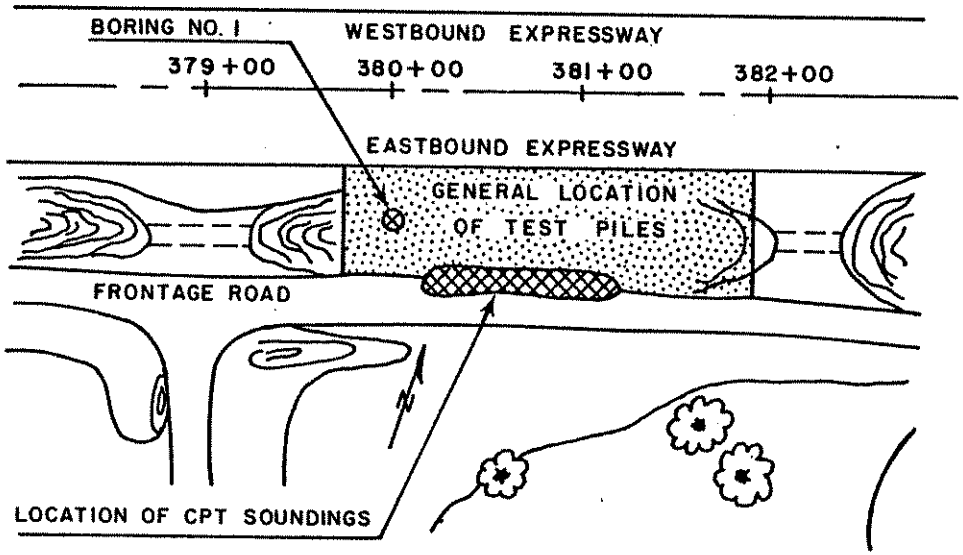

NEW ORLEANS (IIA) SITE

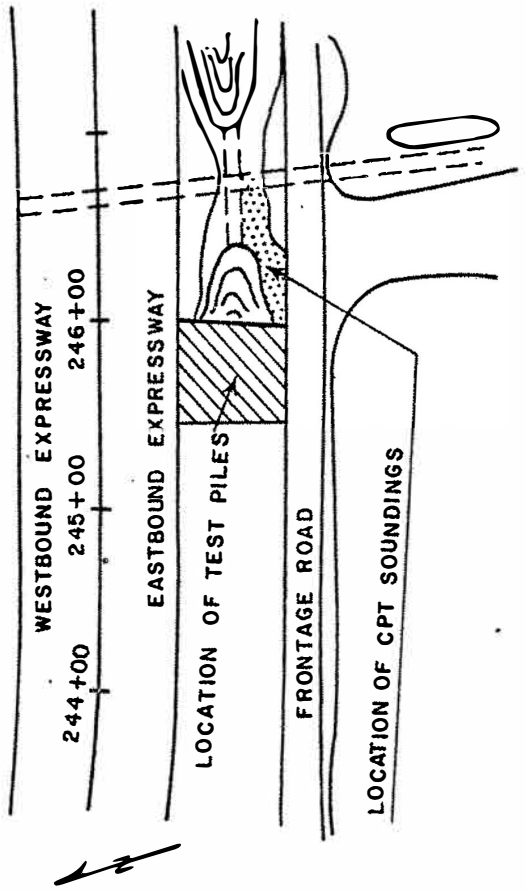
WEST BANK EXPRESSWAY
STATE PROJECT: 283-03-52
PARISH: JEFFERSON
WESTBOUND EXPRESSWAY
EASTBOUND EXPRESSWAY
244+00
245+00
246+00
LOCATION OF TEST PILES
FRONTAGE ROAD
LOCATION OF CPT SOUNDINGS
NEW ORLEANS (I)

TEST PILE PROGRAM

(FRENIER - MANCHAC)

STATE PROJECT: 452-01-25

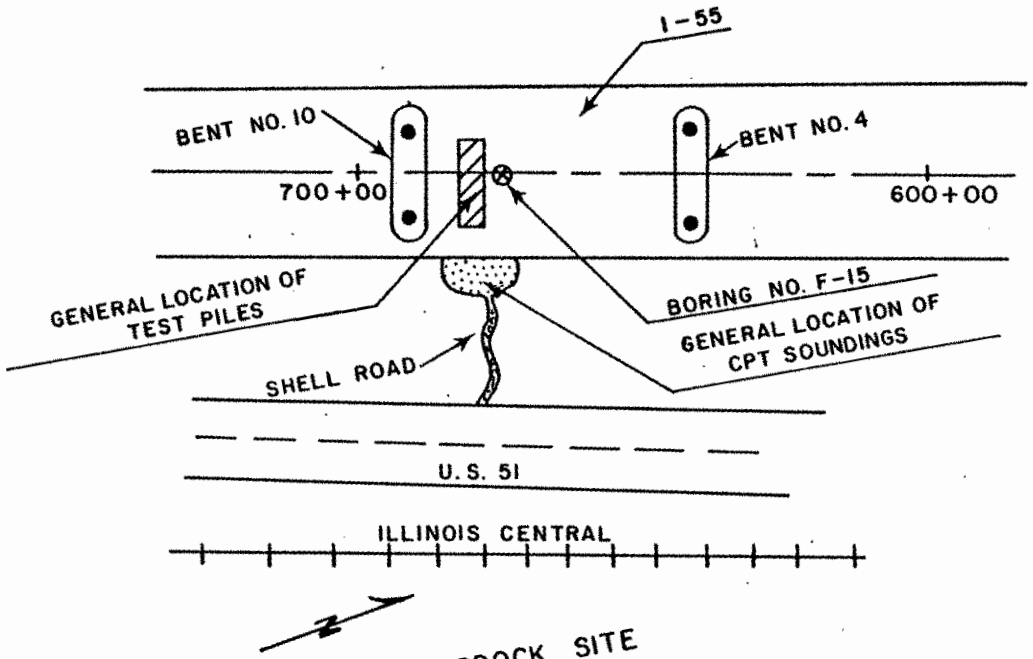

HARDING BLVD. - BRADLEY RD.

SCOTLANDVILLE BYPASS

STATE PROJECT: 450-33-56

EAST BATON ROUGE PARISH

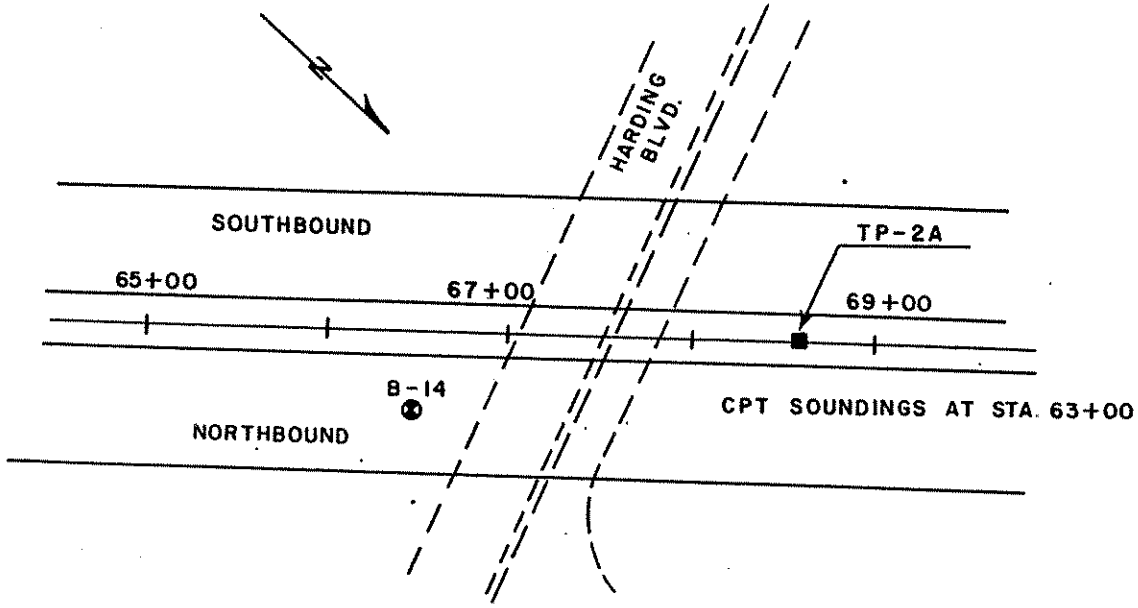

BATON ROUGE (1) SITE

HARDING BLVD. – BADLEY RD.

SCOTLANDVILLE BYPASS

STATE PROJECT 450-33-56

EAST BATON ROUGE PARISH

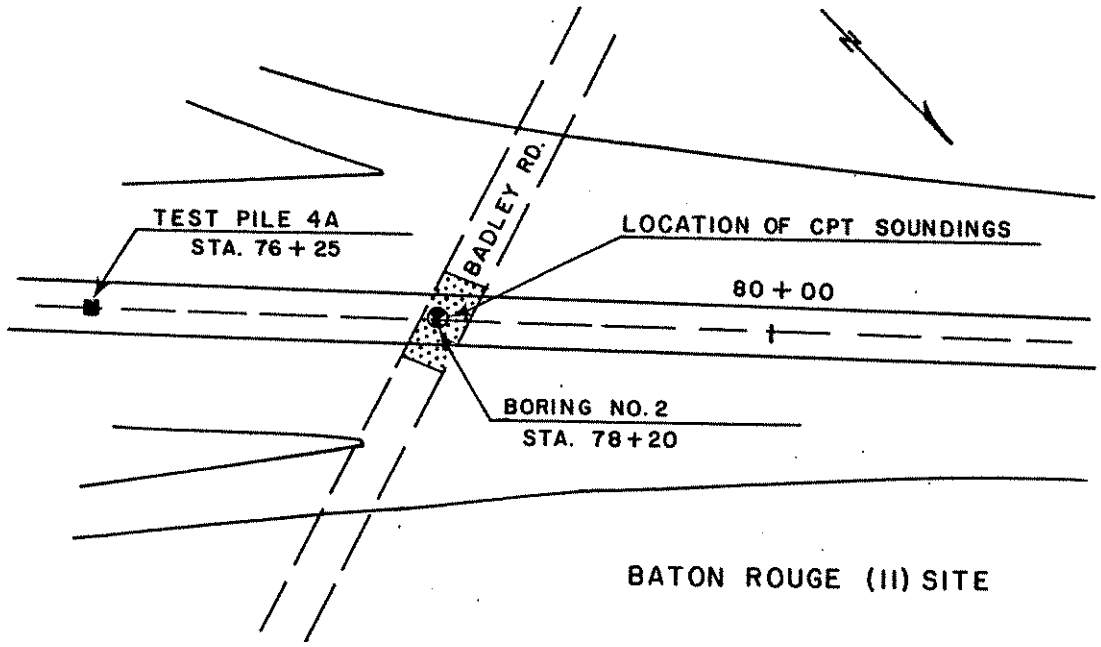

BATON ROUGE (II) SITE

PINEVILLE-TIOGA HIGHWAY

RAILROAD OVERPASS

STATE PROJECT 23-01-12

RAPIDES PARISH

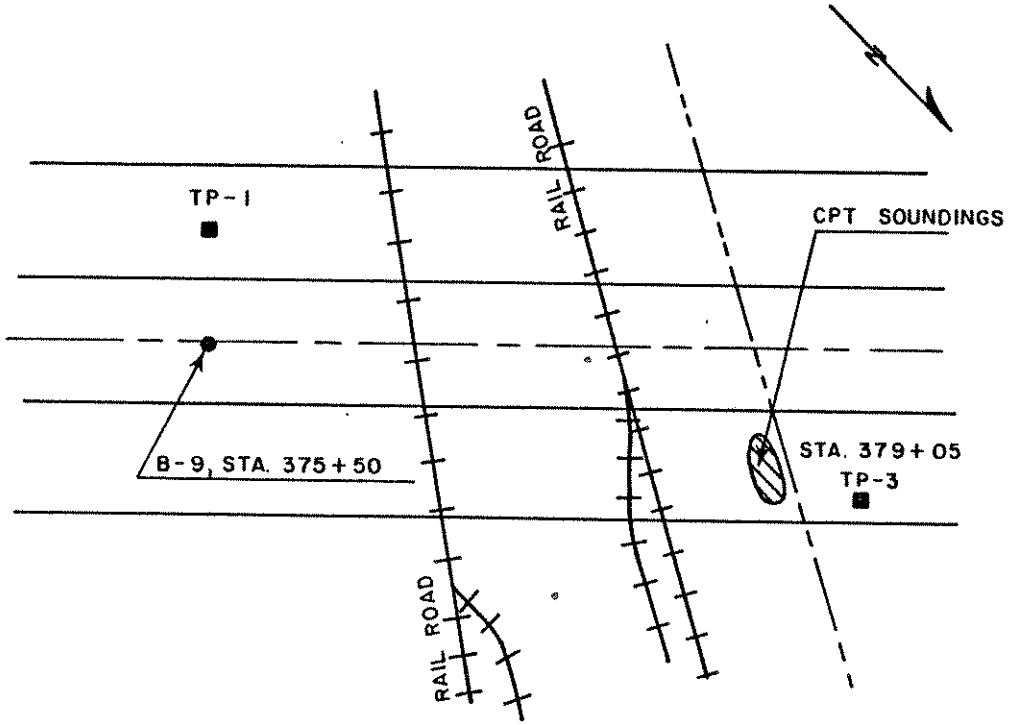

ALEXANDRIA SITE

LAKE BORGNE CANAL BRIDGE

AND APPROACHES

(VIOLET)

STATE PROJECT 46-32-13

SAINT BERNARD PARISH

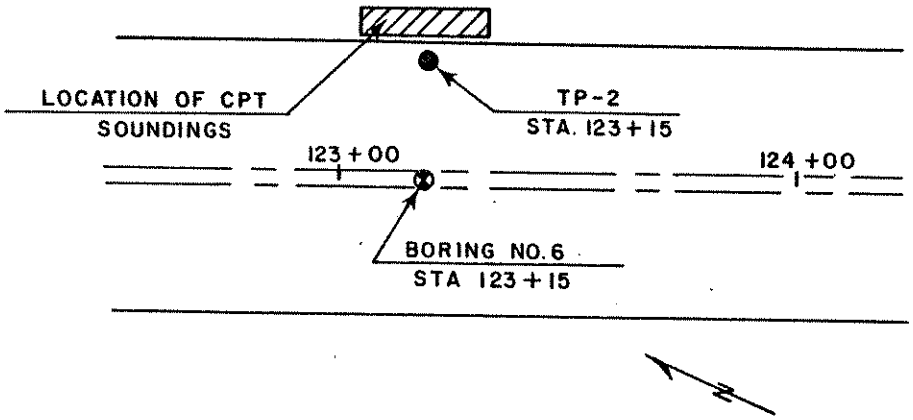

BORGNE (1) SITE

LAKE BORGNE CANAL BRIDGE

AND APPROACHES

(VIOLET)

STATE PROJECT 46-32-13

SAINT BERNARD PARISH

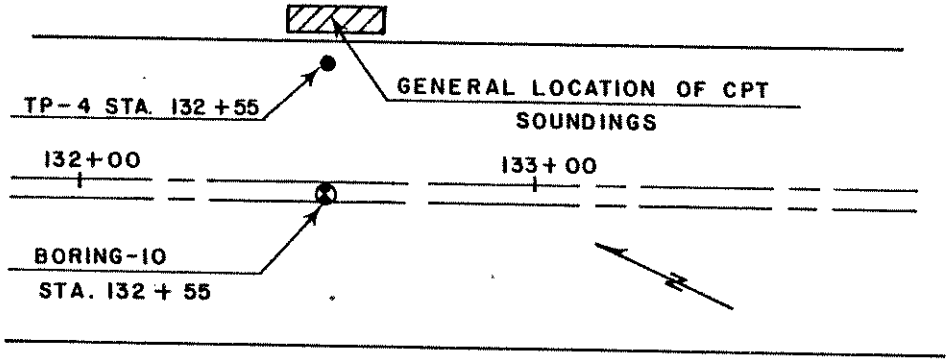

BORGNE (II) SITE

APPENDIX C

SUBSURFACE INFORMATION OF THE SITES

Morgan City Site

Depth (ft)	Soil Type & Color	q_u (TSF)	γ (TCF)	PL (%)	PI (%)
0- 4	Tan & Gray Clay	1.05	0.060	61	41
4- 7	Gray Silty Clay	0.66	0.062	--	--
7- 10	Gray Silty Clay	0.39	0.060	--	--
10- 18	Gray Clay	0.53	0.057	63	42
18- 23	Gray Clay	--	---	--	--
23- 48	Gray Clay	0.60	0.055	70	46
48- 63	Gray Clayey Silt	--	---	--	--
63- 67	Gray Clay	0.76	0.051	--	--
67- 75	Gray Clay	1.81	0.057	--	--
75- 80	Gray Clay	0.68	0.052	94	67
80- 84	Gray Clay	1.04	0.057	--	--
84- 94	Gray Floc. Clay	0.85	0.057	--	--
94- 98	Gray Silty Clay	--	---	--	--
98-108	Gray Clay	0.88	0.058	--	--
108-123	Gray Clay	1.24	0.058	--	--

Boring Number: B-10 Station: 177 + 00

New Orleans (IIA)

Depth (ft)	Soil Type & Color	q_u (TSF)	γ (TCF)	LL (%)	PI (%)
0- 12	Brown Silty Clay	0.40	0.058	49	23
12- 15	Gray Clay	—	0.058	—	—
15- 21	Gray Silty Clay	0.39	0.041	—	—
21- 54	Gray Silty Clay	0.43	0.052	90	62
54- 57	Gray Silty Clay	0.60	0.052	105	73
57- 60	Gray Silty Clay	0.31	0.057	33	15
60- 66	Gray Silty Clay	0.84	0.054	76	51
66- 69	Gray/Brown Silty Clay	0.32	0.060	33	18
69- 75	Gray Brown Sandy Silty Clay	1.20	0.064	73	54
75- 78	Gray Brown Sandy Silty Clay	0.80	0.066	—	—
78- 84	Gray Brown Sandy Silty Clay	1.07	0.064	30	13
84-102	Brown Silty Clay	1.45	0.061	65	41
102-147	Gray Silty Clay	1.85	0.058	72	46

Boring Number: 1

Station: 380 + 00

Houma Site

Depth (ft)	Soil Type & Color	q_u (TSF)	γ (TCF)	LL (%)	PI (%)
0- 4	Gray Silty Clay	0.48	0.048	100	62
4- 8	Gray Silty Clay	0.26	0.053	55	30
8- 13	Gray Fine Sand	—	0.059	--	--
13- 28	Gray Silty Clay	0.37	0.061	37	15
28- 38	Gray Silty Clay	0.57	0.055	63	39
38- 43	Gray Silty Clay	0.74	0.055	76	44
43- 48	Gray Silty Clay	0.65	0.050	65	38
48- 53	Gray Silty Clay	0.41	0.056	51	30
53- 68	Gray Silty Clay	1.29	0.056	73	47
68-141	Gray Silty Clay	1.61	0.057	72	55
141-153	Gray Medium Sand	—	—	--	--
153-157	Gray Fine Sand	—	0.056	—	—

Boring Number: Not Available Station: 41 + 99

New Orleans (I)

Depth (ft)	Soil Type & Color	q_u (TSF)	γ (TCF)	LL (%)	PI (%)
0- 4	Brown Sandy Silty Clay	0.44	0.056	36	14
4- 7	Gray Brown Silty Clay	0.39	0.058	60	37
7- 10	Gray Sandy Silty Clay	0.34	0.062	33	13
10- 13	Gray Silty Clay	0.54	0.054	73	41
13- 16	Gray Silty Clay	0.54	0.053	108	70
16- 19	Gray Silty Clay	0.57	0.053	102	65
19- 40	Gray Silty Clay	0.58	0.053	67	41
40- 43	Gray Silty Clay	0.78	0.051	114	84
43- 46	Gray Silty Clay	0.81	0.054	68	46
46- 58	Gray Silty Clay	0.86	0.051	80	40
58- 61	Gray Medium Silty Sand	--	---	--	--
61- 64	Gray Sandy Silty Clay	0.58	0.057	33	15
64- 67	Gray Silty Clay	0.94	0.057	42	20
67- 79	Gray Silty Clay	1.44	0.052	99	72
79- 85	Gray Brown Silty Clay	1.28	0.061	88	64
85- 88	Brown Sandy Silty Clay	0.98	0.063	39	23
88- 94	Brown Silty Clay	1.80	0.060	93	66
94-100	Brown Silty Clay	1.54	0.063	44	24
100-109	Gray Brown Silty Clay	3.42	0.062	70	50
109-133	Gray Fine Silty Sand		SPT N = 44		

Boring Number: 2 Station: 245 + 00

Ruddock Site

Depth (ft)	Soil Type & Color	q_u (TSF)	SPT (N)
0- 4	Gray & Tan Clay	1.05	--
4- 8	Grown Humus w/ Wood	--	--
8-10	Very Soft Gray Clay	--	--
10-33	Gray Clay w/ Sand	0.20	--
33-46	Tan Gray Clay	1.40	--
46-55	Tan Gray Fine Sand	--	20
55-61	Gray Sand w/ Clay	--	19
61-66	Gray Dense Sand	--	32
66-71	Gray Sand	--	50-10"
71-76	Gray Stiff Clay w/ Sand	--	17
76-79	Gray Clayey Sand	0.20	--
79-82	Gray Silty Clay	0.63	--
82-99	Gray Silty Sand	--	50-8"

Boring Number: F-15 Station: 670 + 75

Baton Rouge (I)

Depth (ft)	Soil Type & Color	q_u (TSF)	γ (TCF)	LL (%)	PI (%)
0- 3	Brown Clayey Silt	2.10	0.058	30	8
3- 8	Brown Silty Clay	2.05	0.062	35	18
8-11	Brown Clay	2.58	0.062	57	35
11-20	Gray Brown Clay	1.60	0.064	68	43
20-23	Brown Silty Clay	0.83	0.060	32	14
23-26	Brown & Gray Clay	2.40	0.059	86	57
26-30	Brown Clay	1.07	0.059	38	18
30-33	Gray Silty Clay	2.59	0.063	50	32
33-54	Brown Clay	4.09	0.065	46	29
54-57	Brown Sandy Silty Clay	2.64	0.062	38	20
57-60	Brown Clay	2.43	0.061	34	16

Boring Number: B-14 Station: 66 + 45

Baton Rouge (II) Site

Depth (ft)	Soil Type & Color	q_u (TSF)	γ (TCF)	LL (%)	PI (%)
0-10	Gray Silty Clay	1.21	0.059	36	15
10-50	Gray Brown Silty Clay	2.76	0.057	105	74
50-56	Gray Silty Clay	2.17	0.062	32	13
56-66	Gray Silty Sandy Clay	2.49	0.063	38	21

Boring Number: 2 Station: 78 + 20

Alexandria Site

Depth (ft)	Soil Type & Color	q_u (TSF)	LL (%)	PI (%)
0- 3	Brown Sandy Loam	--	--	--
3- 6	Gray Brown Medium Fine Sand	--	--	--
6- 8	Black Gray Brown Sandy Loam	0.52	21	4
8-12	Gray Brown Silty Clay	1.28	56	38
12-15	Black Gray Silty Clay	0.75	41	27
15-18	Gray Brown Silty Clay	1.90	46	23
18-21	Brown Gray Silty Sandy Clay	2.22	38	21
21-24	Black Gray Sandy Clay	1.72	48	31
24-27	Brown Black Gray Sandy Clay	2.25	66	46
27-30	Red Brown Silty Clay	3.00	77	56
30-42	Brown Gray Silty Clay	1.77	81	52
42-49	Gray Brown Silty Clay	1.14	84	52
49-57	Brown Silty Clay	1.40	95	67

Boring Number: 9 Station: 375 + 50

Borgne (I) Site

Depth (ft)	Soil Type & Color	q_u (TSF)	SPT (N)	γ (TCF)	LL (%)	PI (%)
0- 20	Gray & Brown Silty Clay	0.28	--	0.044	72	41
20- 26	Gray Silty Clay	0.19	--	0.052	31	11
26- 42	Gray Silty Clay	0.28	--	0.055	43	21
42- 60	Gray Silty Clay	0.52	--	0.048	115	84
60- 66	Gray Silty Clay	0.42	--	0.045	106	76
66- 76	Gray Silty Sand	--	18	---	---	--
76- 78	Gray Silty Clay	0.28	--	0.056	32	15
78- 90	Gray Silty Sand	--	50	0.058	---	--
90-102	Gray Silty Clay	0.50	--	0.056	45	24
102-122	Gray Silty Clay	0.72	--	0.053	50	23

Boring Number: 6 Station: 123 + 15

Borgne (II) Site

Depth (ft)	Soil Type & Color	q_u (TSF)	γ (TCF)	LL (%)	PL (%)
0- 6	Gray Brown Silty Clay	0.27	0.049	104	66
6- 9	Gray Clayey/Silty Sand	—	0.055	—	—
9- 21	Gray Silty Clay	0.22	0.048	82	50
21- 30	Gray Clayey/Silty Sand	—	0.053	—	—
30- 45	Gray Silty Clay	0.38	0.055	61	38
45- 66	Gray Silty Clay	0.43	0.052	114	86
66- 69	Gray Fine Silty Sand	—	—	—	—
69- 72	Gray Clayey Silty Sand	—	—	—	—
72- 84	Gray Fine Silty Sand	—	—	N = 30	
84- 87	Gray Sandy Silty Clay	0.48	0.057	29	11
87-117	Gray Silty Clay	0.98	0.053	53	28
117-120	Gray Fine Silty Sand	—	0.051	22	1
120-123	Gray Sandy Clay	0.25	0.057	30	12

Boring Number: 10 Station: 132 + 55

APPENDIX D

UNDRAINED COHESION INFORMATION

MORGAN CITY SITE

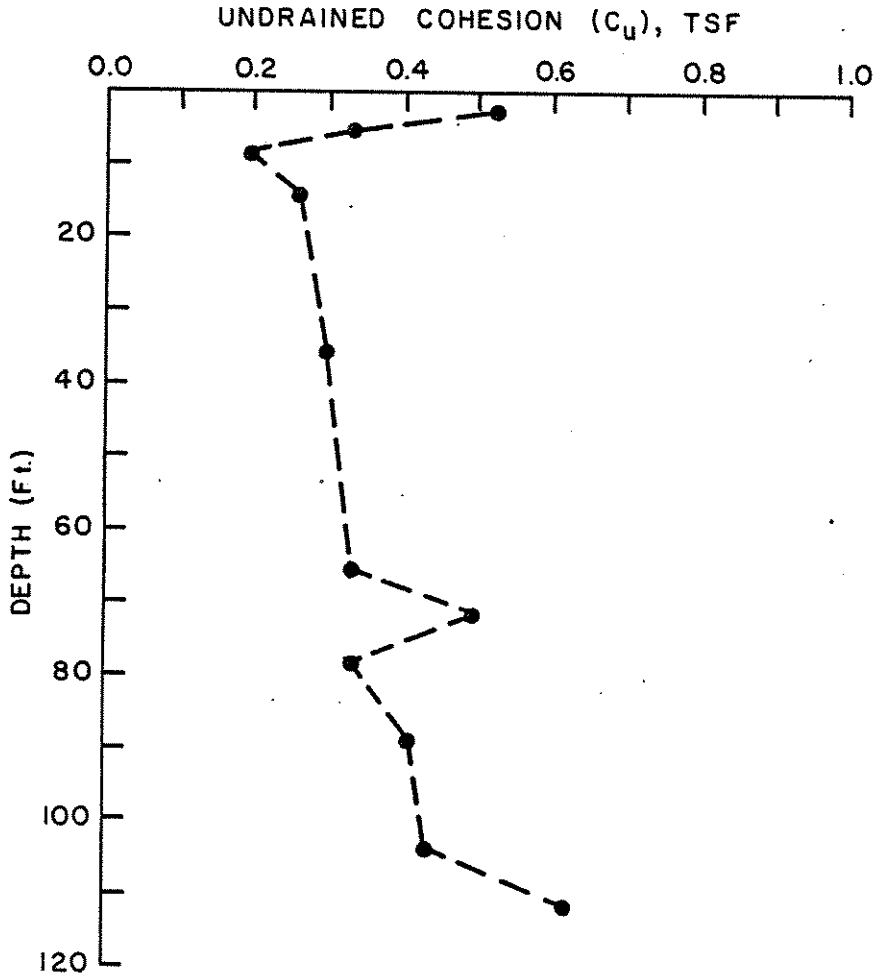

HOUMA SITE

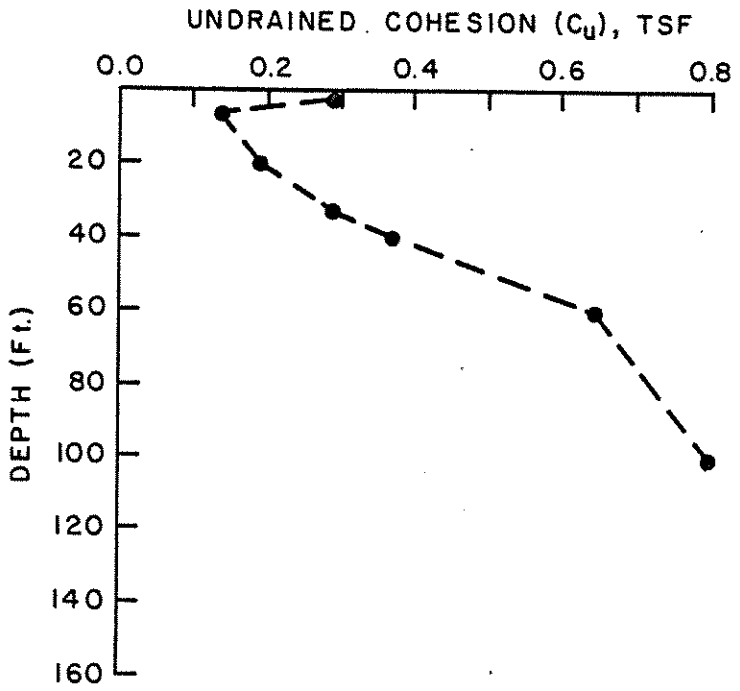
UNDRAINED COHESION (C_u), TSF
0.0
0.2
0.4
0.6
0.8
DEPTH (Ft.)
20
40
60
80
100
120
140
160

NEW ORLEANS (II A) SITE

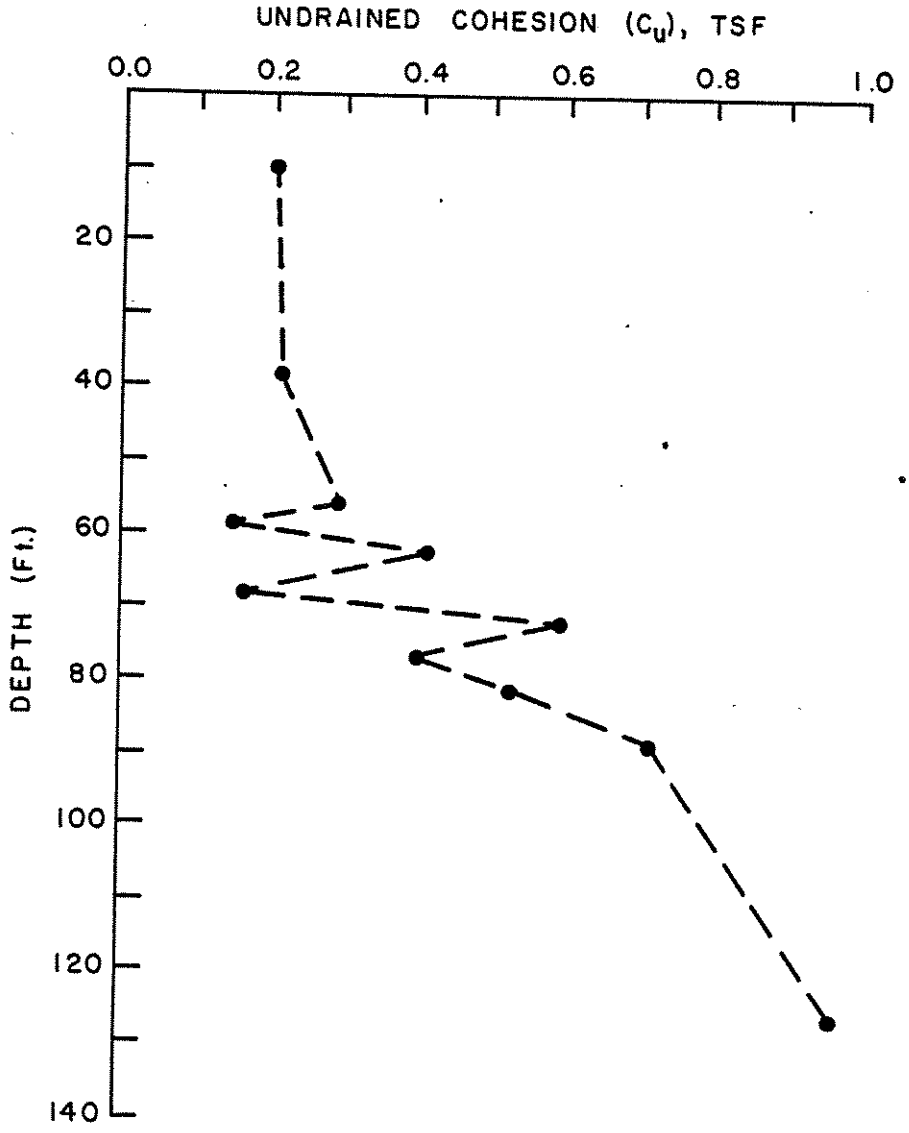

NEW ORLEANS (1)

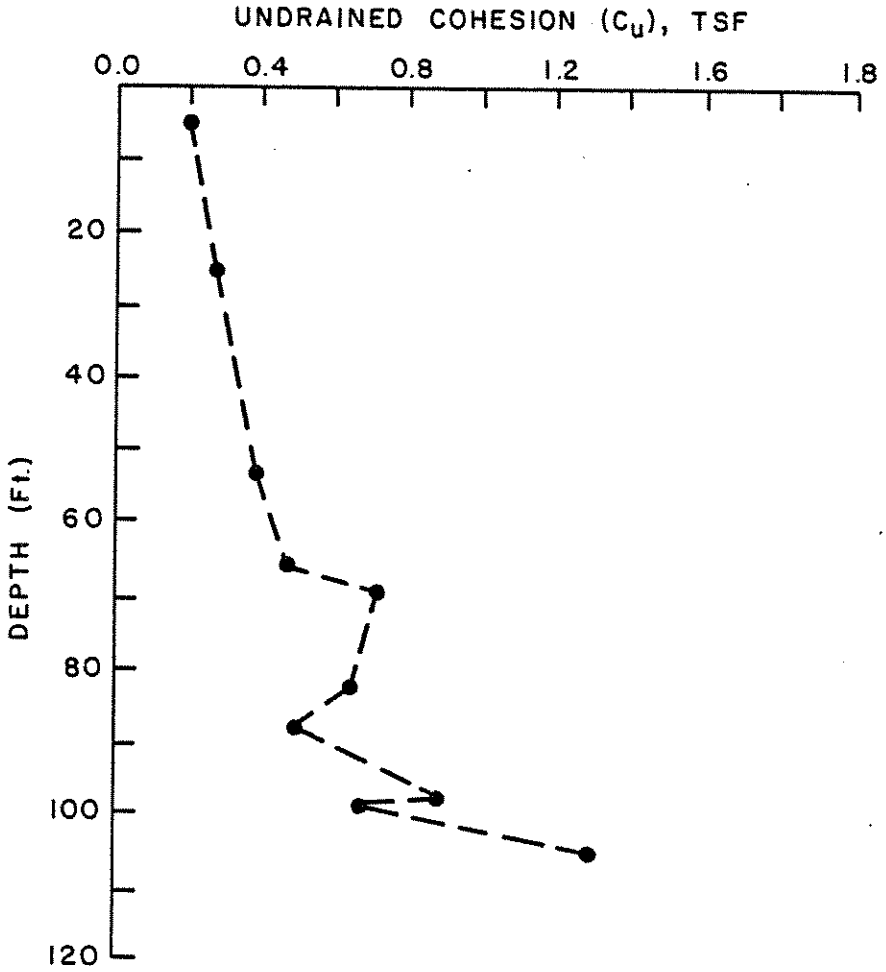

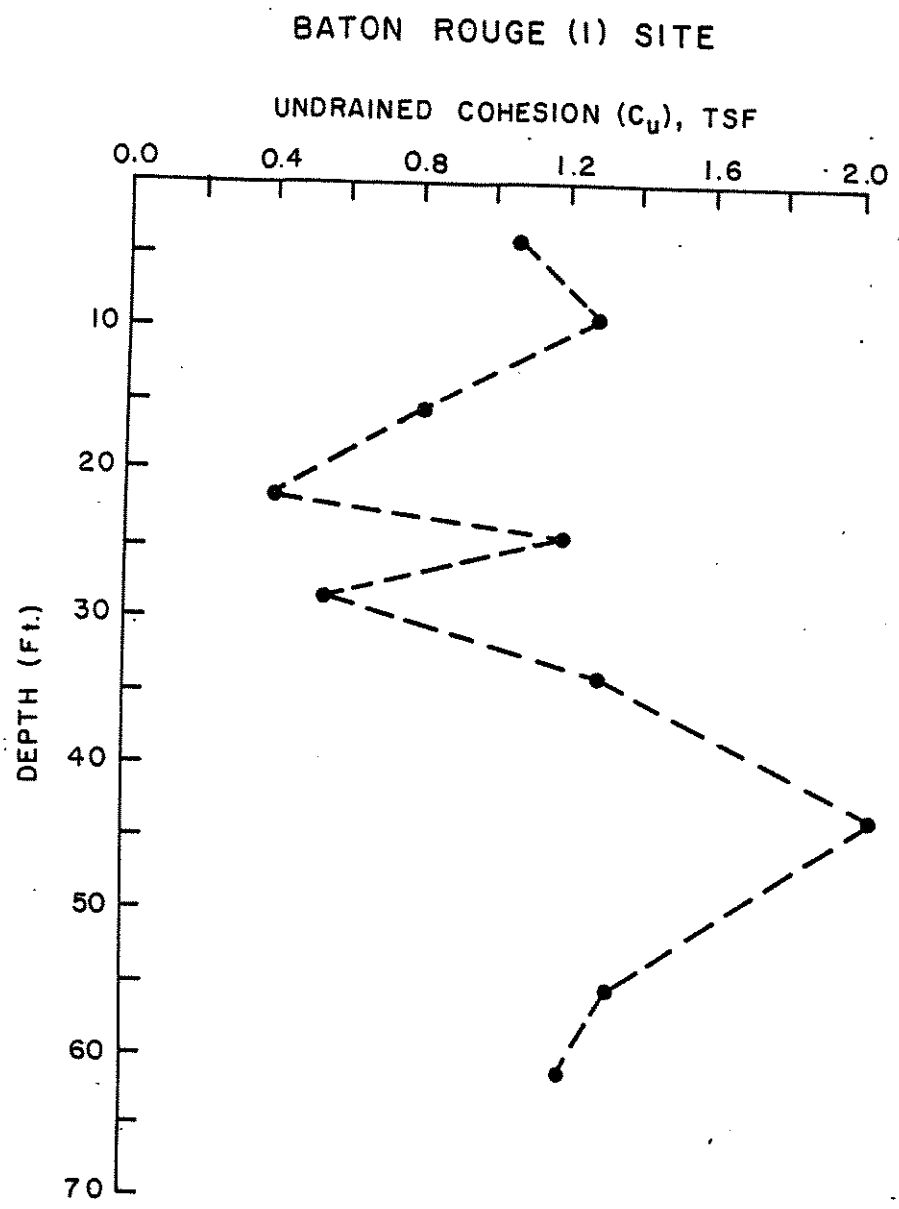
BATON ROUGE (I) SITE
UNDRAINED COHESION (C_u), TSF
0.0
0.4
0.8
1.2
1.6
2.0
10
20
30
40
50
60
70
DEPTH (Ft.)

BATON ROUGE (II) SITE

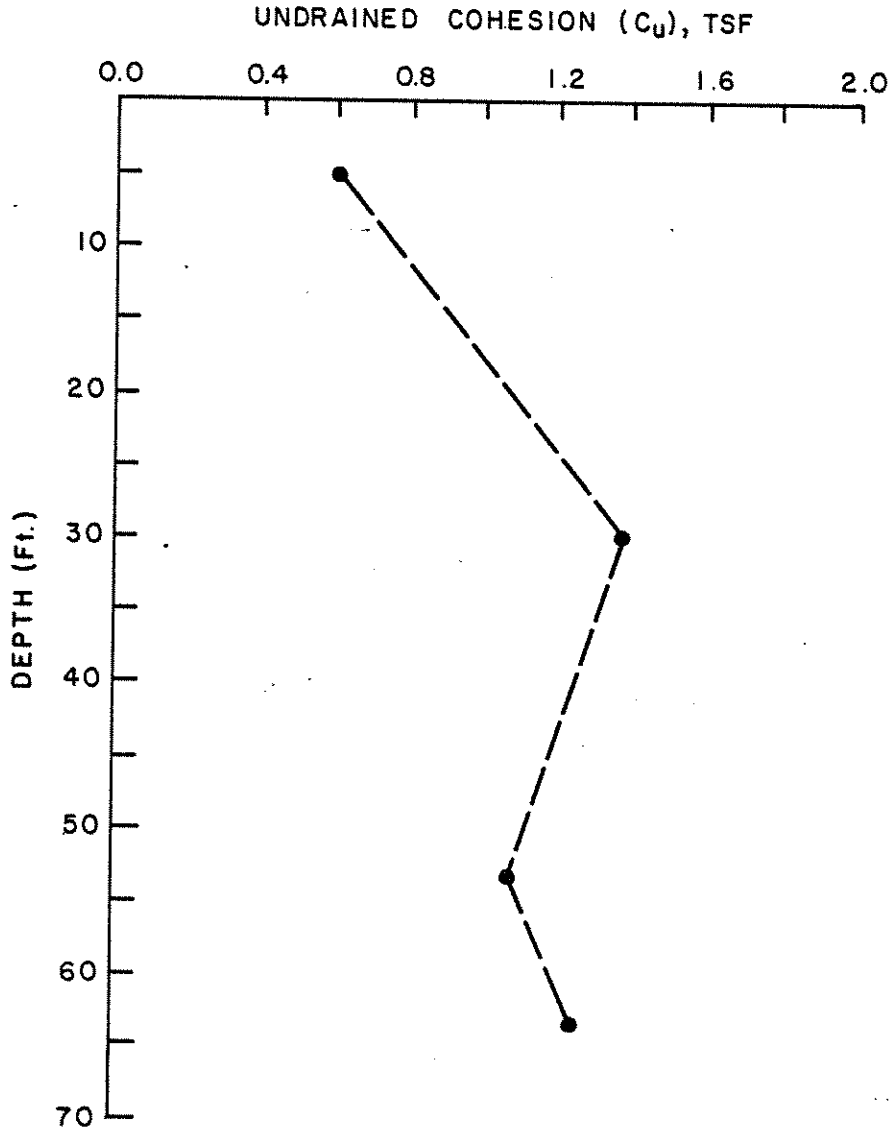

ALEXANDRIA SITE

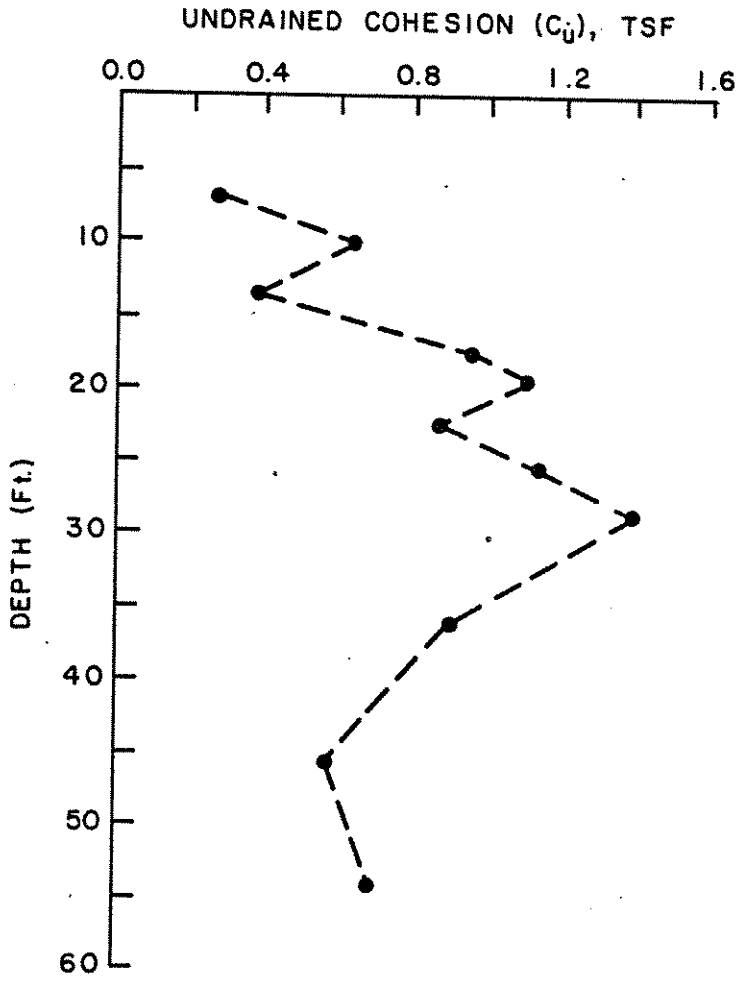

BORGEN (I) SITE

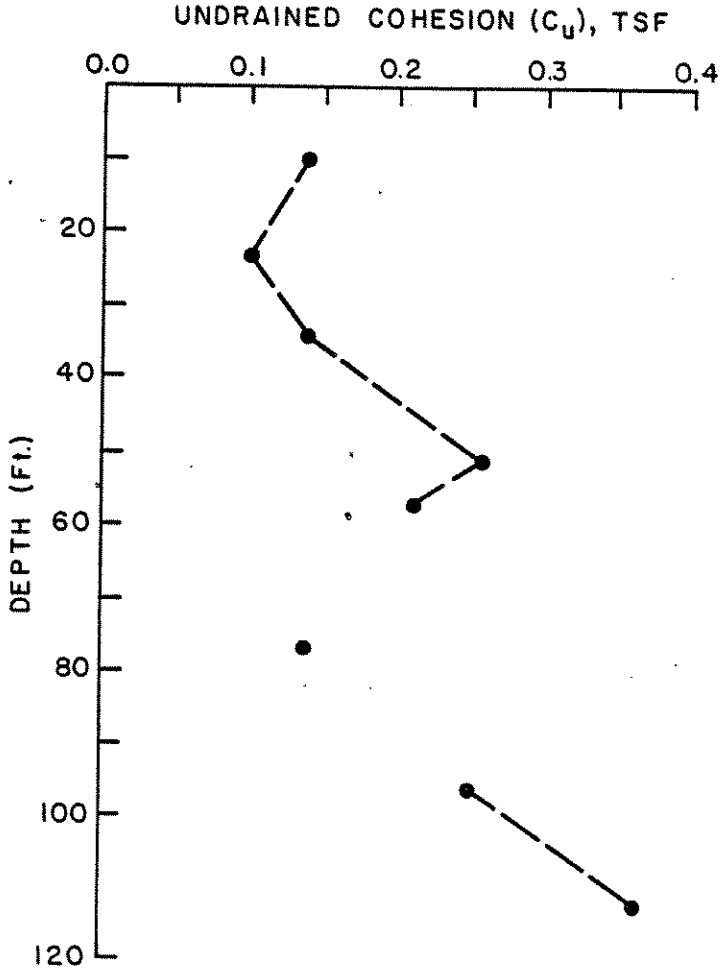

BORGNE (II) SITE

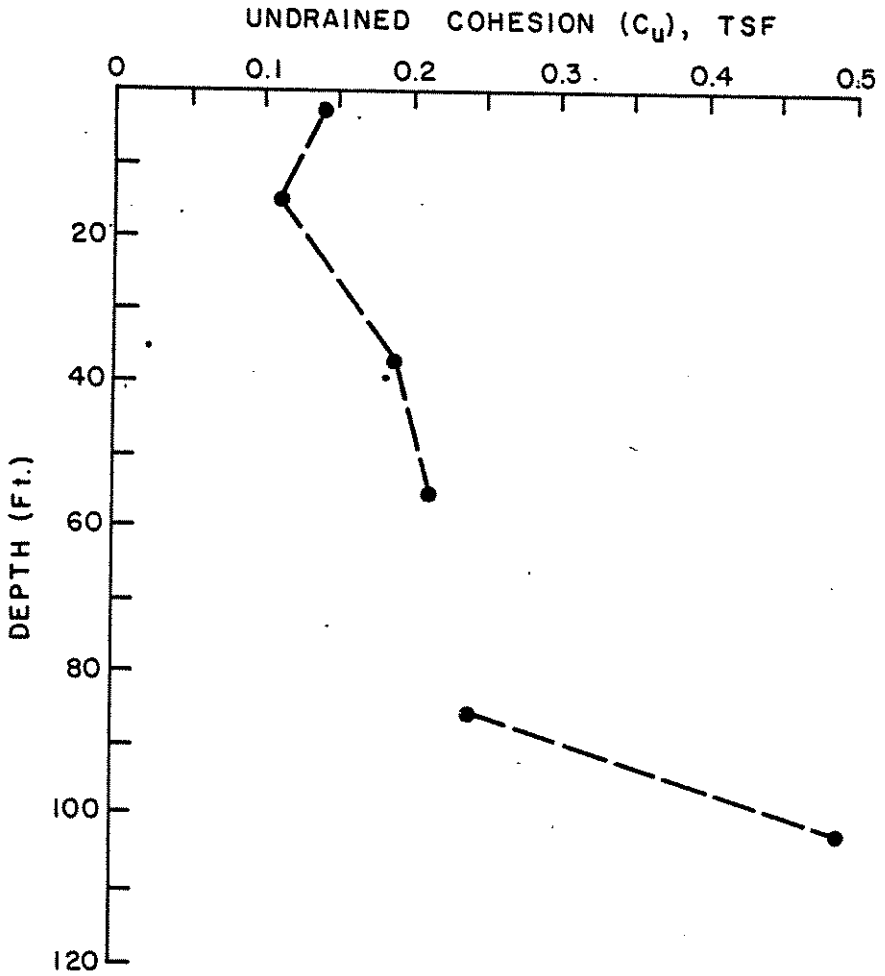

APPENDIX E

CONE PENETRATION PLOTS

MØRGAN

PENETRATION RESULTS TEST NØ=42 (CØNE 60/10)

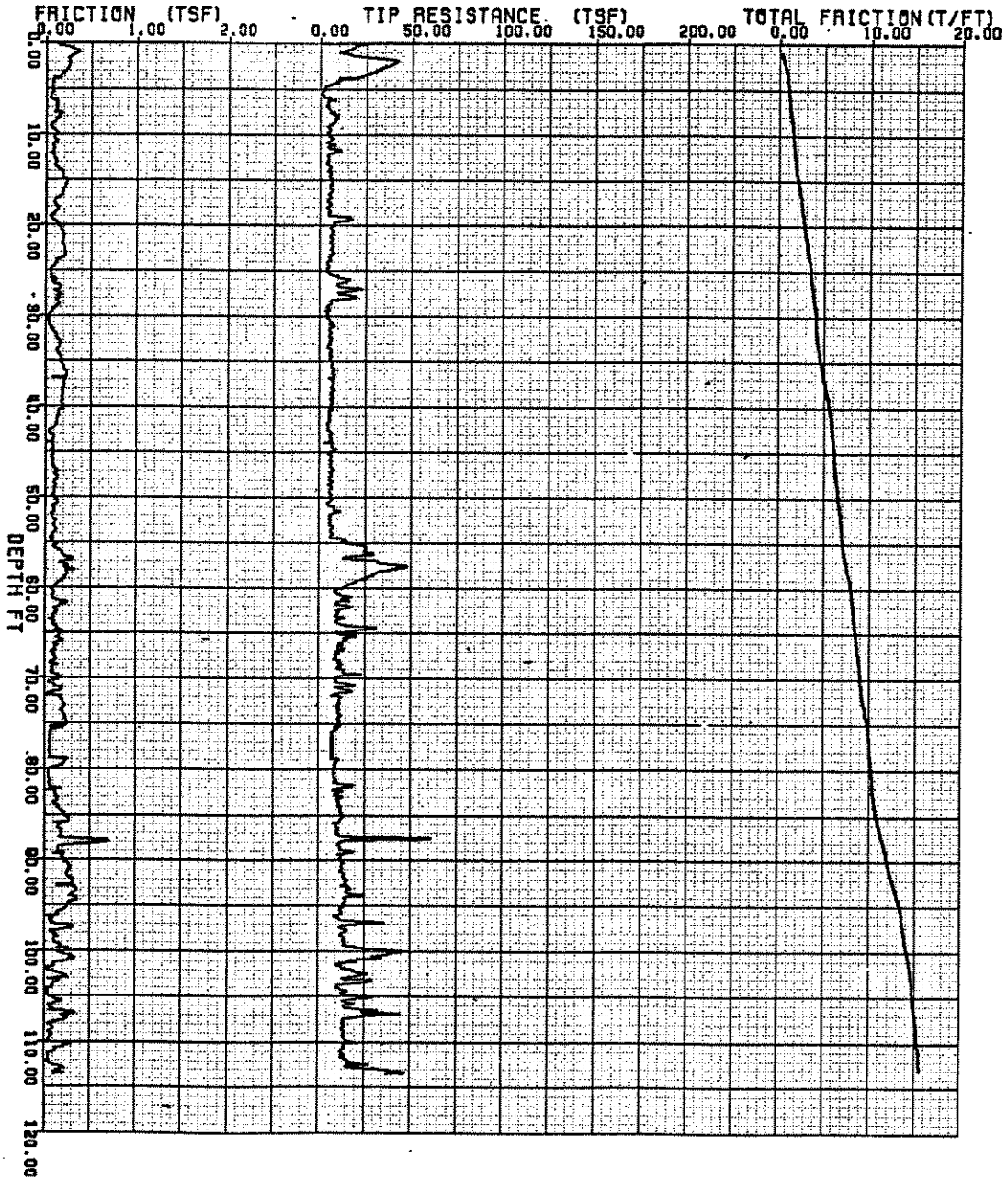

MORGAN

PENETRATION RESULTS TEST NO=41 (CONE 10/10)

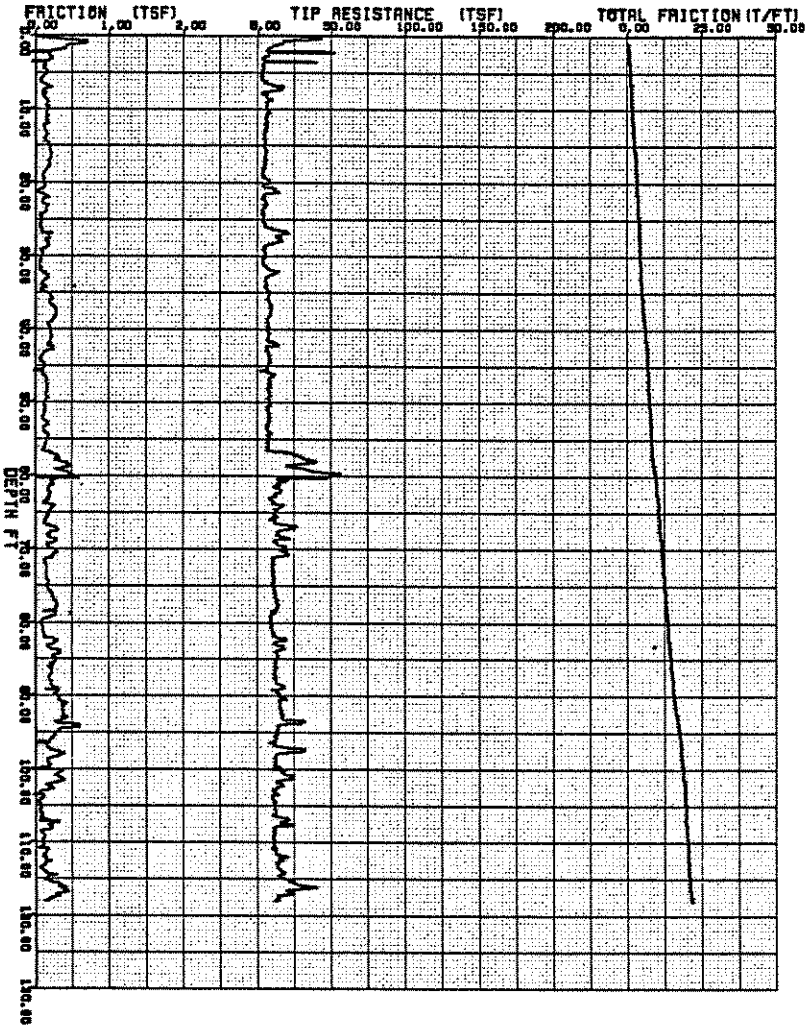

NEW ORLEANS II-A

PENETRATION RESULTS TEST NO=58 (CONE 60/10)

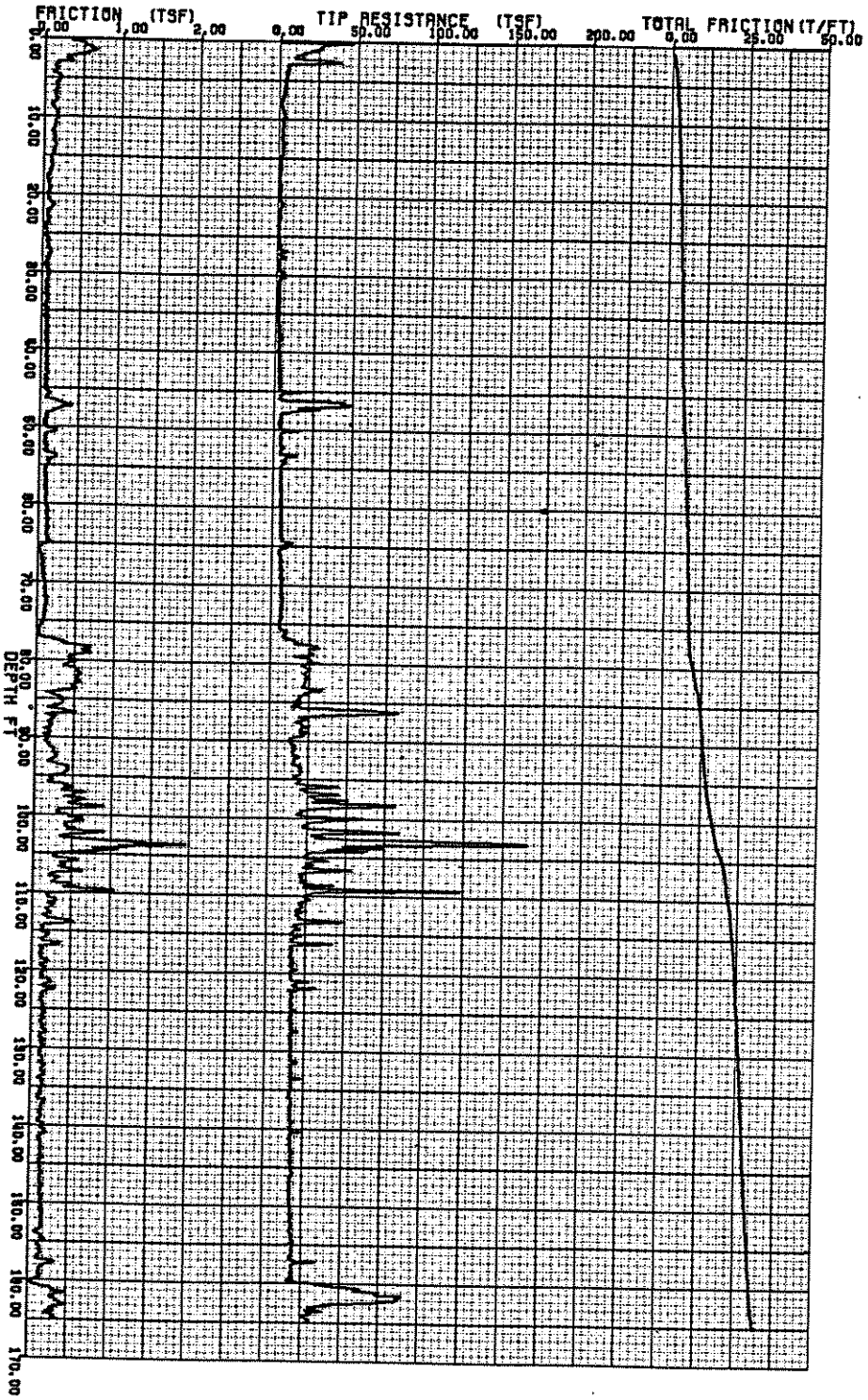

NEW ORLEANS II-A

PENETRATION RESULTS TEST NO=59 (CONE 18/10)

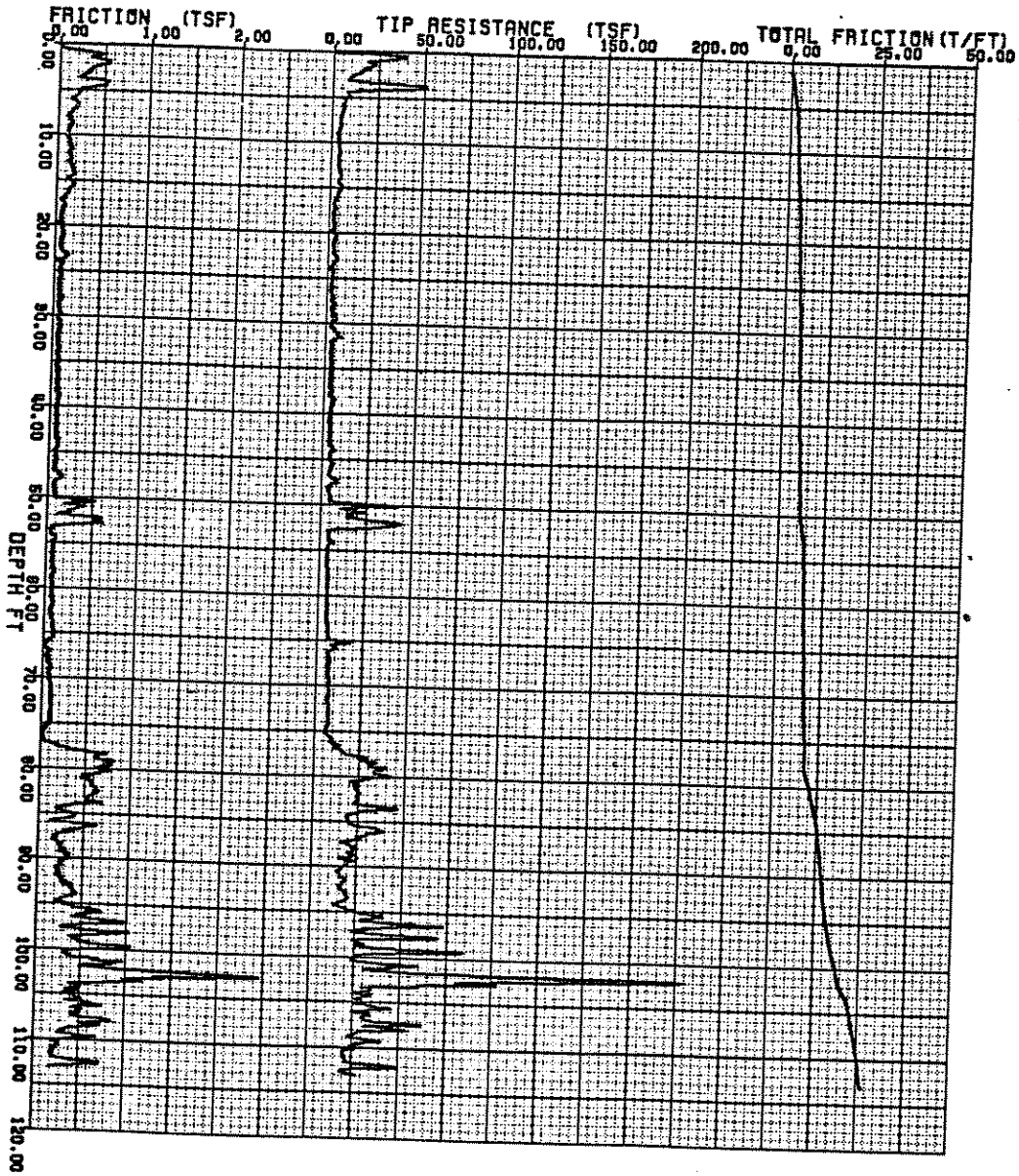

NEW ORLEANS II-A

PENETRATION RESULTS TEST NO=61 (CONE 60/20)

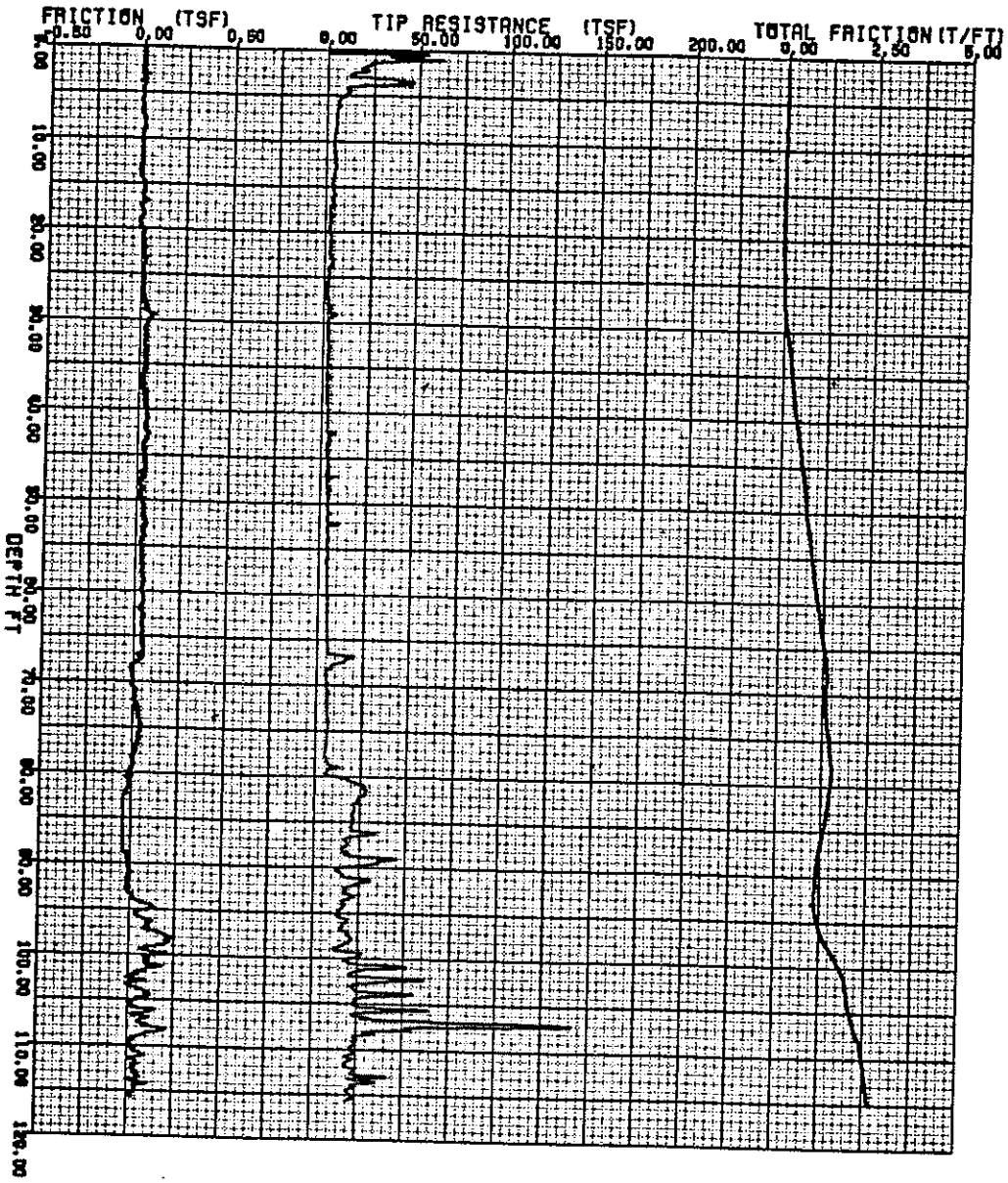

NEW ORLEANS (I)

PENETRATION RESULTS TEST NO=63 (CONE 60/10)

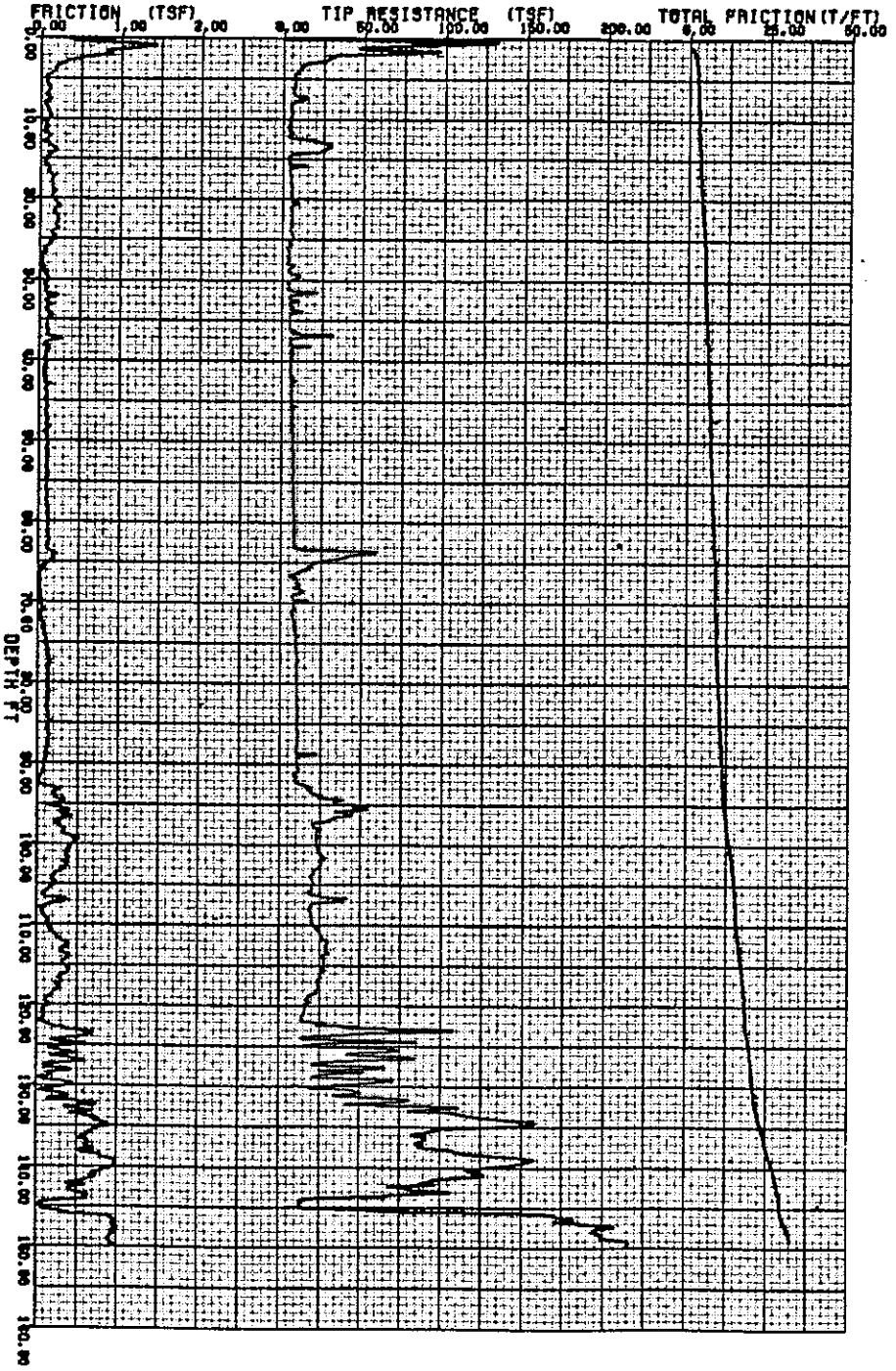

NEW ORLEANS (I)

PENETRATION RESULTS TEST NO=64 (CONE 18/10)

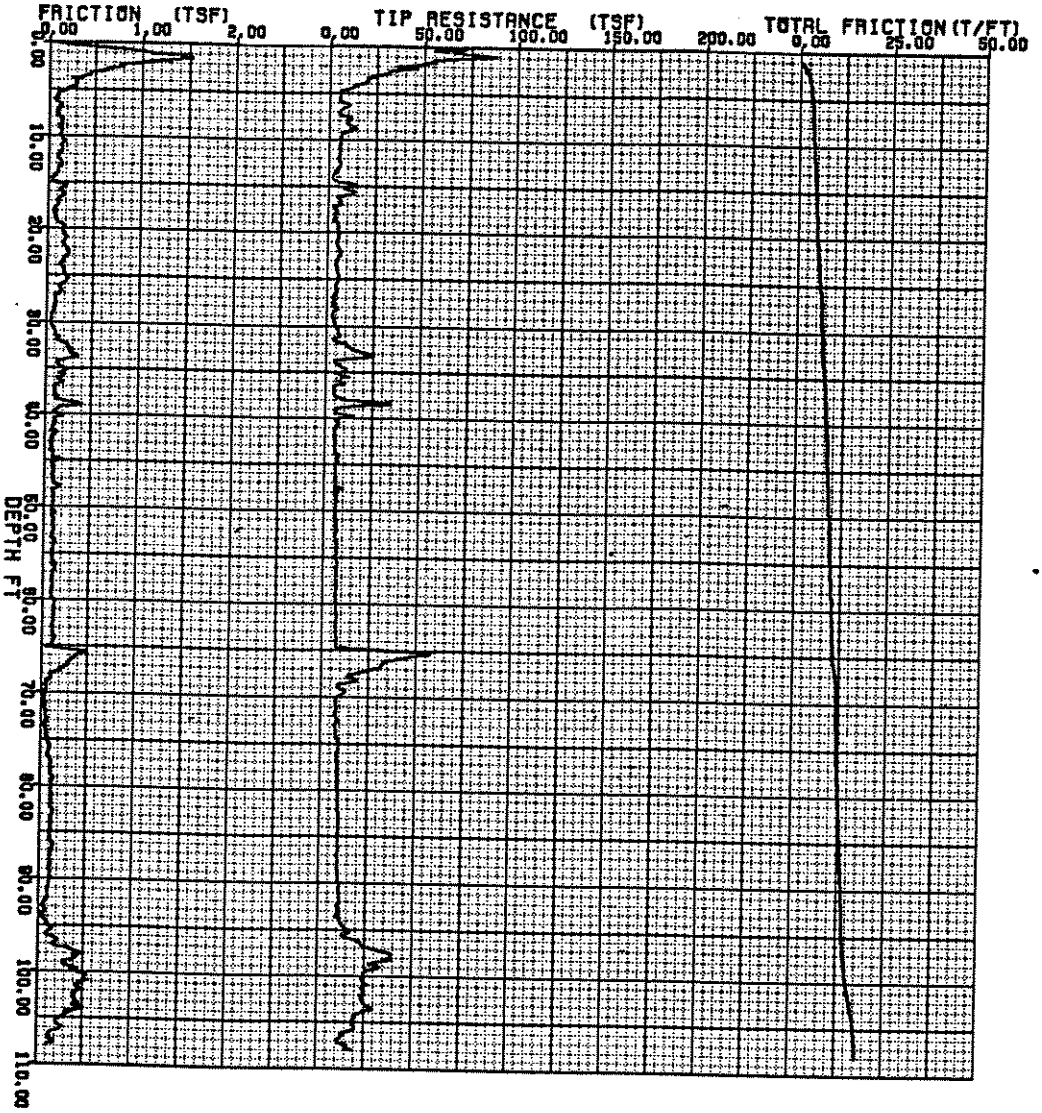

HOUMA

PENETRATION RESULTS TEST NO=54 (CONE 60/10)

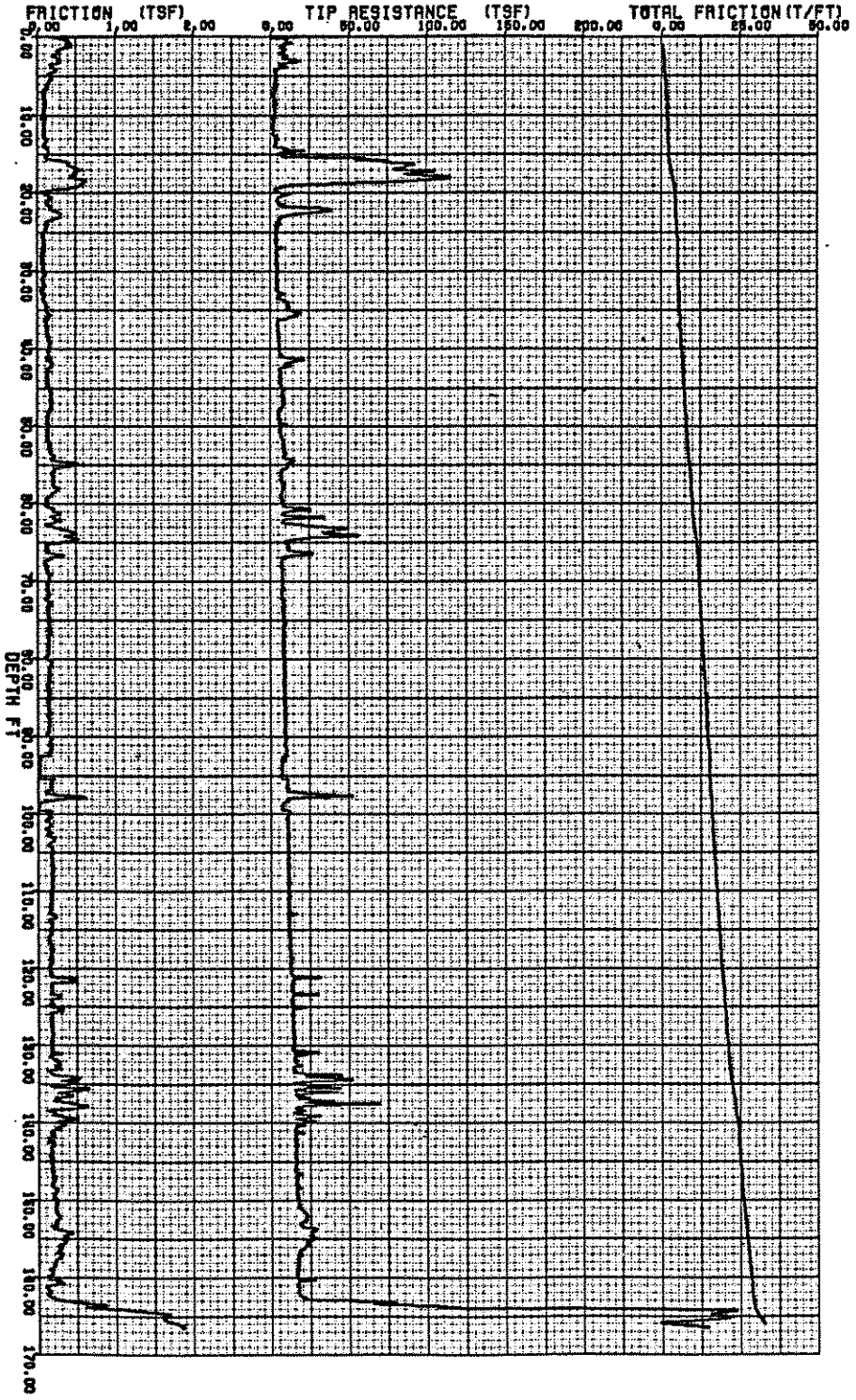

HOUMA

PENETRATION RESULTS TEST NO=55 (CONE 18/10)

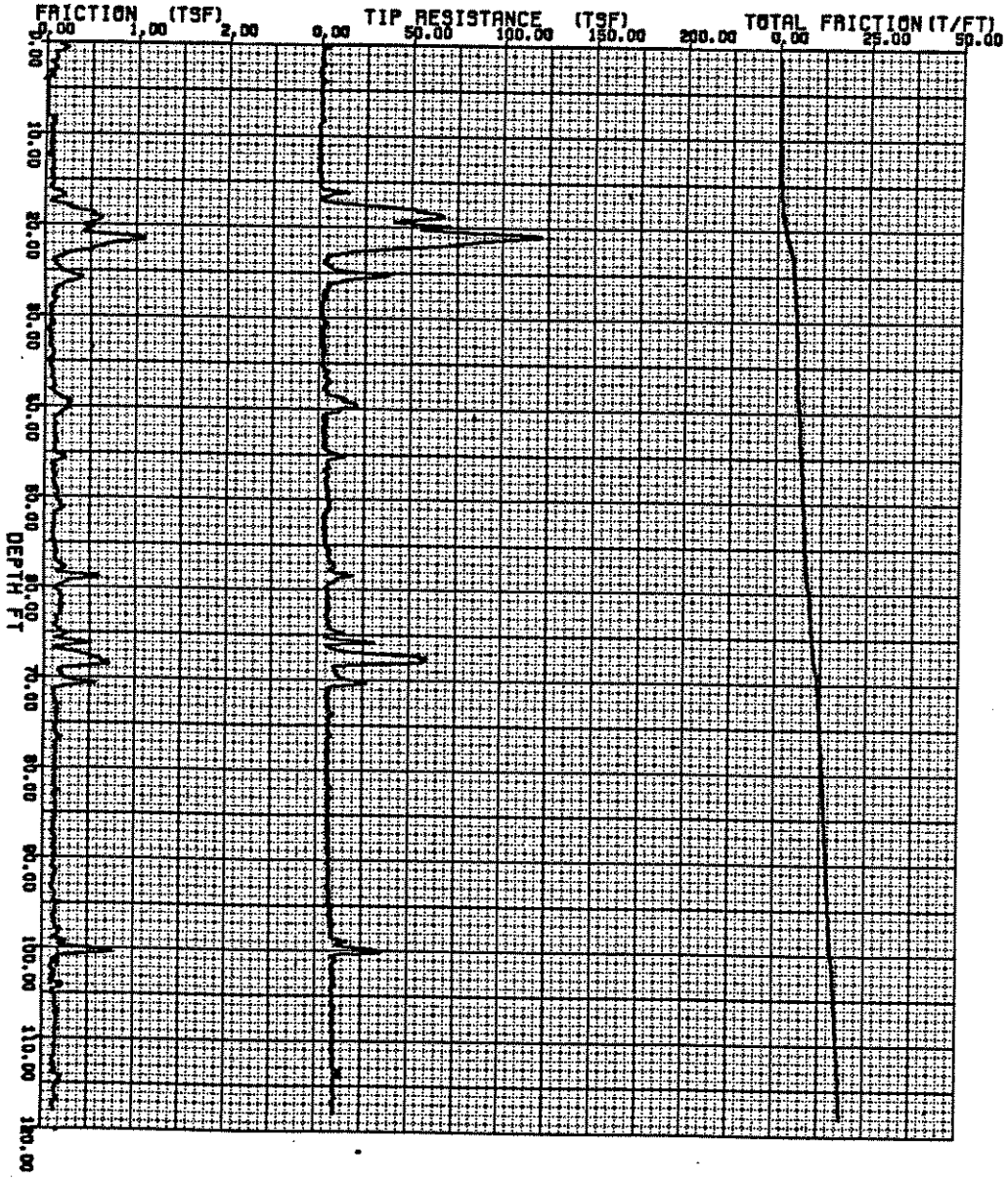

HOUMA

PENETRATION RESULTS TEST NO=56 (CONE 60/20)

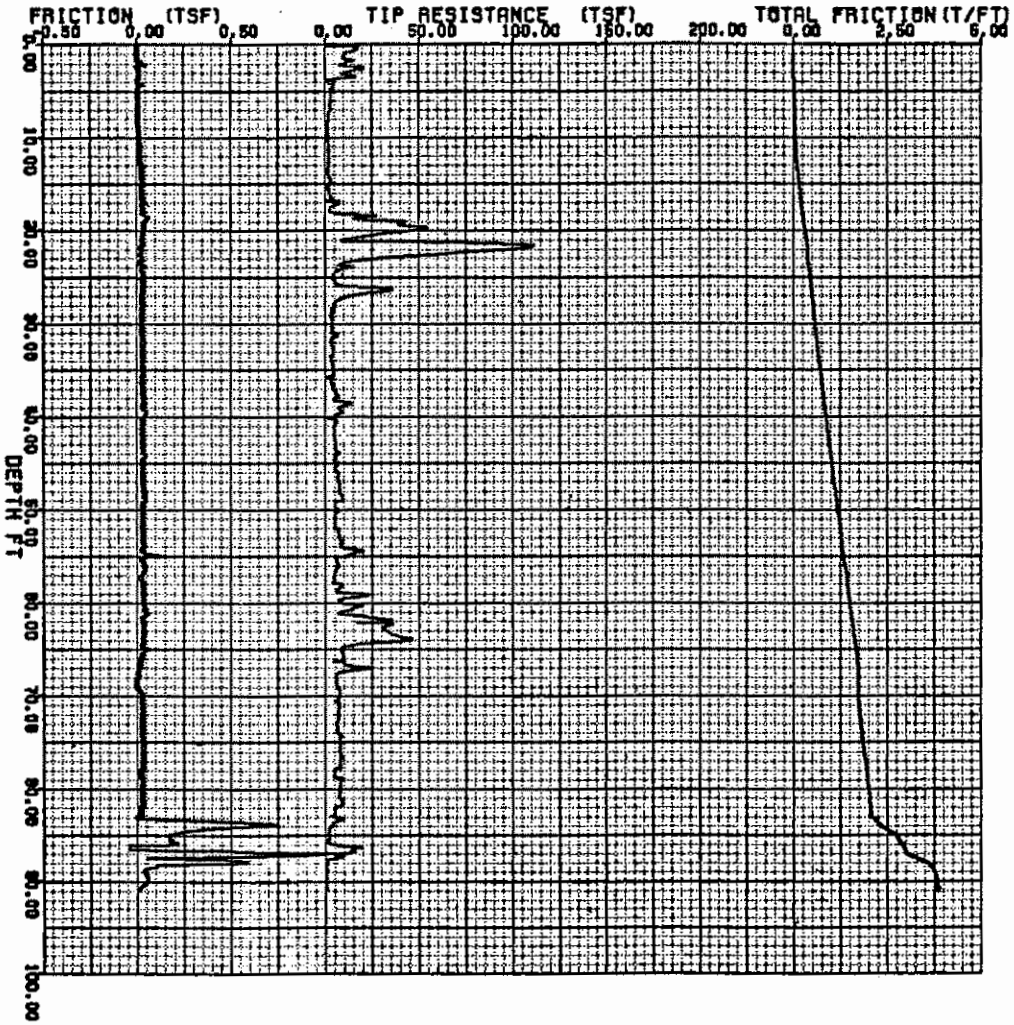

RUDDOCK

PENETRATION RESULTS TEST NO=82 (CONE 60/10)

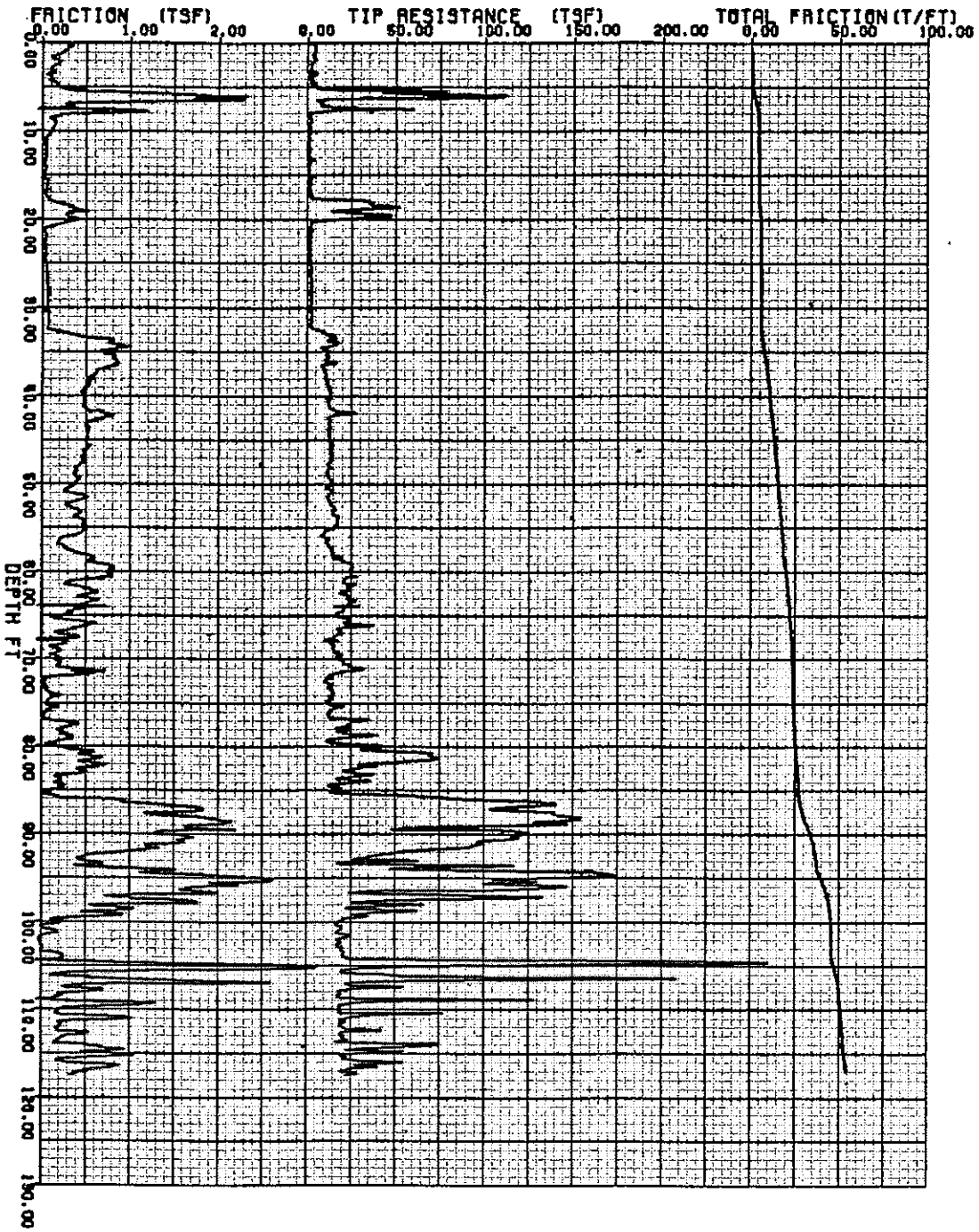

RUDDOCK

PENETRATION RESULTS TEST NO=83 (CONE 18/10)

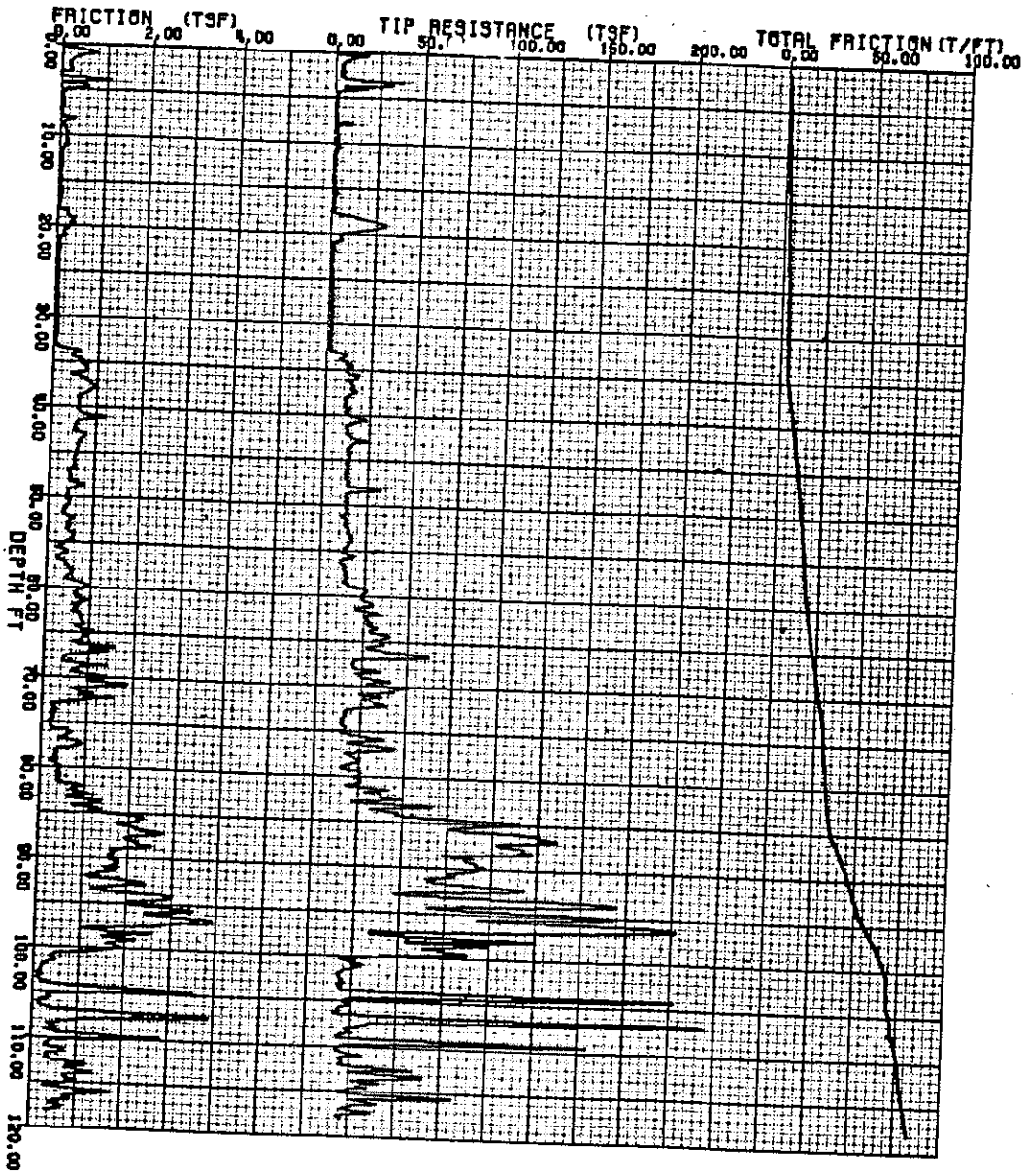

RUDDØCK

PENETRATION RESULTS TEST NØ=84 (CØNE 60/20)

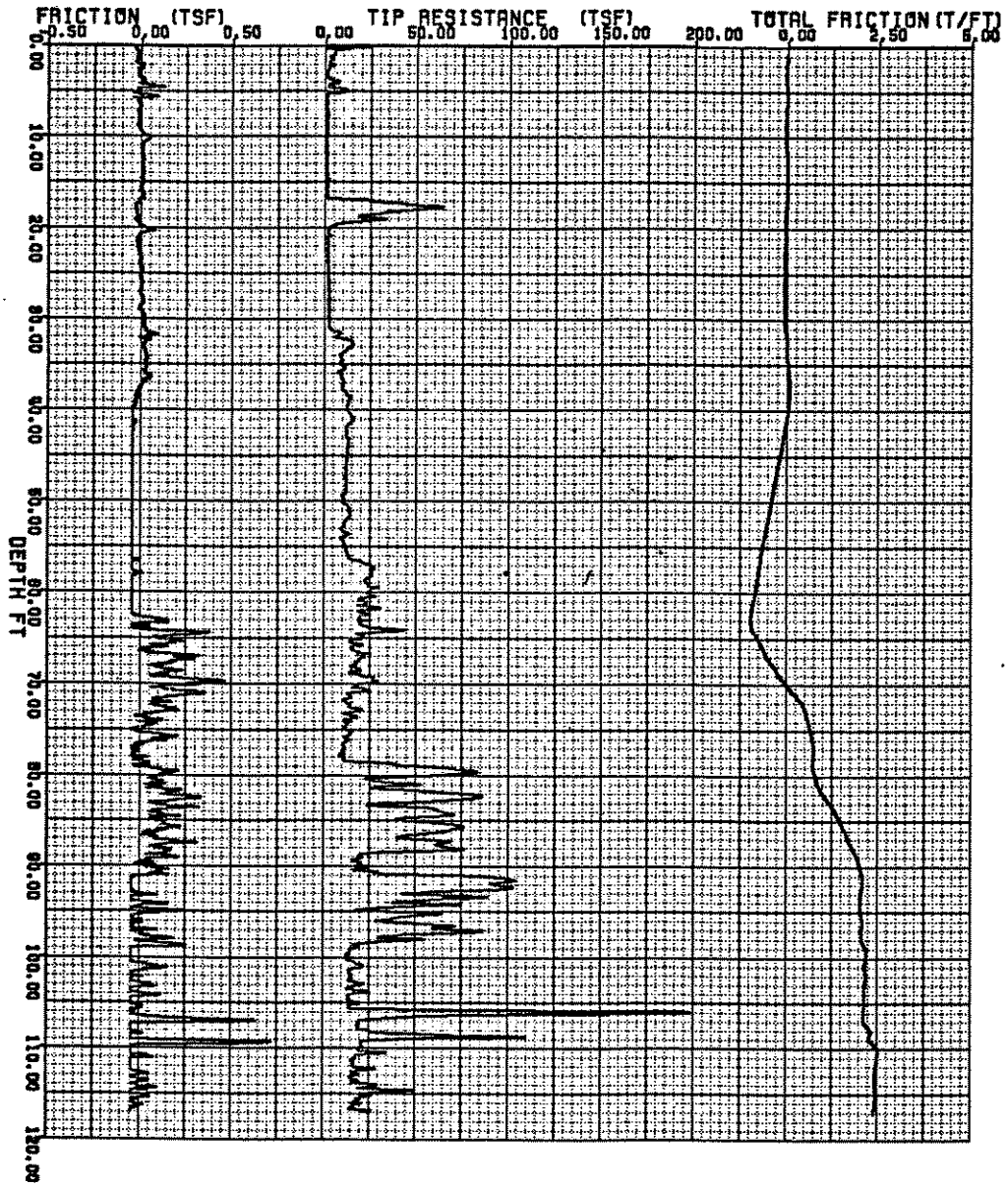

BATØN RØUGE (I)

PENETRATIØN RESULTS TEST NØ=89 (CØNE 60/10)

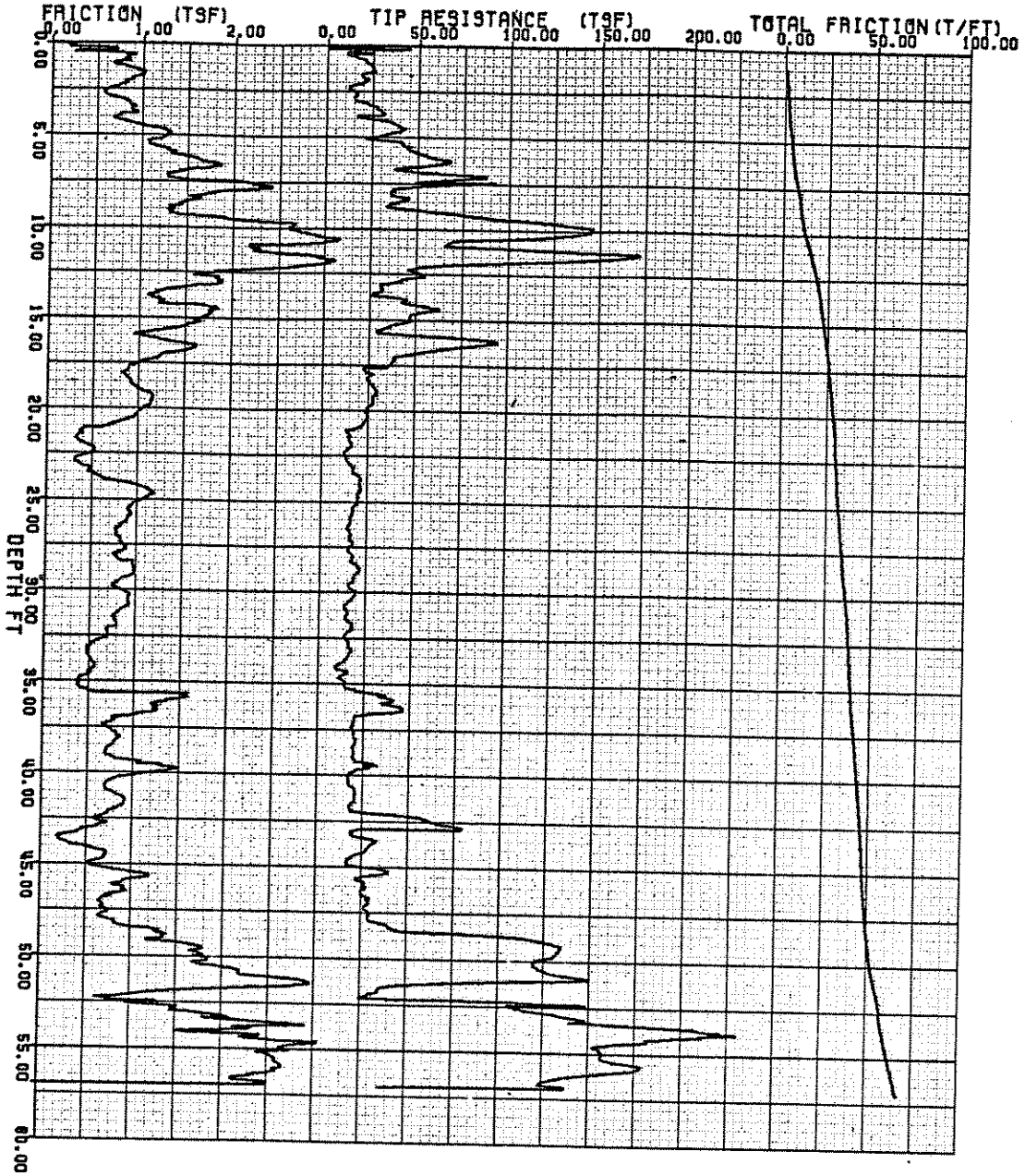

BATON ROUGE (I)

PENETRATION RESULTS TEST NO=91 (CONE 10/10)

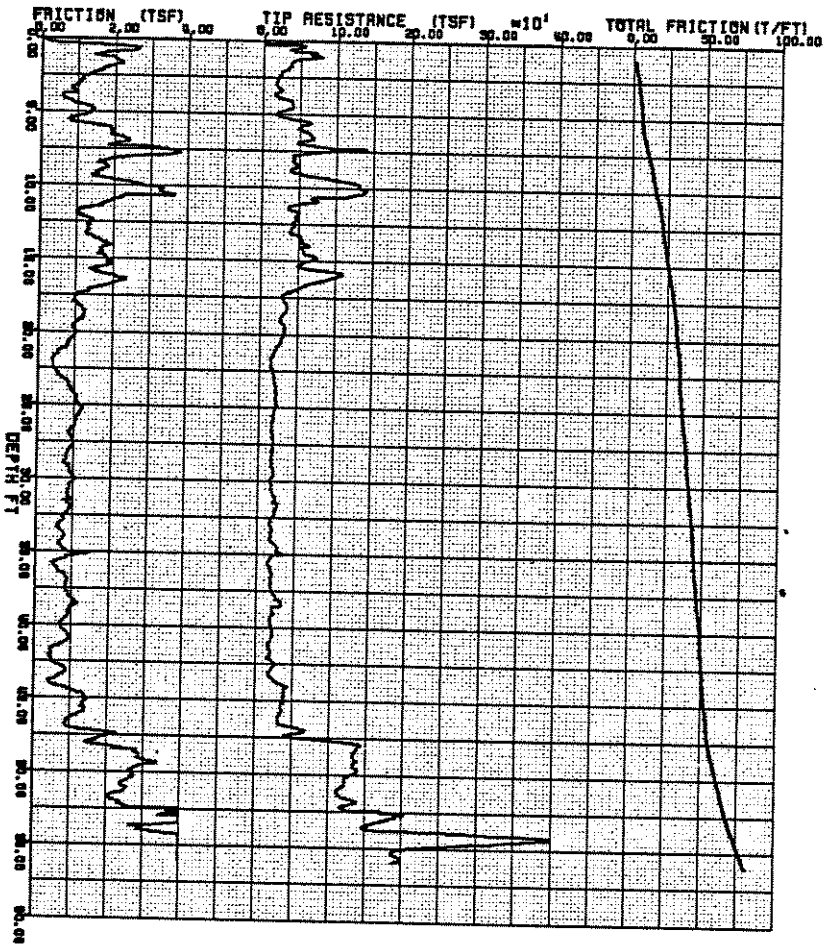

BATON ROUGE (II)

PENETRATION RESULTS TEST NO=94 (CONE 60/10)

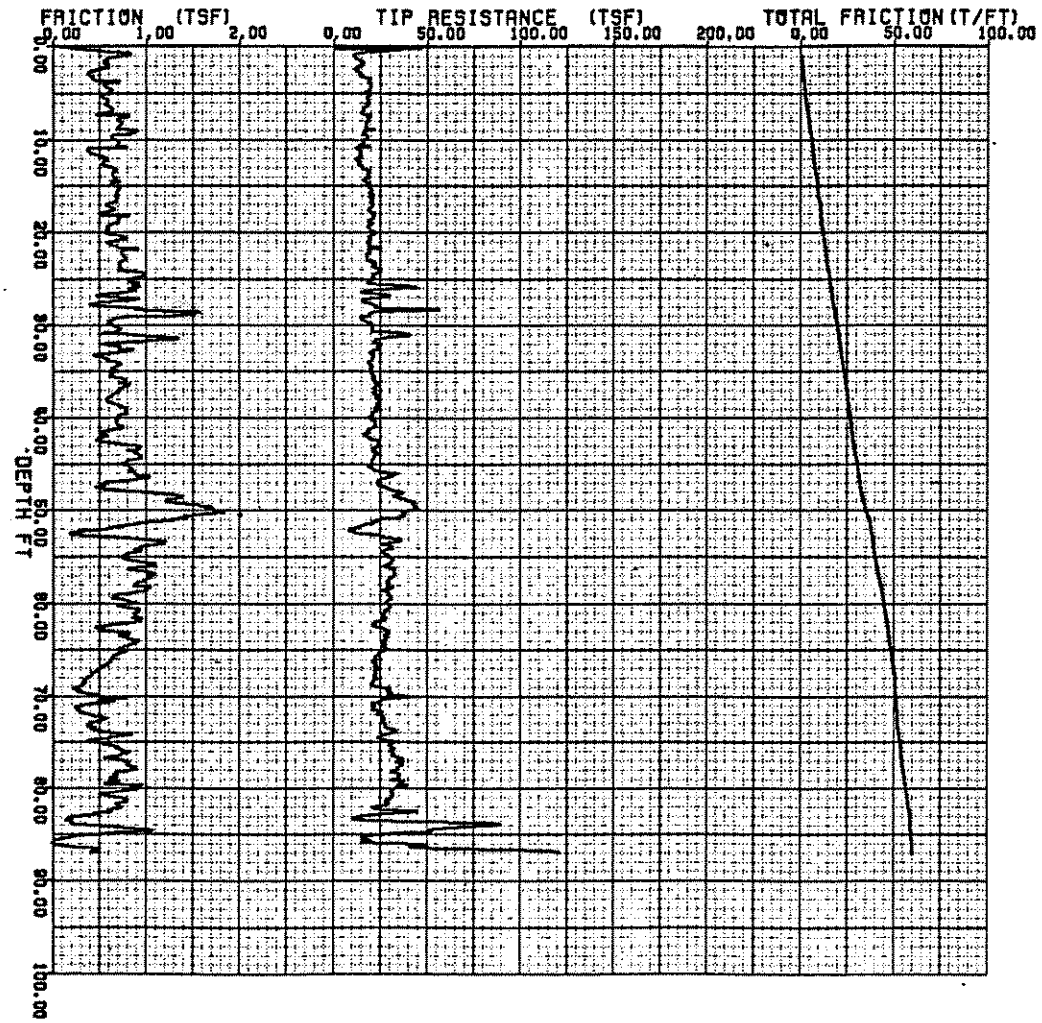

BATON ROUGE (II)

PENETRATION RESULTS TEST NO=95 (CONE 18/10)

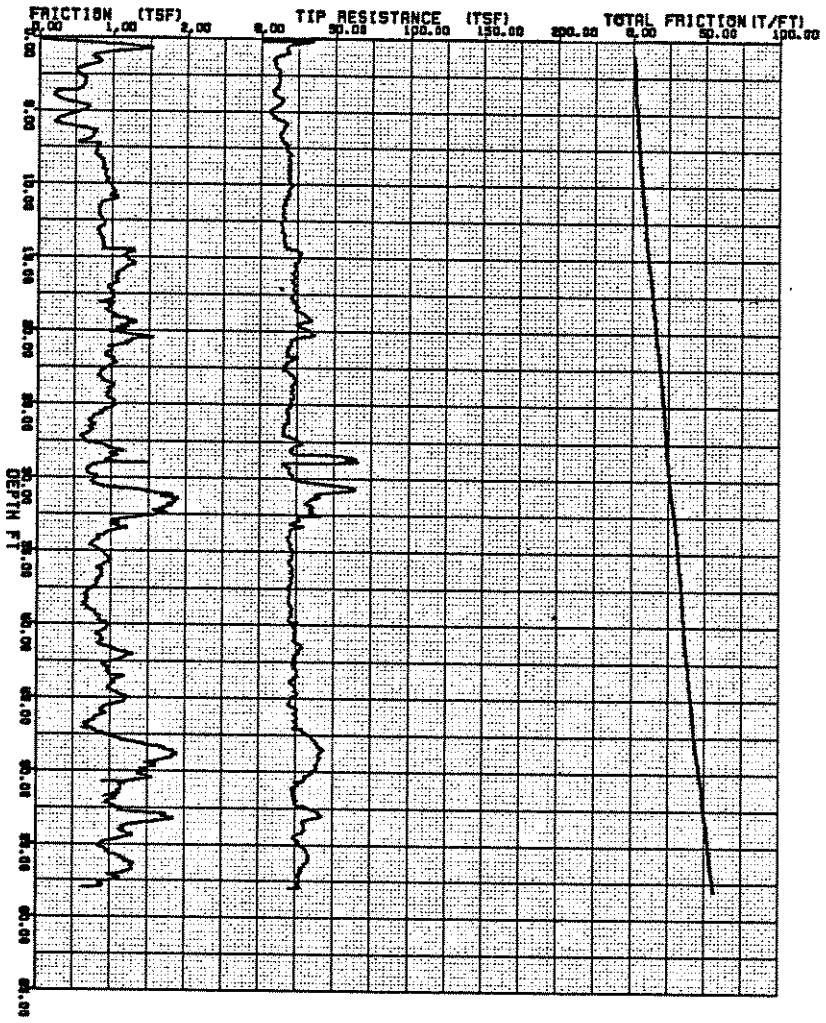

ALEXANDRIA (I)

PENETRATION RESULTS TEST NO=97 (CONE 60/10)

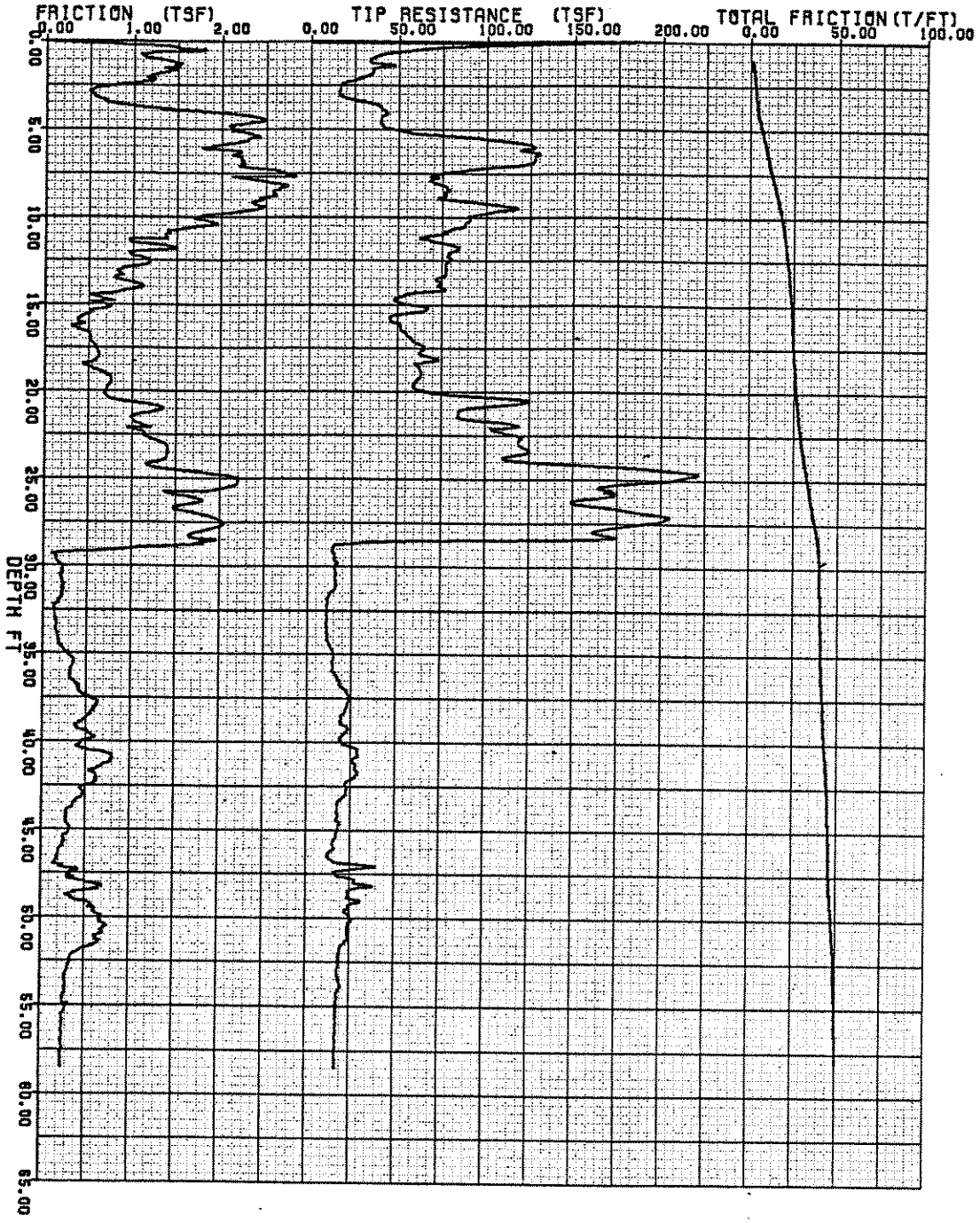

ALEXANDRIA (I)

PENETRATION RESULTS TEST NO=96 (CONE 10/10)

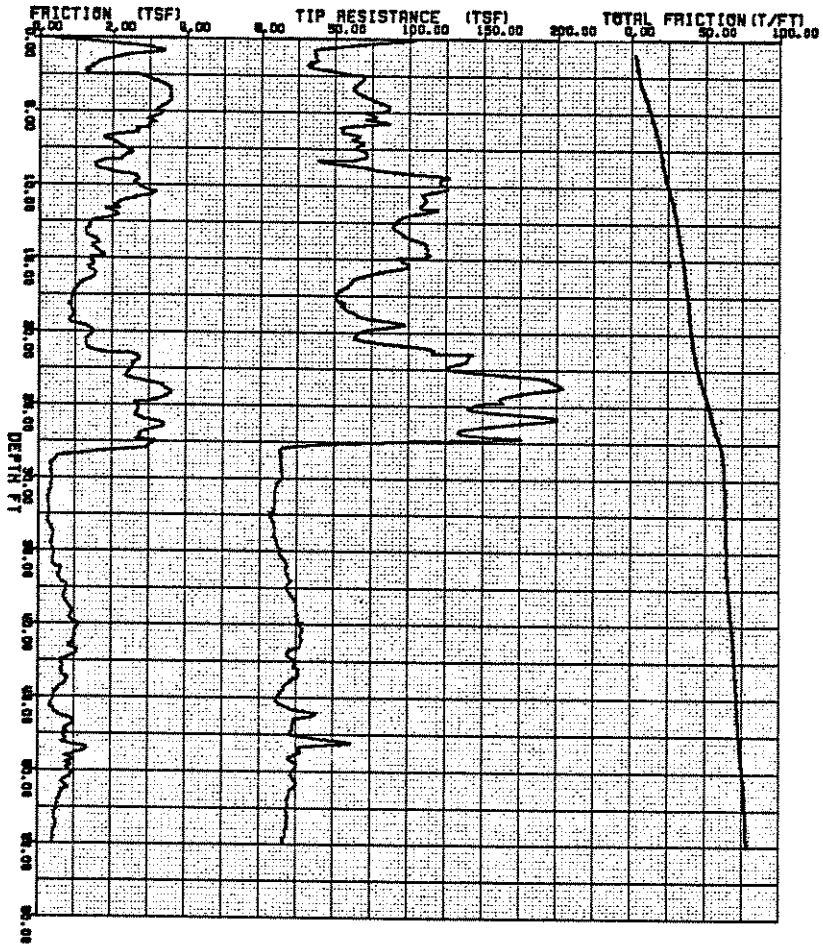

ALEXANDRIA (I)

PENETRATION RESULTS TEST NO=98 (CONE 60/20)

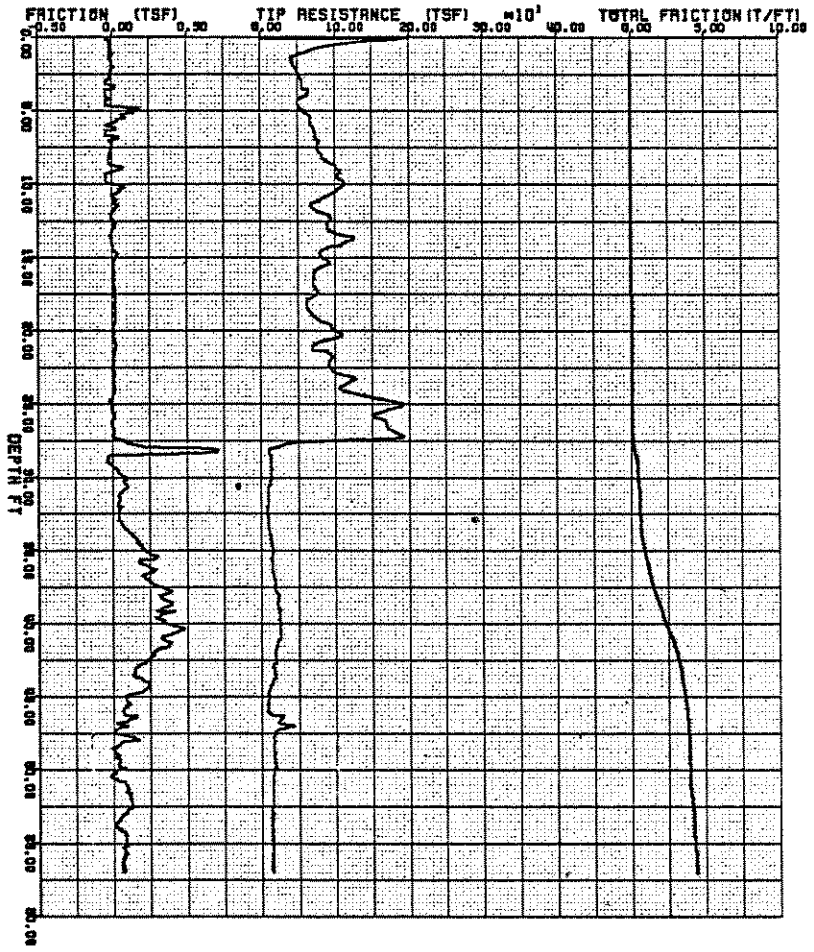

BØRGNE I

PENETRATION RESULTS TEST NØ=163 (CØNE 60/10)

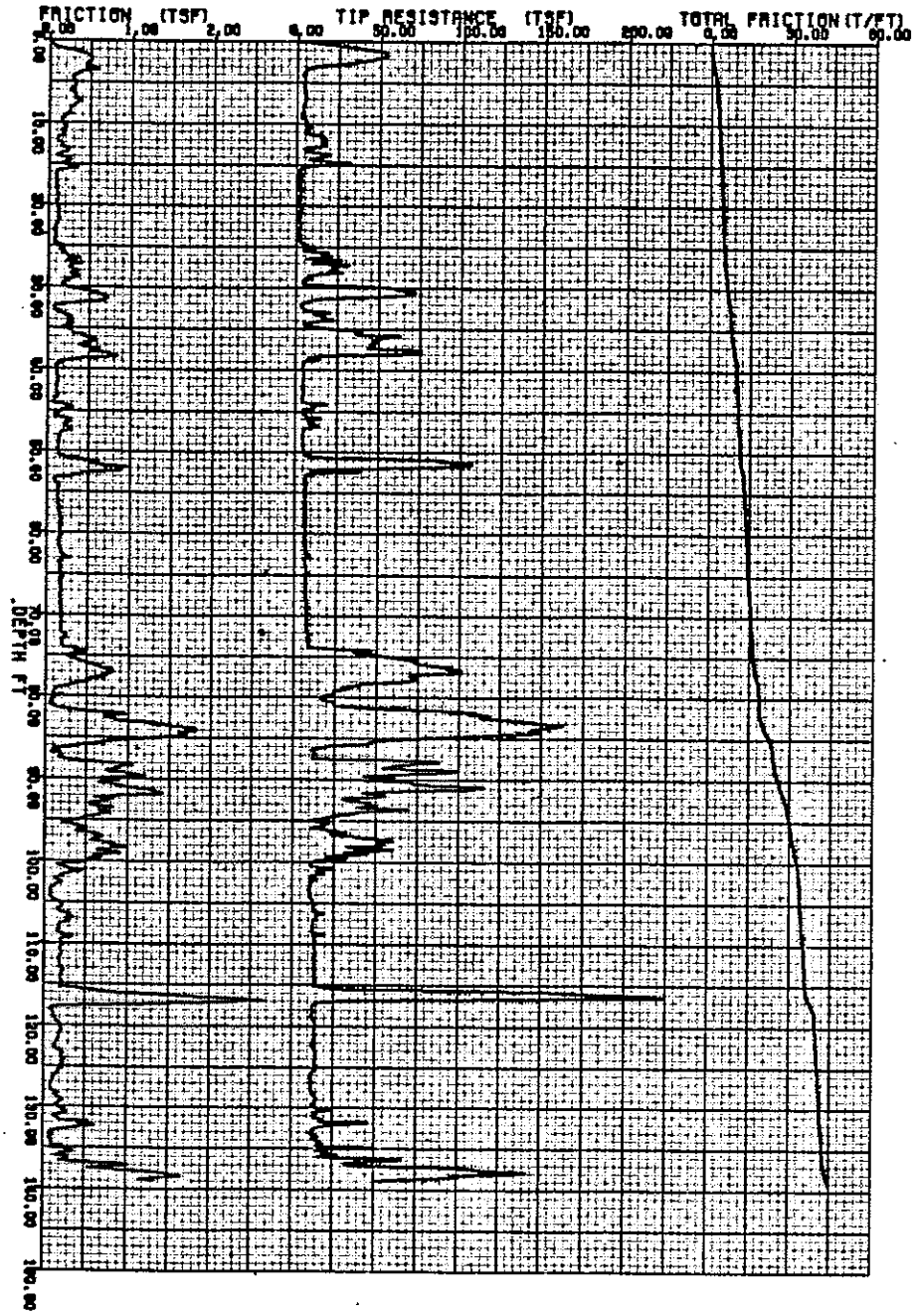

BØRGNE II

PENETRATION RESULTS TEST NØ=114 (CONE 60/10)

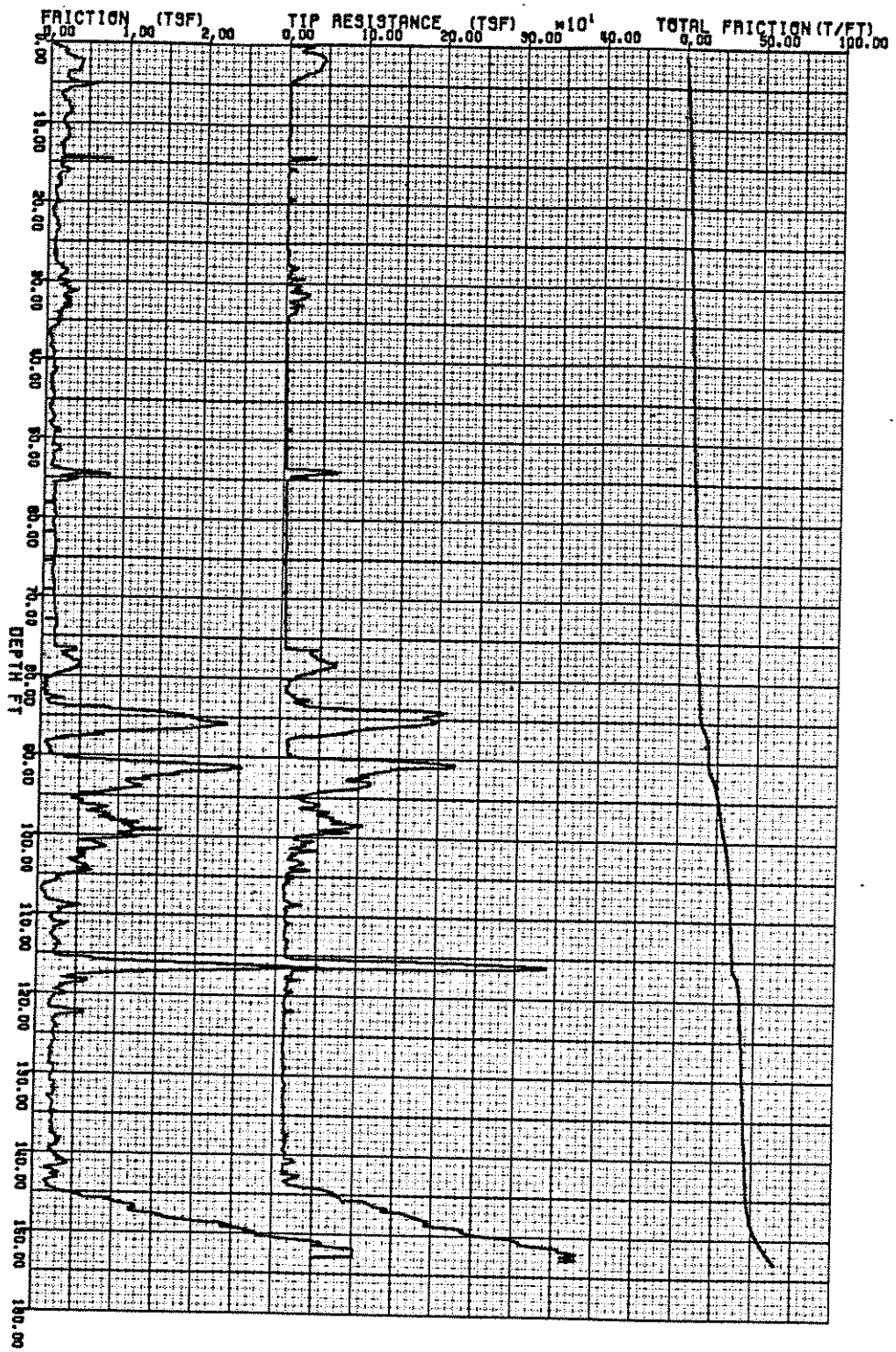

APPENDIX F

TEST PILES' GEOMETRY AND DIMENSION

TEST PILE: 3
NEW ORLEANS (I)
105'
20'
16"ϕ
16"ϕ
8"ϕ
16"ϕ CAST-IN-PLACE CONCRETE
(UNION METAL MONOTUBE)

TEST PILE: 2A
NEW ORLEANS (I)
125'
29"
16"
16"
16"
16"
16"
16"
16"
10¾"ϕ
11⅞"ϕ
12⅞"
13⅞"
14⅜"
15⅜"
16⅞"
16"ϕ CAST-IN-PLACE CONCRETE
(RAYMOND STEP TAPER)

TEST PILE: 1
NEW ORLEANS (I)
125'
18"
18" ⌀ PRECAST CONCRETE PIPE

TEST PILE: 4A
NEW ORLEANS (I)

16" CAST-IN-PLACE CONCRETE
(HLCOR OR CROWEL)

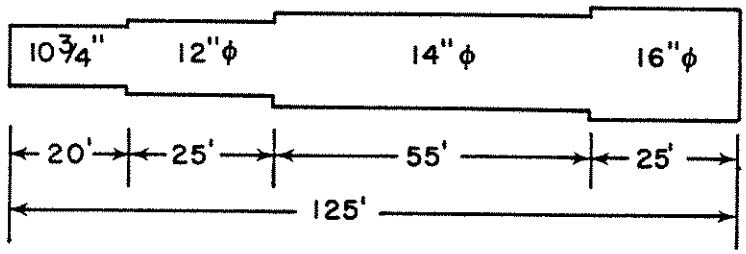

TEST PILE: 5
NEW ORLEANS (I)

16" CAST-IN-PLACE CONCRETE
(PIPE PILE)

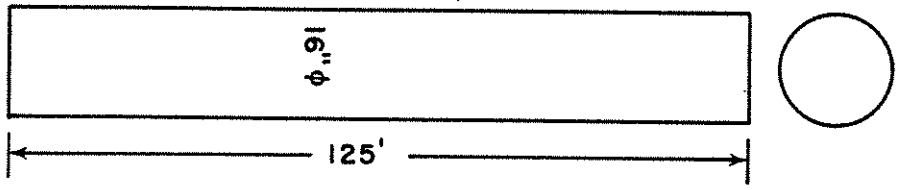

TEST PILE: 6
NEW ORLEANS (IIA)

16" ⊕ PRECAST CONCRETE PILE

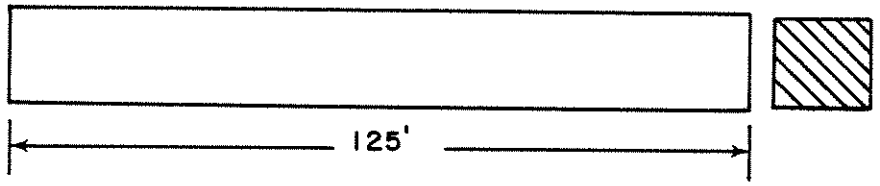

18" ϕ PRECAST CONCRETE PILE
140'
TEST PILE: 7
NEW ORLEANS (IIA)
20" ▽ PRECAST CONCRETE PIPE
105'
TEST PILE: 8
NEW ORLEANS (IIA)
16" ϕ CAST-IN-PLACE CONCRETE
(RAYMOND STEP TAPER)
8 5/8"
9½" 10 3/8" 11 3/8" 12 3/8" 13 3/8" 14 3/8" 15 3/8"
8' 8' 8' 16' 16' 16' 16' 16'
104'
TEST PILE: 9
NEW ORLEANS (IIA)

TEST PILE 10
NEW ORLEANS (11A)

16" ϕ CAST-IN-PLACE CONCRETE
(RAYMOND STEP TAPER)

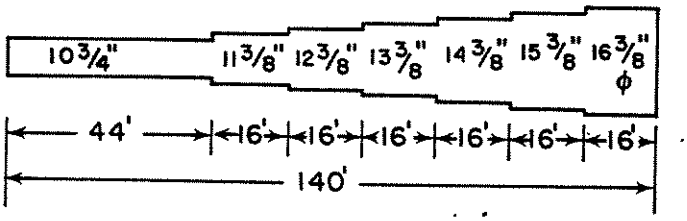

TEST PILE 11
NEW ORLEANS (11A)

14" ϕ CAST-IN-PLACE CONCRETE
(UNION METAL MONOTUBE)

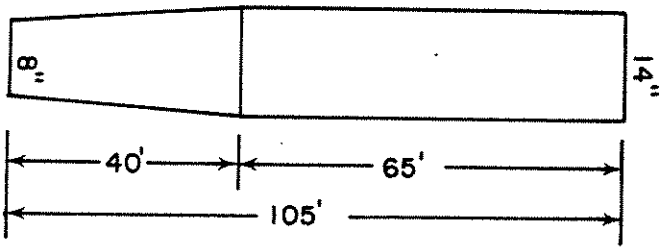

TEST PILE 12
NEW ORLEANS (11A)

16" ϕ CAST-IN-PLACE CONCRETE
(UNION METAL MONOTUBE)

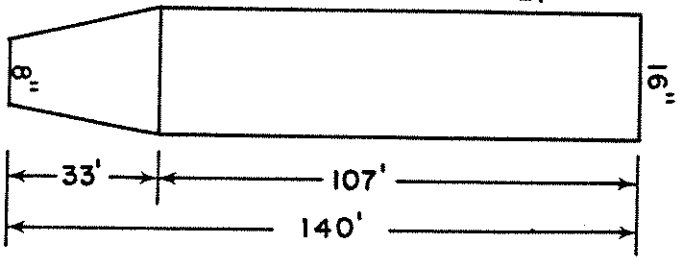

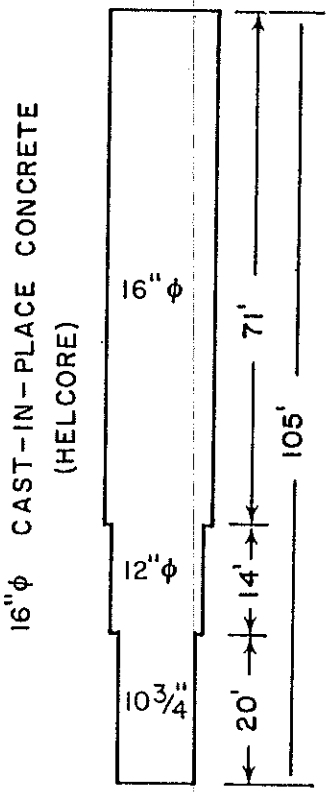

TEST PILE: 13
NEW ORLEANS (11A)

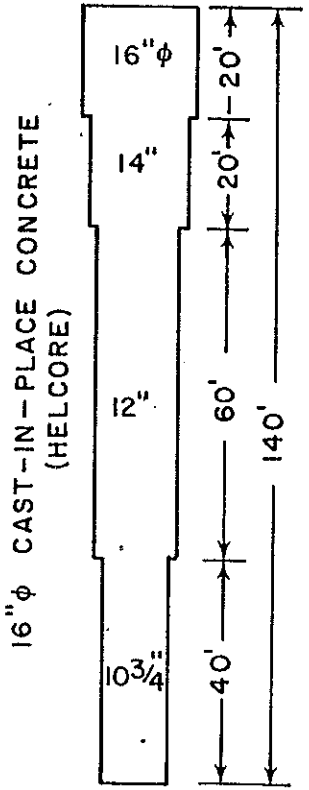

TEST PILE: 14
NEW ORLEANS (11A)

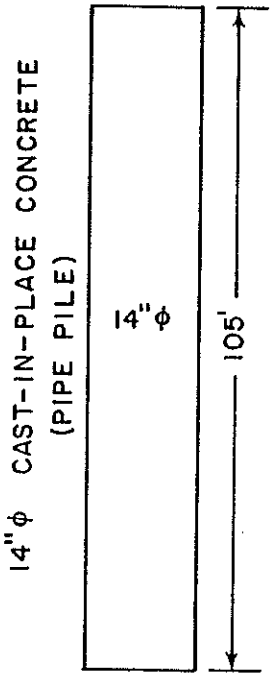

TEST PILE: 15
NEW ORLEANS (11A)

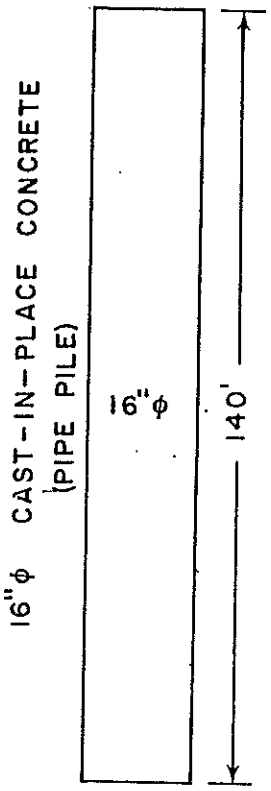

TEST PILE: 16
NEW ORLEANS (IIA)

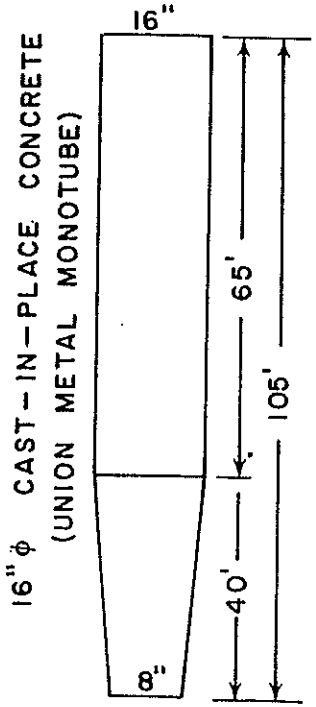

TEST PILE: 17
NEW ORLEANS (IIA)

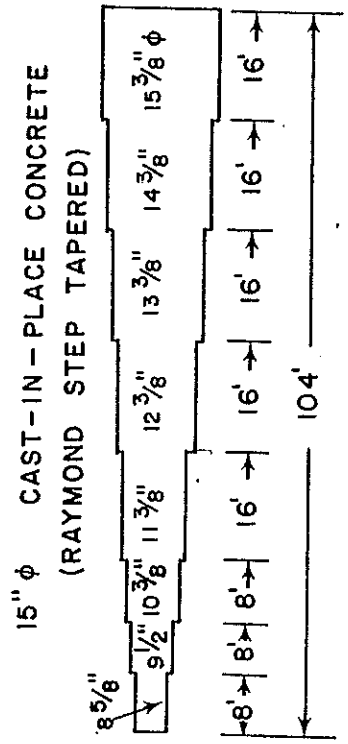

TEST PILE: 18
NEW ORLEANS (IIA)

TEST PILE: 19
NEW ORLEANS (II A)

16"ϕ CAST-IN-PLACE CONCRETE
(RAYMOND STEP TAPER PILE)

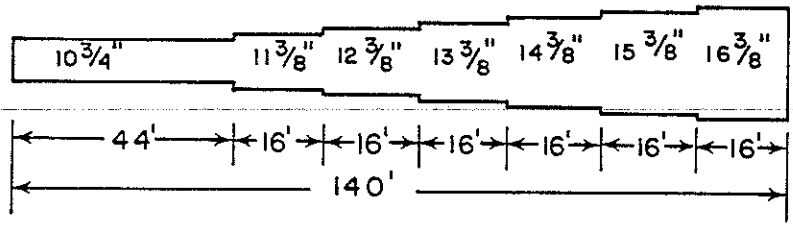

TEST PILE: 1
HOUMA

18" $\square$ PRECAST CONCRETE PILE

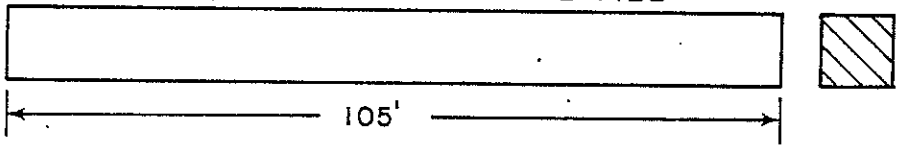

TEST PILE: 2
HOUMA

12"ϕ PRECAST CONCRETE
(PIPE PILE)

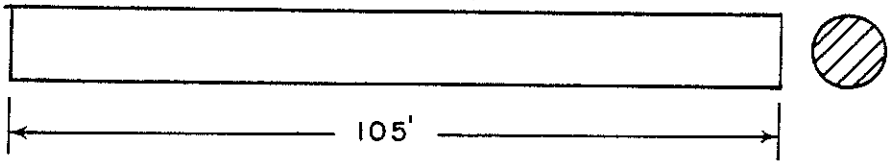

TP-3
HOUMA

14" ø PIPE PILE

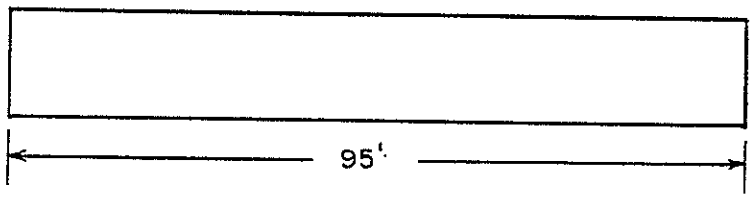

TP-4A
MORGAN CITY

RAYMOND STEP TAPER PILE

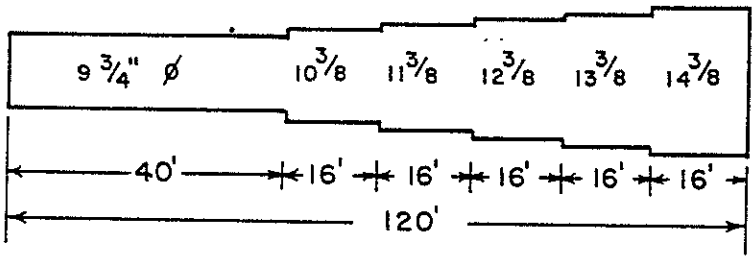

TP-4A
BATON ROUGE (11)

14 ⌀ PRECAST CONCRETE PILE

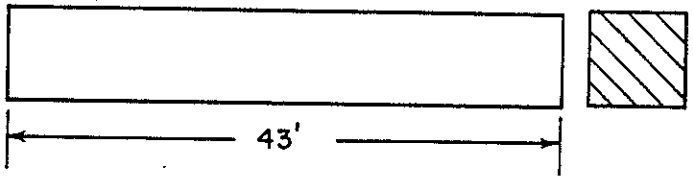

14"φ PRECAST CONCRETE PILE
(RAYMOND STEP TAPER)

TEST PILE: 4
HOUMA

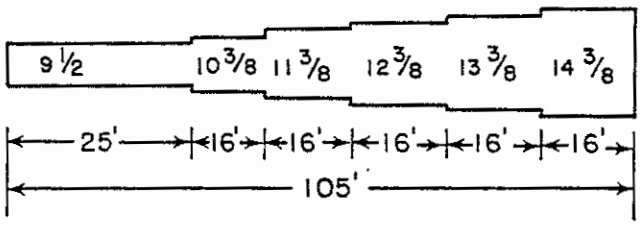

16"φ PRECAST CONCRETE PILE
(RAYMOND STEP TAPER)

TEST PILE: 5
HOUMA

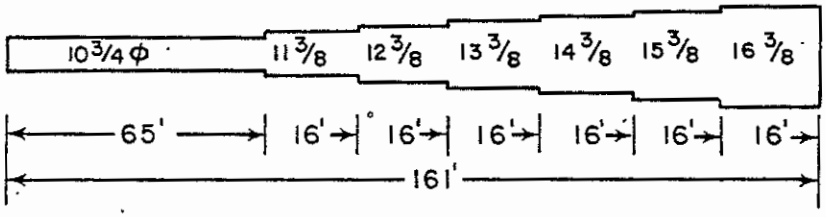

14"φ CAST-IN-PLACE CONCRETE
(UNION METAL MONOTUBE)

TEST PILE: 10
HOUMA

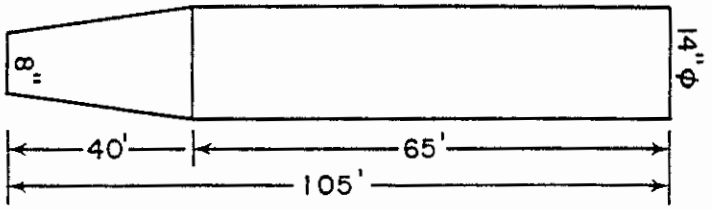

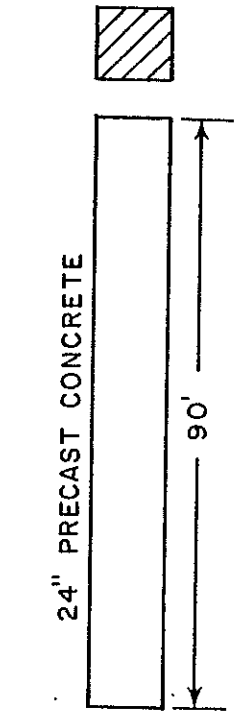

TEST PILE 24-2
RUDDOCK

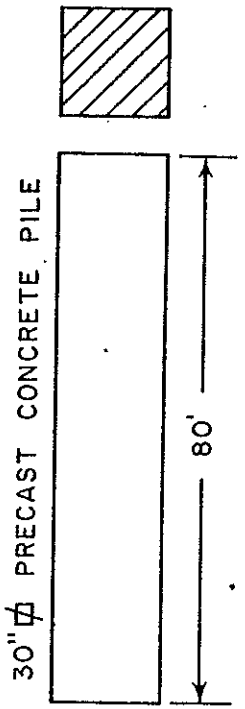

TEST PILE 30-2
RUDDOCK

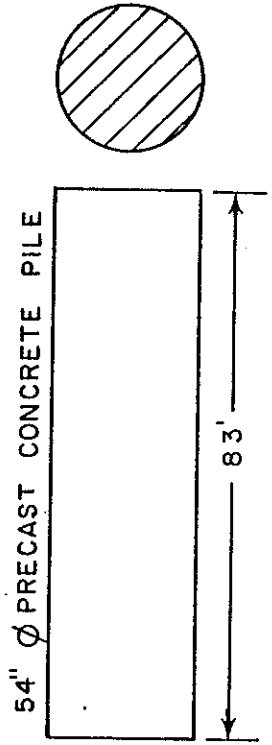

TEST PILE 54-2
RUDDOCK

TEST PILE 24
RUDDOCK

24" ⊕ PRECAST CONCRETE PILE

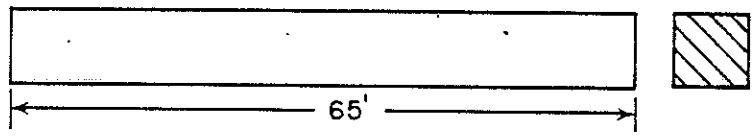

TEST PILE 30
RUDDOCK

30" ⊕ PRECAST CONCRETE PILE

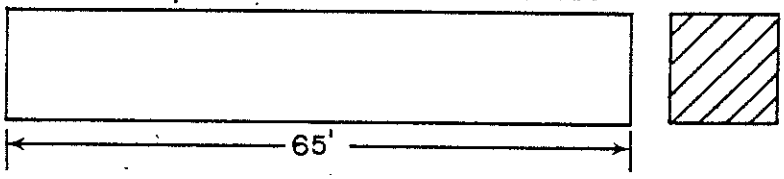

TEST PILE 4A
MORGAN CITY

14" ϕ CAST-IN-PLACE CONCRETE PILE
(RAYMOND STEP TAPER)

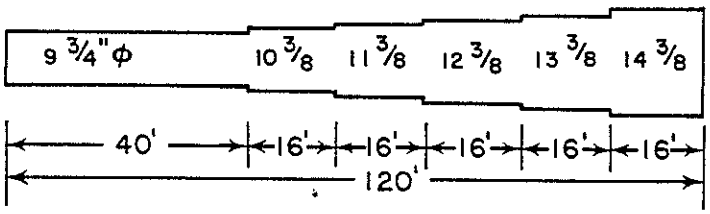

TEST PILE: 1
ALEXANDRIA
14" ⌀ PRECAST CONCRETE PILE
31'
TEST PILE: 2A
BATON ROUGE
14" ⌀ PRECAST CONCRETE PILE
45'
TEST PILE: 4B
MORGAN CITY
14"Φ CAST-IN-PLACE CONCRETE
(RAYMOND STEP TAPER)
9 3/4 Φ
10 3/8
11 3/8
12 3/8
13 3/8
14 3/8
30'
16'
16'
16'
16'
16'
16'
108'

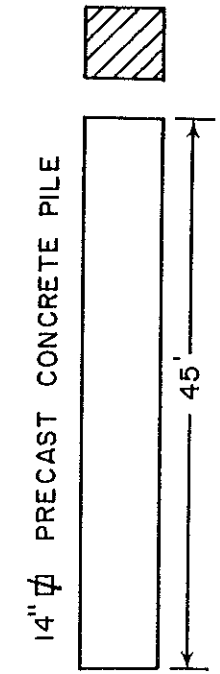

TEST PILE: 3
ALEXANDRIA

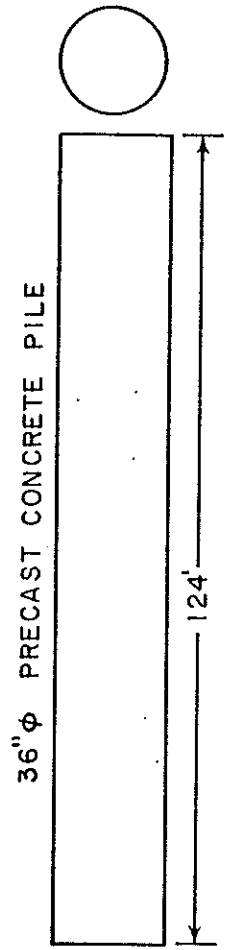

TEST PILE: 2
BORGNE (I)

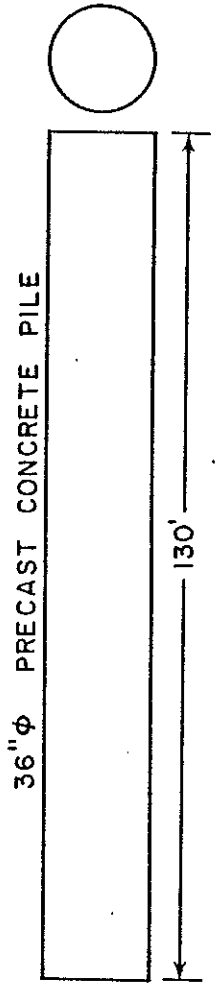

TEST PILE: 4
BORGNE (II)

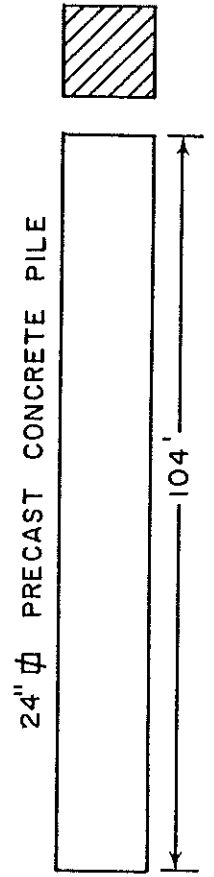

TEST PILE: 5
BORGNE (II)

APPENDIX G

PREDICTION QUOTIENT RESULTS

PREDICTION QUOTIENTS BY CONE-M METHOD

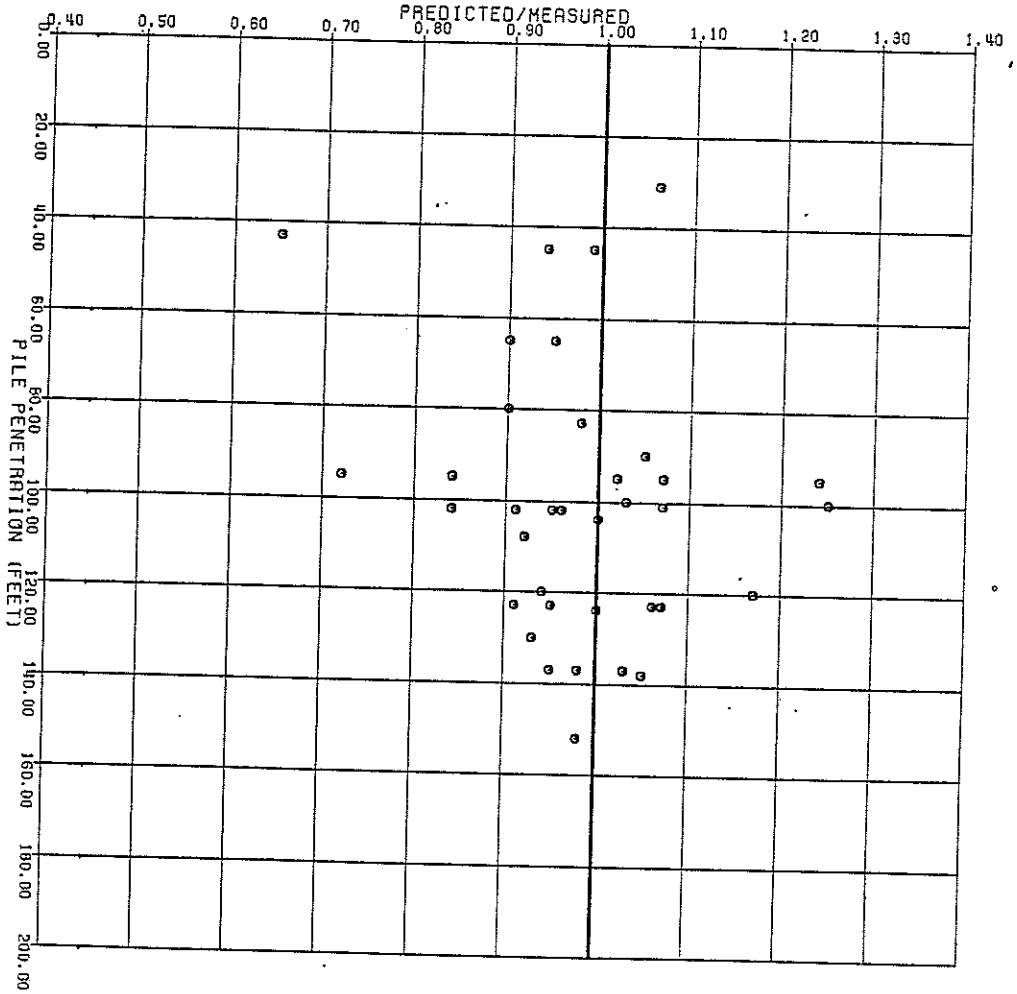

PREDICTION QUOTIENTS BY LAMBDA-CONE METHOD

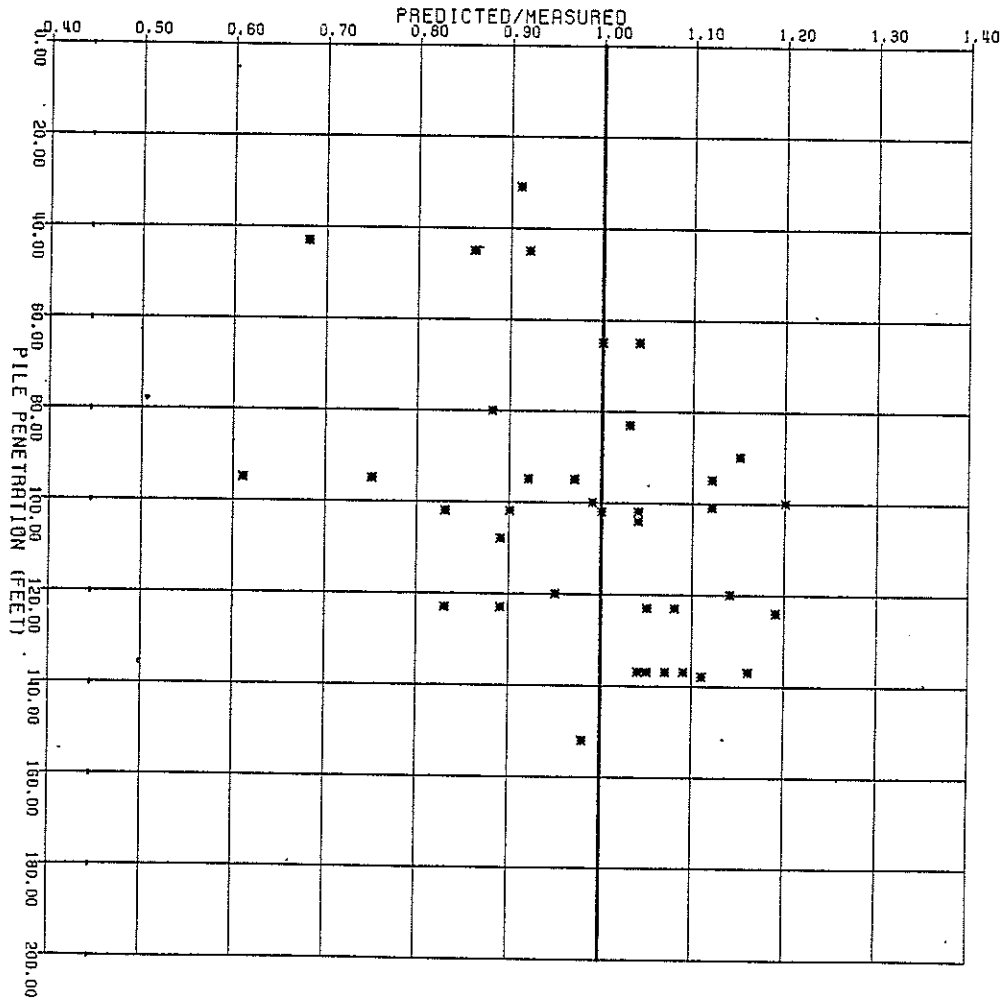

PREDICTION QUOTIENTS BY BETA-CHI METHOD

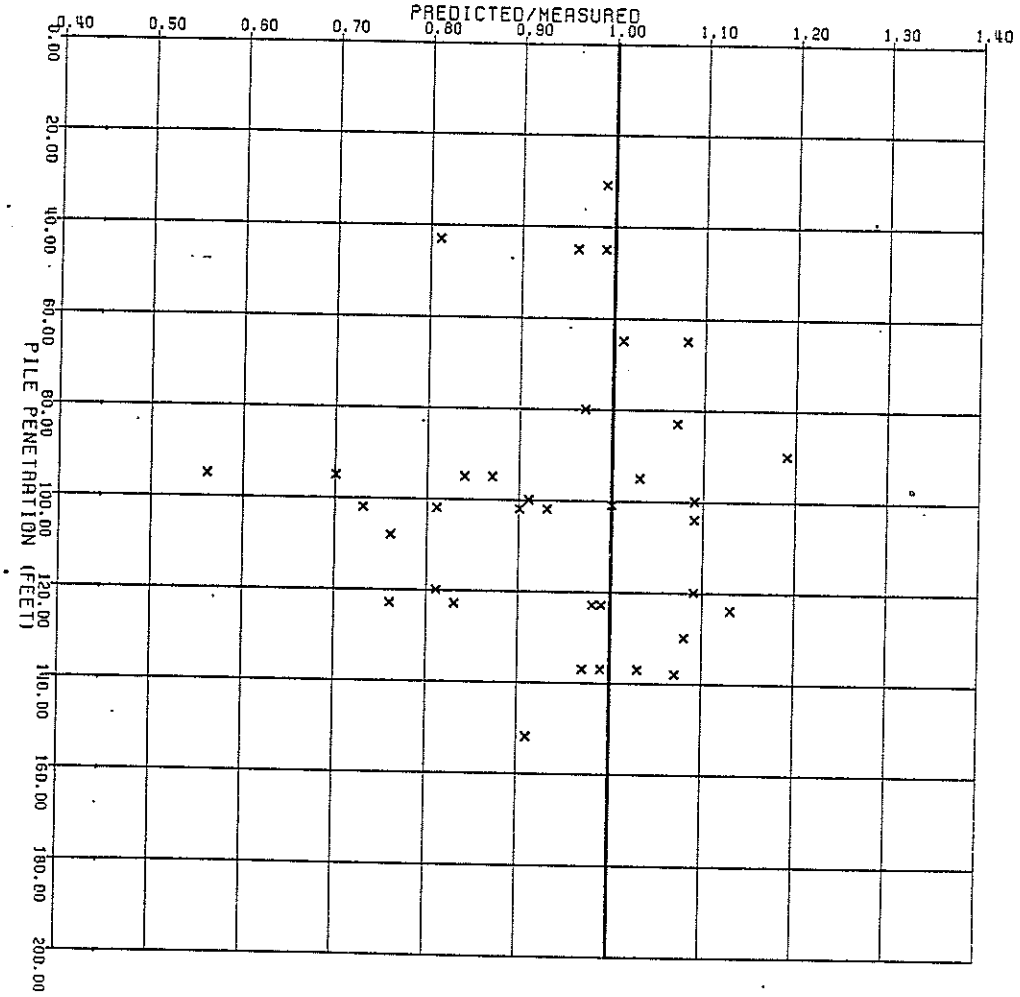

PREDICTION QUOTIENTS BY LAMBDA METHOD

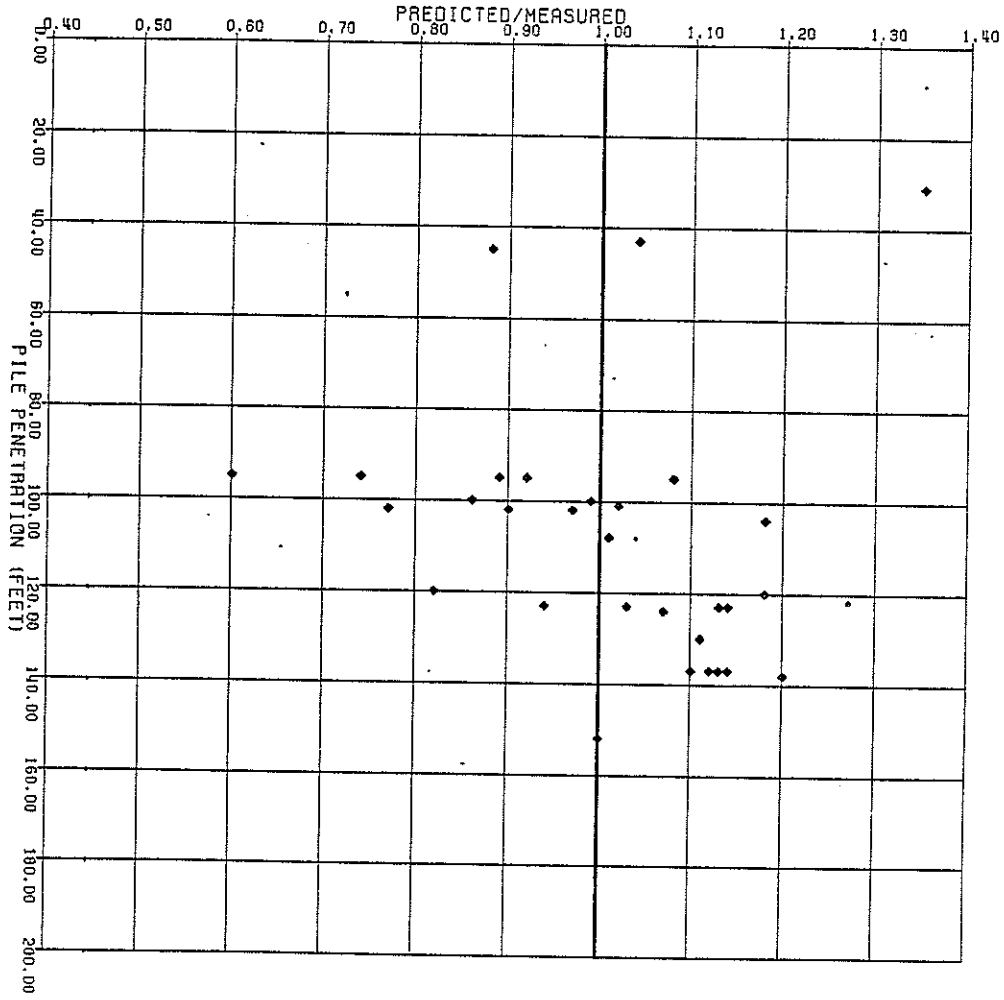

PREDICTION QUOTIENTS BY ALPHA METHOD

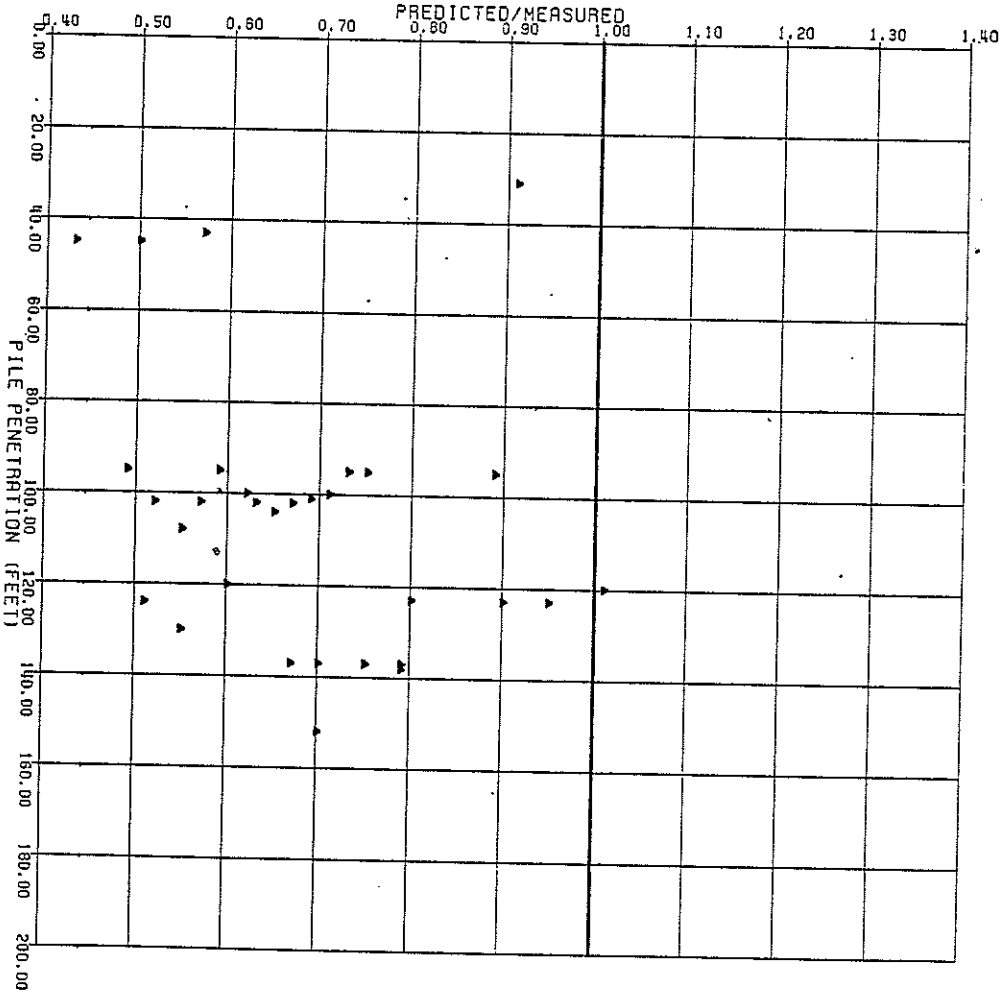

APPENDIX H

EFFECTS OF CONE TIP SHAPE ON LOCAL FRICTION RESULTS

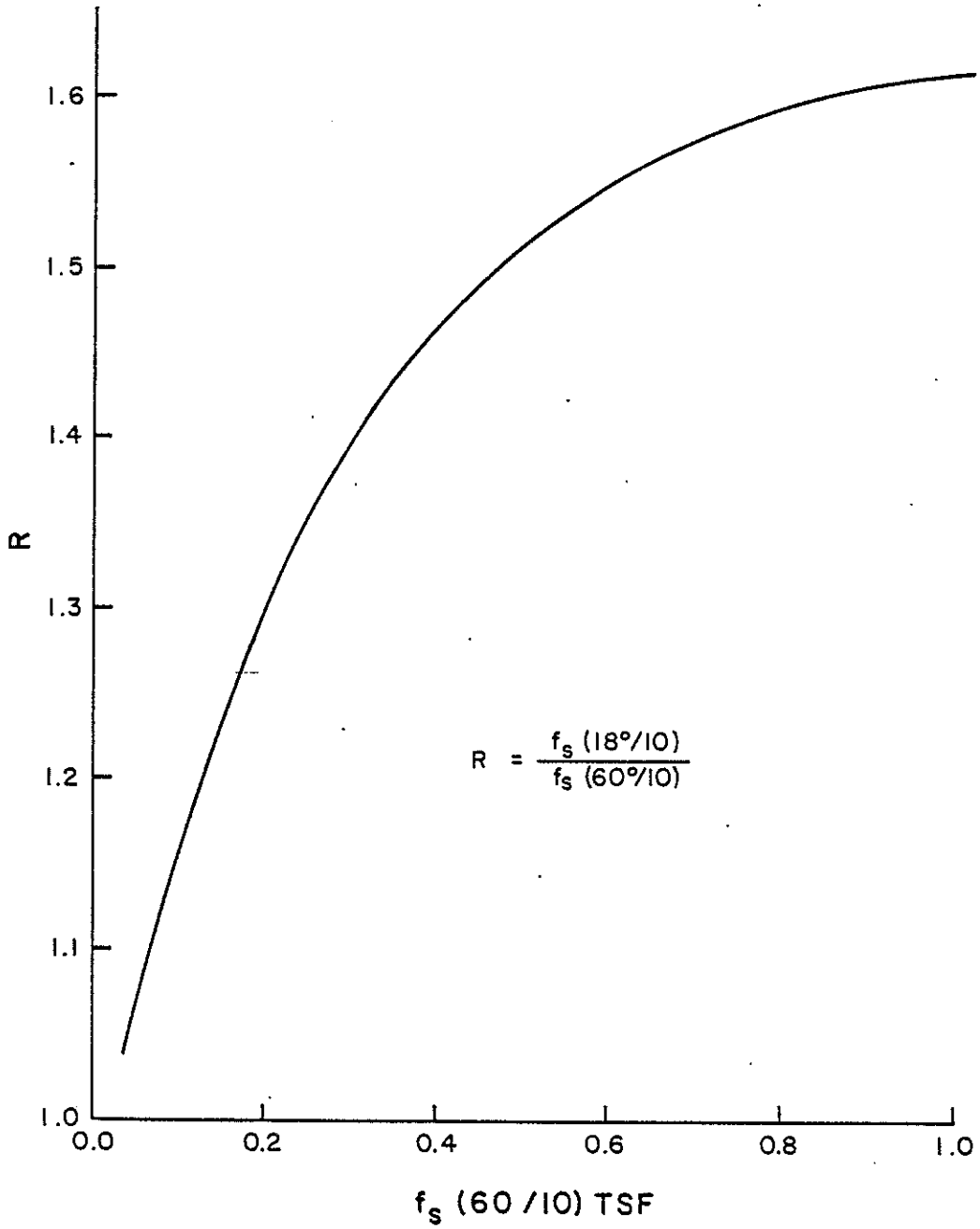
1.6
1.5
1.4
1.3
1.2
1.1
1.0
R
0.0
0.2
0.4
0.6
0.8
1.0
$R = \frac{f_s\ (18°/10)}{f_s\ (60°/10)}$
f_s (60 /10) TSF

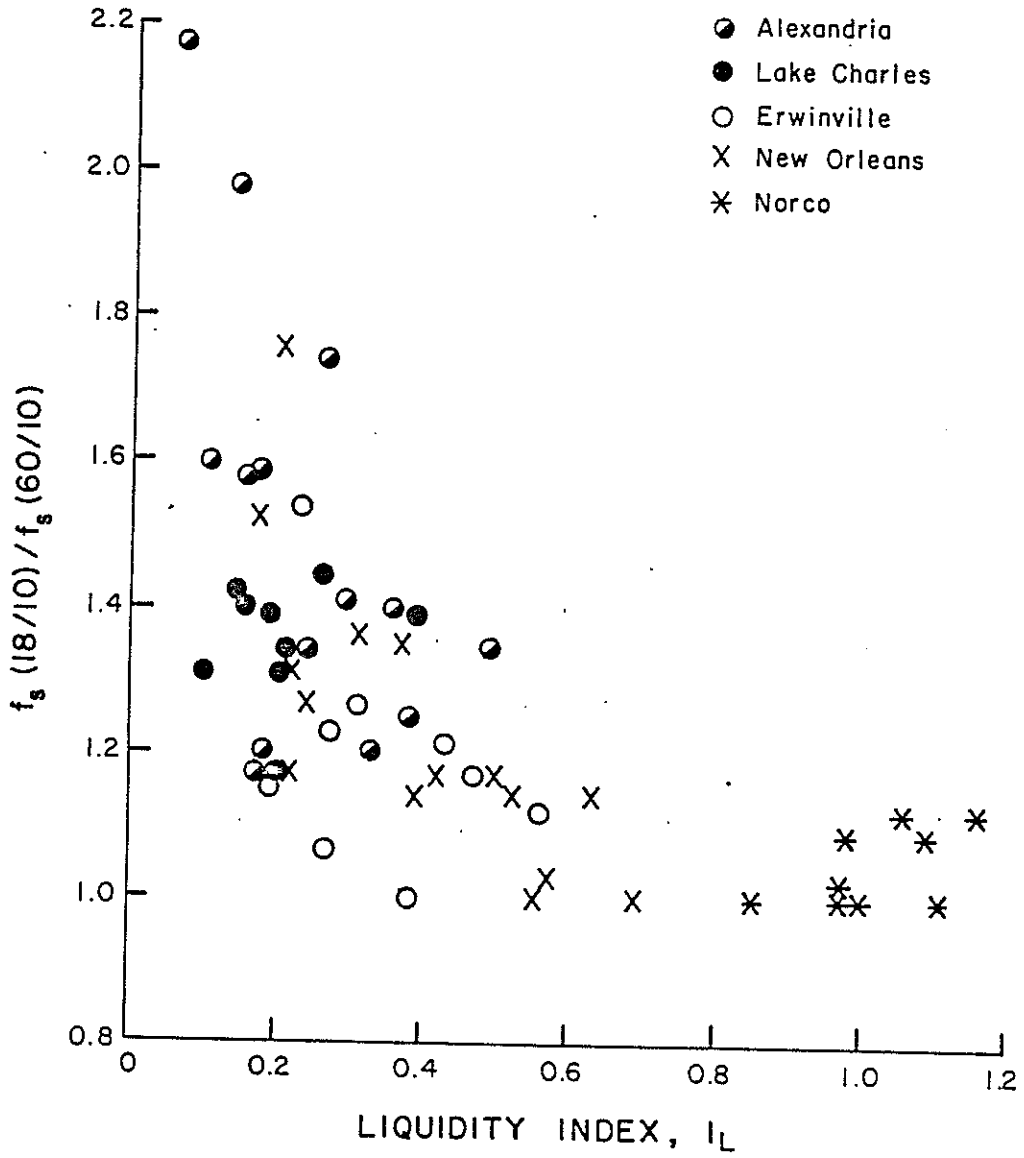
Alexandria
Lake Charles
Erwinville
New Orleans
Norco
2.2
2.0
1.8
1.6
1.4
1.2
1.0
0.8
0
0.2
0.4
0.6
0.8
1.0
1.2
f_s (18/10) / f_s (60/10)
LIQUIDITY INDEX, I_L

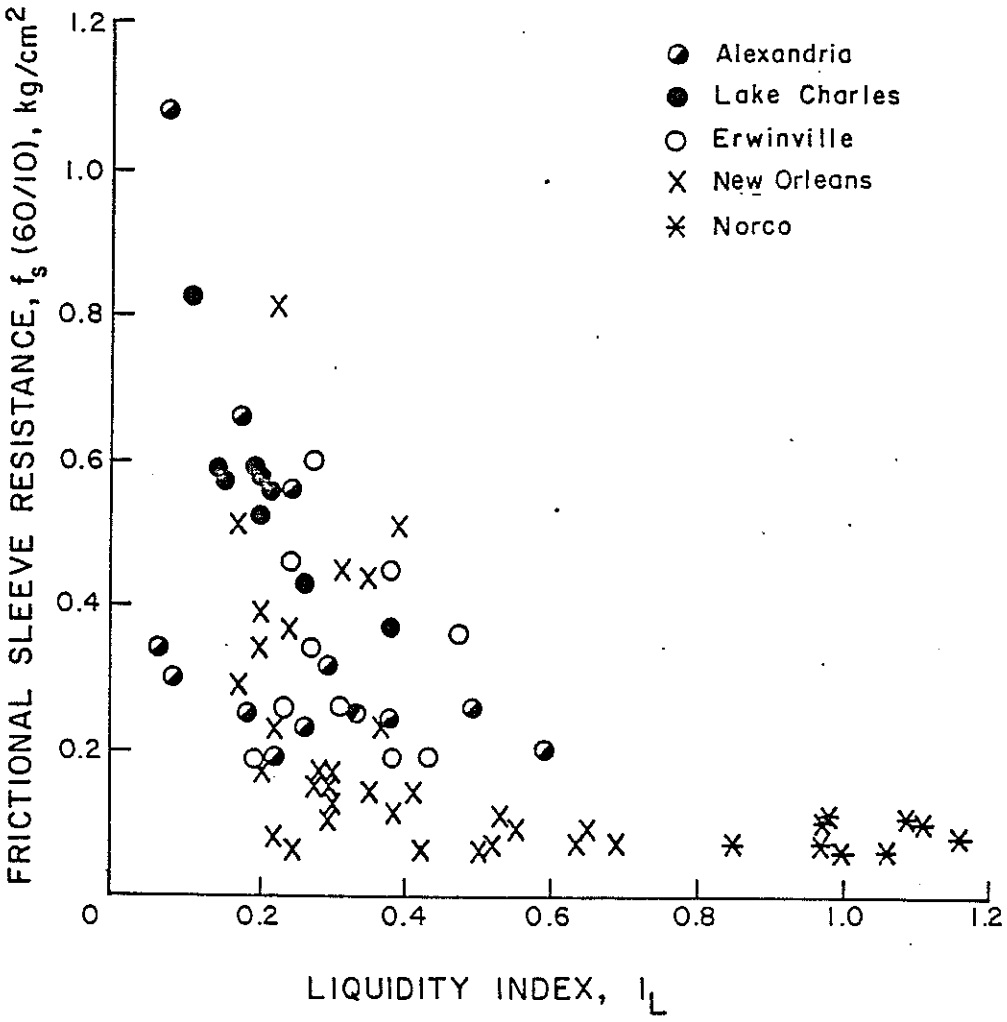
FRICTIONAL SLEEVE RESISTANCE, f_s (60/10), kg/cm^2
1.2
1.0
0.8
0.6
0.4
0.2
0
0.2
0.4
0.6
0.8
1.0
1.2
LIQUIDITY INDEX, I_L
Alexandria
Lake Charles
Erwinville
New Orleans
Norco